

Localization and functional role of RIM3 γ and RIM4 γ , the small members of the RIM protein family

Dissertation

zur

Erlangung des Doktorgrades (Dr. rer.nat.)

der

Mathematisch-Naturwissenschaftlichen Fakultät

der

Rheinischen Friedrich-Wilhelms-Universität Bonn

vorgelegt von

Elena Álvarez-Barón Fuentes

aus

Palencia, Spain

Bonn, 2010

Angefertigt im Institut für Neuropathologie am Universitätsklinikum Bonn mit der Genehmigung der Mathematisch-Naturwissenschaftlichen Fakultät der Rheinischen Friedrich-Wilhelms-Universität Bonn.

1. Referent: Prof. Dr. Susanne Schoch

2. Referent: Prof. Dr. Albert Haas

Tag der mündlichen Prüfung: 25. März 2010

Erscheinungsjahr: 2010

Diese Dissertation ist auf dem Hochschulschriftenserver der ULB Bonn

http://hss.ulb.uni-bonn.de/diss_online elektronisch publiziert.

ERKLÄRUNG

Diese Dissertation wurde im Sinne von § 4 der Promotionsordnung vom 7.1.2004 am Institut für Neuropathologie und Klinik für Epilepsie der Universität Bonn unter der Leitung von Frau Prof. S. Schoch angefertigt.

Hiermit versichere ich, dass ich die vorliegende Arbeit selbständig angefertigt habe und keine weiteren als die angegebenen Hilfsmittel und Quelle verwendet habe, die gemäß § 6 der Promotionsordnung kenntlich gemacht sind.

Bonn, den

Elena Alvarez-Baron

A mis padres

TABLE OF CONTENTS

| | |
|---|------------|
| ERKLÄRUNG | III |
| TABLE OF CONTENTS | V |
| ABSTRACT | XI |
| 1 INTRODUCTION | 1 |
| 1.1 The synaptic vesicle cycle | 2 |
| 1.2 The presynaptic Active Zone | 4 |
| 1.3 The molecular machinery mediating synaptic vesicle exocytosis at the AZ | 6 |
| 1.3.1 The core fusion machinery | 7 |
| 1.3.1.1 SNARES and SNARE regulators | 7 |
| 1.3.1.2 Munc18 | 9 |
| 1.3.1.3 Rab3 | 10 |
| 1.3.2 Active Zone enriched proteins | 11 |
| 1.3.2.1 Bassoon and Piccolo/Azconin | 12 |
| 1.3.2.2 ELKS/ERC/CAST | 14 |
| 1.3.2.3 Liprin- α | 16 |
| 1.3.2.4 Munc13 | 17 |
| 1.3.2.5 RIM | 19 |
| 1.4 RIMs: main components of the scaffolding at the presynaptic Active Zone | 20 |
| 1.4.1 Genomic sequence organization: splice variants and structure | 20 |
| 1.4.2 Protein structure and functional domains | 21 |
| 1.4.3 Interaction partners | 25 |
| 1.4.3.1 Proteins interacting with the N-terminal zinc finger domain | 25 |
| 1.4.3.2 Proteins interacting with the charged domain | 26 |
| 1.4.3.3 Proteins interacting with the PDZ domain | 27 |
| 1.4.3.4 Proteins interacting with the C2 domains | 27 |

| | | |
|----------|--|-----------|
| 1.4.4 | Role of α -RIMs in synaptic function | 30 |
| 1.4.4.1 | UNC-10 deficient <i>C. elegans</i> | 30 |
| 1.4.4.2 | RIM1 α KO mice | 32 |
| 1.4.4.3 | RIM2 α KO mice | 34 |
| 1.4.4.4 | α -RIM DKO mice | 35 |
| 1.4.4.5 | Role of RIM1 β in synaptic function | 35 |
| 1.5 | Presynaptic proteins in neurological diseases | 36 |
| 2 | AIMS OF THE STUDY | 38 |
| 3 | MATERIAL | 40 |
| 3.1 | Equipment | 40 |
| 3.2 | Chemicals | 41 |
| 3.3 | Kits | 43 |
| 3.4 | Cell culture media | 43 |
| 3.5 | Antibodies | 44 |
| 3.6 | Oligonucleotides | 45 |
| 3.6.1 | Sequencing primer | 45 |
| 3.6.2 | <i>In situ</i> hybridization oligonucleotides | 45 |
| 3.6.3 | shRNA sequences | 46 |
| 3.6.4 | Cloning primer | 47 |
| 3.7 | Vectors | 49 |
| 3.7.1 | TOPO cloning vectors | 49 |
| 3.7.2 | Plasmids for cell culture transfection | 52 |
| 3.7.3 | Plasmids for lentivirus production | 54 |
| 3.8 | cDNA and protein sequences | 58 |
| 3.8.1 | RIM1 α | 58 |
| 3.8.1.1 | RIM1 α cDNA (<i>rattus novergicus</i>) | 58 |
| 3.8.1.2 | RIM1 α protein (<i>rattus novergicus</i>) | 60 |
| 3.8.2 | RIM3 γ | 60 |
| 3.8.2.1 | RIM3 γ cDNA (<i>rattus novergicus</i>) | 60 |
| 3.8.2.2 | RIM3 γ protein (<i>rattus novergicus</i>) | 61 |
| 3.8.3 | RIM4 γ | 61 |

| | |
|---|-----------|
| 3.8.3.1 RIM4 γ cDNA (<i>rattus novergicus</i>) | 61 |
| 3.8.3.2 RIM4 γ protein (<i>rattus novergicus</i>) | 61 |
| 3.8.4 Protein alignment | 61 |
| 3.9 URLs | 64 |
| 4 METHODS | 65 |
| 4.1 Molecular biological methods | 65 |
| 4.1.1 Preparation of competent bacteria | 65 |
| 4.1.1.1 Electrocompetent | 65 |
| 4.1.1.2 Chemically competent | 65 |
| 4.1.2 Transformation | 66 |
| 4.1.2.1 Chemical-transformation | 66 |
| 4.1.2.2 Electroporation | 66 |
| 4.1.3 Bacteria culture | 66 |
| 4.1.4 DNA plasmid purification | 67 |
| 4.1.5 Restriction digest, dephosphorylation and ligation | 67 |
| 4.1.6 DNA precipitation | 68 |
| 4.1.7 DNA sequencing | 68 |
| 4.1.8 PCR product purification and gel extraction | 68 |
| 4.1.9 Polymerase chain reaction | 69 |
| 4.1.10 cDNA preparation | 70 |
| 4.1.11 Cloning strategies | 70 |
| 4.1.11.1 Overexpression constructs in pcDNA3.1, pL26 and pLenti LN-EGFP-EF1 α plasmids | 70 |
| 4.1.11.2 cloning of shRNA sequences in the pLVTHM vector | 71 |
| 4.2 Biochemical methods | 72 |
| 4.2.1 Generation of peptides antibodies | 72 |
| 4.2.2 Western blot | 73 |
| 4.2.2.1 Preparation of protein extracts | 73 |
| 4.2.2.2 Subcellular fractionation of adult rat brain | 74 |
| 4.3 Cell culture | 75 |
| 4.3.1 Eukaryotic cell culture | 75 |
| 4.3.2 Primary cell culture | 76 |
| 4.3.2.1 Coverslip treatment | 76 |

| | | |
|------------|--|-----------|
| 4.3.2.2 | Dissection | 76 |
| 4.3.2.3 | Culture preparation | 76 |
| 4.3.3 | Transient transfection of mammalian cells | 77 |
| 4.3.3.1 | HEK 293T | 77 |
| 4.3.3.2 | PC12 | 77 |
| 4.3.3.3 | Primary neurons | 78 |
| 4.4 | Histological and immunohistochemical methods | 78 |
| 4.4.1 | Animals and brain sections | 78 |
| 4.4.2 | Immunohistochemical analyses on paraffin sections | 79 |
| 4.4.3 | Immunohistochemical analyses on cryosections | 79 |
| 4.4.4 | Immunohistochemical analyses on the Retina | 80 |
| 4.4.5 | Free-floating immunohistochemical analyses | 80 |
| 4.4.6 | Immunocytochemistry | 81 |
| 4.5 | Lentivirus production | 81 |
| 4.5.1 | Lentivirus based vector system | 81 |
| 4.5.2 | HEK 293T culture and transfection | 82 |
| 4.5.3 | Viral particle purification | 82 |
| 4.5.4 | <i>In vivo</i> injection of lentivirus particles | 83 |
| 5 | RESULTS | 84 |
| 5.1 | RIM3γ and RIM4γ | 84 |
| 5.1.1 | Localization of RIM3 γ and RIM4 γ | 84 |
| 5.1.1.1 | RIM3 γ and RIM4 γ mRNA expression: <i>In situ</i> hybridization | 84 |
| 5.1.1.2 | RIM3 γ and RIM4 γ protein expression | 87 |
| 5.1.1.2.1 | Generation and characterization of isoform specific antibodies | 87 |
| 5.1.1.2.2 | Tissue distribution of RIM3 γ and rim4 γ proteins | 89 |
| 5.1.1.2.3 | Expression pattern in different brain regions | 89 |
| 5.1.1.2.4 | Developmental expression in rat brain | 91 |
| 5.1.1.2.5 | Association of γ -RIMS with the insoluble synaptic fraction | 91 |
| 5.1.1.3 | Immunofluorescence analyses in rat brain | 94 |
| 5.1.1.3.1 | Light microscopy analysis of RIM3 γ and RIM4 γ localization in rat brain | 94 |
| 5.1.1.3.2 | Immunofluorescence analysis of RIM3 γ and RIM4 γ in primary cultured neurons | 96 |
| 5.1.1.3.3 | Immunofluorescence analysis of RIM3 γ and RIM4 γ expression in the retina | 100 |

| | | |
|------------|---|------------|
| 5.1.1.3.4 | RIM3 γ and RIM4 γ expression in inhibitory neurons | 102 |
| 5.1.2 | Functional investigation of RIM3 γ and RIM4 γ proteins | 105 |
| 5.1.2.1 | Characterization of γ -RIMs targeting sequences | 105 |
| 5.1.2.1.1 | Analysis of the interaction between γ -RIMS and Liprins- α in chromaffin cells | 106 |
| 5.1.2.2 | Analysis of RIM3 γ and RIM4 γ intracellular trafficking in primary hippocampal neurons | 116 |
| 5.1.2.3 | Analysis of γ -RIMs targeting sequences in neurons | 119 |
| 5.1.2.4 | Potential role of Liprins- α and RIM1 α in the synaptic localization of γ -RIMs | 123 |
| 5.1.2.5 | The C2B domain of γ -RIMs is sufficient for the interaction with RIM1 α | 126 |
| 5.1.2.6 | Functional consequences of reduced γ -RIM levels in neurons | 128 |
| 5.1.2.6.1 | Analysis of knockdown efficiency in heterologous cells | 128 |
| 5.1.2.6.2 | shRNAs are isoform specific | 131 |
| 5.1.2.6.3 | Analysis of knockdown efficiency in neurons | 132 |
| 5.1.2.6.4 | RIM3 γ and RIM4 γ knockdown inhibits dendrite morphogenesis | 134 |
| 5.1.2.7 | <i>In vivo</i> experiments | 138 |
| 5.1.2.8 | Phenotype rescue | 143 |
| 5.1.2.8.1 | RIM3 γ and RIM4 γ shRNA sequence with point mutations are ineffective | 144 |
| 5.1.2.9 | Rescue experiments in hippocampal neurons | 145 |
| 5.1.2.10 | RIM3 γ and RIM4 γ are necessary for neurite development | 146 |
| 5.1.2.11 | Loss of RIM3 γ and RIM4 γ specifically affected RIM1 α expression levels | 148 |
| 5.1.2.12 | Loss of RIM3 γ induces a reduction of Liprins- α and GRIP1 expression levels | 150 |
| 5.1.2.13 | Spontaneous synaptic activity in RIM3 γ and RIM4 γ knockdown neurons | 152 |
| 5.2 | Presynaptic proteins in epilepsy | 154 |
| 5.2.1 | Antibodies against Munc18-1 in serum of Rasmussen encephalities patients | 154 |
| 5.2.2 | Neuropathological evaluation of post-surgery biopsy specimens | 157 |
| 6 | DISCUSSION | 160 |
| 6.1 | Expression and subcellular localization of RIM3γ and RIM4γ | 162 |
| 6.1.1 | RIM3 γ is a presynaptic protein, also enriched in the nucleus | 165 |
| 6.1.2 | RIM4 γ is uniformly localized along the axon and dendrites | 167 |
| 6.2 | γ-RIMs targeting sequences | 168 |

| | |
|--|------------|
| 6.3 Determinants of γ-RIM subcellular localization | 170 |
| 6.3.1 Liprins- α do not influence γ -RIMs presynaptic localization | 171 |
| 6.3.2 RIM1 α promotes the synaptic localization of RIM3 γ and RIM4 γ | 173 |
| 6.4 RIM3γ and RIM4γ are necessary for the correct formation of neuronal processes | 176 |
| 6.4.1 Possible mechanisms underlying the loss of neuronal processes | 181 |
| 6.5 Autoantibodies to Munc18, cerebral plasma cells and B-lymphocytes in Rasmussen encephalitis | 185 |
| 7 CONCLUSIONS | 188 |
| 8 OUTLOOK | 190 |
| 9 REFERENCES | 191 |
| 10 LIST OF FIGURES | 209 |
| 11 LIST OF TABLES | 212 |
| 12 ABBREVIATIONS | 213 |
| 13 ACKNOWLEDGMENTS | 217 |

ABSTRACT

RIMs are Active Zone enriched multidomain proteins. In vertebrates, the RIM family is composed of 7 proteins (RIM1 α , 2 α , 1 β , 2 β , 2 γ , 3 γ and 4 γ) encoded by four different genes (RIM1-4). The large members of the RIM protein family are central components of the cytomatrix at the Active Zone and play a key regulatory role in synaptic vesicle exocytosis and presynaptic forms of short- and long-term plasticity. However, so far little was known about the localization and function of the γ -isoforms.

The focus of this study was to gain further insights into the physiological properties of RIM3 γ and RIM4 γ . Therefore, we first investigated their localization. We found the regional distribution of both γ -RIMs to overlap with the full-length isoforms, however, they exhibited a diverging regional and subcellular localization. RIM3 γ was presynaptically localized, whereas RIM4 γ was not restricted to the synapse but also present along the axon and dendrites. In addition, we studied the γ -RIM domains and sequences responsible for the targeting of the proteins, and found the C2B domain to be sufficient for the presynaptic localization of γ -RIMs. Furthermore, we observed that coexpression of the γ -isoforms with RIM1 α , but not with Liprins- α , can promote their synaptic localization.

In order to delineate the function of the γ -isoforms, downregulation of the proteins was performed using lentiviral transduction in primary neuronal cultures and *in vivo*. RIM3 γ or RIM4 γ knock down neurons displayed a striking change in neuronal morphology, whereby they maintained the axon but lost most of their dendrites. In addition, downregulation of γ -RIMs, led to a decrease in the levels of RIM1 α , Liprins- α and GRIP1, suggesting a possible role for γ -RIMs in neuronal morphogenesis, likely via a cascade involving Liprin- α and Liprin- α binding proteins.

1 INTRODUCTION

A century after Santiago Ramon y Cajal presented evidence for the "neuron doctrine", his view of the brain remains the foundation of modern neuroscience. His meticulous morphological and histological examination of the anatomy of the brain revealed the existence of independent cellular units, neurons, leading to a controversial hypothesis: communication of neuronal axons with the soma or dendrites would be established by contact and not by protoplasmic continuity, as thought before. Later, these sites of contact became known as synapses (Charles Sherrington, 1897). Ramón y Cajal postulated that although an axon terminates contiguous to a dendrite of the next neuron, the cleft between the two cells operates as the site of information exchange. The synaptic cleft was first shown in 1954, when improving electron microscope techniques provided strong support for its existence.

Chemical synapses are the main sites for communication between neurons via chemical messengers, known as neurotransmitters. When an action potential arrives at the presynaptic nerve terminal, neurotransmitters are rapidly released into the synaptic cleft, diffuse, and activate the receptors that are localized in the postsynaptic membrane (reviewed in C. Südhof and Starke, 2008; Carr and Munson, 2007; Stevens, 2003; Südhof, 2008a; Südhof, 2004).

Synapses exhibit a very characteristic asymmetric organization with a presynaptic nerve terminal (bouton) where synaptic vesicles are localized, a synaptic cleft, and a postsynaptic neurotransmitter response machinery, the postsynaptic density (PSD) (Fig. 1.1).

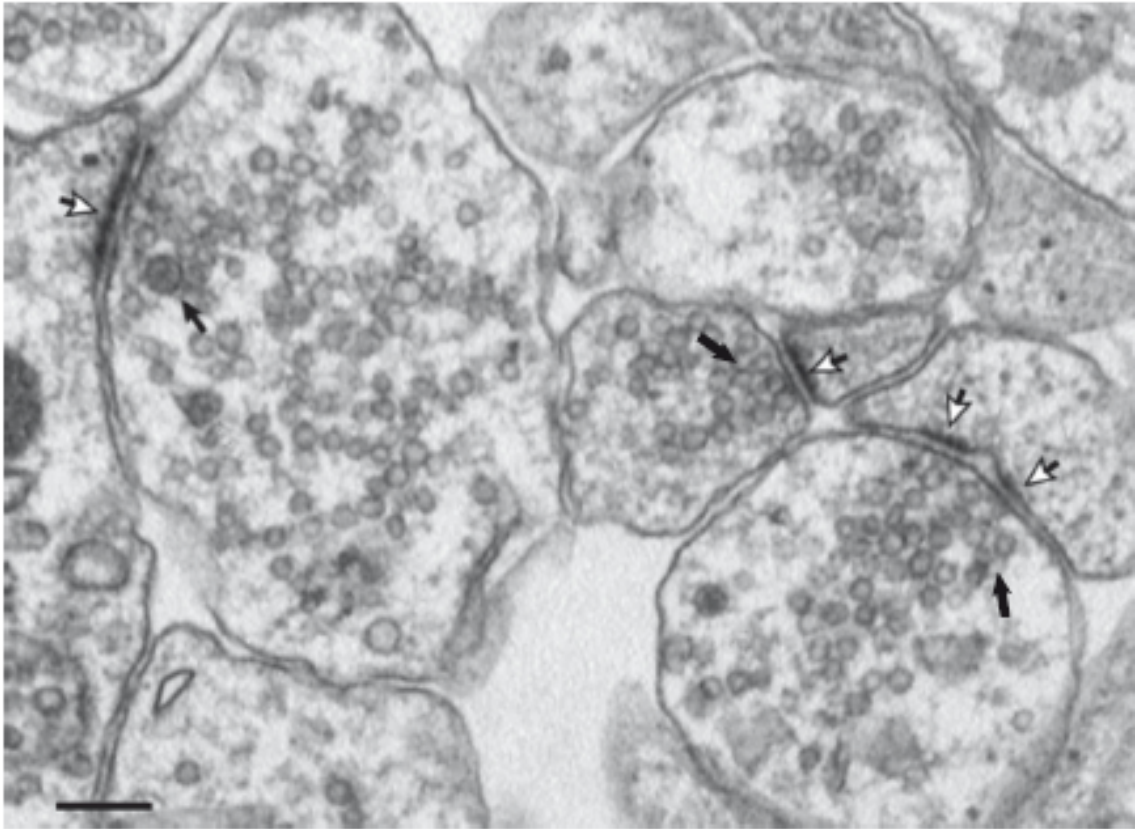


Fig. 1.1 Electron micrograph of a synapse

The electron micrograph shows synapses between cortical mouse neurons (C. Südhof and Starke, 2008). Black arrows point out the presynapse whereas white arrows mark postsynaptic densities, illustrating the asymmetric organization of the synapses.

1.1 The synaptic vesicle cycle

Presynaptic nerve terminals mediate the rapid fusion of synaptic vesicles (SVs) after calcium entry. When an action potential arrives in the bouton, presynaptic voltage gated calcium channels open, resulting in the influx of Ca^{2+} ions, thereby triggering synaptic vesicle fusion and subsequent neurotransmitter release.

Synaptic vesicles take part in fast and repeated rounds of release. For this purpose, the vesicles go through a trafficking cycle that can be divided into different steps (Fig. 1.2). Initially, neurotransmitters are actively transported into synaptic vesicles, which are subsequently targeted to a specialized area of the

presynaptic plasma membrane, the Active Zone (Südhof, 2004). After docking at the Active Zone, the vesicles become fusion competent in a multi-step maturation process, called priming. In response to an action potential and the influx of Ca^{2+} through voltage-gated calcium channels, the mature vesicles are able to fuse with the presynaptic plasma membrane to release the transmitters.

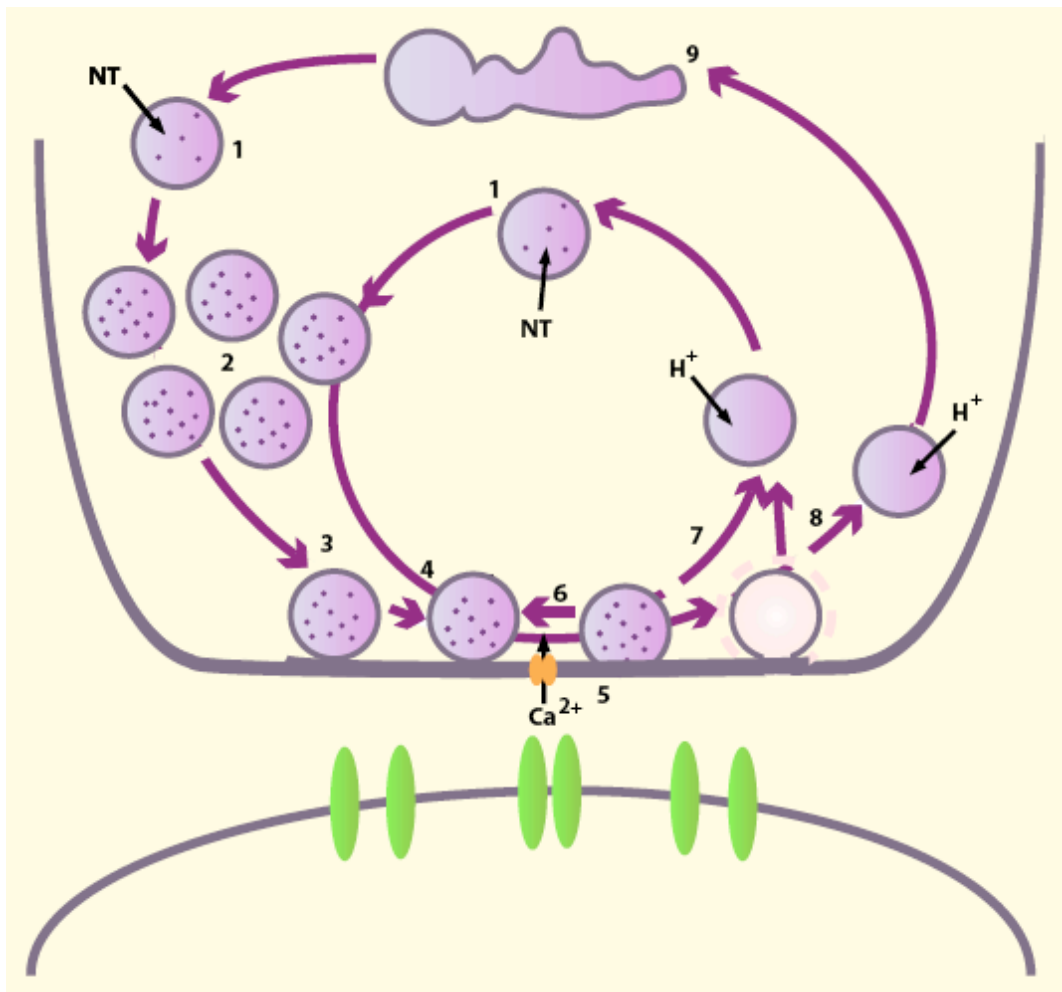


Fig. 1.2 The synaptic vesicle cycle

1. Neurotransmitter refilling; 2. SV clustering (Reserve Pool, RP); 3. Docking; 4. Priming (Readily Releasable Pool, RRP); 5. Fusion; 6. Kiss and stay; 7. Kiss and Run; 8. Endocytosis via clathrin coated pits; 9. Endosome (modified from Südhof, 2008a).

After exocytosis, synaptic vesicles are recycled and reused, via different endocytotic pathways: kiss-and-stay, vesicles are reacidified and refilled without undocking, remaining in the readily releasable pool (RRP); kiss-and-run,

vesicles undock and recycle locally to reacidify and refill with neurotransmitters; and endocytosis via clathrin coated pits, vesicular membrane and proteins of fully fused vesicles are taken up, reacidified and refilled with neurotransmitters either directly or by passing through the recycling endosome (Südhof, 2004).

1.2 *The presynaptic Active Zone*

The Active Zone is the compartment of the presynaptic plasma membrane where neurotransmitter release takes place (Dresbach *et al.*, 2001). The regulation of synaptic vesicle fusion is under a tight spatial and temporal control, requiring a close proximity of synaptic vesicles, voltage gated calcium channels and necessary regulatory proteins at the Active Zone (Siksou *et al.*, 2007).

The Active Zone protein network is composed of scaffolding proteins, fusion proteins, ion channels, signalling molecules and cell adhesion molecules (Schoch and Gundelfinger, 2006). Furthermore, microfilaments and associated proteins have been implicated in different steps of the SV cycle (Dresbach *et al.*, 2001). This orchestra of proteins is responsible for the function of the Active Zone. The organization and function of the cytomatrix at the Active Zone (CAZ) is crucial for determining the neurotransmitter release site during development, and its alignment to the postsynaptic densities (PSD). The CAZ is involved in organizing the neurotransmitter release machinery, the localization of presynaptic membrane proteins and in coupling synaptic vesicles to Ca²⁺ channels. Moreover, the components of the CAZ play a role in certain forms of presynaptic plasticity (Dresbach *et al.*, 2001; García-Junco-Clemente *et al.*, 2005; Schoch and Gundelfinger, 2006).

However, the molecular mechanisms underlying the organization and function of the CAZ are still not fully understood. In the last years numerous studies

have been performed trying to resolve the ultrastructural composition of the AZ, indicating that the structure of the cytomatrix depends on the type of synapse and the animal species under study (Zhai and Bellen, 2004).

Classical electron microscopy analyses of vertebrate synapses using tissue fixed with aldehydes have shown that presynaptic dense projections are organized into a hexagonal network, in which cone shaped particles alternate with small depressions (Fig. 1.3). A net of cytoskeletal filaments interconnects the electron-dense cone-shaped particles, and long filamentous strands project into the presynaptic bouton (Schoch and Gundelfinger, 2006). These projections are thought to represent the molecular guides that direct synaptic vesicles to their release sites, represented as slots. However, recent evidence indicates that the usage of aldehyde fixatives leads to an artificial aggregation of filaments (Fig. 1.3 A).

New techniques applying quick freezing without aldehydes to preserve the tissue for electron microscopy revealed short filaments connecting adjacent SVs and longer filaments projecting from the AZ membrane (Siksou *et al.*, 2007). A given vesicle is connected to 1.5 neighbouring ones. The synaptic morphology observed after high pressure freezing differs from that after aldehyde fixation. In the presynaptic terminal, synaptic vesicles are less densely distributed, connected via filaments and not anymore hexagonally organized (Fig. 1.3 B).

A more recent EM study performed in rat neocortex by conical electron tomography, showed the Active Zone to be constructed of a variable number of distinct "synaptic units" (Zampighi *et al.*, 2008). These entities include a polyhedral cage and seven surrounding vesicles. In addition, filaments of different lengths connect the vesicles. The short strands form a mesh between vesicles of the same "synaptic unit", whereas the long filaments connect different units. These synaptic ensembles let the vesicles dock at the Active

Zone (Fig. 1.3 C).

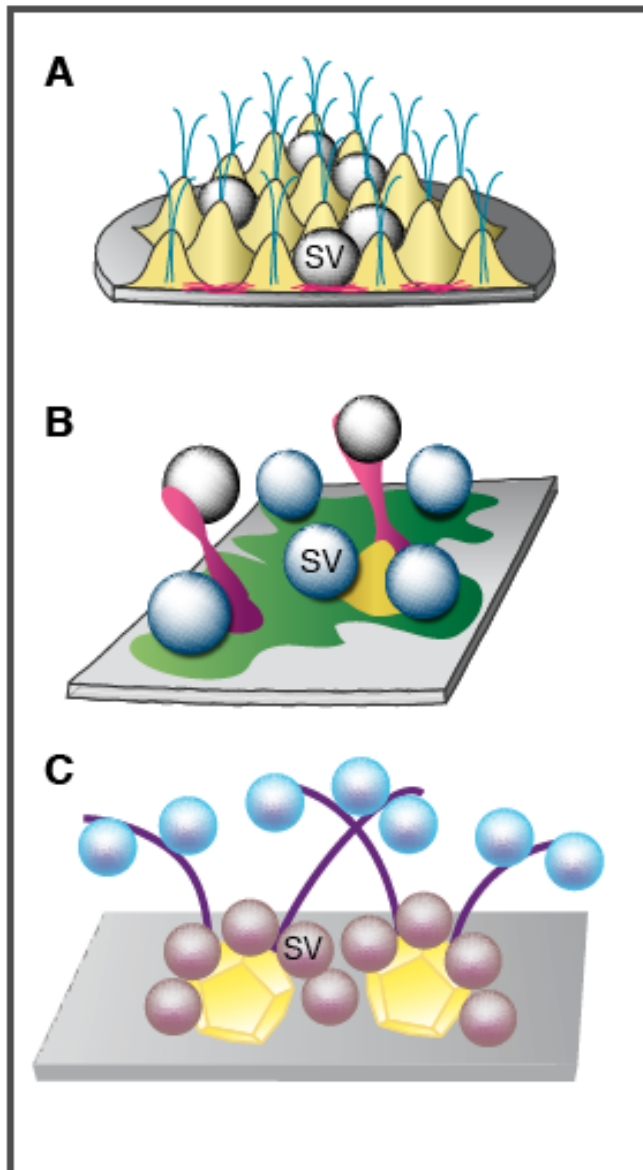


Fig. 1.3 Models of Active Zone ultrastructure

The ultrastructure of the presynaptic Active Zone observed by electron microscopy, differs depending on the method used for fixation of the tissue samples. **A** After aldehyde fixation, the Active Zone shows a highly organized ultrastructure composed of docked synaptic vesicles among cone-shaped particles and filaments reaching into the cytoplasm. **B** High pressure freezing results in a more asymmetric ultrastructure, with short filaments connecting synaptic vesicles with the plasma membrane and long strands linking diverse neurotransmitter vesicles. **C** Conical electron microscopy shows that the ultrastructure of the Active Zone consists of synaptic units. These units contain a hexagonal cage, a corona of vesicles and interconnecting filaments.

1.3 The molecular machinery mediating synaptic vesicle exocytosis at the AZ

Synaptic vesicle exocytosis shares many basic principles and homologous proteins with other membrane fusion processes in the cell e.g. SNARE proteins (soluble N-ethylmaleimide-sensitive factor attachment protein receptors), Munc18 or Rab3. In addition to this elementary machinery, synaptic vesicles

use a set of unique components to achieve the high temporal and spatial precision that distinguishes neurotransmitter release from other fusion processes (Sun *et al.*, 2003). At present, the precise composition of the CAZ is not entirely resolved, but five CAZ-enriched proteins, including RIMs, Munc13s, Bassoon, Piccolo/Aczonin, ELKS and Liprins, are thought to organize the molecular structure of the CAZ (García-Junco-Clemente *et al.*, 2005; Gundelfinger and tom Dieck, 2000; Rosenmund *et al.*, 2003; Schoch and Gundelfinger, 2006).

1.3.1 The core fusion machinery

All intracellular membrane fusion processes (excluding mitochondrial fusion) are thought to be mediated by a core fusion machinery composed of four families of proteins: SNARE-proteins, SM-proteins (for Sec1/Munc18-like proteins), Rab-proteins, and Rab-effectors (Südhof, 2008a). Synaptic transmission requires two conserved protein families that are universally involved in membrane fusion reactions: SNARE proteins and Sec1/Munc18-like proteins (SM proteins). They are essential for intracellular membrane fusion (Deák *et al.*, 2009a; Lang and Jahn, 2008; Malsam *et al.*, 2008; Rizo and Rosenmund, 2008). In recent years, tremendous progress has been made in elucidating the molecular composition and mechanism underlying the fusion process (Rickman and Duncan, 2009).

1.3.1.1 SNARES AND SNARE REGULATORS

SNAREs (soluble NSF-attachment protein receptors) represent a large family of proteins, characterized by a ~60-residue sequence known as the SNARE motif (Rizo and Südhof, 2002). In the synapse, Synaptobrevin-2 is located on synaptic vesicles (v-SNARE), whereas Syntaxin1 and SNAP-25 reside at the presynaptic plasma membrane (t-SNARE). An important step in the fusion of the synaptic vesicles is the SNARE complex, which is formed by four SNARE

motifs (two from SNAP25 and one each from Syntaxin1 and Synaptobrevin-2). Formation of the complex provides the necessary energy to pull synaptic vesicles and presynaptic membranes into close proximity, leading to fusion (Rizo and Rosenmund, 2008).

Analysis of knockout phenotypes in different species and the application of neurotoxins have shown that SNARE complex formation is essential for synaptic fast calcium-triggered exocytosis (Bronk *et al.*, 2007; Deák *et al.*, 2004; Sørensen *et al.*, 2002). Fine tuning of the fusion process is regulated by the specific features of the three proteins contributing to SNARE complex formation and their interaction to other proteins such as Complexin1 and Synaptotagmin1 (Malsam *et al.*, 2008). Docked synaptic vesicles at the Active Zone undergo a maturation process that leads, among other changes, to SNARE complex assembly. After priming, synaptic vesicles may undertake two different release pathways: asynchronous release, which is Synaptotagmin-1 and Complexin independent, and synchronous release in response to Ca^{2+} influx that depends on these proteins (Südhof, 2008a). Binding of Complexin to the SNARE complex stabilizes its assembly and avoids spontaneous fusion by inhibiting the transfer of energy generated by the complex formation to the synaptic plasma membranes (Maximov *et al.*, 2009). This intermediate state between synaptic vesicle priming and fusion with the synaptic plasma membrane has been named superpriming. It has been suggested that calcium binding to Synaptotagmin-1 induces the simultaneous interaction of Synaptotagmin1 with the SNARE complex and phospholipids of the presynaptic plasma membrane, inducing displacement of Complexin and subsequent synaptic vesicle fusion (Tang *et al.*, 2006). In contrast, other studies have proposed that Complexin and Synaptotagmin1 can bind simultaneously to the SNARE complex (Schaub *et al.*, 2006) and that Complexin not only prevents but also promotes synaptic vesicle fusion (Xue *et al.*, 2007; Yoon *et al.*, 2008), indicating that binding of

Complexin and Synaptotagmin-1 to the SNARE complex fine-tunes synaptic vesicle fusion (reviewed in Malsam *et al.*, 2008; Rizo and Rosenmund, 2008; Südhof and Rothman, 2009).

1.3.1.2 MUNC18

SM proteins are hydrophilic 60–70-kDa polypeptides with a high degree of homology throughout the whole sequence. The human genome contains seven Sec1/Munc18 proteins, three of which are involved in exocytotic processes, but not only in the brain. Munc18a (Munc18-1), Munc18b (Munc18-2), and Munc18c (Munc18-3) exhibit different expression patterns, with Munc18-1 exclusively being found in the brain (Rodkey *et al.*, 2008).

UNC-18 was the first identified SM protein, in *C. elegans* (Gengyo-Ando *et al.*, 1993). The mammalian homologue, Munc18-1 (also called nSec1 or RbSec1), a neuron-specific protein, was isolated by its ability to bind to Syntaxin1 (Hata *et al.*, 1993). Mutational studies on SM proteins have revealed a complete block of membrane fusion, indicating that intracellular membrane traffic requires an SM protein (Rizo and Südhof, 2002).

At mammalian synapses, deletion of Munc18-1 has severe consequences. Loss of Munc18-1 completely blocks synaptic activity, revealing a phenotype stronger than observed after deletion of the SNARE proteins synaptobrevin or SNAP-25 (Deák *et al.*, 2004; Schoch *et al.*, 2001; Verhage *et al.*, 2000; Washbourne *et al.*, 2002). KO mice show an absolute deficit in neurotransmitter release without changes in synaptic vesicle docking, suggesting a post-docking role for Munc18-1 (Verhage *et al.*, 2000). Mutant mice are completely paralyzed and die instantaneously after birth, probably because of a breathing deficit (Verhage *et al.*, 2000).

Recent studies suggest Munc18 to act at different exocytotic steps (Burgoyne *et al.*, 2009). Initially the Syntaxin1 interaction was thought to be only compatible

with the closed conformation of Syntaxin1, which is incompatible with SNARE complex formation (Misura *et al.*, 2000). However, new findings showed that Munc18-1 can also bind to a half-open conformation of Syntaxin1 (Zilly *et al.*, 2006) as well as to the assembled SNARE complex (Dulubova *et al.*, 2007). This last interaction is involved in organizing the formation of SNARE complexes (Deák *et al.*, 2009b; Dulubova *et al.*, 2007). In the current understanding Munc18-1, via different modes of interaction either with the SNARE protein Syntaxin1 or the assembled SNARE complex itself, acts at different stages of the fusion process. However, the underlying molecular mechanism and the relevance of these multiple binding modes still have to be resolved in detail (Burgoyne *et al.*, 2009).

1.3.1.3 **RAB3**

Rab proteins are members of the Ras superfamily of small GTPases, which play an important role in vesicular trafficking of different secretory processes (Grosshans *et al.*, 2006). In humans, there are at least 60 Rab proteins, of which Rab3 has been implicated in regulating exocytosis of neurotransmitters and hormones. The Rab3 family consists of four isoforms, Rab3A, B, C, and D, which are differentially expressed in neuronal and endocrine tissues. Rab3A is the most abundantly expressed isoform in brain. Like other Rab proteins, Rab3 cycles between a synaptic vesicle-associated GTP-bound form and a cytosolic GDP-bound form (Li and Chin, 2003).

Rab3 has been proposed to play an important role in regulating synaptic vesicle release. In *C. elegans* mutants, synaptic transmission is altered. Synaptic vesicles are able to cluster but show no tight binding to the Active Zone (Gracheva *et al.*, 2008; Nonet *et al.*, 1997). However, in mice deficient for Rab3A no major phenotype has been observed. Deletion of Rab3A does not affect synaptic transmission, but Rab3A is necessary for mossy fiber long-term

potentiation (Castillo *et al.*, 1997). Rab3 is not essential for synaptic membrane trafficking, docking and priming of SVs, but is able to modulate the basic release machinery. Ablation of all Rab3 isoforms showed that Rab3 is required for survival in mice and that the four isoforms are functionally redundant (Schlüter *et al.*, 2004).

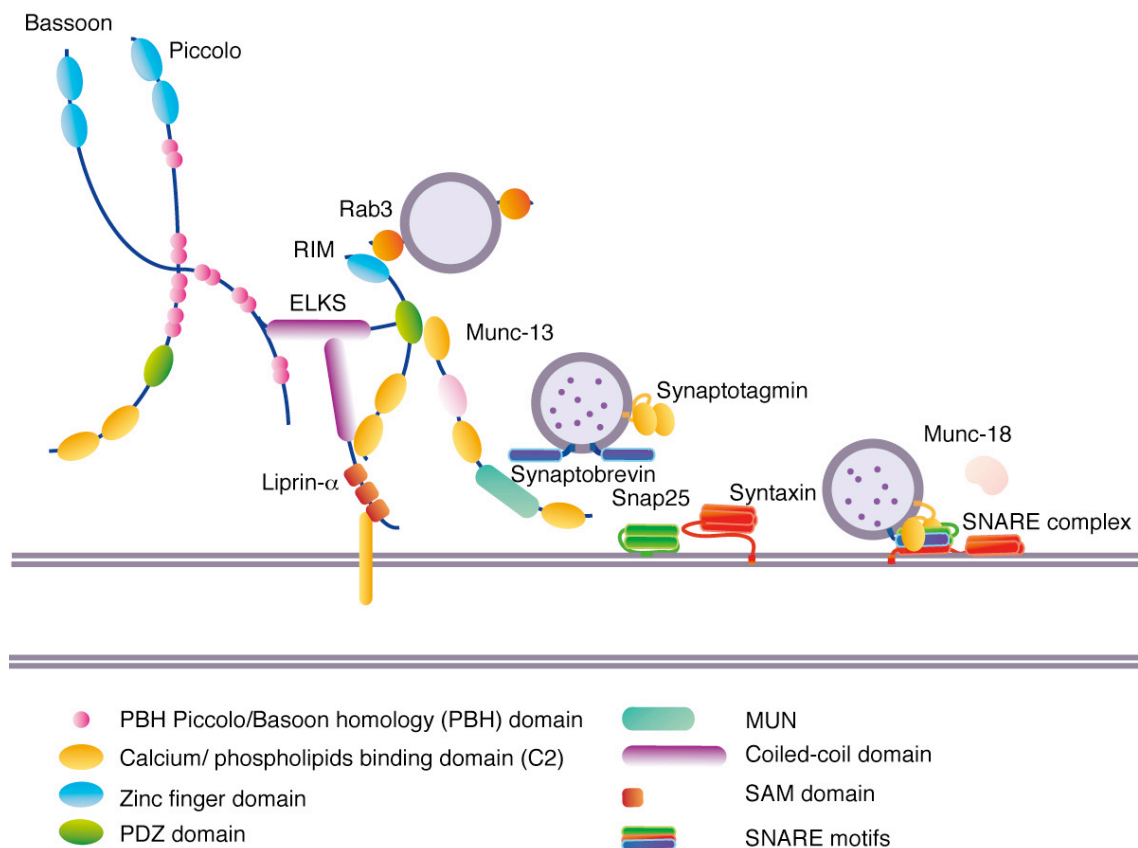


Fig. 1.4 Components of the “core machinery” for synaptic vesicle fusion and of the “cytomatrix at the Active Zone”

Cartoon showing the structure and interactions of the main proteins implicated in synaptic vesicle fusion and specific Active Zone enriched proteins (Ziv and Garner, 2004).

1.3.2 Active Zone enriched proteins

Synaptic vesicle fusion only takes place at highly specialized regions of the presynaptic membrane, called Active Zones. The protein network at the Active Zone is composed of AZ-specific and various other proteins, participating

together in multiple steps of the synaptic vesicle cycle. To date, five families of Active Zone enriched proteins have been identified: Piccolo/Bassoon, ELKS, Munc13, Liprins- α and RIMs (reviewed in Schoch and Gundelfinger, 2006).

1.3.2.1 BASSOON AND PICCOLO/AZCONIN

Piccolo and Bassoon are the two largest CAZ enriched proteins. Structurally, both proteins consist of two Zn²⁺ finger domains and three coiled coil (CC) domains. Piccolo but not Bassoon also contains a PDZ domain and two C2-domains (C2A and C2B) in its C-terminal region (Fenster *et al.*, 2000; tom Dieck *et al.*, 1998).

Interestingly, whereas other Active Zone enriched proteins like RIMs and Munc13 are expressed in both *C. elegans* and *Drosophila* (Brose *et al.*, 1995; Wang *et al.*, 1997), homologs of Bassoon and Piccolo appear to be specific for vertebrates (Altrock *et al.*, 2003).

The functions of the two largest CAZ proteins have been difficult to characterize because of their enormous sizes (> 400 kDa). Both are expressed very early during neuronal development and are among the first proteins to arrive at newly forming synapses (Leal-Ortiz *et al.*, 2008). After a first axo-dendritic contact, Active Zones are able to assemble within a few minutes. Considering this short period of time, it has been postulated that there might be preassembled Active Zone precursor vesicles in the soma, which are axonally transported and fuse with the presynaptic membrane to form a new presynaptic bouton (Goldstein *et al.*, 2008). PTVs constitute one of the mechanisms responsible for the delivery of proteins such as Munc13 and RIMs to the Active Zone (Zhai *et al.*, 2001), but not for synaptic vesicles proteins (Ziv and Garner, 2004). Furthermore, both proteins play a role in the regulation of synaptic transmission in excitatory as well as in inhibitory synapses.

To date no mouse deficient for Piccolo has been reported and the Bassoon KO

is not completely genetically deleted. Because the central region of Bassoon has been shown to be sufficient for presynaptic targeting of the protein and its association to the CAZ (Dresbach *et al.*, 2003), deletion of the central region (between 1692 – 3263aa) of Bassoon was used to create a knockout (KO) mouse. However, this mouse still expresses a truncated protein. Phenotypically, Bassoon *-/-* mutant mice develop spontaneous epileptic seizures (Altrock *et al.*, 2003). Structurally, mutant hippocampal synapses exhibit a normal ultrastructure (Altrock *et al.*, 2003), while in the retina, lack of Bassoon disturbs the formation of functional ribbons, special retinal CAZ-structures at the Active Zone. Synaptic ribbons are not able to attach to the presynaptic membrane and remain floating in the cytoplasm (tom Dieck *et al.*, 2005). Electrophysiological analyses of Bassoon KOs in acute slices and autaptic cultures showed a reduction in synaptic transmission due to an increase in the number of silent synapses, and not because of changes in the transmission properties of the remaining active synapse (Altrock *et al.*, 2003).

So far, the effects of an ablation of Piccolo have only been studied via a knockdown approach in primary neuronal cultures. The result of that study did not reveal a role of Piccolo in synapse formation. However, Piccolo negatively regulates SV exocytosis via modulation of Synapsin1 dynamics (Leal-Ortiz *et al.*, 2008). This function was specific and not shared by Bassoon, indicating that Piccolo has a distinctive role in the recruitment of SVs from the reserve pool to the Active Zone (Leal-Ortiz *et al.*, 2008).

Noteworthy, Piccolo like other CAZ proteins can be regulated by alternative splicing. The C2A-domain of Piccolo binds calcium ions with low affinity but high specificity. Alternative splicing removes 9 amino acids leading to an increase in the calcium affinity and impedes C2 domain dimerization (Garcia *et al.*, 2004).

In accordance with their large size and multi-domain structure, multiple interacting proteins have been identified for Bassoon and Piccolo. Both proteins

interact with ELKS via their third CC domain (Takao-Rikitsu *et al.*, 2004) and with two members of the C-terminal binding protein family, CtBP1 and CtBP2 (tom Dieck *et al.*, 2005). In addition, Piccolo is able to interact with multiple proteins such as GIT1 (Kim *et al.*, 2003), Abp1 (Fenster *et al.*, 2003), profilin, and PRA-1 (Fenster *et al.*, 2000), implicated in actin-binding and endocytosis.

1.3.2.2 ELKS/ERC/CAST

ELKS proteins, whose name derives from their high content in the amino acids glutamate (E), leucine (L), lysine (K), and serine (S), are the most recently identified proteins to be enriched at the Active Zone (reviewed in Schoch and Gundelfinger, 2006). They were discovered by two independent approaches, a mass spectrometry analysis of rat synaptosomes (Ohtsuka *et al.*, 2002) and in a yeast-two hybrid screen as binding partner for the RIM1 PDZ domain (Wang *et al.*, 2002). This family of proteins, previously known as ERC and CAST (CAZ-associated structural protein), is composed of four coiled-coil domains and a putative COOH-terminal consensus motif for binding to PDZ domains.

Mammals contain two ELKS genes, ELKS1 and ELKS2. Interestingly, alternative splicing of the ELKS1 C-terminus produces two isoforms, ELKS1 α and ELKS1 β , with specific tissue distributions and biochemical properties (Wang *et al.*, 2002). Whereas ELKS1 α is exclusively synthesized outside of the brain, ELKS1 β is brain specific, and can be found in two different forms, insoluble and synaptically localized, or soluble and cytoplasmically distributed (Wang *et al.*, 2002). Recent studies have revealed that the ELKS2 gene encodes for several proteins. ELKS2 α , previously named ELKS2, is a brain specific insoluble protein, which becomes detectable only after other synaptic proteins are synthesized (around embryonic day 14.5) (Wang *et al.*, 2002). ELKS2 β , produced by an internal promoter in the ELKS2 gene, is weakly expressed during postnatal development and becomes undetectable on day 20.

In addition, ELKS2 can be alternatively spliced, leading to two different variants, the full length protein ELKS2B and a protein lacking the C-terminal RIM binding sequence, ELKS2A (Kaeser *et al.*, 2009). In summary, the ELKS2 gene encodes four main proteins ELKS2 α A, ELKS2 α B, ELKS2 β A and ELKS2 β B, with ELKS2 α B being the main isoform.

ELKS interacts through its coiled coil domain with RIM1, Liprin- α , Bassoon and Piccolo. The binding of ELKS and RIM1 is extremely specific, the last three amino acids [IWA] of ELKS are essential for its binding. In addition, the central region of ELKS directly binds Bassoon at the region containing the third coiled-coil domain. Binding of Bassoon and Piccolo to ELKS is competitive, suggesting that distinct complexes, Bassoon-ELKS-RIM1-Munc13-1 and Piccolo-ELKS-RIM1-Munc13-1, may exist at synapses (Takao-Rikitsu *et al.*, 2004). Binding of ELKS is necessary, at least in part, for the localization of RIM1 at the Active Zone (Ohtsuka *et al.*, 2002). Nevertheless, deletion of ELKS in *C. elegans* does not modify RIM localization, and does not result in changes of synaptic activity, indicating that ELKS proteins are not essential for Active Zone ultrastructure and neurotransmitter release in the worm (Deken *et al.*, 2005). Interestingly, deletion of Bruchpilot (BRP), an ELKS related protein recently discovered in *Drosophila*, reveals a strong phenotype (Wagh *et al.*, 2006). BRP contains a N-terminus with a high homology to ELKS and a C-terminus including several coiled-coil domains, but lacks the RIM-PDZ interaction motif present in ELKS. Flies lacking BRP show a loss of T-bars (electron dense projections) in the Active Zone and defective calcium channel clustering. In addition, evoked synaptic transmission is reduced at the NMJ (Wagh *et al.*, 2006). These data, in contradiction to the results obtained in *C. elegans*, indicate that BRP is necessary for Active Zone ultrastructure maintenance and neurotransmission in the fly.

Recent studies analyzing the function of ELKS in mutant mice have shown that deletion of ELKS1 is lethal, whereas ELKS2 ablation does not impair survival (Kaeser *et al.*, 2009). Electrophysiological analyses of the ELKS2 KO showed that ELKS2 controls synaptic transmission in inhibitory but not in excitatory neurons (Kaeser *et al.*, 2009). Deletion of ELKS2 induces an increase in neurotransmitter release in inhibitory synapses due to an enlargement of the RRP. Interestingly, no significant ultrastructural changes were detected in neurons lacking ELKS2, indicating that ELKS are not essential for a correct formation of the Active Zone in mammals (Kaeser *et al.*, 2009).

1.3.2.3 LIPRIN-ALPHA

Even though Liprin- α proteins are not restricted to the presynaptic boutons, data from invertebrates indicates that they play an important role in the formation and maintenance of Active Zones (Dai *et al.*, 2006; Kaufmann *et al.*, 2002; Zhen and Jin, 1999). Liprins- α are highly evolutionarily conserved scaffolding proteins (Zürner and Schoch, 2008). They were first characterized by their ability to bind to the cytoplasmic domains of the Leukocyte common antigen-related family of receptor protein tyrosine phosphatases (LAR) (Serra-Pagès *et al.*, 1998). Structurally, Liprins- α have an N-terminal coiled-coil domain that acts as a dimerization domain and a C-terminal Liprin homology (LH) domain, composed of three sterile alpha motifs (SAMs), that interacts with LAR and other proteins (Stryker and Johnson, 2007). In contrast to invertebrates, where only one Liprin gene can be detected, vertebrates express four Liprin- α (1-4) proteins. Liprin- α 2 and Liprin- α 3 are expressed exclusively in mammalian brain, while Liprin- α 1 and Liprin- α 4 are also found in non-neuronal tissues (Serra-Pagès *et al.*, 1998). So far, various pre- and postsynaptically localized interaction partners of Liprins- α have been identified: CASK (Olsen *et al.*, 2005), the motor protein KIF1 α (Shin *et al.*, 2003), the scaffolding protein GRIP1 (Ko *et al.*, 2003a;

Wyszynski *et al.*, 2002), GIT1 (Kim *et al.*, 2003), RIM1 α (Schoch *et al.*, 2002), ELKS (Dai *et al.*, 2006) and indirectly Piccolo (Kim *et al.*, 2003). Binding of Liprins- α to GRIP and GIT1 has been shown to be necessary for the proper transport of AMPA receptors (Ko *et al.*, 2003a), whereas binding to KIF1 is important for the axonal transport of some presynaptic proteins, as shown in *C. elegans* and *Drosophila* KOs (Miller *et al.*, 2005; Shin *et al.*, 2003).

In *C. elegans*, loss of Syd2/Liprin results in a decrease in the levels of Synaptobrevin, Synaptotagmin, Syntaxin and Rab3 proteins at the presynapse, and an increase in axonal localization, indicating that they are not properly transported (Zhen and Jin, 1999). In addition, *C. elegans* and *Drosophila* mutants show defects in the organization and an abnormal size of the Active Zone (Kaufmann *et al.*, 2002; Zhen and Jin, 1999).

In summary, based on evidence mainly obtained from analyses in invertebrates, Liprins- α have been associated with presynaptic maturation, axonal targeting, vesicular trafficking of other synaptic proteins, spine formation and sustenance, as well as Active Zone organization and structure maintenance (reviewed in Schoch and Gundelfinger, 2006; Spangler and Hoogenraad, 2007). However, to date there is still rather incomplete information available about their function in vertebrates.

1.3.2.4 MUNC13

The first data about the Munc13 protein family came from a screen for uncoordinated movements in *C. elegans*, in which UNC-13 was one of the first proteins discovered to be implicated in synaptic transmission (Ahmed *et al.*, 1992; Maruyama and Brenner, 1991).

Whereas invertebrates possess only one Munc13 gene, mammals contain four different genes (Kohn *et al.*, 2000). The mammalian Munc13 family consists of four different large proteins: Munc13-1, Munc13-2, Munc13-3 and Munc13-4

(Koch *et al.*, 2000). In addition, the Munc13-2 gene generates two splice variants with diverging N-termini and different localization, bMunc13-2 (brain specific) and ubMunc13-2 (ubiquitously expressed) (Betz *et al.*, 2001).

Munc13 proteins are highly homologous molecules containing conserved C terminal C₁ and C₂ domains, a central Munc homology domain (MUN) and an N-terminal domain that differs among all members. Munc13-1, -3 and bMunc13-2 proteins are brain specific, whereas the ubMunc13-2 isoform and Munc13-4 are also found outside the central nervous system, where they seem to play a role in fusion processes (Koch *et al.*, 2000) (Higashio *et al.*, 2008).

Munc13-1 is an Active Zone specific protein with an essential role in neurotransmission. Loss of Munc13-1 in mice leads to death in the first hours of life (Augustin *et al.*, 1999b). Several studies in *Drosophila*, *C. elegans* and mice, have shown that Munc13 is indispensable for synaptic vesicle priming and therefore the establishment of the readily releasable pool. Neurons lacking Munc13-1 are able to dock but they do not become fusion competent (Augustin *et al.*, 1999b; Varoqueaux *et al.*, 2002). Morphologically, Munc13-1 knockout neurons form ultrastructurally normal synapses. The number of docked vesicles remains unchanged, but they are not capable to fuse because of their immature state (Betz *et al.*, 1998). However, recent electron microscopy experiments, after high-pressure freeze fixation in *C. elegans*, have revealed a decrease in the number of synaptic vesicles in close proximity to the electron dense filaments at the presynaptic plasma membrane, indicating a connection between synaptic vesicle localization and the maturation processes (Gracheva *et al.*, 2008; Weimer *et al.*, 2006). The defects in synaptic vesicle priming in neurons lacking Munc13 have been linked to its interaction with Syntaxin. Munc13 has been postulated to bring Syntaxin to its open conformation, since overexpression of a constitutively open conformation of Syntaxin rescues the UNC-13 phenotype in *C. elegans* (Richmond *et al.*, 2001). However, NMR

analyses have not been able to detect a direct interaction between Munc13 and Syntaxin (Basu *et al.*, 2005).

The key role of Munc13 in synaptic transmission is demonstrated by the complete loss of spontaneous and evoked synaptic activity in mice lacking both, Munc13-1 and -2 (Varoqueaux *et al.*, 2002). In addition to the priming function, Munc13 plays an important role in presynaptic plasticity. Neurons lacking Munc13-1 show short-term depression after high frequency stimuli (Rosenmund *et al.*, 2002). Interestingly, this phenotype is restricted to a subpopulation of neurons using Munc13-1 as priming factor, while Munc13-2 dependent synapses, show short term facilitation (Koch *et al.*, 2000; Rosenmund *et al.*, 2002).

Each Munc13 domain has been related to a different function of the protein. The Munc13 C-terminus domain has been found to be indispensable for its priming activity, whereas the N-terminus contains modulatory domains like the phorbol ester/diacylglycerol (DAG) binding C1 domain (Rhee *et al.*, 2002). Activation of Munc13-1 by phorbol esters leads to enhancement of neurotransmitter release (Betz *et al.*, 1998). In addition Munc13-1 binds to DOC 2 α (Orita *et al.*, 1997) via the C-terminus and RIM1 α (Betz *et al.*, 1997) and Calmodulin (Junge *et al.*, 2004) through its N-terminus.

In summary, Munc13 play an essential role in synaptic vesicle priming, leading Syntaxin1 to the conformational change necessary for SNARE complex assembly and therefore making synaptic vesicles competent to fuse with the synaptic plasma membrane.

1.3.2.5 RIM

See RIMs: main components of the scaffolding at the presynaptic Active Zone (1.4).

1.4 RIMs: main components of the scaffolding at the presynaptic Active Zone

1.4.1 Genomic sequence organization: splice variants and structure

RIMs are central components of the presynaptic cytomatrix at the Active Zone. They are multidomain proteins, first discovered in a yeast two-hybrid screen as an effector of the synaptic vesicle protein Rab3 (Wang *et al.*, 1997). In contrast to invertebrates, where (UNC-10) is the only RIM family member known, in vertebrates the RIM protein family is composed of 7 members (RIM1 α , 1 β , 2 α , 2 β , 2 γ , 3 γ and 4 γ) encoded by four different genes (RIM1-4) (Wang and Südhof, 2003). RIM1 α was the first member of the RIM family to be discovered and up to now has been studied in most detail. Due to the presence of three internal promoters, the RIM2 gene generates three independent transcripts (2 α , 2 β , 2 γ). Recently, a second promoter was discovered in the RIM1 gene as well, resulting in two transcripts, RIM1 α and the newly discovered RIM1 β (Kaesler *et al.*, 2008a). RIM1 and RIM2 are widely spliced at three canonical positions, splice sites A, B and C respectively (Wang and Südhof, 2003). The positions of the splice sites are conserved between the RIM1 and RIM2 genes. Splice site A is located in the Zinc finger domain (Wang and Südhof, 2003). Alternative splicing of this site can result in the disruption of the Rab3 binding domain. Splice site B is located between the C2A domain and the proline rich RIM-BP binding region, and splice site C is situated between the RIM-BP interaction sequence and the C2B domain. In contrast, the RIM3 γ and RIM4 γ genes are not spliced (Wang and Südhof, 2003). Splice site B at the RIM1 gene contains six exons that can be independently spliced, potentially generating 64 different splice variants. In contrast, exons 26-28 at the RIM1 splice site C can only be

spliced in or out as a unit in order to avoid a reading frame disruption (Wang and Südhof, 2003).

So far, only little is known about the expression of the potential splice variants of RIM1 α and RIM2 α , and the role of alternative splicing on RIM function has not been addressed yet.

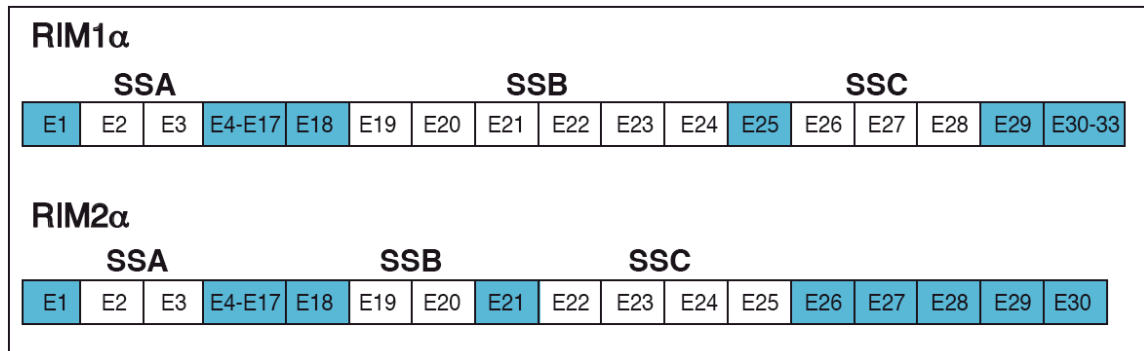


Fig. 1.5 Alternatively spliced exons in RIM1 α and RIM2 α .

Splice sites A, B and C are conserved in RIM1 and RIM2 in vertebrates. Splice site A (SSA) consist of exons 2 and 3. Alternative splicing at SSA disrupts Rab3 binding to α -RIMs. In mammals, the RIM1 genes contains six variable exons for splice site B (SSB) that can be spliced independently, resulting in 64 potential exon combinations. Splice site C (SSC) is relatively homologous between RIM1 and RIM2 (61% identity) and must be spliced as a block to avoid disruption of the reading frame. Alternatively spliced exons are shown in white, and constitutive exons in blue.

1.4.2 Protein structure and functional domains

RIM1 α , the prototypical member of the RIM family, is a multidomain protein. However, not all RIM isoforms contain the whole set of domains (Schoch and Gundelfinger, 2006; Wang *et al.*, 2002). The alpha-isoforms, RIM1 α and RIM2 α are composed of an amino-terminal zinc-finger motif, a PDZ domain and two carboxy-terminal C₂ domains (C2A and C2B). RIM2 β lacks the whole zinc finger domain, whereas in RIM1 β only the N-terminal Rab3-binding sequence of RIM1 α is absent (Kaeser *et al.*, 2008a). In contrast, the gamma isoforms contain only the C2B domain after a short isoform-specific N-terminal sequence

(Wang and Südhof, 2003).

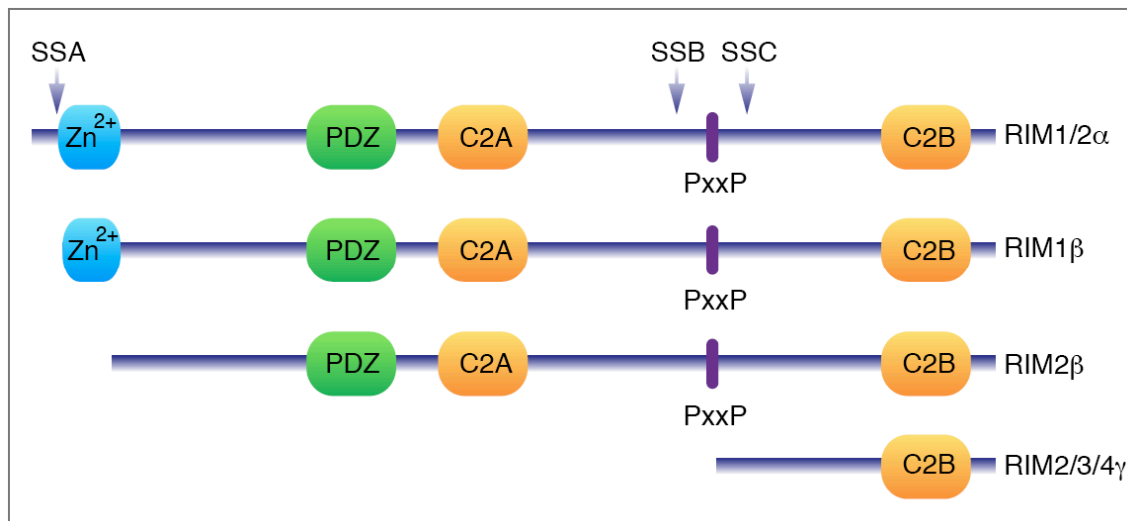


Fig. 1.6 Domain structure of the RIM protein family

The α -RIM isoforms contain the complete set of domains and binding motifs, whereas the other members of the family lack some of them; RIM2 β does not contain the zinc finger domain, and in RIM1 β only the Rab3 binding motif is absent. The γ -isoforms, in contrast, comprise only the C2B domain and isoform-specific N-termini. Abbreviations: Zn²⁺ zinc finger domain; PxxP proline rich domain; SS splice site.

In recent years tremendous progress has been made in elucidating the three-dimensional structure and function of the RIM domains in order to gain further insight into their physiological relevance.

N-Terminal Zinc Finger Domain. The N-terminal region includes two domains that mediate two binding activities: an α -helical Rab3-binding region and a Munc13-binding zinc-finger domain (Wang *et al.*, 2001). Through the simultaneous binding of Munc13 and Rab3 to the RIM N-Terminal domain, these proteins constitute a tripartite protein complex (Dulubova *et al.*, 2005).

Charged domain. The N-terminal zinc-finger domain of RIM is followed by a highly charged sequence containing phosphorylation consensus sequences for Ca²⁺/calmodulin-dependent protein kinases and protein kinase A (PKA). A first analysis of RIM1/2 phosphorylation suggested that phosphorylation of residues ser-241 and ser-287 of RIM1 α and ser-335 of RIM2 α , enables α -RIMs to bind

the adaptor protein 14-3-3 (Sun *et al.*, 2003). Subsequent investigations have shown that RIM1 α is phosphorylated at Ser-413 by protein kinase A, and that this phosphorylation also permits the interaction between RIM1 α and 14-3-3 (Lonart *et al.*, 2003).

PDZ domain. α/β -RIMs also contain a PDZ domain that binds ELKS C-terminal residues (GIWA) with an unusual specificity. Any change in these four amino acids disrupts the interaction between RIMs and ELKS. In addition, the Active Zone protein Piccolo, which also interacts with ELKS through its PDZ domain, does not bind this C-terminal sequence, corroborating the specificity of interaction between RIMS and ELKS (Lu *et al.*, 2005). The RIM1 PDZ is not important for the localization and function of RIM at the *C. elegans* Active Zone (Deken *et al.*, 2005).

C2-domain. α/β -RIMs contain two degenerated C2 domains, C2A and C2B, which are separated by alternatively spliced sequences. In contrast, γ -RIMs only consist of an isoform specific N-terminal and a C2B domain (Wang *et al.*, 1997). The RIM C2 domains are atypical because they do not contain the consensus calcium binding sites that have been defined in the Synaptotagmin C2 domains and that are present in the Rabphilin C2 domains. In addition, they have been shown not to bind to phospholipids (Wang *et al.*, 2000). The structure of both RIM C2 domains has been well defined using crystallography and NMR spectroscopy studies (Dai *et al.*, 2005; Guan *et al.*, 2007).

The RIM C2A domain was shown to bind *in vitro* to the SNARE protein SNAP-25, and the calcium sensor Synaptotagmin1 (Coppola *et al.*, 2001). However, a subsequent study that reported the crystal structure of the RIM2 C2A domain, did not detect a significant binding affinity to these proteins (Dai *et al.*, 2005). Interestingly, the RIM C2A domain possesses a highly positively charged surface, a single mutation of an arginine in this domain has been linked to the autosomal dominant cone-rod dystrophy (CORD7) (Barragan *et al.*, 2005; Johnson *et al.*,

2003; Michaelides *et al.*, 2005).

The RIM C2B domain is present in all members of the RIM protein family (Wang and Südhof, 2003). In addition, RIM C2B domains have been shown to bind to several proteins, suggesting that they might play an important role in the function and localization of all members of the RIM protein family. The RIM C2B domain has been shown to interact with Liprins- α (Schoch *et al.*, 2002), with Synaptotagmin1 (Coppola *et al.*, 2001; Schoch *et al.*, 2002), the ubiquitin ligase SCRAPPER (Khanna *et al.*, 2006; Yao *et al.*, 2007) and calcium channels (Khanna *et al.*, 2006; Kiyonaka *et al.*, 2007). However, crystallography and NMR studies of the C2B domain, could not verify neither a direct interaction between RIM and Synaptotagmin1, nor binding between the minimal RIM binding domain of Liprin- α and the isolated C2B domain (Guan *et al.*, 2007). In addition, a crystal structure analysis revealed dimerization of the C2B domains, which might play an important role in RIM function. Moreover, C2B domains require adjacent N-and C-terminal sequence for an adequate folding, suggesting that they might be also mandatory for the interaction to other proteins (Guan *et al.*, 2007).

Proline rich SH3 interaction motif. A proline rich sequence can be found between the two C2 domains. This conserved region is the binding site for the RIM binding proteins (RIM-BPs). Interestingly, the RIM-BP binding motif is located between the alternative splice sites B and C (Wang *et al.*, 2000). The interaction between RIMs and RIM-BPs takes place via the second of three Src-homology 3 domains (SH3) of RIM-BPs. This binding has been postulated to function as link between RIM proteins and calcium channels (Hibino *et al.*, 2002).

1.4.3 Interaction partners

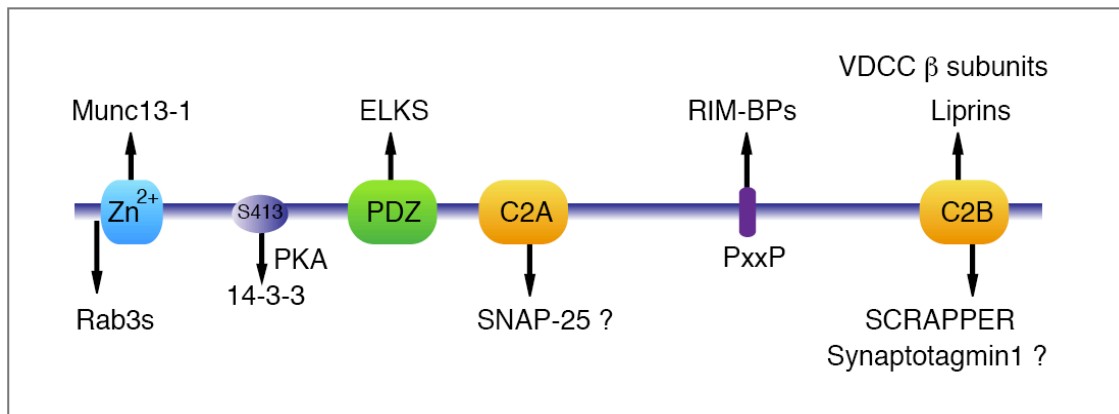


Fig. 1.7 Interacting molecules of α -RIMs

This cartoon depicts the domain structure of α -RIMs and the site of interaction for the known binding partners.

In the last years various binding partners have been identified for the different RIM domains.

1.4.3.1 PROTEINS INTERACTING WITH THE N-TERMINAL ZINC FINGER DOMAIN

RAB3 is a small GTPase attached to the synaptic vesicle membrane (Fischer von Mollard *et al.*, 1990). RIM1 was originally identified as an effector for the GTP-bound form of Rab3 (Wang *et al.*, 1997). This interaction is dependent on GTP and is mediated by two sequences in RIM, the helix- α 1 and the SGAWFY sequence at the end of helix- α 2 (Wang *et al.*, 2001). Through this interaction α -RIMs could form a linker between synaptic vesicles and the Active Zone plasma membrane. The binding between Rab3 and RIM1 α , but not RIM2 α , is potentially modulated by alternative splicing of the RIM splice site A (Fukuda, 2004).

MUNC13 binding to α -RIMs takes place through the interaction between the RIM zinc finger domain and the N-terminal C2 domain of Munc13. Disruption of this association impedes synaptic vesicle maturation, causing a loss of fusion competence and a reduction in the readily releasable pool (Betz *et al.*, 2001).

The RIM1 α zinc finger interacts with the C2A domain of Munc13, competing with Munc13 homodimerization. This switch between homo- and heterodimerization of the Munc13-RIM interaction might play a role in the regulation of synaptic vesicle priming (Dulubova *et al.*, 2005).

As both, Rab3 and Munc13 bind to the zinc finger domain, it was initially postulated that the interactions of these proteins with RIM1 α were mutually exclusive (Betz *et al.*, 2001). However, further NMR Spectroscopy and X-ray crystallography studies of the RIM2 α zinc finger domain have shown that although Munc13-1 binding weakly alters the RIM2 α /Rab3a interaction, Rab3a and Munc13-1 bind to different regions, allowing for the formation of a tripartite Rab3A/ α -RIM/Munc13-1 complex. This complex is involved in priming of synaptic vesicles and potentially in synaptic plasticity response adaptation (Dulubova *et al.*, 2005).

1.4.3.2 PROTEINS INTERACTING WITH THE CHARGED DOMAIN

PKA directly phosphorylates RIM1 α at two sites, Ser413 and Ser1458 (Lonart *et al.*, 2003). In culture, it has been shown that phosphorylation at Ser413 is required for the induction of LTP at the cerebellar parallel fiber synapse. However, recent studies using a knock-in mouse carrying the mutation S413A, suggest that phosphorylation of RIM1 α at Ser413 is not necessary for presynaptic LTP, learning and memory (Kaesler *et al.*, 2008b).

14-3-3 are ubiquitous phosphoserine-binding proteins, that play a role in synaptic transmission. Phosphorylated RIM can interact with 14-3-3 adapter proteins at different sites (Simsek-Duran *et al.*, 2004; Sun *et al.*, 2003). Interaction between RIM1 and 14-3-3, through the phosphorylated Ser413, has been related to presynaptic LTP (Simsek-Duran *et al.*, 2004). However, recent

experiments have shown that disruption of this interaction does not impair LTP (Kaeser *et al.*, 2008b).

cAMP-GEFII. RIM2 was found to interact with cAMP-GEFII, a cAMP sensor. This interaction mediates cAMP-induced calcium-dependent secretion, in a PKA independent manner, in pancreatic β -cells (Kashima *et al.*, 2001; Ozaki *et al.*, 2000).

1.4.3.3 PROTEINS INTERACTING WITH THE PDZ DOMAIN

The **ELKS** interaction to the RIM PDZ domain was suggested to be, at least in part, responsible for the synaptic localization of RIM1 (Ohtsuka *et al.*, 2002; Wang *et al.*, 2002). However, deletion of ELKS in *C. elegans* does not alter the localization of RIM1, indicating that ELKS are not necessary for RIM localization (Deken *et al.*, 2005). Interestingly, ELKS2 KO mice showed a significant increase in RIM1 α solubility (Kaeser *et al.*, 2009), consistent with an increase of ELKS soluble fraction in RIM1 α/β DKO (Kaeser *et al.*, 2008a), suggesting that the interaction between RIM1 α and ELKS2 is important for the integration (cross-linking) of these proteins at the Active Zone.

1.4.3.4 PROTEINS INTERACTING WITH THE C2 DOMAINS

SNAP-25 binding to RIMs was shown to take place through the RIM C2A domain in a calcium-dependent manner *in vitro*. This interaction would directly link RIM to SNARE complex, and thereby to the core fusion machinery (Coppola *et al.*, 2001). However, crystallography and NMR studies did not find evidence for a significant binding affinity between SNAP-25 and the RIM C2A domain (Dai *et al.*, 2005).

PICCOLO. Direct interaction between Piccolo and RIM2 has only been described in β -pancreatic cells. Piccolo dimerization through its C2A domain

switches from homodimer to a RIM2-piccolo heterodimer form in a calcium dependent manner (Shibasaki *et al.*, 2004)

SYNAPTOTAGMIN 1 was shown to bind to the RIM1 α C2A and C2B domains *in vitro*. Pull-down experiments revealed an association between RIMs and Synaptotagmin1, and Calcium binding studies furthermore showed a calcium dependent coupling of the RIM C2B domain with the synaptic vesicle protein Synaptotagmin1 (Coppola *et al.*, 2001; Schoch *et al.*, 2002). However, after crystallography studies, no significant affinity between both proteins could be found (Dai *et al.*, 2005).

LIPRINS- α were identified as binding partners for the C2B domain of RIMs (Schoch *et al.*, 2002). However, crystallography and NMR analyses, using the minimal described binding domains, have shown that surrounding sequences of both domains are necessary for this interaction (Guan *et al.*, 2007).

Liprin- α associates with the motor protein KIF1A and is involved in the transport of several proteins, eg. AMPARs, GRIP1, GIT1 (Okada *et al.*, 1995; Shin *et al.*, 2003). In addition, KIF1A coimmunoprecipitates specifically RIM and GIT1 (Shin *et al.*, 2003), suggesting a possible role of Liprin- α as link between motor proteins and RIM, indicating that Liprin- α might be involved in RIM1 α trafficking

RIM-BP (RIM-binding protein) interacts with the proline rich region of RIMs through its second SH3 interaction motif. Interestingly, RIM-BPs can interact simultaneously with RIM and with the alpha subunit of L- and T-type voltage-gated calcium channels, acting as bridge between RIM proteins and these channels (Hibino *et al.*, 2002).

CALCIUM CHANNELS. The RIM C2B domain was found to interact with the β_4 -subunit of voltage-gated calcium channels. Interestingly, most proteins interacting with voltage-gated calcium channels bind the pore forming α -subunit, also known as Ca_v . This interaction has been shown to couple synaptic vesicles

to calcium channels, and to regulate the calcium entry through the modulation of the channel inactivation properties (Kiyonaka *et al.*, 2007).

SCRAPPER. The synapse-associated E3 ubiquitin ligase binds to RIM1 and ubiquitinates the protein (Yao *et al.*, 2007). In recent years, proteasome activity in neurons has been a field of increasing interest, because of its role in the modulation of synaptic transmission (Tai and Schuman, 2008). The ubiquitination of RIM1 α by SCRAPPER leads to its degradation, thereby modulating synaptic plasticity (Yao *et al.*, 2007).

SAD-B KINASE, a synaptic vesicle associated serine/threonine kinase, has been recently shown to specifically phosphorylate RIM1 α near the C2B domain (Inoue *et al.*, 2006). SAD-B, as well as the SAD-1 kinase, the *C. elegans* homolog, have been implicated in presynaptic differentiation and axon/dendrite polarization (Crump *et al.*, 2001; Kishi *et al.*, 2005). In neurons, SAD-B is involved in the regulation of neurotransmitter release, as overexpression of wild type SAD-B results in an increase of mEPSP frequency, whereas SAD-B lacking its kinase activity leads to a decrease (Inoue *et al.*, 2006). Effects on neurotransmitter release might be dependent on phosphorylation of SAD-B targets, such as RIM1 α (Inoue *et al.*, 2006).

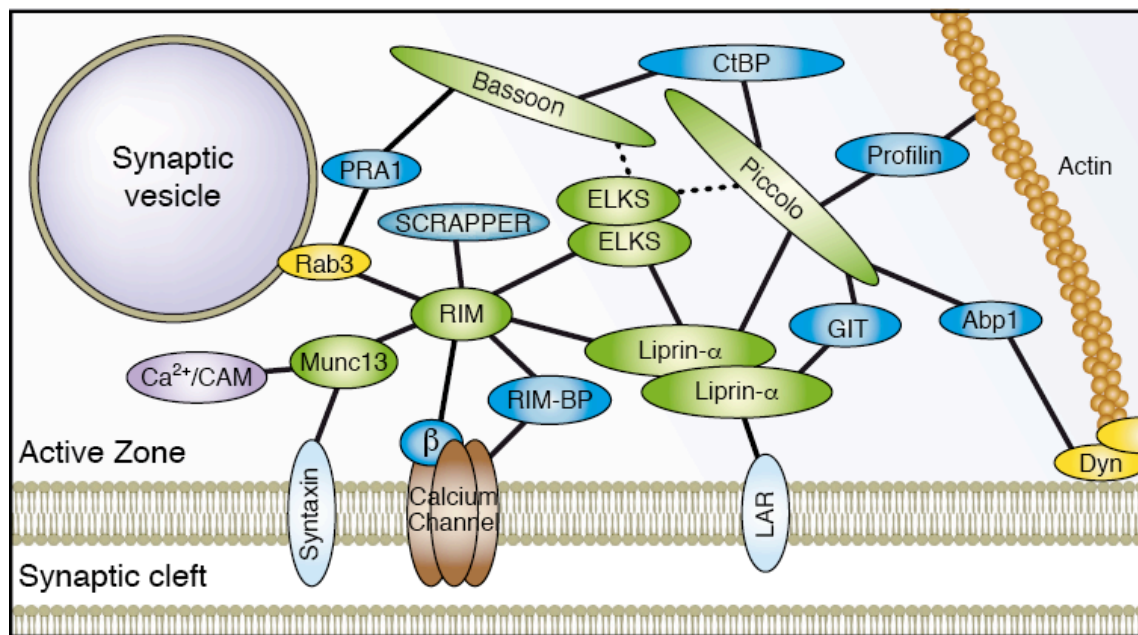


Fig. 1.8. Direct and indirect proteins interaction of RIM1 α at the Active Zone

Represented in green are Active Zone enriched proteins and their most prominent binding partners. Modified from (Mittelstaedt *et al.*, 2008, NWG).

1.4.4 Role of α -RIMs in synaptic function

As described above, α -RIMs form a scaffold at the Active Zone by interacting directly and indirectly with all other CAZ enriched proteins. In addition, they are linked to synaptic vesicles via Rab3, and linked to calcium channels directly or indirectly. Characterization of the invertebrate *C. elegans* lacking UNC-10/RIM, as well as α -RIM knockout mice have contributed to the understanding of the functional role of RIM1 α and RIM2 α in synaptic function.

1.4.4.1 UNC-10 DEFICIENT *C. ELEGANS*

Loss of UNC-10/RIM in *C. elegans* leads to behavioural and physiological deficits (Koushika *et al.*, 2001). UNC-10 mutant worms are smaller and show locomotor defects. Ultrastructural analysis after aldehyde fixation of the tissue showed no changes in the size and composition of the presynapse. Furthermore, no changes in the levels of the RIM binding proteins Rab3 and

UNC-13 were observed (Koushika *et al.*, 2001). However, subsequent electron microscopy studies using high pressure freezing in order to preserve the tissue in a more native state provided new insights into the synaptic ultrastructure of wild type and mutant worms, showing a clustering of synaptic vesicles near electron dense projections. Loss of UNC-10 resulted in a significant decrease of vesicles contacting the membrane adjacent to these dense projections (Weimer *et al.*, 2006), thus implying a role of UNC-10/RIM in the targeting of synaptic vesicles to the presynaptic density through its interaction with Rab3 (Gracheva *et al.*, 2008). This fact was corroborated by the analysis of Rab3 mutants, showing a decrease in the number of synaptic vesicles attached to the presynaptic densities (Gracheva *et al.*, 2008). In addition, Gracheva and collaborators showed a colocalization of UNC-10 and the calcium channel UNC-2 at presynaptic densities, suggesting that RIM is required for the targeting of synaptic vesicles to the presynaptic densities and thereby into proximity of calcium channels.

Electrophysiological characterization of worms lacking UNC-10/RIM found changes in spontaneous and evoked synaptic activity. Deletion of UNC-10 leads to a significant decrease in evoked EPSCs together with a reduced frequency of mini-EPSC. However the amplitude of the mini events was not altered compared to controls. These data indicated that UNC-10/RIM is not necessary for the fusion process itself because of the presence of spontaneous activity, but it might be required for the maturation of synaptic vesicle to a fusion-competent state (Koushika *et al.*, 2001). To further investigate the role of UNC-10/RIM in priming, an open form of Syntaxin was overexpressed in UNC-10 deficient worms. The open, but not the closed, form of Syntaxin was able to rescue the UNC-10/RIM phenotype, suggesting that UNC-10/RIM plays a role in priming (Koushika *et al.*, 2001). In addition, deletion of the RIM interacting protein UNC-13 in *C. elegans* lead to a similar but stronger phenotype, with a

total deficit in synaptic vesicle priming. This phenotype could also be rescued by overexpression of the open form of Syntaxin (Richmond *et al.*, 2001). These data indicate that UNC-10 via its interaction to UNC-13 coordinates synaptic vesicle maturation to a fusion competent state, driving Syntaxin to an open conformation necessary for SNARE complex assembly and therefore for synaptic vesicle priming.

1.4.4.2 RIM1 α KO MICE

Detailed analyses of RIM1 α and RIM2 α single KO mice, as well as, double knockout (DKO) mice, have provided new insights into the function of α -RIMs in vertebrates. RIM1 α deficient mice are viable and fertile (Schoch *et al.*, 2002) but show relevant impairments in synaptic transmission (Calakos *et al.*, 2004; Castillo *et al.*, 2002; Schoch *et al.*, 2002).

Synapses lacking RIM1 α do not undergo ultrastructural changes. Electron microscopy analysis of synapses in the hippocampal CA1 region, using aldehyde fixation, revealed no alterations in synaptic density, the size of Active Zones, or the number of docked vesicles (Schoch *et al.*, 2002). Moreover, RIM1 α KO mice displayed no changes in the expression of any interaction partner, apart from Munc13-1. Levels of this protein are decreased to 40% compared to wild type mice. In addition, a small increase in the expression of several postsynaptic proteins (GRIP, Shank, PSD-95, SynGAP) was detected (Schoch *et al.*, 2002).

The physiological consequences of RIM1 α absence have been studied in cultured neurons and in acute slice preparations. Electrophysiological analysis of neurons lacking RIM1 α yielded similar results as observed in *C. elegans* (Gracheva *et al.*, 2008; Koushika *et al.*, 2001), supporting the hypothesis that RIM1 α is necessary for the maturation of synaptic vesicles into a fusion competent state (Schoch *et al.*, 2002). Analyses of hippocampal slices as well

as of autapses of RIM1 α KO primary cultured neurons, have verified the role of RIM1 α in priming (Schoch *et al.*, 2002). This feature is corroborated by the decrease in release probability in the mutant mice because RIM1 α enhances the release probability by increasing the RRP size (Calakos *et al.*, 2004; Schoch *et al.*, 2002).

Additionally, RIM1 α plays a key role in short- and long-term synaptic plasticity, but its effect depends on the type of synapse (Schoch *et al.*, 2002). In CA1 excitatory neurons, the Schaffer collateral/commissural fiber synapses, RIM1 α maintains a normal neurotransmitter release and is necessary for short-term potentiation. In contrast to this, in mossy fiber synapses in the CA3 region of the hippocampus and at the parallel fibre/Purkinje cell synapse in the cerebellum, deletion of RIM1 α has no visible effect on acute neurotransmitter release, but abolishes LTP (Castillo *et al.*, 2002). These differences in the effect of RIM1 α deletion in excitatory synapses have been associated with the different mechanisms underlying synaptic plasticity. In neurons where long-term plasticity principally involves a presynaptic PKA-dependent component, deletion of RIM1 α impairs LTP. In contrast, in neurons with a postsynaptic NMDA-receptor dependent LTP, loss of RIM1 α does not induce changes in long-lasting plasticity (Castillo *et al.*, 2002). Furthermore, RIM1 α has been implicated in the late phase of NMDA-receptor dependent LTP (L-LTP) of Schaffer collateral synapses and the corticoamygdaloid pathway, where activation of PKA and NMDARs, is necessary for this form of plasticity (Huang *et al.*, 2005).

The effect of RIM1 α on presynaptic long-term potentiation in mossy fiber synapses and cerebellar parallel fibers has been associated with the phosphorylation of RIM1 α Ser-413 by protein kinase A, and the subsequent binding of the phosphorylated RIM to the adaptor protein 14-3-3 (Lonart *et al.*, 2003; Simsek-Duran *et al.*, 2004). However, recent experiments using knock-in

mice with the point mutation S413A, which avoids phosphorylation, have shown that phosphorylation of Ser413 is not necessary for LTP (Kaesler *et al.*, 2008b).

In addition to excitatory synapses, in inhibitory synapses RIM1 α also plays a role in synaptic plasticity (Chevalleyre *et al.*, 2007). CB1 receptor-dependent LTD at inhibitory synapses requires RIM1 α and cAMP/PKA signalling as shown by the loss of LTD induction in RIM1 α KOs and after the pharmacological block of PKA in the amygdala and hippocampus (Chevalleyre *et al.*, 2007).

Taken together, long lasting changes in the release machinery mediated by PKA signalling and RIM1 α represent a general mechanism for presynaptic regulation of long-term plasticity at both excitatory and inhibitory synapses (McBain and Kauer, 2009). Additionally, behavioural studies were performed by Powell *et al.*, finding that RIM1 KOs have learning and memory deficits (Powell *et al.*, 2004). This phenotype might be associated with the impairments in synaptic plasticity.

1.4.4.3 RIM2 α KO MICE

RIM1 α and RIM2 α are highly homologous proteins, and are expressed in overlapping but diverging patterns. In contrast to the RIM1 α KO, ablation of RIM2 α does not lead to a remarkable phenotype. RIM2 α Knockout mice show no changes in either excitatory or in inhibitory neurotransmission. In addition, loss of RIM2 α in the hippocampus does not alter synaptic plasticity processes or release probability (Schoch *et al.*, 2006). These results contrast with data obtained from RIM1 α KO mice, where synaptic transmission and facilitation is significantly impaired (Castillo *et al.*, 2002; Schoch *et al.*, 2002), indicating a compensatory effect of RIM1 α in neurons lacking RIM2 α .

1.4.4.4 α -RIM DKO MICE

Whereas RIM1 α and RIM2 α KOs are viable, deletion of both proteins is lethal. Mice die immediately after birth, most likely due to breathing problems (Schoch *et al.*, 2006). α -RIM deficient neurons do not undergo changes in number or size of synapse. In addition, no ultrastructural changes can be detected. Ablation of both isoforms does not alter expression levels of other synaptic proteins, with exception of Munc13-1. Nevertheless, there are no significant changes between Munc13-1 expression when compared to the RIM1 α KO (Schoch *et al.*, 2006).

The effects of α -RIM ablation have been studied in detail at the NMJ of E18.5 embryos. The NMJ of α -RIM DKO mice exhibits developmental aberrations without changes in synaptic ultrastructure, or spontaneous synaptic activity. However, synapses are unable to mediate normal calcium triggered neurotransmitter release, indicating that α -RIMs are necessary for a proper maintenance of calcium-triggered exocytosis (Schoch *et al.*, 2006).

1.4.4.5 ROLE OF RIM1 β IN SYNAPTIC FUNCTION

Recently, Kaeser *et al.* showed that the RIM1 gene generates an additional isoform, RIM1 β , due to the presence of an internal promoter. The domain structure of RIM1 β is identical to the one of RIM1 α , except that it lacks the N-terminal Rab3 binding sequence. RIM1 β and RIM1 α show overlapping expression patterns. Nevertheless, RIM1 β is preferentially expressed in caudal brain region, in contrast to RIM1 α that is mostly found in the frontal brain area.

Deletion of both RIM1 proteins impairs survival, consistent with a higher expression of RIM1 β in posterior brain regions and the overall upregulation of RIM1 β in the RIM1 α KO mice. In general, deletion of RIM1 β exacerbates the RIM1 α KO phenotype, with the exception of mossy fibers LTP. These Long

Term Potentiation effects in the RIM1 α ablated mouse are Rab3-dependent and RIM1 β lacks the binding sequence for this protein (Kaeser *et al.*, 2008a).

The RIM1 DKO also presents some differences in the composition of the AZ. Munc13-1 protein levels are extremely reduced. In addition, the solubility of ELKS, RIM-BPs and Liprins and Munc13-1 is increased, pointing to a key role of RIM1 proteins as scaffolding and stabilizer of other Active Zone proteins (Kaeser *et al.*, 2008a). Changes in the localization of these proteins might also be responsible for the impairment in short-term plasticity, due to a decrease in the release probability.

1.5 Presynaptic proteins in neurological diseases

Neurodegenerative diseases, aging, epilepsy and other neurological syndromes are associated with changes in the structure and function of synapses.

Several presynaptic proteins that are linked to the release machinery have been associated with the development of neuropathological events. α -Synuclein plays a critical role in Parkinson disease. The work of Krüger and colleagues showed that point mutations in the α -Synuclein sequence lead to a change in the conformation, inducing protein aggregation (Krüger *et al.*, 1998). α -Synuclein is a major component of Lewy bodies. Interestingly, α -Synucleins bind to the synaptic vesicle protein CSP α (cysteine string protein α). Deletion of the presynaptic co-chaperone CSP α accelerates neurodegenerative processes (Fernández-Chacón, 2004). This phenotype can be rescued by moderate overexpression of synucleins, and is aggravated if synucleins are deleted (Chandra *et al.*, 2005).

Also in neurological diseases like schizophrenia and autisms, there is an implication of synaptic proteins. Components of the presynaptic release

machinery and the cytomatrix of the Active Zone have been implied to play a role in schizophrenia (Weidenhofer *et al.*, 2006; Weidenhofer *et al.*, 2009). Particularly, the expression of RIM2, RIM3 and Piccolo was up-regulated in the amygdala of patients with schizophrenia as compared to controls (Weidenhofer *et al.*, 2006). In addition, RIM1 α knockout mice show a specific impairment in learning and memory, and trigger schizophrenia-related behaviours (Powell *et al.*, 2004). In the case of autisms, several mutations have been found in the genes coding for Neuroligins (postsynaptic) and Neurexins (presynaptic) (Südhof, 2008b).

An involvement of presynaptic proteins has been described in other neurological disorders, like epilepsy. Epileptic phenotypes have been observed in several mouse models in which presynaptic proteins were ablated, eg. in the KO mice of Active Zone protein bassoon (Altrock *et al.*, 2003), synaptic vesicles proteins synapsin1 (Terada *et al.*, 1999) and SV2A (Crowder *et al.*, 1999). Interestingly, SV2A is known to be the high affinity binding site for the wide-used antiepileptic drug levetiracetam (Lynch *et al.*, 2004). In humans, mutations in synapsin1 have been found in a family with epilepsy (Garcia *et al.*, 2004). Furthermore, antibodies against the S/M protein Munc18, essential component of the synaptic vesicle fusion machinery, were found in one patient with Rasmussen Encephalitis, a rare form of epilepsy, characterized by severe seizures and degeneration of one brain hemisphere (Yang *et al.*, 2000)

Therefore, accumulating evidence suggests that a better understanding of the molecular mechanism underlying the regulation of synaptic vesicle fusion and the associated plasticity, might result in the discovery of novel therapeutic approaches for different neurological disorders.

2 AIMS OF THE STUDY

Chemical transmission at the synapse is a tightly regulated process, which is characterized by its high speed, precision and spatial restriction to the Active Zone as well as by its plasticity. To ensure the perfect coordination of the ensemble of processes involved, the execution machinery needs to be tightly organized at the molecular level, both structurally and functionally. In recent years, RIM1 α and RIM2 α have emerged as key players in synaptic function with a regulatory role in synaptic vesicle exocytosis at the Active Zone and in presynaptically mediated forms of short- and long-term synaptic plasticity. However, so far the smallest members of the RIM gene family, RIM3 γ and RIM4, have not been studied in detail. It is therefore still unresolved if γ -RIMs function in concert with full length RIMs or are components of completely unrelated molecular processes.

The main objective of the present study was to improve the understanding of the molecular and physiological function and regulation of γ -RIM proteins in neurons. For this purpose, the following goals were addressed.

1. The first aim was to thoroughly resolve the spatial and cellular expression patterns of RIM3 γ and RIM4 γ in the rat brain. Knowledge about their distribution and subcellular localization, in relation to the full-length isoforms, is instrumental to understand their physiological relevance. Therefore, it should be examined if both γ -RIM isoforms are coexpressed with the full length RIM proteins, and associated with the CAZ.

2. The second goal was to gain insight into the molecular mechanism underlying the subcellular localization of γ -RIMs and to identify potential regions important for γ -RIM targeting.
3. The third aim was to elucidate the physiological relevance of RIM3 γ and RIM4 γ . Therefore a loss-of-function approach via RNA interference, using lentiviral transduction of neurons *in vitro* as well as *in vivo* should be applied.

An additional goal of this thesis was to address the involvement of presynaptic proteins in human neurological disorders. Accumulating evidence points to the involvement of components of the presynaptic release machinery in neurological disorders, e.g. schizophrenia, epilepsy. To gain further insight into the role of presynaptic proteins in epilepsy, serum of Rasmussen patients were examined for the presence of autoantibodies against presynaptic proteins.

3 MATERIAL

3.1 *Equipment*

| Equipment | Model | Company |
|----------------------------------|---------------------------------------|---------------------|
| Acrylamid electrophoresis system | Mini-PROTEAN 3 Electrophoresis System | BioRad |
| Agarose electrophoresis system | SUB-CELL GT | BioRad |
| Analytical balance | BP210S | Sartorius |
| Autoclave | H + P Varioklav 75T | |
| Balance | SBC53 | SCALTEC |
| Capillary Sequencer | 3130/xl/ Genetic Analyzer | Applied Biosystems |
| Centrifuge | 1-15K | Sigma |
| Centrifuge | 5415C | eppendorf |
| Confocal microscop | FV300 | Olympus |
| Cryostat | HM 560 | MICROM |
| Electroporator | MicroPulser Electroporator | BioRad |
| Gel documentation system | Alphamager | AlphaInnotech |
| Incubator | T6 | Heraeus Instruments |
| infrared imaging System | Oyssey | Odyssey, Li-cor |
| Inverse microscop | Axiovert | Zeiss |
| Microtome | Microm HM 335 E | Microm |
| PCR-Cycler | UNOII | Biometra |
| pH-Meter | HI 9025 | HANNA Instruments |
| Photometer | BIO | eppendorf |
| Pipettes | 10, 20, 100, 200, 1000 | Gilson |
| Power Supplies Agarose | PHERO-stab.500 | BIOTEC-FISCHER |
| Power Supplies Agarose | Power Pack 25 | Biometra |
| Shaker | 3031 | GFL |
| Spectrophotometer | ND-1000 | NanoDrop |
| Thermo Shaker | compact | Eppendorf |

| Equipment | Model | Company |
|-----------------|---------------------------------------|-----------------------|
| Transfer System | Mighty Small Transphor/ Hofer TE22 | Amersham |
| Ultrasonicator | UP50H | Hilscher |
| Vibratome | Vibratome 1000 | Geneq |
| Vortex | Vortex-Genie 2 | Scientific Industries |

Table 3.1 Lab equipment

3.2 Chemicals

| Product | Company |
|---|---------------|
| 6 x loading buffer | Fermentas |
| Acetic acid | Roth |
| Acrylamid | Roth |
| Agarose | peqLab |
| Ammoniumpersulfat (APS) | Roth |
| Ampicillin | Roth |
| Aqua ad iniectabilia | Delta Select |
| Bovine serum albumin (BSA) | Sigma-Aldrich |
| Bromphenolblue | Roth |
| Calcium chloride | Sigma-Aldrich |
| Chloroform | Roth |
| Citric acid | Sigma-Aldrich |
| Complete Mini Protease Inhibitor | Roche |
| Cryo-preserving medium (Tissue-Tek) | Dako |
| DAB (3,3'-Diaminobenzidin-Tetrachlorid) | Sigma-Aldrich |
| Denhardt's solution | Roth |
| Diethylpyrocarbonate (DEPC) | Roth |
| Dimethylsulfoxide (DMSO) | Roth |
| Ethanol | Fluka |
| Ethidiumbromide | Merck |
| Fish gelatine | Sigma-Aldrich |
| Formamide | Roth |
| Glycerol | Sigma-Aldrich |
| HCl 2N | Merck |

| Product | Company |
|---------------------------|--------------------------|
| Isofluorane | Sigma-Aldrich |
| Isopropanol | Fluka |
| Kanamycin | Sigma-Aldrich |
| LB-Agar | LabM/idg |
| LB-Medium | LabM/idg |
| Lipofectamine 2000 | Invitrogen |
| Magnesium chloride | Merck |
| Methanol | Merck |
| Milk powder | Roth |
| Nitrocellulose Membrane | GE Healthcare |
| Paraformaldehyd | Roth |
| PBS | Biochrom AG |
| Penicilin | Sigma-Aldrich |
| RNAse away | Molecular BioProducts |
| Saccharose | Sigma |
| Sodium acetic | Merck |
| Sodium chloride | Merck |
| Sodium Citrate | Sigma-Aldrich |
| Sodium Hydroxid 2N | Merck |
| Sodiumdodecylsulfat (SDS) | Roth |
| Sodiumhydrogenphosphat | Merck |
| β -Marscaptoethanol | Roth |
| TEMED | Roth |
| TESPA | Sigma-Aldrich |
| Tris-Base | Sigma |
| Tris-HCl | Roth |
| Triton-X-100 | Roche |
| Trizol | Sigma |
| Trypan-Blue | Invitrogen |
| Urea | Sigma-Aldrich |
| Xylol | Merck |

Table 3.2 Chemicals

3.3 Kits

| Use | Name | Company |
|---|--|-----------------------|
| cDNA-Synthesis | First-strand cDNA Synthesis Fermentas | Fermentas |
| DNA gel extraction | QIAquick Gel extraction kit | Qiagen |
| mRNA purification | Dynabeads mRNA direct | Invitrogen |
| PCR Purification | QIAquick PCR Purification Kit | Qiagen |
| Plasmid purification Maxi Endotoxin frei | EndoFree Plasmid Maxi kit | Qiagen |
| Plasmid purification Midi | Pure Link Midi kit | Invitrogen |
| Plasmid purification Mini | Pure Link Mini kit | Invitrogen |
| RNA extraction | RNeasyMinikit | QIAGEN, Hilden |
| Sequencing | PRISM Big Dye Terminator | Applied Biosystems |
| Sequencing reaction purification | DyeEx 2.0 | Qiagen |
| Western Blot chemiluminescent reagent | ECL Amersham | GE Healthcare |

Table 3.3 Commercial kits

3.4 Cell culture media

| Cell culture medium/solution | Company |
|---|-----------------------|
| Dulbecco's Modified Eagle's Medium (DMEM) | (GibcoBRL, Eggenheim) |
| Basal Medium Eagle (BME) | (GibcoBRL, Eggenheim) |
| Fetales calf serum (FCS) | (GibcoBRL, Eggenheim) |
| Opti-MEM | (GibcoBRL, Eggenheim) |
| Phospate saline buffer (PBS) | (GibcoBRL, Eggenheim) |
| Hank's Buffered Salt Solution (HBSS) | (GibcoBRL, Eggenheim) |
| Penicillin-Streptomycin | (GibcoBRL, Eggenheim) |
| Glucose | (GibcoBRL, Eggenheim) |
| B27 | (GibcoBRL, Eggenheim) |

Table 3.4 Cell culture media and solutions

3.5 Antibodies

| PRIMARY ANTIBODIES | |
|-------------------------------|-------------------|
| Antibody | Company |
| α -Tubulin (ab7750) | Abcam |
| Bassoon (10040715) | Stressgene |
| β -Tubulin (05-661) | Chemicon |
| RFP (AB3528) | Millipore |
| GFP (SC 101525) | Santa Cruz |
| GFP FITC conjugated (AB42560) | Abcam |
| GRIP1 (611319) | BD Bioscience |
| Liprins- α | Pineda AK Service |
| MAP2 (MAB3418) | Chemicon |
| Munc18 (610337) | BD Bioscience |
| PSD-95 (75-028) | NeuroMab |
| RIM1 (610907) | BD Bioscience |
| RIM1/2 (140203) | SySy |
| RIM3 | Pineda AK Service |
| RIM4 | Pineda AK Service |
| Synapsin (106001) | SySy |
| Synaptophysin (101011) | SySy |

Table 3.5 Primary antibodies

| SECONDARY ANTIBODIES | |
|---------------------------|-------------------------|
| Antibody | Company |
| Biotin-anti mouse IgG | Jackson immuno research |
| Biotin-anti rabbit IgG | Jackson immuno research |
| Cy3-anti mouse IgG | Jackson immuno research |
| Cy3-anti rabbit IgG | Jackson immuno research |
| Cy5-anti mouse IgG | Jackson immuno research |
| Cy5-anti rabbit IgG | Jackson immuno research |
| FITC-anti mouse IgG | Jackson immuno research |
| FITC-anti rabbit IgG | Jackson immuno research |
| HRP-anti mouse IgG | Vector Laboratories |
| HRP-anti rabbit IgG | Vector Laboratories |
| IRDye 680-anti mouse IgG | LI-COR Odyssey |
| IRDye 680-anti rabbit IgG | LI-COR Odyssey |

| | |
|---------------------------|----------------|
| IRDye 800-anti mouse IgG | LI-COR Odyssey |
| IRDye 800-anti rabbit IgG | LI-COR Odyssey |

Table 3.6 Secondary antibodies

3.6 Oligonucleotides

3.6.1 Sequencing primer

| TEMPLATE | PRIMER | 5'-SEQUENCE-3' |
|----------------------------|-----------------|------------------------|
| PLentiLN-EGFP-EF1 α | EF1 α fw | CTCAAGCCTCAGACAGTGGTTC |
| pLVTHM | H1 fw | TCGCTATGTGTTCTGGGAAA |
| pLVTHM | SP6 rv | ATTTAGGTGACACTATAG |
| TOPO TA | M13 fw | CTGGCCGTCGTTTTAC |
| TOPO TA | M13 rv | CAGGAAACAGCTATGAC |
| CT-GFP TOPO, pcDNA 3.1 | T7 | GTAAAACGACGGCCAG |
| CT-GFP TOPO | GFP rv | GGTAAGCTTTCCGTATGTAGC |
| NT-GFP TOPO | GFP fw | CGACACAATCTGCCCTTTTCG |
| NT-GFP TOPO, pcDNA 3.1 | BGH rv | TAGAAGGCACAGTCGAGG |
| PL26 (pLenti-Syn) | Lenti fw | CTGGTCGAGCTGGACGGCGACG |

Table 3.7 Primer for sequencing

3.6.2 *In situ* hybridization oligonucleotides

| GEN | POSITION | 5'-SEQUENCE-3' |
|---------------|----------|---|
| RIM3 γ | 496-540 | GCTGGGATCCACAGATCTCACCGCTGATGCTGGAG CTCCTCACTA |
| RIM3 γ | 231-275 | GCAATGCCCGTCTCTGTGCTCCGTCGAATGTTGCT GCGCAGCTTC |
| RIM4 γ | 156-200 | ATGGACTCATGGCTGGCTTGGCGTAACGTCCGGCT GGGCATCTCC |

Table 3.8 *In situ* hybridization probe sequences

3.6.3 shRNA sequences

R3SHRNA1 FW **CGCGTCCCC**GGCAAGGTTCTACAGGTGAT**TTCAAGAGAT**CACCTGTAGAACCTTGCC**TTTTTGAAAT**

R3SHRNA1 RV **AGGGG**CCGTTCCAAGATGTCCACT**AAGTTCTCT**AGTGGACATCTTGGAACGG**AAAACCTTAGC**

R3SHRNA2 FW **CGCGTCCCC**CGCCAAGATGGTGGCTATTGTT**TTCAAGAGA**ACAATAGCCACCATCTTGCG**TTTTTGAAAT**

R3SHRNA2 RV **AGGGG**GCGTTCTACCACCGATAACA**AAGTTCTCT**TGTTATCGGTGGTAGAACCGC**AAAACCTTAGC**

R3SHRNA3 FW **CGCGTCCCC**GCCACCTATATCAAGGCTTAC**TTCAAGAGA**GTAAGCCTTGATATAGGTGGC**TTTTTGAAAT**

R3SHRNA3 RV **AGGGG**GCGTGGATATAGTTCCGAATG**AAGTTCTCT**CATTCGGAACCTATATCCACCG**AAAACCTTAGC**

R3SHRNA4 FW **CGCGTCCCC**GGAGCACCAACAGTAACAGCT**TTCAAGAGA**AGCTGTTACTGTTGGTGCTCC**TTTTTGAAAT**

R3SHRNA4 RV **AGGGG**CCTCGTGGTTGTCATTGTCGA**AAGTTCTCT**TCGACAATGACAACCACGAGG**AAAACCTTAGC**

R4SHRNA1 FW **CGCGTCCCC**GGATGTGGAGATCGGTTTACA**TTCAAGAGA**TGTAAACCGATCTCCACATCC**TTTTTGAAAT**

R4SHRNA1 RV **AGGGG**CCTACACCTCTAGCCAAATGT**AAGTTCTCT**TACATTTGGCTAGAGGTGTAGG**AAAACCTTAGC**

R4SHRNA2 FW **CGCGTCCCC**CGTGGGTTGGTACAAGCTCTT**TTCAAGAGA**AAGAGCTTGTACCAACCCACG**TTTTTGAAAT**

R4SHRNA2 RV **AGGGG**CCTACACCTCTAGCCAAATGT**AAGTTCTCT**TTCTCGAACATGGTTGGGTGC**AAAACCTTAGC**

R4SHRNA3 FW **CGCGTCCCC**GGAGGAGTTTGTCTAGCTTCA**TTCAAGAGA**TGAAGCTAGACAAACTCCTCC**TTTTTGAAAT**

R4SHRNA3 RV **AGGGG**CCTCCTCAAACAGATCGAAGT**AAGTTCTCT**ACTTCGATCTGTTTGAGGAGG**AAAACCTTAGC**

R4SHRNA4 FW **CGCGTCCCC**ATCACTGGACCCGTTGTACAAC**TTCAAGAGA**GTTGTACAACGGGTCCAGTGAC**TTTTTGAAAT**

R4SHRNA4 RV **AGGGG**TAGTGACCTGGGCAACATGTTG**AAGTTCTCT**CAACATGTTGCCAGGTCACTG**AAAAACCTTAGC**

3.6.4 CLONING PRIMER

| CLONING PRIMER FOR FLUORESCENT PROTEINS | | | | | |
|--|-----|-----|---|-----------------|----------------|
| TEMPLATE | FW | RV | 5'-SEQUENCE-3' | ENZYME | VECTOR |
| CHERRY | 797 | 798 | GCGGGATCCGAATTCGTACCGGTCGCC | BamHI, EcoRI | pcDNA3.1, pL26 |
| CHERRY | 798 | 797 | GCGCAATTGTTACTTGTACAGCTCGTCCATG | MfeI | pcDNA3.1, pL26 |
| GFP | 799 | 800 | GCGAGATCTACCATGGATGGTGAGCAAGGGCGAGGAG | BglII | pcDNA3.1, pL26 |
| GFP | 800 | 799 | GCGGAATTCGGATCCTCCTCCTCCCTTGTACAGCTCGTCC ATGCC | BamHI, EcoRI | pcDNA3.1, pL26 |
| CLONING PRIMER FOR γ -RIM FULL LENGTH | | | | | |
| GEN | FW | RV | 5'-SEQUENCE-3' | ENZYME | VECTOR |
| RIM3 γ | 805 | 806 | GCGGAATTCCACCATGTTTAACGGGGAGCCTGG | EcoRI | pcDNA3.1, pL26 |
| RIM3 γ | 806 | 805 | GCGGAATTCGGAGCACGAGGGGCTGGTGG | EcoRI | pcDNA3.1, pL26 |
| RIM3 γ | 807 | 808 | GCGGAATTCATGTTTAACGGGGAGCCTGG | EcoRI | pcDNA3.1, pL26 |
| RIM3 γ | 808 | 807 | GCGGAATTCTTAGGAGCACGAGGGGCTGGTGG | EcoRI | pcDNA3.1, pL26 |
| RIM4 γ | 809 | 810 | GCGGGATCCACCATGGAGCGCTCGCAGAGC | BamHI | pcDNA3.1, pL26 |
| RIM4 γ | 810 | 809 | GCGGAATTCAGATCGCTCGCCACAGGG | EcoRI | pcDNA3.1, pL26 |
| RIM4 γ | 811 | 812 | GCGGGATCCATGGAGCGCTCGCAGAGC | BamHI | pcDNA3.1, pL26 |
| RIM4 γ | 812 | 811 | GCGGAATTCTTAAGATCGCTCGCCACAGGG | EcoRI | pcDNA3.1, pL26 |

| CLONING PRIMER FOR γ -RIM DELETION CONSTRUCTS | | | | | |
|--|------|-----------------|----------------------------------|--------|----------------------|
| GEN | FW | RV | 5'-SEQUENCE-3' | ENZYME | VECTOR |
| RIM3 γ | 1534 | 1535 | GCGGAATTCTATGGTGGGACGACAGACACTGG | EcoRI | pLenti-EF1 α |
| RIM3 γ | 1535 | 1534, 36, 37 | GCGGAATTCTTAGGAGCACGAGGGGCTGGTGG | EcoRI | pLenti-EF1 α |
| RIM3 γ | 1536 | 1535 | GCGGAATTCTATGGAAGGGGCCACCAAGAAG | EcoRI | pLenti-EF1 α |
| RIM3 γ | 1537 | 1535 | GCGGAATTCTATGACCACCACAGCCAAGAAAC | EcoRI | pLenti-EF1 α |
| RIM4 γ | 1538 | 1539 | GCGGAATTCTATGACACCCATGGGGGATGTG | EcoRI | pLenti-EF1 α |
| RIM4 γ | 1539 | 1538, 40 | GCGGAATTCTTAAGATCGCTCGCCACAGG | EcoRI | pLenti-EF1 α |
| RIM4 γ | 1540 | 1539 | GCGGAATTCTATGGACAGCCGGAGGCTGAAG | EcoRI | pLenti-EF1 α |
| RIM3 γ | 1050 | 1051 | CCCCCATGGGAGATGTGCAC | | pCDNA3.1/NT-GFP-TOPO |
| RIM3 γ | 1224 | 1051 | AGCAAAGCACACTGCAGCTC | | pCDNA3.1/NT-GFP-TOPO |
| RIM3 γ | 1227 | 1051 | ACCACCACAGCCAAGAAAC | | pCDNA3.1/NT-GFP-TOPO |
| RIM4 γ | 1056 | 1057 | CTGGCTACCACACCCATG | | pCDNA3.1/NT-GFP-TOPO |
| RIM4 γ | 1225 | 1057 | ATGAACTCCTTCGATGATGAGG | | pCDNA3.1/NT-GFP-TOPO |
| RIM4 γ | 1057 | 1056, 1225 | CCGAAGCAGGGGACCTGTGG | | pCDNA3.1/NT-GFP-TOPO |

Table 3.9 Primers used for DNA amplification

3.7 Vectors

3.7.1 TOPO cloning vectors

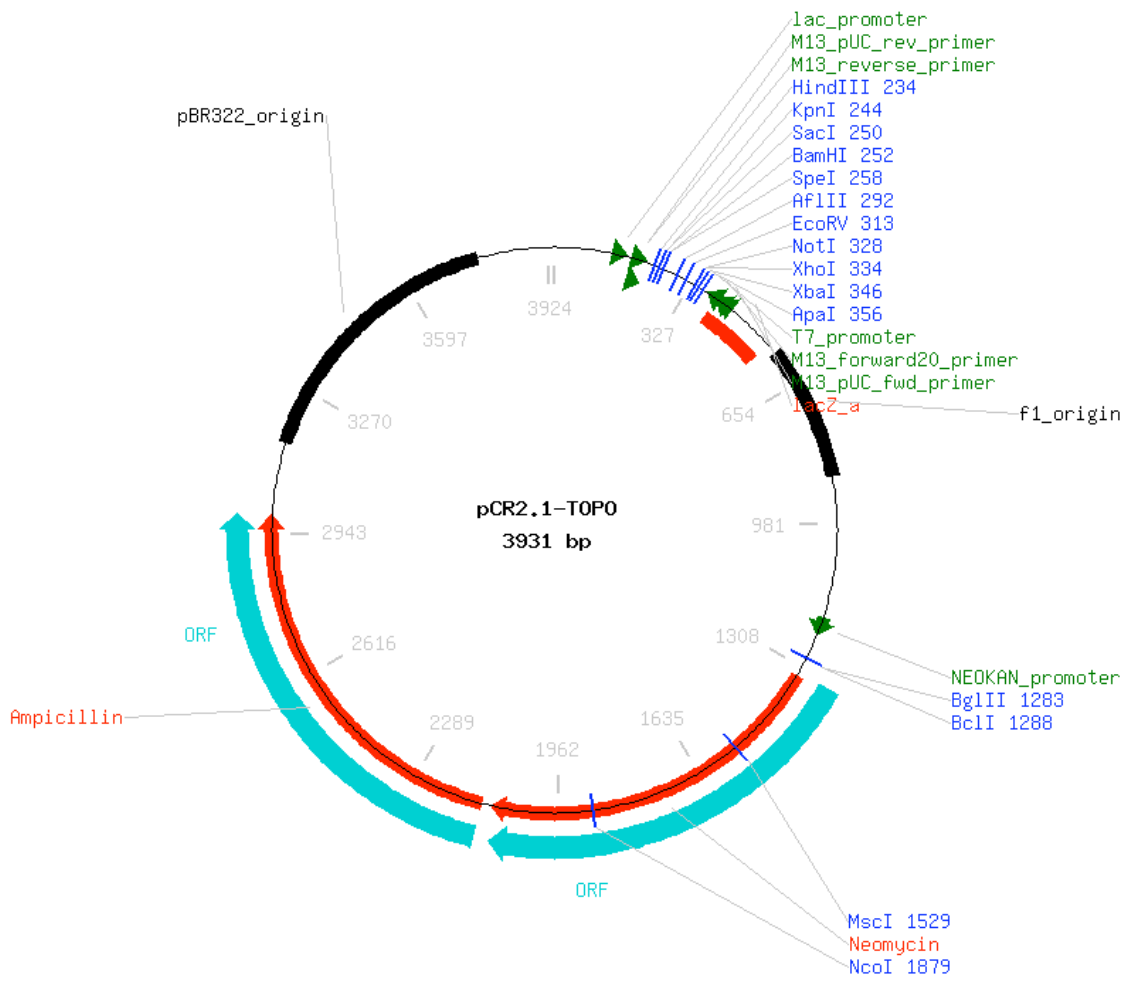


Fig. 3.1 TOPO TA cloning vector (Invitrogen)

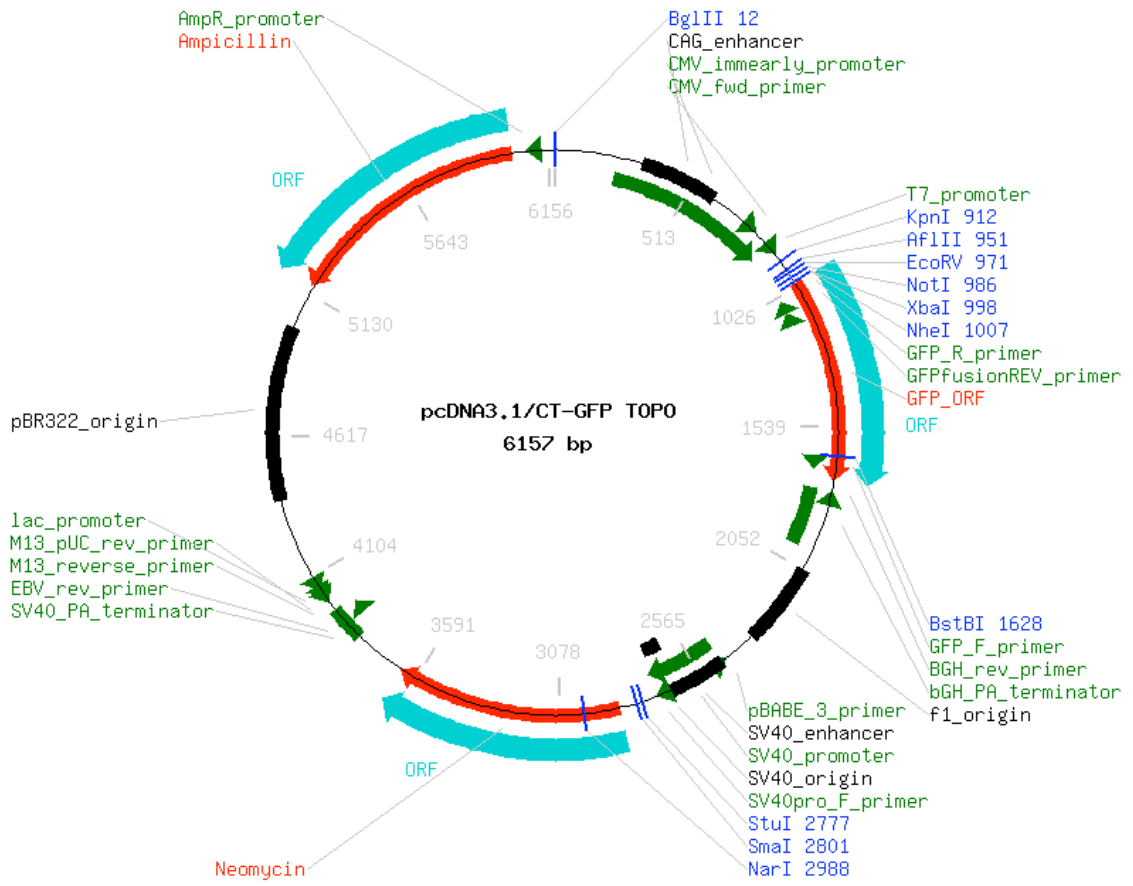


Fig. 3.2 pcDNA 3.1 CT-GFP TOPO vector (Invitrogen)

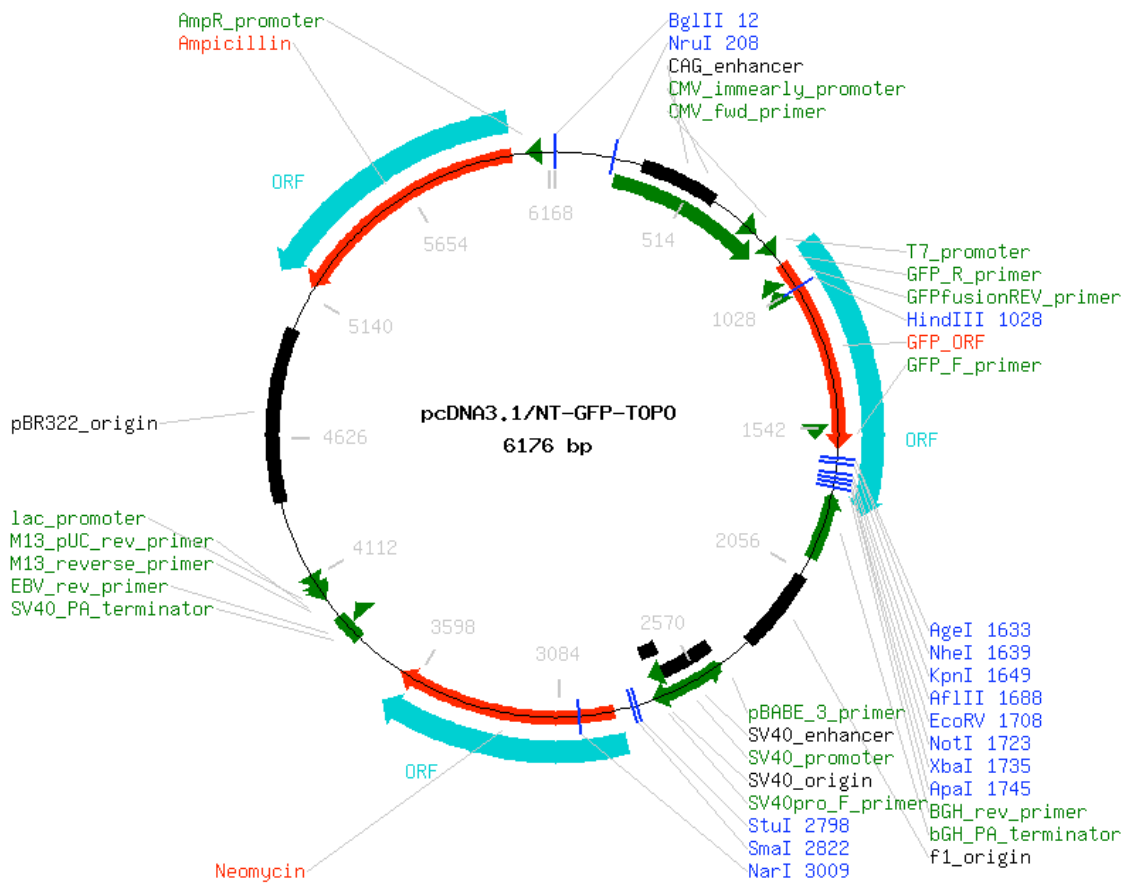


Fig. 3.3 pcDNA 3.1 NT-GFP TOPO vector (Invitrogen)

3.7.2 Plasmids for cell culture transfection

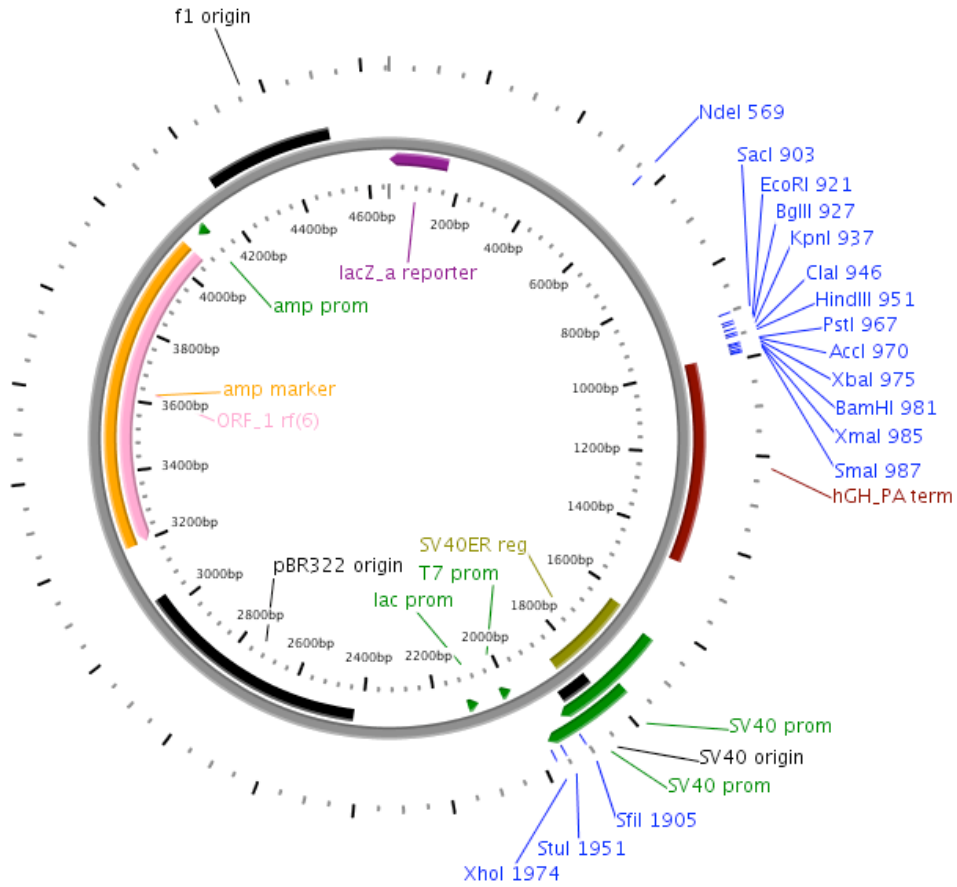


Fig. 3.4 pCMV5 vector (T.S Lab)

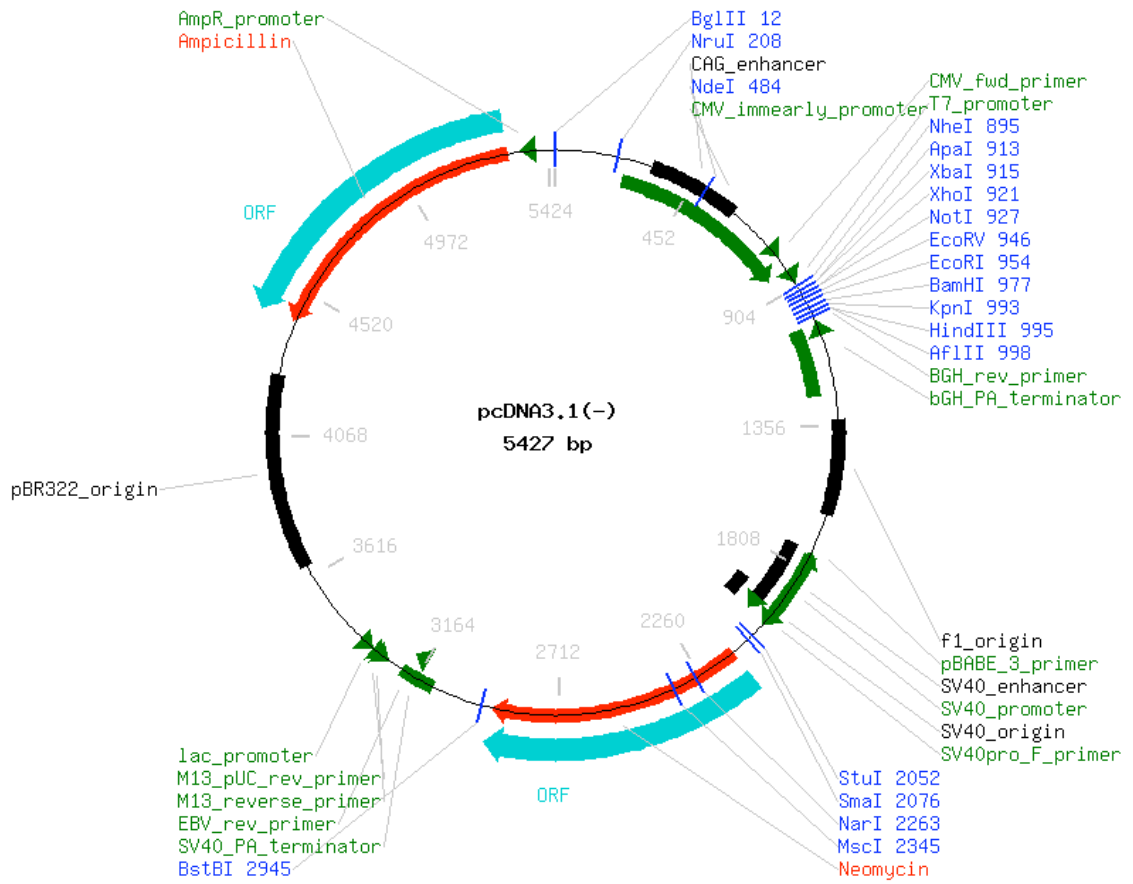


Fig. 3.5 pCDNA 3.1 vector (Invitrogen)

3.7.3 Plasmids for lentivirus production

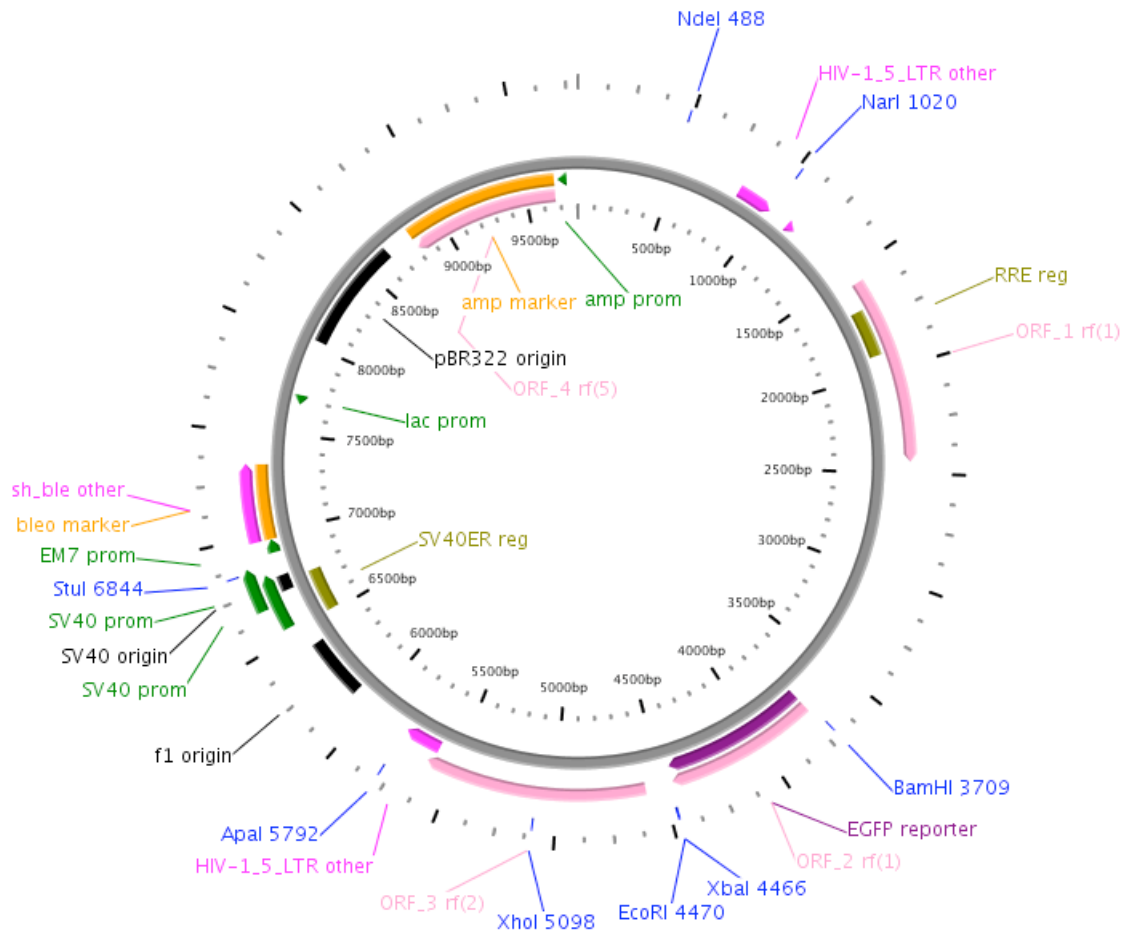


Fig. 3.6 pL26 vector (M.Schwarz Lab)

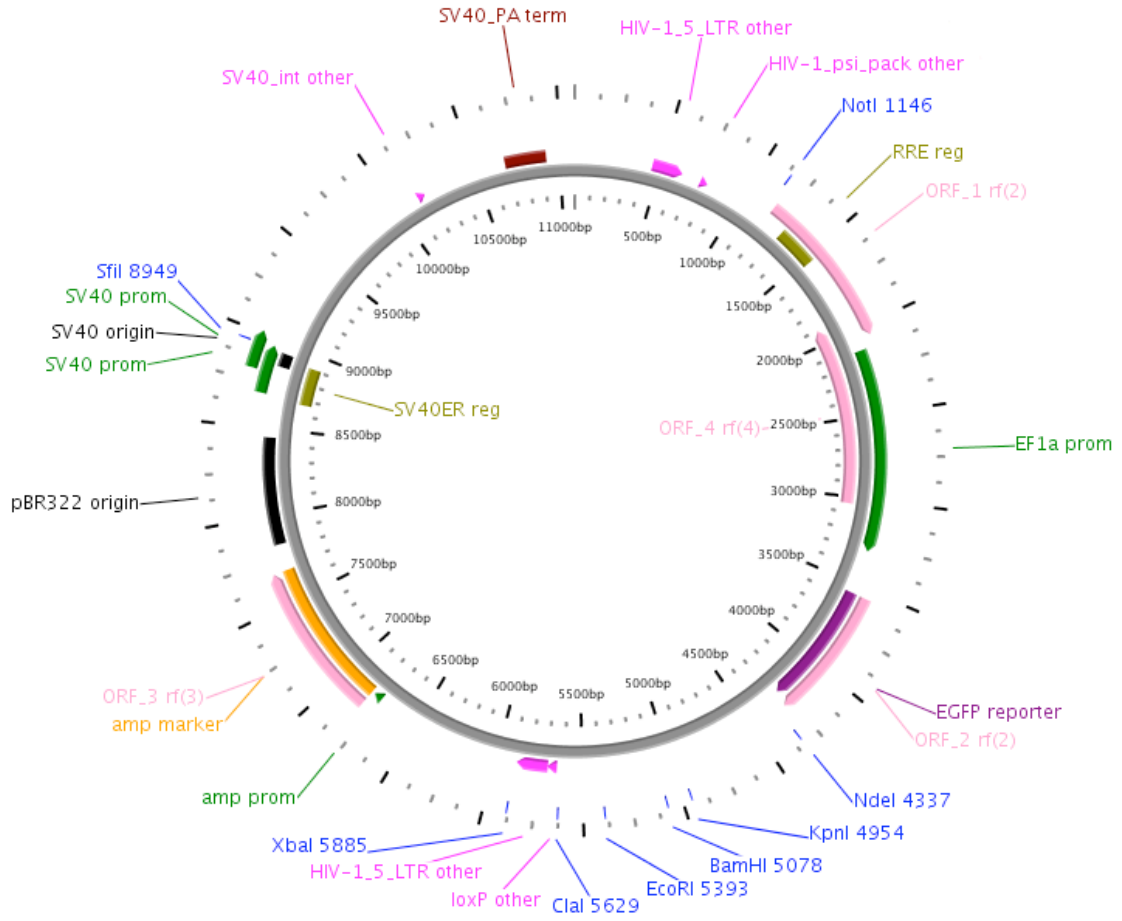


Fig. 3.7 pLVTHM vector (Trono Lab)

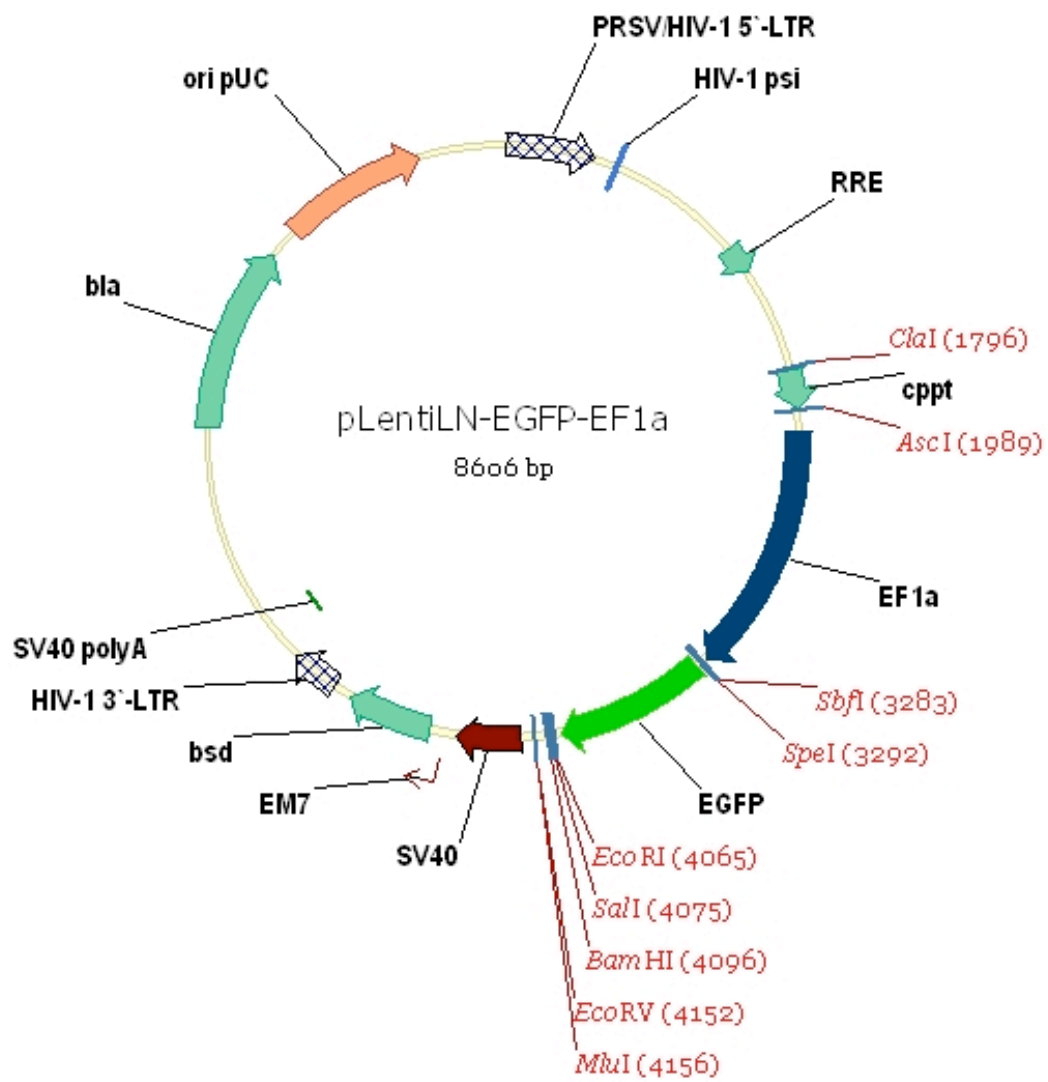


Fig. 3.8 pLentiLN-EGFP-EF1α plasmid (Trono Lab)

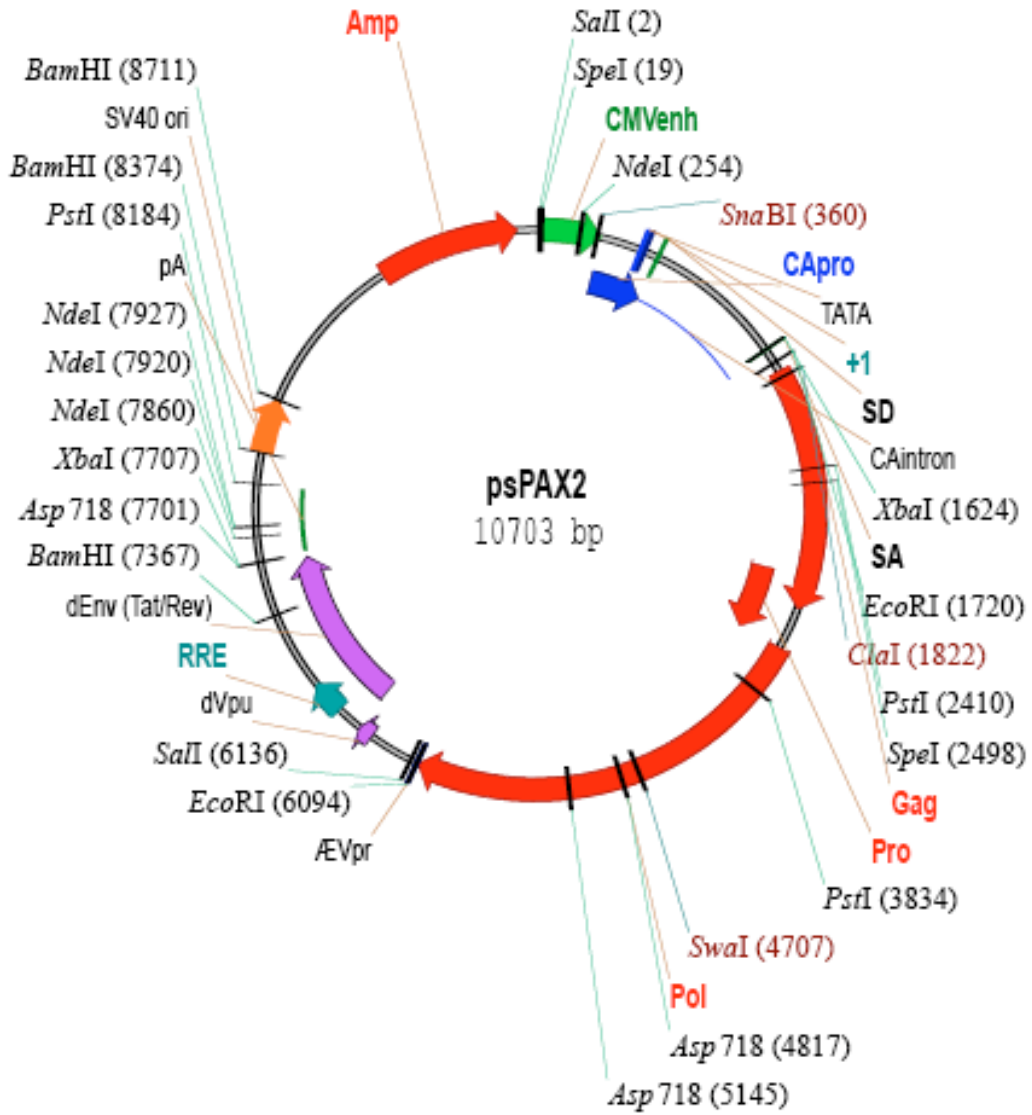


Fig. 3.9 psPAX2 packaging plasmid second generation (Trono Lab)

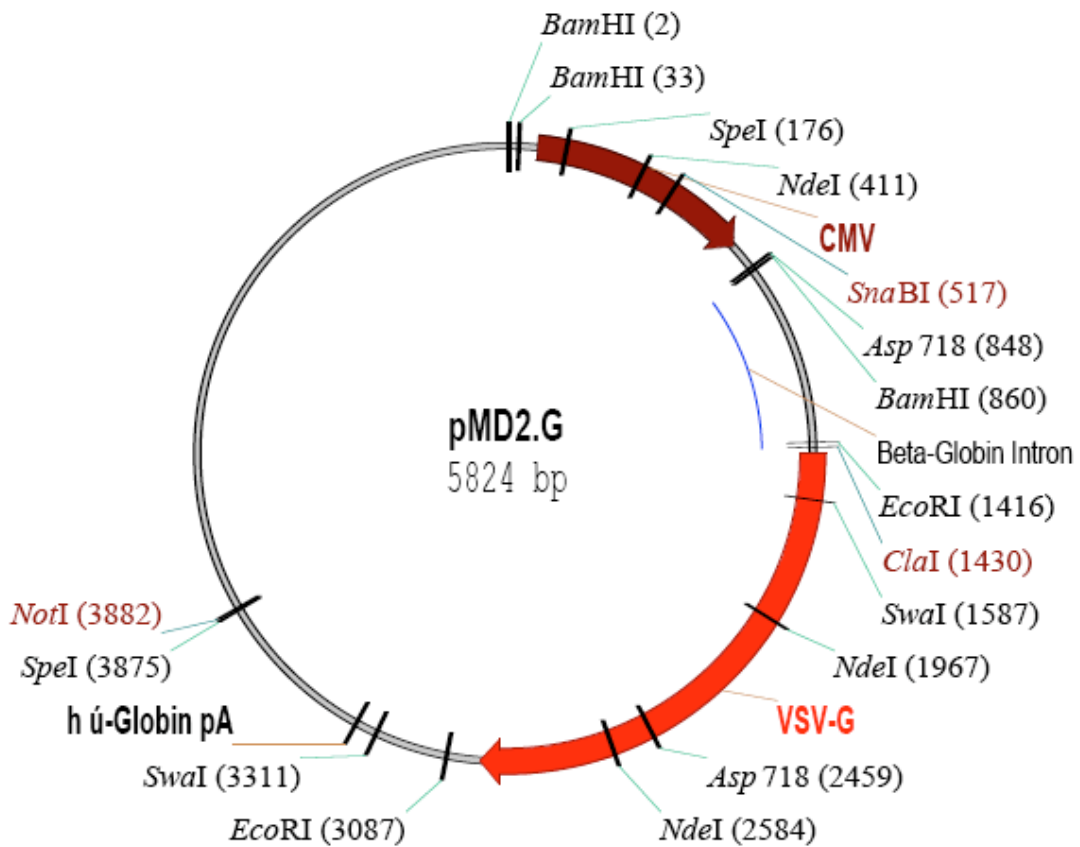


Fig. 3.10 pMD2.G envelope plasmid second generation (Trono Lab)

3.8 cDNA and protein sequences

3.8.1 RIM1 α

3.8.1.1 RIM1 α cDNA (*RATTUS NOVERGICUS*)

```

CGGGCGGCCCCGGCCCCGGCCCCGGCCCCGGCCCCGGCCAGCGCAGCCCCGGCGCCCGGCGCTCCGGAGCTC
AGCGCCAGCCCTCGCCCCCTCGCCGTGCCTCCGCTGCCCGCCCCGCGGCCAAGGCTGGGCTGCGGGA
GGCCGCCGGGCGGCCCCGAGCCTCGCCAGGGCGACCCAAACAAAGGCAGCATCCGGGCTCGGCGGGAGGC
AGAGCATCATGAGAGACTGGGTCTCGCTGTCCCCGGCTCCGCTGCTGCTGCCGCTGCCGCCGCCCGC
CGCCGCCGCTGCCGCTGCCGCCGCCAGGAGGGCTTCGCTGTGAGCGTTGGAAAGCAGGGGCGCAGCTGCG
GGGCGTGAATCCGAAAGGTGAGAGCCAGAGCCAGCGAGCCGAGGGGGCGGGCAGGCCACGAAAAATGTCC
TCGGCCGTGGGGCCCCGAGGTCCTCGCCACCCACGGTGCCTCCCCCTATGCAAGAAGTCCCCGACCTGA
GCCACCTGACCGAGGAGGAGGGAACATTATCATGGCAGTGTGGACCGCAGAAAGGAGAGGAGGAAAA
AGAAGAGGCCATGCTCAAGTGTGTTGTTCAGGGACATGGCGAAGCCTGCTGCCTGCAAAACACCAAGAAA
GCTGAAAGCCAGCCCCATCAACCACCACTGAACATTTTCAGATGTGTCTGTGTTCCAGAAAGCCAAGCA
GCGAAGAGGGAGGCCAGAAAGAGACTGGAGATTGCATCAACAGTTTGAAGCTACAAGGAGCAAGTGAG
AAAAATCGGAGAGGAAGCGAGGCGTTACCAGGGCGAGCACAAGGATGATGCCCCGACGTGTGGAATCTGT
CATAAGACAAAGTTTGTGATGGATGTGGCCATCTCTGCTCCTATTGTGCGACCAAGTTCTGTGCACGCT
GCGGAGGCCGTGTGTCTCTGCGATCGAACAATGAGGACAAAGTGGTTATGTGGGTATGCAATTTATGTGCG
AAAGCAACAAGAAATCTTAACGAAATCTGGAGCGTGGTTCTTTGGAAGTGGCCCTCAGCAGCCTAGTCAA
GATGGGACTCTGAGTGACACGGCCACAGGTGCTGGATCTGAGGTGCCAAGAGAAAAGAAAGCAAGGCTCC
    
```

AAGAGCGATCAAGGTCTCAGACGCCCTTGAGTACAGCAGCTGTCTCTTCCCAAGACACTGCTACCCCCGG
TGCACCGTTGCACAGGAACAAAGGGGCTGAGCCCTCACAGCAAGCCTTGGGTCTTGAACAGAAGCAGGCA
TCAAGATCAAGAAGCGAGCCACCGAGGGAAAGGAAGAAGGCTCCAGGGCTTTCAGAGCAGAATGGCAAGG
GAGGCCAGAAGAGCGAGCGCAAACGTGTCCCAAGTCTGTGGTGCAACCCGGGGAAAGGGATCGCGGATGA
GAGGGAGAGGAAAGAGAGGGCGGGAAACCCGCAGGTTGGAGAAAGGGCGCTCCCAGGACTACTCAGACCGG
CCTGAGAAACCGCACAATGGCAGGGTGGCGGAAGACCAGAAGCAGAGGAAGGAGGAGGTACCAGACTA
GGTACCAGCAGCGACCTAACCTGGCTCGCTACCCGGTGAAGGCGCCGCCAGAGGAGCAGCAGATGCGCAT
GCACGCCCGGGTGTCCCAGCGAGGCACGAGCGGCCACAGCGACGTGGCGCTCCCGCACACCGAGGCA
GCTGCCCGCCGGCCGGCTGAGGCCACGGCGGGCAAGCGCGCCGCGCCACCGCAGGGTCTCTCCCCCGG
AGTCCCCGCGCGCACGCGCGGGCGGCCAGCCTCCACCGAGCACGGGCCACCGCCGCGCGGCCAGC
CCCCGGTCCCAGAGCCACCCGAGCCGCGCTCCCCGAGCCGCTCCGTAAGCAGGGCCGCTGGACCCG
GGCTCGGCCGTGCTTCTGCGCAAGGCCAAGCGCGAGAAGGCGGAGAGCATGCTGCGGAACGACTCGCTGA
GCTCCGATCAGTCCGAGTCCGTGCGGCCATCCCCGCCAAGCCTCACCGGCCAAGCGGGGAGGCAAGAG
ACGTCAGATGTCGGTGTGAGCAGCTCGGAGGAGGAGGGCGTGTCCACACCGGAGTACACGAGCTGCGAGGAC
GTGGAGCTGGAGAGCGAGAGCGTGTGAGCGAGAAAGGTGACTTGGATTACTACTGGTTGGATCCCGCCACGT
GGCACAGCAGGGAAACGTGCGCTATCAGTTTCGCATCCTGTAACGTGGCAGCCGTCTAAAGAGGGGAGATCG
ACTAATCGGCCGTGTTATTTCTTAACAAAAGAACAACCATGCCCAAAGAATCAGGTGCATTATTGGGTCTG
AAGGTGGTTGGAGGAAAAATGACGGACTTAGGGCGCCTTGGTGTCTTTCATCACCAAAGTAAAGAAGGGCA
GCCTGGCAGACGTCGTCCGACACCTAAGAGCAGGGGACGAAGTCTTAGAGTGGAAATGGTAAACCCCTGCC
GGGAGCAACAACGAAGAAGTTTACAACATTATCTTAGAATCAAAATCAGAACCTCAAGTTGAGATTATT
GTTTCAAGGCTATTGGTGACATCCCCAGGATCCCTGAGAGTCCCATCTCCCTGGAGTCCAGTCCAGTCAA
GTTCCTTTGAATCTCAGAAAATGAAAAGGCCCTTCTATTTCTGTTATTTCTCCAACCGCCCTGGAGCTCT
GAAAGATGCCCCACAAGTCTTACCAGGGCAACTCTCAGTGAAGCTATGGTATGATAAAGTGGGGCACCAG
CTGATTGTAAATGTTCTACAAGCAACAGATCTACCCCTTAGAGTAGATGGCCGTCCCAGGAATCCCTATG
TAAAAATGTATTTCTTCCAGATAGAAGCGACAAAAGTAAAAGGAGAACCAAAACAGTAAAGAAACTTCT
AGAGCCAAAATGGAACCAGACATTTGTCTACTCACACGTACATCGTAGAGATTTTCGAGAGCGAATGTTA
GAGATTACCGTGTGGGACCAGCCGAGAGTACAGGACGAAGAGAGTGAATTTCTTGGAGAGATCCTCATAG
AGTTGGAAACAGCGCTTTTAGATGATGAGCCCATTGGTATAAACTCCAGACACATGACGAATCTTCACT
ACCTCTGCCTCAGCCATCACCGTTCATGCCAGGGCGGCATATTCATGGAGAGAGCTCCAGCAAAAAGCTA
CAAAGATCTCAGCGAATCAGTGATAGTGACATCTCAGATTATGAGGTTGATGATGGTATTGGAGTAGTGC
CTCCAGTGGGTTATAGAGCTAGTGCTAGAGAGAGTAAAGCAACCACGTTAACAGTGCCAGAGCAACAAAG
AACTACACATCACCGCTCACGTTCCGTGTCTCCTCATCGCGGCATGATCAGGGAAGGCCCTCGTTACGT
TTACCAAATGTGCCATTACAGAGGAGCTTAGATGAAATTCATCCAACACGAAGGTACGTTCTCCAAACC
GACACCATGATGCTTCCCAGAGCCGCGCCATCAGATCCAGACATGTGGAAAGTCAATATTCTCAGAGA
GCCAGACAGTGAGCTTCTCATGCTGCCAGAGCAAAAACGAGGACGAAGTGCAGAAAAGCTACACATGACC
AGTGAACGTCAGCCCTCTCTTGACAGGGCTAGGAGTGCTAGTACCAACTGCTTGAGACCAGATACTAGTT
TGCATTCACCAGAACGAGAAAGGCACTCCAGAAAAGTCTGAAAAGATGTAGCATCCAAAAACAGTCTAGGAA
AGGCACAGCCTCTGATGCAGACAGAACGCACCGACAAGGAAGCCCAACCCAGTCTCCTCCAGCAGACACA
TCCTTCGGCAGTCCCGTGGAAAGACAGCTCCACAGGTGCCAGTTCGAAGCGGCAGTATAGAACAAGCAA
GCTTAGTAGTGGAGGAGCGAACGAGACAGATGAAAAGTAAAAGTTTACCAGATTTAAGCAGACAACAGGGTC
TGGGTCTAGTCAAGAACTTGACCACGAGCAATACTCCAAGTACAACATACATAAAGATCAGTACAGAAGC
TGTGATAACGCGTCTGCCAAGTCTTCAGATAGTGATGTGATGATGTCAGTGTGTCGCCCATTTCCAGAGCCAGCA
GTACCTCACGCCTCAGCAGCACAAGCTTTATGTGAGAGCAGTCTGAGCGCCCCAGGGGTAGGATCAGTTC
ATTTACCCCCAAAATGCAAGGCAGACGGATGGGGACTTCAGGAAGAGCCATCATCAAGAGCACCAGTGT
AGTGGAGAGATATATACACTGGAACGTAATGACGGTAGCCAGTCCGACACGGCCGTAGTACCCTCGGAG
CCGGTGGAAAGAAACGAAGATCCAGCCTGAGCGCCAAAAGTGGTAGCCATTGTGTCTCGAAGAAGCAGGAG
CACGTCACAGCTCAGCCAGACAGAGTCCGGCCACAAGAAGTTGAAAAGCACCATCCAGAGGAGTACGGAA
ACAGGAATGGCAGCTGAAAATGCGGAAGATGGTGAGACAGCCGAGCCGGGAGTCCACGGATGGCAGCATCA
ACAGTTATAGCTCGGAAGGAAACTTGATATTTCTGGAGTTCGAGTAGGACCCGACAGTCAGTTCAGTGA
TTTCTTGTGATGGGTTGGGACCAGCGCAGCTCGTTGGCCGTGAGACGCTCGCCACCCCGGCCATGGGCGAT
ATCCAAATCGGGATGGAGGATAAGAAGGGTCAGTTGGAGGTTGAGGTTATCAGAGCCCGGAGCCTTACAC
AAAACCTGGTTCCAAATCTACACCCGCTCCCTATGTGAAAAGTATATCTTTTGGAAAATGGAGCCTGTAT
TGCCAAAAGAAAGACAAGAATTGCACGGAAAACCTCTCGATCCTTTGTATCAGCAGTCCCTGGTTTTTGTAT
GAAAGTCCACAGGGTAAAGTTCTTCAGGTGATTGTCTGGGGTACTATGGAAGAATGGACCACAAATGCT
TTATGGGTGTGGCTCAAATCTTGTGGAAGAACTTGATCTATCCAGCATGGTGTATTGGATGGTATAAAT
GTTCCCTCCGCTCCTCACTGGTGGATCCCACTCTCGCTCCCTGACCCGCGGGCTTCCCAATCATCTCTG
GAAAGTACTTCCGGCCCTCCCTGCATCCGGTATAGTAAACTCTATCCTTCCAGCAAACTCATACTT
CAGGATAATTATCAGAACCAGATTATTTATGATCAAGAGCATTGTTGGAGACAGACAATCAACTTGTGT
TTTGCCGTGTAGTAGTTTTTCGATAATATGTCCAAATTGTTGTTTAAAATATGGCTTCATATGACAGAACA
AAGCAAGTCAAGTCAAAATTCAGTAAGAACGGACATGCTAGTGAGAGCCACTTCACACTTCTTGCAAATA
GGAAAACAAAAGAGGAAACCTCAAATTCACACACACACACATAACACACCAAATTTGAACAAACTGGAA
ATTCTCACTCTGTGAAAAGGTGTACTTCACATGTTTCTGCACAGACCACAAGCAGTGTGTTTCCCTAGT

GTTTGAGATTCTTCAGTTCTGTGTGCTTTTCGTTGTTTGTGTGCTGTTTGCTGATTCTTTTTGCCCCGTTG
 CCTCTCTTTCTCTGTCTTCATTGTATTTATTATTTCCGCTAGCTTTTTTTTTTTTTCATTTTTTTTTTGTCTT
 TGTCTTTCTTTGCTTTGCCATGACAGGATTAGGTGGTGTAAACAGAGACTGCTTC

3.8.1.2 RIM1 α PROTEIN (*RATTUS NOVERGICUS*)

MSSAVGPRGPRPPTVPPPMQELPDLSHLTFEERNIIMAVMDRQKEEEEKEEAMLKCVVRDMAKPAACKTP
 RNAESQPHQPLNIFRCVVCVPRKPSSEEGGPERDWRLHQOFESYKEQVRKIGEEARRYQGEHKDDAPTCCG
 ICHKTKFADGCGHLCSYCRTKFCARCGGRVSLRSNNEDKVVMMVCNLCRKQOEILTKSGAWFFGSGPQQP
 SQDGTLSDTATGAGSEVPREKKARLQERSRSQTPLSTAAVSSQDTATPGAPLHRNKGAEPSQQALGPEQK
 QASRSRSEPPRERKKAPGLSEQNGKGGQKSERKRVKSVVQPGEGIADERERKERRETRRLEKGRSQDYS
 DRPEKRDNGRVAEDQKORKEEYQTRYRSDPNLARYPVKAPPEEQQMRMHARVSRARHERRHSDVALPHT
 EAAAAAPAEATAGKRAPATARVSPPEPRARAAAAQPPTEHGPPPPRPAPGPAEPPEPRVPEPLRKQGR
 DPGSAVLLRKAKREKAESMLRNDLSLSDQSESVRPSPPKPHRPRKGGKRRQMSVSSSEEEGVSTPEYTS
 EDVELESESVSEKGDLDYYWLDPATWHSRETSPISSHPVTWQPSKEGDRLIGRVLNKRRTTMPKESGALL
 GLKVVGGKMTDLGRLGAFITKVKKGLADVGHLAGDEVLEWNGKPLPGATNEEVYNIILESSEKSEQVE
 IIVSRPIGDIPRIPESSHPPLESSSSSFESQKMERPSISVISPTSPGALKDAPQVLPGLSVKLWYDKVG
 HQLIVNVLQATDLPPRVDGRPRNPYVKMYFLPDRSDKSKRRTKTVKKLLEPKWNQTFVYSHVHRRDFRER
 MLEITVWDQPRVQDEESEFLGEILIELETALLDDEPHWYKLOTHDESSLPLPQSPFMPRRRIHGESSK
 KLQRSQRISDSDISDYEVDDGIGVPPVGYRASARESKATTLTVPEQORTTHHRSRSVSPHRGDDQGRPR
 SRLPNVPLQRSLEIHPTRRSRSPTRHHDASRSPADHRSRHVESQYSSEPDSELLMLPRAKGRSAESLH
 MTSELQPSLDRARSASTNCLRPDTSLSHSPERERHSRKSERCSIQKQSRKGTASDADRTHRQGSPTQSPPA
 DTSFGSRRGRQLPQVPVRSISIEQASLVVEERTQMKVVKVHRFKQTTGSGSSQELDHEQYSKYNHDKDY
 RSCDNASAKSSSDVSDVSAISRASSTSRLSSTFSMSEQSERPRGRISSFTPKMQGRRMGTSGRAIKST
 SVSGEITYTLERNDGSQSDTAVGTVGAGGKRRSSLSAKVVAIVSRRSRSTSOLSQTESGHKKLSTIQRS
 TETGMAAEMRKMVRQPSRESTDGSINSYSSEGNLIFPGVRVGPDSQFSDFLDGLGPAQLVGRQTLATPAM
 GDIQIGMEDKVLQVIEVEVIRARSLTQKPGSKSTPAPYVKVYLLENGACIAKKKTRIAKRTLDPLYQQSLV
 FDESPQKVLQVIVWGDYGRMDHKCFMGVAQILLEELDLSSMVIWYKLFPPSSSLVDPPTLAPLTRRASQS
 SLESSGPPCIRS

3.8.2 RIM3 γ

3.8.2.1 RIM3 γ cDNA (*RATTUS NOVERGICUS*)

CCTGTCTCTCTGACTGGATTTCGTTATCATGACCCTGGATTCTGGCCATACTCAAGAATTAGCACCTCGG
 GCTTGGCAGATATAAGTCCAAATCCCAGGAGAAGATCTGATTGGCTCTGAGGGACTTAGGTGCTACTCT
 GAACCACCCAGCTTTAATCTGCTGGGAGGGATCACAAGGTGAGATGTGAAGGAGGCTCCTGGAACCTTCC
 TCTGGTGTGTGCGTGGGTCACTATTAGCCAGATCCTGTGCATCACATTGCTTCCCCCTGGAAGCCTGCCCT
 GATTGCCTTTACCTTCTTCTCTGAAAATCGGTGTCTCAACAGAAGTGAAGCTCTGTGCAGACTTGGGGCT
 GTGCTGTTGAGAGACACAGCCCCTTGTGATGCGGAGCGTACACAGCAGACTCAGCAACTCGAATTGCCCT
 GAAGCCCTGCCATCCTGGGGACCATGTTTAACGGGGAGCCTGGTCCAGCCTCGGCTGGGGCCTCCAGGAA
 TGTAGTGAGGAGCTCCAGCATCAGCGGTGAGATCTGTGGATCCCAGCAAGCCGGAGGCGGGGCCGGGACC
 ACCACAGCCAAGAAACGGCGCAGCAGCCTGGGCGCCAAGATGGTGGCTATTGTGCGCTTGACCCAGTGGA
 GCAAAAGCACACTGCAGCTCCCCAGCCTGAAGGGGCCACCAAGAAGCTGCGCAGCAACATTGACGGAG
 CACAGAGACGGGCATTGCCGTGGAGATGCGGAGCCGTGTAACCCGCCAGGGCAGCCGGGAGTCTACCGAT
 GGGAGCACCACAGCAACAGCTCCGAGGGCACGTTTATTTTCCCACACGGCTTGGAGCTGAAAGCCAGT
 TCAGTGACTTTCTGGATGGCCTGGGACCAGCCAGATAGTGGGACGACAGACACTGGCCACACCCCCAT
 GGGAGATGTGCACATTGCCATCATGGACCGGAGTGGCCAGCTGGAGGTAGAAGTGATTGAAGCTCGGGGC
 CTGACCCCCAAACCAGGCTCCAAATCCCTCCCAGCCACCTATATCAAGGCTTACCTGCTGGAGAACGGGG
 CATGTGTGGCCAAGAAAAGACAAAGGTGGCCAAGAAGACTTGTGATCCCTTGTACCAGCAAGCTTTGCT
 CTTTGTATGAGGGGCCCAAGGCAAGTTCTACAGGTGATCGTCTGGGGAGACTATGGCCGTATGGACCAC
 AAGTGCTTATGGGTATGGCCAGATCATGACTGGACGAGCTGGACCTGAGTGTGCTGTGGTCACTGGTGGT
 ACAAATCTTCCCCACATCCTCTGTGGCCGACTCCACACTTGGATCCCTCACCAGGCGCCTGTCTCAGTC
 CTCCTTGGAGAGTGCCACCAGCCCCCTCGTGCTCCTAAGGACCTCGATGAAGACAAGAGGCCAGGGCTAT
 TGGGGGAAGGGAGCCTGCTGGACCCACCACCCCTGTACATAGTCTCCATGACCTTCTGGACCCCTTACC
 CTGCTGCATGCCTGTGGCCACTGGGCTTGTCCCAGCTGGCAGTGGAGACTGTAGTGTGTGTCTGTGTGTC
 TCTCTCTGTGTATGTGTGTGTGTATGTGTGTGTGTTGAGCTTGAACGCTTTCTTTATTGATGGCG

3.8.2.2 RIM3 γ PROTEIN (*RATTUS NOVERGICUS*)

MFNGEPGPASAGASRNVVRSISSISGEICGSQQAGGGAGTTTAKKRRSSLGAKMVAIVGLTQWSKSTLQLP
 QPEGATKKLRSNIRRSTETGIAVEMRSRVTRQGSRESTDGSTNSNSSEGTFIFPTRLGAESQFSDFLDGL
 GPAQIVGRQTLATPPMGDVHIAIMDRSGQLEVEVIEARGLTPKPGSKSLPATYIKAYLLENGACVAKKKT
 KVAKKTCDPLYQQALLFDEGPQGVVQVIVWGDYGRMDHKCFMGMAQIMLDELDSLAVVTGWYKFFPTSS
 VADSTLGSLTRRLSQSSLESATSPSCS

3.8.3 RIM4 γ

3.8.3.1 RIM4 γ cDNA (*RATTUS NOVERGICUS*)

ATGGAGCGCTCGCAGAGCCGCCTCAGCCTGTCCGCCTCCTTCGAGGCGCTCGCCATCTACTTCCCCTGCA
 TGAACCTCTTCGATGATGAGGACGCAGCAGACAGCCGGAGGCTGAAGGGTGCCATCCAGAGAAGCACAGA
 GACAGGGCTGGCCGTGGAGATGCCAGCCGGACGTTACGCCAAGCCAGCCATGAGTCCATCGAGGACAGC
 ATGAATAGCTATGGCTCAGAGGGCAACCTGAACTATGGAGGAGTTTGTCTAGCTTCGGATGCCAGTTCA
 GTGACTTCTGGGGAGCATGGGGCCAGCACAGTTTGTGGGCCGCGAGACCCTGGCTACCACACCCATGGG
 GGGTGTGGAGATCGGTTTACAGGAGCGGAACGGTCAGCTGGAGGTGGACATCATCCAGGCACGCGGGCTG
 ACTGCCAAGCCAGGCTCGAAGACACTGCCAGCTGCCTATATCAAGGCCTATCTGCTGGAAAATGGTGTCT
 GCATTGCCAAGAAGAAGACCAAGTGGCCCGCAAGTCACTGGACCCATTGTACAACCAGGTGCTTCTGTT
 TCCTGAGAGTCCCCAGGGCAAAGTCTGCAGGTAATTGTGTGGGGAAACTACGGACGAATGGAGCGGAAG
 CAGTTCATGGGCGTGGCTCGAGTGTCTGGAGGAACTGGACTTGACCACCCTGGCCGTGGGTTGGTACA
 AGCTCTTCCCCACCTCCTCCATGGTGGACCCAGCCACAGGTCCCCTGCTTCGGCAGGCATCCCAGCTGTC
 CCTCGAGAGCACCGTGGGGCCCTGTGGCGAGCGATCTTAA

3.8.3.2 RIM4 γ PROTEIN (*RATTUS NOVERGICUS*)

MERSQSRLSLSASFEALAIYFPCMNSFDEDAADSRRLKGAIQRSTETGLAVEMPSRTLQASHESIEDS
 MNSYGSEGNLNYGGVCLASDAQFSDFLGSMGPAQFVGRQTLATTPMGGVEIGLQERNQLEVDIIQARGL
 TAKPGSKTLPAAAIKAYLLENGVCIAKKKTQVARKSLDPLYNQVLLFPESPQGVVQVIVWGNVGRMERK
 QFMGVARVLLLELDLTTLAVGWYKLFPTSSMVDPATGPLLRQASQLSLESTVGPCCGERS

3.8.4 Protein alignment

| | |
|------|---|
| RIM1 | MSSAVGPRGPRPPTVPPPMQELPDLSHLTEEERNIIMAVMDRQEEEEKEEAMLKCVVRDMAKPAACKTPRNAESQPHQP |
| RIM3 | ----- |
| RIM4 | ----- |
| | |
| RIM1 | PLNIFRCVVCVPRKPSSEEGGPERDWRLHQQFESYKEQVRKIGEEARRYQGEHKDDAPTGGICHKTKFADGCGHLCSYCRT |
| RIM3 | ----- |
| RIM4 | ----- |
| | |
| RIM1 | KFCARCGRVSLRSNNEKVVMMVCNLCRKQQEILTKSGAWFFGSGPQQPSQDGLSDTATGAGSEVPREKKARLQERSR |
| RIM3 | ----- |
| RIM4 | ----- |

RIM1 SQTPLSTAAVSSQDTATPGAPLHRNKGAEPSQQALGPEQKQASRSRSEPPREKKA PGLSEQNGKGGQKSERKRVPKSVV

RIM3 -----

RIM4 -----

RIM1 QPGEGIADERERKERRETRRLEKGRSQDYSDRPEKRDNGRVAEDQKQKKEEYQTRYRSDPNLARYPVKAPPEEQMRMH

RIM3 -----

RIM4 -----

RIM1 ARVSRARHERRHSDVALPHEAAAAAPA EATAGKRAPATARVSPPESPRARAAAQPTEHGPPPPRPAPGPAEPPEPRV

RIM3 -----

RIM4 -----

RIM1 PEPLRKQGRLDPGSAVLLRKAKREKAESMLRNDLSLSDQSESVRPSPPKPHRPKRGGKRRQMSVSSSEEEGVSTPEYTSC

RIM3 -----

RIM4 -----

RIM1 EDVELESESVSEKGDLDYYWLDPATWHSRETSPISSHVPTWQPSKEGDR LIGRVILNKRTTMPKESGALLGLKVVGKMT

RIM3 -----

RIM4 -----

RIM1 DLGRLGAFITKVKKGLADVVGHLAGDEVLEWNGKPLPGATNEEVYNIILESKSEPQVEIIVSRPIGDI PRIPESHPP

RIM3 -----

RIM4 -----

RIM1 LESSSSSFESQKMERPSISVISPTSPGALKDAPQVLPQQLSVKLWYDKVGHQLIVNVLQATDLPPRV DGRPRNPFVKMYF

RIM3 -----

RIM4 -----

RIM1 LPDRSDKSKRRTKTVKKLLEPKWNQTFVYSHVHRRDFRERMLEITWVDQPRVQDEESEFLGEILIELETALLDDEPHWK

RIM3 -----

RIM4 -----

RIM1 LQTHDESSLPLPQPSFMPRRHIHGESSSKLQORSQRISDSDISDYEVDDGIGVPPVGYRASARESKATTLTVPEQORT

RIM3 -----

RIM4 -----

RIM1 THHRSRSVSPHRGDDQGRPRSRLLPNVPLQRSLEIHPTRRSRSPTRHHASRSPADHRSRHRVVSQYSSSEPDSELLMLPRA

RIM3 -----

RIM4 -----

RIM1 KRGRSAESLHMTSELOPQLDRARSASTNCLRPDTSLHSPERERHSRKSERCISIQKQSRKGTASDADRTHRQGSPTQSPPA

RIM3 -----

RIM4 -----

RIM1 DTSFGSRRGRQLPOVPVRSGSIEQASLVVEERTROMKVKVHRFKQTGSGSSQELDHEQYSKYNIHKDQYRSCDNASAKS

RIM3 -----

RIM4 -----

RIM1 SDDSDVSDVSAISRASSTSRSSSFMSEQSERPRGRISSTPKMQGRRMGTSGRAIIKSTSVSGEIIVTLERNDCSQSDTA

RIM3 -----MFCNCEPQPASAG-----ASRNVVRSSSISGEICGSQQAGG-----G

RIM4 -----MERSQS-----

RIM1 VGTVEAGGKKRRSSLSAKVVAIV--SRRSRSTSOLSQTESGKPKLKSIIQRSTETGVAAEMR--KVMRQPSRESTDGSINS

RIM3 AGTTTA--KKRRSSLGAKMVAIVGLTQMSKSTLQLPQPEGATKKLRSNIRRSTETGLAVEMRSRVTRQGSRESTDGSINS

RIM4 -----RLSLSASFETAIYFPCMNSFDEDEDAD--SRLKGAIIQRSTETGLAVEMPSRTLRQASHESIEDSMNS

RIM1 YSSEGNLIFPEVVRVGPDSQFSDFLDGLGPAQLVGRQTLATPAMGDIQIGMEDKKGQLEVEVIRARSLTQKPGSKSLPAPY

RIM3 NSSEGNLIFPEVVRVGPDSQFSDFLDGLGPAQLVGRQTLATPMPGDVEIAIMDRSGQLEVEVIEARGLTQKPGSKSLPAPY

RIM4 YGSEGNLNYGVVCLASDAQFSDFLGSMPAQVGRQTLATPMPGGVEIGLQERNQGLEVDIICARGLTAKPGSKTLPAAY

RIM1 VKVYLLENGACTIAKKKTRIAKRTLDPLYQOQLVFDSEPOGKVLQVIVWGDYGRMDHKCFMGVAQILLEELDLSMVIQWY

RIM3 IKAYLLENGACVAKKKTKVAKKTCDFLYQOQLVFDSEPOGKVLQVIVWGDYGRMDHKCFMGVAQIMLDELDSLAVVTQWY

RIM4 IKAYLLENGVCIAKKKTKVARKSLDPLYNOQLVFDSEPOGKVLQVIVWGNVGRMERKQFMGVARVLLLELDLTLAVGWY

RIM1 KLFPPSSSLVDPTLAPLERRASQSSLESSESGPFCIRS

RIM3 KLFPTSSVADSTLGSLETRRLSQQSSLESATSPSCS--

RIM4 KLFPTSSMVDPATCPLELROASQLSLESTVGFCEGERS

3.9 *URLs*

| | |
|----------|---|
| BLAST | http://blast.ncbi.nlm.nih.gov/Blast.cgi |
| ClustalW | http://www.ebi.ac.uk.clustalw/index.html |
| Dialign | http://bibiserv.techfak.uni-bielefeld.de/dialign/ |
| ENSEMBL | http://www.ensembl.org/ |
| LOctree | http://cubic.bioc.columbia.edu/cgi-bin/var/nair/loctree/query |
| NCBI | http://www.nlm.nih.gov/ |
| NucPred | http://www.sbc.su.se/~maccallr/nucpred/cgi-bin/single.cgi |
| pTARGET | http://bioapps.rit.albany.edu/pTARGET |
| T-coffee | http://tcoffee.vital-it.ch/cgi-bin/Tcoffee/tcoffee.cgi/index.cgi |

4 METHODS

4.1 *Molecular biological methods*

4.1.1 Preparation of competent bacteria

4.1.1.1 ELECTROCOMPETENT

A single colony of the desired bacterial strain (DH5 α or Stbl2) was inoculated in 100 ml LB medium and incubated while shaking over night at 37°C. Cells were diluted 1:100 in one liter of LB-medium and shaken at 37°C until an OD₆₀₀ of 0.5 to 0.7 was reached. Cells were recollected by centrifugation (15 min at 4000 x g_{max}) at 4°C and resuspended in one liter of ice-cold 10% glycerin in sterile H₂O. Cells were washed with 0.5 and 0.25 liters of 10% Glycerin in water, and subsequently they were resuspended in 4 ml of 10% glycerin, aliquoted, flash frozen in liquid Nitrogen, and stored at -80°C.

4.1.1.2 CHEMICALLY COMPETENT

A single colony was inoculated in 25 ml LB medium and incubated for 6-8 hours at 37°C and 250 rpm. 2 ml from the starter culture were added to 250 ml LB medium and incubated overnight at 20°C and 100 rpm. When the bacterial culture reached an OD₆₀₀ of 0,55, it was cooled down on ice for 10 minutes. The ice-cold bacteria culture was centrifuged 10 minutes by 2500 rpm and 4°C. The pellets were resuspended in 80 ml Inoue-transformation buffer (Inoue *et al.*, 1990), centrifuged again and resuspended in 20 ml Inoue buffer. 1,5 ml DMSO were added to the cell suspension, which after careful mixing was aliquoted on a liquid nitrogen bath.

4.1.2 Transformation

4.1.2.1 CHEMICAL-TRANSFORMATION

50 µl of competent bacteria were thawed on ice. An appropriate amount of DNA, 5 µl of a ligation reaction or 1 µl DNA for retransformation of plasmid DNA, was added and together with the cells incubated for 20 minutes on ice. Afterwards the transformation reaction was heat shocked at 42°C for 42 seconds and directly chilled on ice. 200 µl LB-Medium were added and incubated for 45 minutes to 1 hour at 37°C in a thermo shaker. Subsequently, the cells were cautiously plated on selection plates.

4.1.2.2 ELECTROPORATION

20 µl of competent bacteria were thawed on ice. An appropriate amount of DNA, 1 µl ligation reaction, was added, mixed and incubated for one minute on ice in an electroporation cuvette (0.1 cm, BioRad). Subsequently, an electric pulse (Micropulser electroporator, BioRad) of 1.80 kV was administered. Then the cells were immediately removed from the cuvette with 200 µl LB-Medium and allowed to recover for 45 minutes to 1 hour at 37°C in a thermo shaker. After recovery, the cells were carefully plated on selection plates.

4.1.3 Bacteria culture

To cultivate *E. coli* strains, LB medium was inoculated with bacteria (colony from an agar plate, glycerol stock or preparatory culture) and agitated for 12-16 h at 37°C and 200 rpm, unless otherwise stated. The bacteria were preserved as colonies on agar plates at 4°C up to 6 weeks, or as glycerol stock (50% glycerol in LB medium w/o) at -80°C for long-term storage.

4.1.4 DNA plasmid purification

Purification of plasmid DNA was performed using commercial kits (“mini”, “midi” and “maxi” purification kits), following the manufacture’s instructions. DNA concentration was determined by spectrophotometric analysis, according to the extinction coefficient at 260 nm for double stranded DNA: 1 OD₂₆₀ = 50 mg/ml.

Plasmid mini preparation was used for restriction analysis and sequencing of clones after ligation. Plasmid midi-kit was employed to prepare DNA for digestion, cloning and cell culture transfection. For virus production and neurons transfection, endotoxin-free maxi kit (Quiagen GmbH, Germany) preparation was used to obtain high quality DNA.

4.1.5 Restriction digest, dephosphorylation and ligation

To subclone fragments into the appropriate vectors, both vector and insert were digested using restriction endonucleases for 2-3 hours at 37°C, or overnight. To prevent self ligation, the cut vector DNA was dephosphorylated using 5 units of shrimp alkaline phosphatase (SAP) for one hour at 37°C. T4 DNA ligase was used to ligate both sticky and blunt DNA ends.

For a typical ligation reaction, 100ng of vector DNA and insert were used at a molecular ratio of 1:3. The ligation reaction was performed at 37°C for one hour or at 16°C overnight. TA cloning of PCR products into TOPO-TA, CT-GFP TOPO and NT-GFP TOPO vectors (Invitrogen, Carlsbad, CA) was performed according to manufacturer’s instructions.

To increase the colony yield of the ligation, the DNA was precipitated and the total amount of precipitated DNA was resuspended in 2-5 µl and transformed in competent bacteria.

4.1.6 DNA precipitation

The volume of DNA was adjusted to 400 μ l and subsequently precipitated for at least 15 minutes at -80°C in the presence of sodium acetate (3.5 M, 35 μ l) and ethanol (100%, 1 ml). After 30 minutes of centrifugation at full speed a tiny white pellet was visible, which was washed with 70% ethanol before being resuspended in 2-6 μ l distilled water.

4.1.7 DNA sequencing

Sequencing of plasmid DNA was carried out using BigDye Terminator v3.1 cycle sequencing kit (Applied Biosystems) and specific primers (Table 3.7) for each vector. The sequencing PCR reaction was purified via gel filtration on a spin column (DyEx 2.0 spin kit, Qiagen). PCR fragments were separated, monitored and analyzed in a capillary sequencer (Applied Biosystems 3130/xl/ Genetic Analyzer). Sequence analysis was carried out using Lasergene 8 software SeqMan.

4.1.8 PCR product purification and gel extraction

PCR products were purified using commercially available purification kit (MicroSpin Cycle-pure kit, Peqlab). Purification procedure was followed as recommended by the manufacturer with slight modifications at the elution step. DNA was recovered in small amounts of dH₂O or elution buffer (10 mM Tris pH 8.5).

For gel extraction the DNA was fractionated on an agarose gel, visualized under UV light, excised from the gel and purified using commercial kits (MicroSpin Gel extraction kit, Peqlab). The nucleic acid was eluted from the agarose and used for further applications.

4.1.9 Polymerase chain reaction

DNA was amplified using Polymerase chain reaction (PCR). The PCR reaction mix included double-stranded template DNA, single-stranded primers, deoxyribonucleosides (dNTPs), buffer, salt, and high fidelity *Taq*-polymerase or Platinum *Taq*-polymerase (Invitrogen, Carlsbad, CA). PCR reaction mixes were composed as listed below:

| PCR reaction | Volume |
|------------------------------|-----------------------|
| 10x Polymerase Buffer | 2 μ l |
| Magnesium chloride (25 mM) | 1,2 μ l |
| 5' Primer (10 pmol/ μ l) | 0,5 μ l |
| 3' Primer (10 pmol/ μ l) | 0,5 μ l |
| dNTP-Mix (25 mM) | 0,5 μ l |
| Template DNA | 2 μ l (50-500 ng) |
| Polymerase | 0,2 μ l |
| H ₂ O | <i>ad</i> 20 μ l |

Basic PCR cycling parameters were as follows:

| PCR cycle | Temperature | Time |
|------------------------------|-------------|--------------|
| Step 1: initial denaturation | 95 °C | 3 minutes |
| Step 2: denaturation | 95 °C | 30 s |
| Step 3: annealing | 50-60 °C | 40 s |
| Step 4: extension | 68/72 °C | 1 minutes/kb |
| Step 5: final extension | 68/72 °C | 10 minutes |

4.1.10 cDNA preparation

Total RNA was extracted from whole brain or brain regions after homogenization in TRI reagent (Sigma-Aldrich, Germany) using the SV Total RNA isolation system (Promega, Madison, WI). Subsequently mRNA purification was performed using Dynabeads Oligo(dT)₂₅ kit (Invitrogen, Carlsbad, CA).

RNA samples were stored at -80°C or directly used for cDNA preparation. Reverse transcription was carried out using 5 µg of total RNA and the RevertAid™ Premium Reverse Transcriptase (Fermentas GmbH, Germany) with random hexamer primers, or 5 µl of Dynabeads derived mRNA solution with oligo (dT) primers.

4.1.11 Cloning strategies

4.1.11.1 OVEREXPRESSION CONSTRUCTS IN pcDNA3.1, PL26 AND PLENTI LN-EGFP-EF1 α PLASMIDS

Green fluorescent protein (GFP) or red fluorescent protein (mcherry) were amplified by PCR and cloned into the pcDNA3.1 and pL26 vector as described (Fig. 4.1). Full length and deletion sequences of RIM3 γ and RIM4 γ were generated by PCR using suitable primers (Table 3.9), and subsequently inserted into pcDNA3.1 or pL26 modified vectors. For cloning of RIM3 γ , EcoR1 restriction enzyme was used, whereas cloning of RIM4 γ was performed using EcoRI/BamHI restriction sites (Fig. 4.1). The nucleotide sequence of all constructs was verified by DNA sequencing.

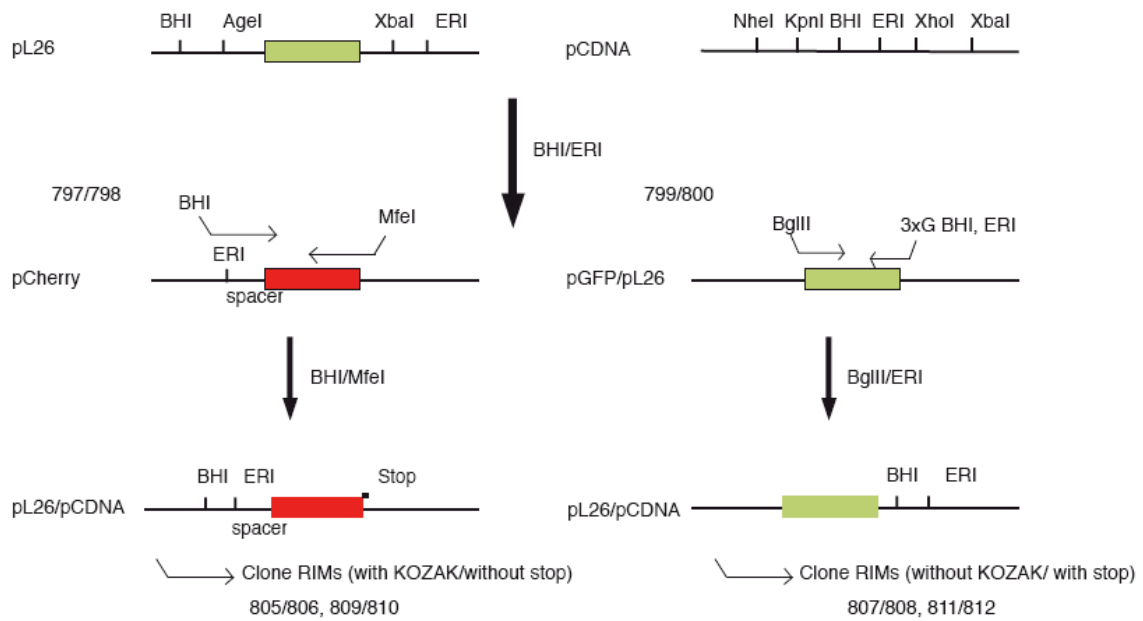


Fig. 4.1 Cloning strategy for pcDNA3.1 and pL26 vectors

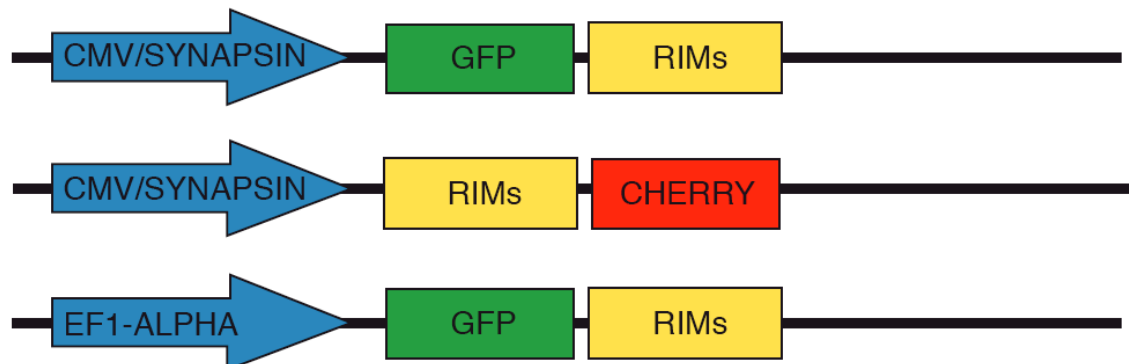


Fig. 4.2 Schematic depiction of the overexpression plasmids

4.1.11.2 CLONING OF shRNA SEQUENCES IN THE PLVTHM VECTOR

For RNAi experiments, two single-stranded DNA oligonucleotides were designed (3.6.3), annealed, phosphorylated and cloned into the pLVTHM vector (Fig. 3.7) using MluI and ClaI restriction enzymes. All constructs were verified by DNA sequencing.



Fig. 4.3 Structural organization of lentiviral shRNA constructs

Cartoon showing the structure of the lentiviral vector used for the cloning of the shRNAs sequences. The pLVHTM cloning vector (Trono Lab) contains a green fluorescent marker (GFP) under the control of the EF1 α promoter, and the shRNA sequence under the control of the H1 promoter *in situ* hybridization.

Radioactive ISH was performed on 12 mm cryosections. Frozen rat brain sections were mounted on silane-coated glass slides, fixed with 4% (w/v) paraformaldehyde in PBS, dried in ascending ethanol concentrations and stored under ethanol until hybridization. The sequences of the ISH probes used, are listed in Table 3.8.

Probes were labeled with [³⁵S]dATP using terminal deoxyribonucleotidyl transferase (Fermentas, St. Leon-Rot, Germany). Each section was hybridized for 15-20 h in 150 μ l hybridization buffer (50 % deionized formamide / 10% (v/v) dextran sulphate / 0.3 M NaCl / 30 mM Tris/HCl (pH 8) / 4 mM EDTA / 1x Denhardt's / 0.4 mg/ml polyadenylic acid / 0.5 mg/ml denatured salmon sperm DNA) containing the amount of radiolabeled probe equating to 400.000 counts. Brain slices were hybridized at 42°C overnight, washed at RT and 57°C for 45 min and dried in ethanol. Afterwards, they were exposed to X-Ray films (KODAK BIOMAX MR; Kodak, Rochester, NY) for two to four weeks and to nuclear track emulsion (NBT2, Kodak) for up to three months.

4.2 Biochemical methods

4.2.1 Generation of peptides antibodies

RIM3 γ and RIM4 γ peptide antibodies were raised against the N-terminal amino acid sequence NH₂-CSKSTLQLPQPEGATK-CONH₂ (RIM3 γ) and NH₂-

CFDDEDAADSRRLKGAIQR-CONH₂ (RIM4 γ) after an epitope analysis (Janin, 1979; Parker *et al.*, 1986) by Pineda antibody service (<http://www.pineda-abservice.de/>). Antibodies were purified from rabbit immunosera by affinity chromatography on a column to which the synthetic peptide was linked covalently.

4.2.2 Western blot

4.2.2.1 PREPARATION OF PROTEIN EXTRACTS

TISSUE PROTEIN EXTRACTION

Rat brain regions, and other tissues were collected at different time points and frozen or directly used for protein extraction. Tissue weight was determined, lysis buffer added (1ml buffer/ 100 mg tissue), and homogenized using an ultrasonicator (UP50H, Hilscher).

CELL PROTEIN LYSATES

To prepare protein extracts from HEK 293T cells, they were transfected with the desired plasmid DNA using lipofectamine 2000 (Invitrogen, Carlsbad, CA). 48 hours post-transfection cells were washed with cold phosphate saline buffer and lysed in 250 ml ice-cold buffer with 2% detergent (SDS), 10 mM EDTA in PBS (pH 7.4) containing a protease inhibitor mixture (Roche).

Protein homogenates from neurons were prepared from 6 well plates after lentiviral infection. The cells were washed, collected with a cell scraper, resuspended in 60 ml lysis buffer, and shortly ultrasonicated.

PROTEIN QUANTIFICATION, ELECTROPHORESIS

Protein concentration of cell and tissue extract samples was determined using a nanodrop (ND-1000). The protein extracts were adjusted to a final concentration of 5mg/ml using 6x SDS-loading buffer and lyses buffer. Samples

were heated to 95°C for 5 minutes, 50 µg protein were loaded and size fractionated on 10% SDS-polyacrylamide gel electrophoresis (PAGE) gels, and transferred to nitrocellulose membrane. Membranes were preincubated for one hour at room temperature (RT) in blocking solution (5% gelatin/ 0,1% Tween/ PBS), and then incubated with the primary antibodies for 1 hour at RT. Secondary antibodies were IR-labeled (Odyssey) and used at a 1:10.000 dilution. The immunoblots were developed with an infrared imaging System (Odyssey, Li-cor).

4.2.2.2 SUBCELLULAR FRACTIONATION OF ADULT RAT BRAIN

Eight Wistar rat brains (4 weeks old) were rapidly dissected, the cerebellum was removed, and the remaining tissue was washed in ice-cold homogenization buffer (0,32M sucrose/100 mM EDTA, 5mM HEPES). The entire isolation procedure was performed at 4°C, all buffers included complete protease block mix (Roche) to avoid proteolysis and instruments used were detergent free. A sample of every isolation step was stored for Western blot analyses.

Pooled brains were desegregated in homogenization buffer (10 ml/brain) using a Teflon-glass mechanical tissue homogenizer and centrifuged for 10 minutes at 3000 rpm (Beckman, J-20). The pellet (P1, nuclear fraction) was discarded and the supernatant (S1, crude synaptosomal fraction) centrifuged at 10.000 rpm (Beckman, J-20) for 20 minutes. The synaptosomal cytosol fraction (S2) was removed and the crude synaptosomal pellet fraction (P2) was resuspended in a small volume, overlaid on a sucrose density gradient and spun for two hours and 24.600 rpm (Beckman, SW28). After centrifugation two different fractions could be distinguished: myelin in the 850/1000 mM interphase and synaptosomes in the 1000/1200 mM. The synaptosomes were carefully collected and divided in two fractions; one was used for postsynaptic densities

(PSD) preparation and the other for synaptic vesicle (SV) and synaptic plasma membrane (SPM) enrichment.

SYNAPTIC PLASMA MEMBRANES

Synaptosomes were lysed by dilution into 10 volumes ice-cold water, and homogenized through 3 strokes at 2000 rpm. Afterwards HEPES-KOH buffer (pH 7,4) was added to a 1% final concentration and centrifuged for 20 minutes at 16.500 rpm (Beckman, SS-34). The resulting pellet contained synaptic plasma membranes (SPM) and the supernatant was again centrifuged for 2 hours at 50.000 rpm (Beckman, 50 Ti), obtaining a pellet containing the synaptic vesicle fraction (SV).

POSTSYNAPTIC DENSITY PREPARATION

Synaptosomes were adjusted to a final volume of 1 ml ice cold homogenization buffer containing 0,5% (w/v) Triton X-100, rotated for 20 minutes and centrifuged 20 minutes at 24.000 x g. The resulting pellet (TX1) was resuspended in 500 ml homogenization buffer containing 1% Triton X-100 (w/v), again rotated and centrifuged for 60 minutes. Supernatant of the 0,5% (w/v) or 1% (w/v) Triton X-100 soluble fraction (TX1 supp and TX2 supp respectively) and the Triton X-100 insoluble fraction of the SPM (TX1 and TX2), together with previous aliquots were analyzed by immunoblotting.

4.3 Cell culture

4.3.1 Eukaryotic cell culture

All cell lines were cultured in humidified incubators supplied with 5% CO₂ at 37°C. Cells were passaged every 3-4 days and plated in a 1:5-1:20 dilution. HEK293T, cells were culture in DMEM 4.5 g/l glucose supplemented with 10% heat inactivated FCS and antibiotics (100 units/ml penicillin and 100 mg/ml

streptomycin). PC12 cells were maintained in the same medium with 10% horse serum and 5% FCS.

4.3.2 Primary cell culture

Primary neurons were prepared as described by (Kavalali *et al.*, 1999) with some modifications.

4.3.2.1 COVERSLIP TREATMENT

The treatment of the coverslip is crucial for neuronal adhesion and survival. Coverslips were backed at least 16 hours by 240 °C. Sterile coverslips were coated overnight by incubation with Poly-L-Lysin (0,1 mg/ml in borat buffer) at 37 °C and subsequently washed three times with sterile distilled water.

4.3.2.2 DISSECTION

The pregnant rat or mouse was sacrificed, and the uterus containing the embryos (E16-E19) removed. Embryo heads were dissected and placed in a Petri dish with iced cold dissection medium (10 mM HEPES in HBSS). The cortex and the hippocampus of every pup were isolated and separately collected in 5 ml dissection solution, trypsin was added to a final concentration of 0,025-1% depending on the amount of tissue, and incubated for 10 minutes at 37 °C. Subsequently, the enzyme solution was gently removed and the hippocampal and cortex preparation were washed twice with ice cold plating medium and once with BME.

4.3.2.3 CULTURE PREPARATION

The tissue suspension was collected in 1 ml BME medium and dissociated by pipetting 50 times trough a blue pipette tip. The cell suspension was collected in a new falcon tube after passing trough a cell filter and resuspended in 4 ml BME. The cells were counted using a Neubauer chamber and diluted to an

appropriate concentration for seeding. After three hours the medium was replaced with fresh BME.

4.3.3 Transient transfection of mammalian cells

4.3.3.1 HEK 293T

HEK 293T cells were transfected to express proteins of interest for Western Blot analyses. Cells were cultured in 10 cm dishes and transfected with plasmid DNA using lipofectamine 2000 reagent (Invitrogen, Carlsbad, CA), when they were 80-90% confluent. The DNA/lipofectamine complex formation was prepared, according to the manufacturers instructions, in serum and antibiotic free medium Optimem (Invitrogen, Carlsbad, CA), but cells were maintained and transfected in DMEM containing 10% FCS, penicillin/streptomycin. 48-72 hours after transfection, medium was discarded. The cells were quickly washed, collected in 500 ml PBS and centrifuged at 4 °C for 5 minutes and 4000 rpm. Cell pellets were conserved by -80 °C or directly lysed for protein extraction.

4.3.3.2 PC12

The transient transfection of PC12 cells was carried out in 24-well culture dishes for immunofluorescence analyses. Cells were plated on poly-L-Lysin coated coverslips at a 40% confluence. Transfection was carried out using lipofectamine 2000 (Invitrogen, Carlsbad, CA). Less transfection reagent was used, as recommended, to decrease toxicity. DNA/lipofectamine complexes were prepared in Optimem and transfection was carried out in PC12 growth medium without antibiotics to increase transfection efficiency. 36 hours after transfection cells were fixated using 4% PFA, washed and mounted using VECTASHILD.

4.3.3.3 PRIMARY NEURONS

Hippocampal primary neurons were cultivated on poly-L-Lysin coated coverslips in 24 wells culture dishes. Transfection was carried out at DIV3-5 using 1 ml lipofectamine 2000 reagent (Invitrogen, Carlsbad, CA) and 1-2 mg DNA. Prior to transfection, 500 ml growing medium (BME) was removed from each well, collected and conserved by 37 °C and 5% CO₂. DNA/transfection reagent complex formation was completed in Optimem and added to the neurons. In order to increase cell survival, neurons were washed with fresh BME 2-3 hours after transfection to avoid lipofectamine toxicity effects. Finally, the previously collected culture medium was added together with fresh medium. Primary neurons were grown till DIV 13-15 and analyzed using confocal microscopy (FV300, Olympus).

4.4 Histological and immunohistochemical methods

4.4.1 Animals and brain sections

The studies were carried out on brains of Wistar rats if not otherwise stated (Charles River, Sulzfeld, Germany). All animal use procedures were carried out in accordance with the European communities Council Directive of 24 November 1986 (86/609/EEC). Rats were anesthetized by Isoflurane (Baxter, Deerfield, IL, USA) inhalation prior to decapitation. If necessary, animals were perfused through the heart before brain removal. Intracardial perfusion of PBS was followed by perfusion of 4% paraformaldehyde solution in phosphate saline buffer.

4.4.2 Immunohistochemical analyses on paraffin sections

4 μm slices were sagittally cut from paraffin embedded brains on a Microm HM 335 E microtom. Brain slices were deparaffinized and rehydrated using xylene, a decreasing ethanol serie of a 100%, 95%, 70% (v/v) and PBS, for 5 to 10 minutes each. For antigen retrieval, brain slices were incubated in citrate buffer and microwaved for 20 min, and afterwards cooled down for 20-30 minutes at RT. After a short rinse with PBS, the slices were permeabilized for 30 minutes in 0.5% Triton X-100 PBS and subsequently blocked in PBS 10% goat serum, 1% BSA, 0,3% Triton X-100. First the silices were incubated with affinity-purified antibodies (Table 3.5) in block buffer overnight at 4 °C in a humidified chamber, followed by washing with PBS and by incubation with fluorescence-labeled or biotin-labeled secondary antibodies and streptavidin-fluorescein incuabation for 1h at RT (Table 3.5). After washing off excess antibody with PBS, slices were covered using vectashield-hard set mounting medium (Vector Laboratories, Inc Burlingame, CA).

4.4.3 Immunohistochemical analyses on cryosections

Isolated brains were sectioned sagittaly and cryopreserved by TissueTek embedding medium (Sakura Finetek Europe B.V., Zoeterwoude, The Netherlands), and directly frozen in liquid nitrogen on an isopentane bad. Sections of 12 μm thickness were cut with a Microm HM 560 Microtom (Microm, Walldorf, Germany), and directly used or conserved at -20°C. Brain slices were fixated in 4% PFA for 30 minutes. After a short rinse with PBS, the slices were permeabilized for 30 minutes in 0.5% Triton X-100 PBS and subsequently blocked in PBS 10% goat serum, 1% BSA, 0,3% Triton X-100. First, slices were incubated with affinity-purified antibodies in block buffer overnight at 4 °C in a humidified chamber, followed by PBS washing and fluorescence-labeled or

biotin-labeled secondary antibodies and streptavidin-fluorescein (Table 3.5) incubation for 1 h at RT. After washing off excess antibody with PBS slices were covered using vectashield-hard set mounting medium (Vector Laboratories, Inc Burlingame, CA).

4.4.4 Immunohistochemical analyses on the Retina

Mouse, rat or bovine eyes were isolated, embedded in Tissue-Tek (Sakura Finetek Europe B.V., Zoeterwoude, The Netherlands), and directly frozen in liquid nitrogen. 10 μm slices were cut with a Microm HM 560 Microtom (Microm, Walldorf, Germany). Eye sections were heat fixated 10 minutes by 60 $^{\circ}\text{C}$, cooled down and blocked for one hour in 1% BSA/PBS. The first antibody was diluted in block solution and incubated overnight at 4 $^{\circ}\text{C}$. Excess antibody was washed off three times ten minutes using iced cold PBS, followed by fluorescence-labeled secondary antibody incubation for one hour at room temperature. After washing excess antibody, the sections were covered using vectashield-hard set mounting medium (Vector Laboratories, Inc Burlingame, CA).

4.4.5 Free-floating immunohistochemical analyses

Wistar rats were anesthetized and perfused transcardially with PBS for 5 minutes, followed by 20 minutes of perfusion with 4% PFA/PBS (pH 7,4). After removal, the brain was postfixed in the same fixative (4 $^{\circ}\text{C}$, 90 minutes) and equilibrated in 30% sucrose for 24 hours. The cerebellum was discarded and the forebrain was embedded in agarose and subsequently cut in 100 μm horizontal sections on a vibratome (Vibrotome 1000, genqe). Free-floating slices were conserved in PBS or immunostained directly.

4.4.6 Immunocytochemistry

Primary cultures of rat hippocampal and cortical neurons 9-15 DIV were quickly washed with PBS and fixed with 4% PFA in PBS for 10-15 minutes at room temperature. After three washing steps with PBS, cells were permeabilized in 0,3 % Triton X-100/PBS for 10 minutes. Directly after permeabilization a blocking step was carried out by incubating the cells in Blocking buffer (10% Goat Serum, 1% BSA, 0.1% Triton X-100 in PBS) for at least 30 minutes, after which a primary antibody containing solution (blocking buffer) was applied and incubated over night at 4 °C. After three washes with PBS, fluorochrome-labeled secondary antibody (Table 3.5) was applied, and incubated for 1 hour at room temperature. Finally, cells were washed 3 times with PBS and coverslips were mounted with the embedding medium using vectashield-hard set mounting medium (Vector Laboratories, Inc Burlingame, CA) and left to dry over night at room temperature.

4.5 *Lentivirus production*

4.5.1 Lentivirus based vector system

The production of functional lentiviral particles is performed by cotransfection of vectors including a packaging vector expressing the structural proteins Gag and Pol as well as most of the viral accessory proteins; an envelope vector expressing heterologous surface glycoproteins (vesicular stomatitis virus, VSV-G); and a transfer vector for heterologous protein expression.

In order to improve the biosafety of the human immunodeficiency virus type 1 (HIV-1) derived expression systems all accessory genes except Tat and Rev were deleted (second generation of lentiviral vectors). Further improvements lead to the third generation of HIV-1 based vectors where the tat gene was

ablated, and the gag/pol and rev genes were placed on two separate expression cassettes (Cockrell and Kafri, 2007).

Transfer vectors used for expression contained the transgene expression cassette as well as the necessary elements required for packaging and reverse transcription. If these vectors were tat-dependent, ie. pLVTHM, second generation of packaging vectors was required (pM2DG, psPAX2). In all other cases the third generation (ViraPower, Invitrogen, Carlsbad, CA) was used.

4.5.2 HEK 293T culture and transfection

Lentiviral particles were produced by transfection of three or four plasmids in HEK 293T cells using lipofectamine 2000 reagent (Invitrogen, Carlsbad, CA). Cells were plated in 10 cm culture dishes a day before, to achieve 50-60% confluency on transfection day. The transfection reaction was performed in Optimem with 30-40 µg DNA including all vectors and 60 µl lipofectamine. Shortly before applying the transfection mix to the cells, the culture medium was replaced with BME.

HEK 293T cells for lentivirus production were only used till passage 40-50, because older passages did not produce the required efficiency.

4.5.3 Viral particle purification

48 hours after transfection, medium containing viral particles was harvested, filtrated through a 45 µm filter and directly used or concentrated. VSV-G derived viral particles could be concentrated by ultracentrifugation at 29600 rpm (SORVALL, 90 SE) for two hours. Pellets were resuspended in 10 µl HBSS when used for *in vivo* experiments and in 200 µl for cell culture approaches. Virus stocks were stored at -80 °C.

4.5.4 *In vivo* injection of lentivirus particles

Newborn rats were anesthetized and immobilized by covering them with ice for 3-5 minutes. Directly afterwards, pups were freehand injected with 1 μ l virus suspension/HBSS in both ventricles, immediately warmed up for recovery, and returned to the mother. To test the effect of the shRNAs *in vivo*, rat brains were analyzed by immunohistochemistry at days p7, p14 and p21. At least 3 rats per group and time point were examined using FITC couple antibody to GFP.

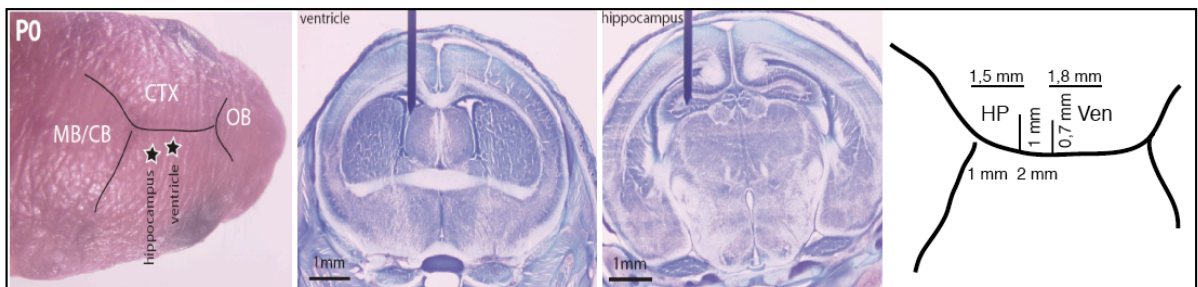


Fig. 4.4 Schematic depiction of the injection of lentiviral particles in the ventricle and Hippocampus

Cartoon showing the coordinates for the correct position of the capillary containing lentivirus particles for the injection procedure. Viral particles were injected in both ventricles or Hippocampi of P0 Wistar rats. (modified from Pilpel *et al.*, 2009).

5 RESULTS

5.1 *RIM3 γ* and *RIM4 γ*

RIMs are multidomain scaffolding proteins specifically enriched at the Active Zone. The RIM protein family consists of 7 members (Wang and Südhof, 2003; Wang *et al.*, 2000), of which RIM1 α and RIM2 α , the isoforms containing the full set of domains, have been studied in most detail. RIM3 γ and RIM4 γ , the smallest members of the RIM protein family, are composed of a C-terminal C2B domain and an isoform specific N-terminal sequence. To date, the localization and function of these truncated RIM variants has not been examined yet.

5.1.1 Localization of RIM3 γ and RIM4 γ

A first step in elucidating the functional role of RIM3 γ and RIM4 γ is to study their cellular and subcellular localization. Therefore, their expression was analyzed at the mRNA and protein level in order to learn if they are present in the same compartments as the α -RIM isoforms.

5.1.1.1 RIM3 γ AND RIM4 γ mRNA EXPRESSION: *IN SITU* HYBRIDIZATION

To study the expression pattern of RIM3 γ and RIM4 γ in the adult rat brain, their mRNA distribution was analyzed by *in situ* hybridization. Therefore, based on sequence alignments of all RIM isoforms, specific oligonucleotides were designed for each isoform (Table 3.8). These radioactively (³⁵S) labeled isoform specific probes were used to detect RIM3 γ and RIM4 γ mRNA in sagittal brain sections of adult rat (p28). Radioactive probes specifically hybridized to the

respective RIM3 γ and RIM4 γ transcripts. The labeling of the mRNA could be abolished by excess addition of unlabeled oligonucleotides in the hybridization mix (data not shown), confirming the specificity of the observed signal (Fig. 5.1, Fig. 5.2).

Negative X-ray film images showed that RIM3 γ and RIM4 γ transcripts in adult rat brain exhibit distinct, but overlapping expression patterns. In the case of RIM3 γ , the strongest mRNA expression was found in the cerebellum and thalamus (Fig. 5.1A). In addition, high expression levels were detected in cortex, olfactory bulb and hippocampus (Fig. 5.1A). The highest expression levels for RIM4 γ were observed in the cerebellum and cortex, followed by the olfactory bulb and hippocampus (Fig. 5.2A).

To allow for an expression analysis on the single cell level, the radioactively labeled sections were dipped in photo-emulsion and developed after two months. Dark field images of emulsion-dipped tissue revealed that cerebellar RIM3 γ is mainly expressed in the granule cell layer, Purkinje cells also expressed RIM3 γ , albeit at low levels. In the cortex, RIM3 γ was predominantly expressed in layers II/III followed by layer V (Fig. 5.1C). In addition, RIM3 γ mRNA was mainly detected in the dentate gyrus (Fig. 5.1D), in thalamus (Fig. 5.1F) and in the olfactory bulb external plexiform layer (Fig. 5.1E).

RIM4 γ showed certain differences in the expression pattern within brain regions. Also at higher resolution the expression pattern of RIM4 γ differed from the one detected for RIM3 γ . In the cerebellum, the highest expression levels of RIM4 γ were found in Purkinje cells (Fig. 5.2B), followed by the granule cell layer. In the cortex, RIM4 γ was uniformly expressed throughout all cortical layers (Fig. 5.2C). In contrast to RIM3 γ , RIM4 γ mRNA levels in the hippocampus were higher in the CA1 region (Fig. 5.2D). In the olfactory bulb, RIM4 γ was highly expressed in the glomerular and plexiform layers (Fig. 5.2E).

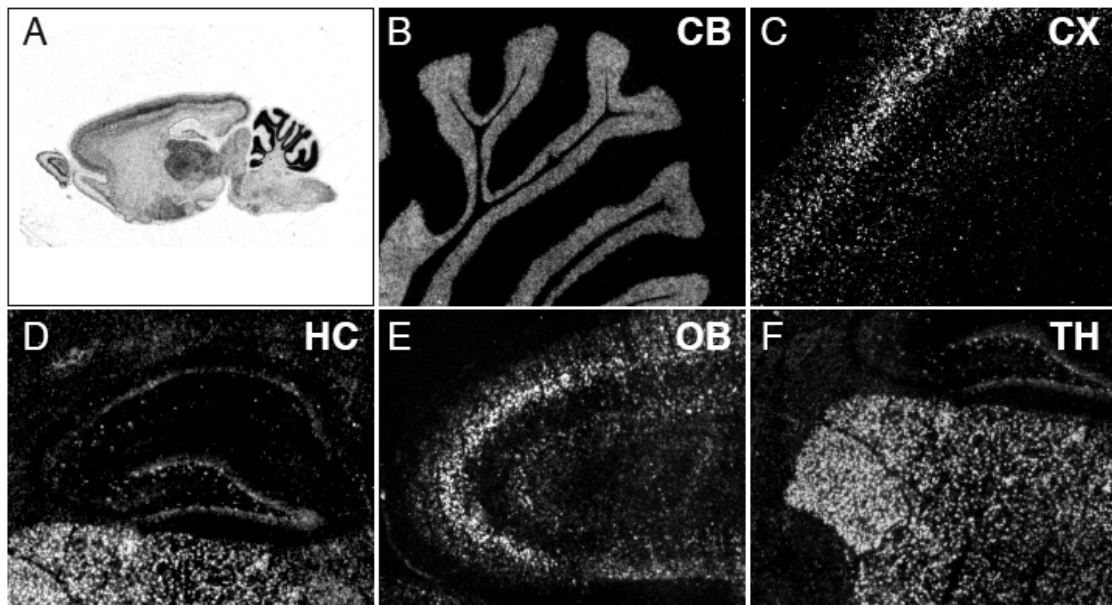


Fig. 5.1 Localization of RIM3 γ mRNA in adult rat brain

A. In situ hybridization micrographs showing RIM3 γ mRNA distribution in the whole brain. RIM3 γ was ubiquitously present in the brain, showing highest expression levels in the cerebellum, cortex, hippocampus, olfactory bulb and thalamus. Negative controls with excess unlabeled oligonucleotides were devoid of signal (results not shown). B-F. Higher resolution pictures of emulsion-dipped sections revealed elevated expression levels in the cerebellar granule cell layer (B), cortical layers II/III and V (C), and gyrus dentatus (D). In addition, a strong signal was detected in the glomerular and plexiform layers of the olfactory bulb (E), as well as in the thalamus (F). Abbreviations: CB cerebellum; CX cortex; HC hippocampus; OB olfactory bulb; TH thalamus.

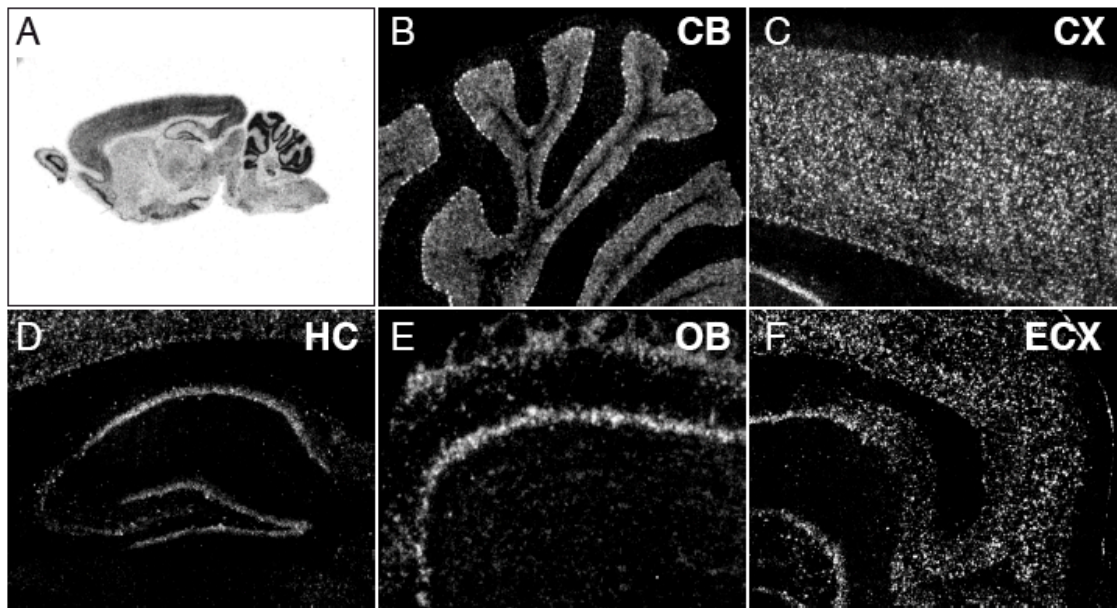


Fig. 5.2 Localization of RIM4 γ mRNA in adult rat brain

A. X-Ray film image showing RIM4 γ transcript distribution in p28 rat brain. RIM4 γ mRNA was found to be ubiquitously distributed. The highest expression levels were detected in cerebellum, cortex, entorhinal cortex, hippocampus and olfactory bulb. Negative controls with excess unlabeled oligonucleotides were devoid of signal (results not shown). B-F. Emulsion-dipped section images revealed high levels of RIM4 γ in the Purkinje and granule cell layer of the cerebellum (B), in all cortical layers (C), as well as in enthorinal cortex (F). In addition, RIM4 γ was strongly expressed in hippocampal CA1 region (D), glomelular and plexiform layers of the olfactory bulb (E). Abbreviations: CB cerebellum; CX cortex; HC hippocampus; OB olfactory bulb; TH thalamus.

5.1.1.2 RIM3 γ AND RIM4 γ PROTEIN EXPRESSION

5.1.1.2.1 Generation and characterization of isoform specific antibodies

RIM3 γ and RIM4 γ exhibit a high degree of sequence homology, even in their isoform specific N-terminal region. In order to study the localization of the two proteins, isoform specific antibodies were generated to allow for specific detection of RIM3 γ and RIM4 γ proteins. RIM3 γ and RIM4 γ polyclonal antibodies were raised against two peptides that had been selected by epitope analysis. The selected sequences, NH₂-CGCGAGTTTAKKRRSSL-CONH

(RIM3 γ) and NH₂-CFDDEDAADSRRLKGAIQR-CONH₂, (RIM4 γ), were localized in the N-terminus of the proteins and did not exhibit homology with other members of the RIM protein family.

To control for the specificity of the antibodies, all members of the RIM protein family were overexpressed in HEK 293T cells and analyzed by Western blotting. No cross-reactivity was detected between either of the newly generated antibodies against RIM3 γ (Fig. 5.3A) and RIM4 γ (Fig. 5.3B) and other members of the RIM protein family.

The newly generated antibodies only reacted with the respective antigens, producing a band of the predicted molecular mass, 32 kDa (RIM3 γ) and 29 kDa (RIM4 γ), and did not recognize other members of the RIM protein family.

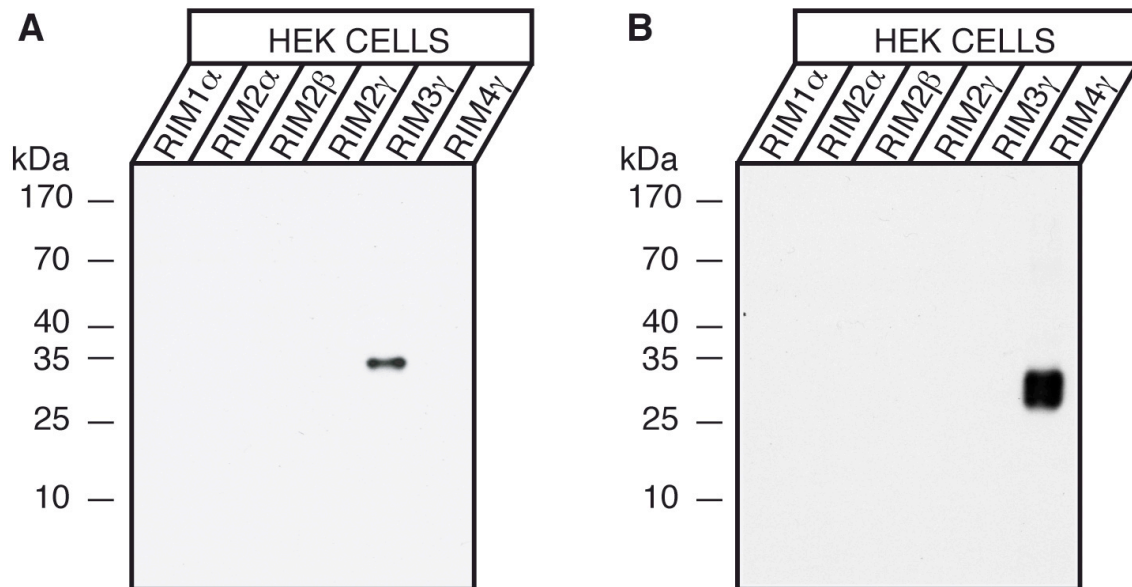


Fig. 5.3 Specificity of newly generated RIM3 γ and RIM4 γ antibodies

Homogenates of HEK 293T cells transfected with the indicated full length RIM expression plasmids were analyzed by immunoblotting with affinity-purified antisera against RIM3 γ (A) and RIM4 γ (B). The two antibodies were specific for the respective isoforms (peptides) they were raised against.

5.1.1.2.2 Tissue distribution of RIM3 γ and rim4 γ proteins

In order to study the localization of both RIM γ -isoforms, homogenates from several tissues of adult rat were assayed by Western blotting. Immunoblotting with RIM3 γ specific antibody revealed a specific 32 kDa band, corresponding to the calculated molecular weight, only in brain (Fig. 5.4). The RIM4 γ antibody also reacted strongly with the brain homogenate fraction, revealing a specific band at the predicted size of 29 kDa (Fig. 5.4). In addition, weak signals were detected in muscle and liver tissues. However, these signals remained after incubation of the blot with antibodies previously preabsorbed with the immunogen (peptid-block), showing these bands to be unspecific (data not shown). Immunoblot analyses revealed a highly restricted expression of RIM3 γ and RIM4 γ as both proteins were exclusively expressed in brain.

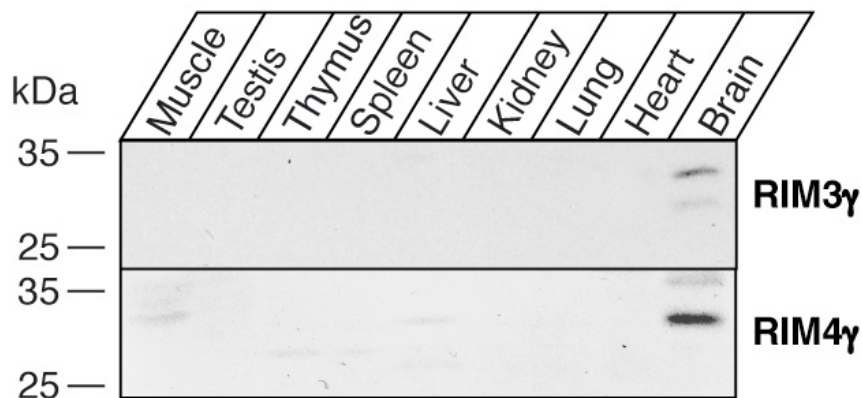


Fig. 5.4 γ -RIMs are brain specific proteins

The indicated adult rat tissues were isolated, homogenized and equal protein amounts were loaded for Western Blot analysis. Specific bands corresponding to the molecular weight of RIM3 γ (32 kDa) and RIM4 γ (29 kDa) were only detected in brain.

5.1.1.2.3 Expression pattern in different brain regions

To confirm the previously observed regional distribution of RIM3 γ and RIM4 γ mRNA at the protein level, various brain regions were isolated and analyzed by immunoblotting. The specificity of the detected bands was controlled by incubating the blots with antibodies previously preabsorbed with the

immunogen (peptid-block). The highest expression levels of RIM3 γ were detected in the cerebellum and olfactory bulb, followed by cortex and hippocampus. RIM4 γ was strongly expressed in cerebellum and cortex, but also in hippocampus and olfactory bulb. Both proteins only showed weak expression in the brainstem (Fig. 5.5).

In accordance with the mRNA expression levels (Fig. 5.1, Fig. 5.2), RIM3 γ and RIM4 γ proteins could be detected ubiquitously throughout the brain, albeit at diverging expression levels (Fig. 5.5).

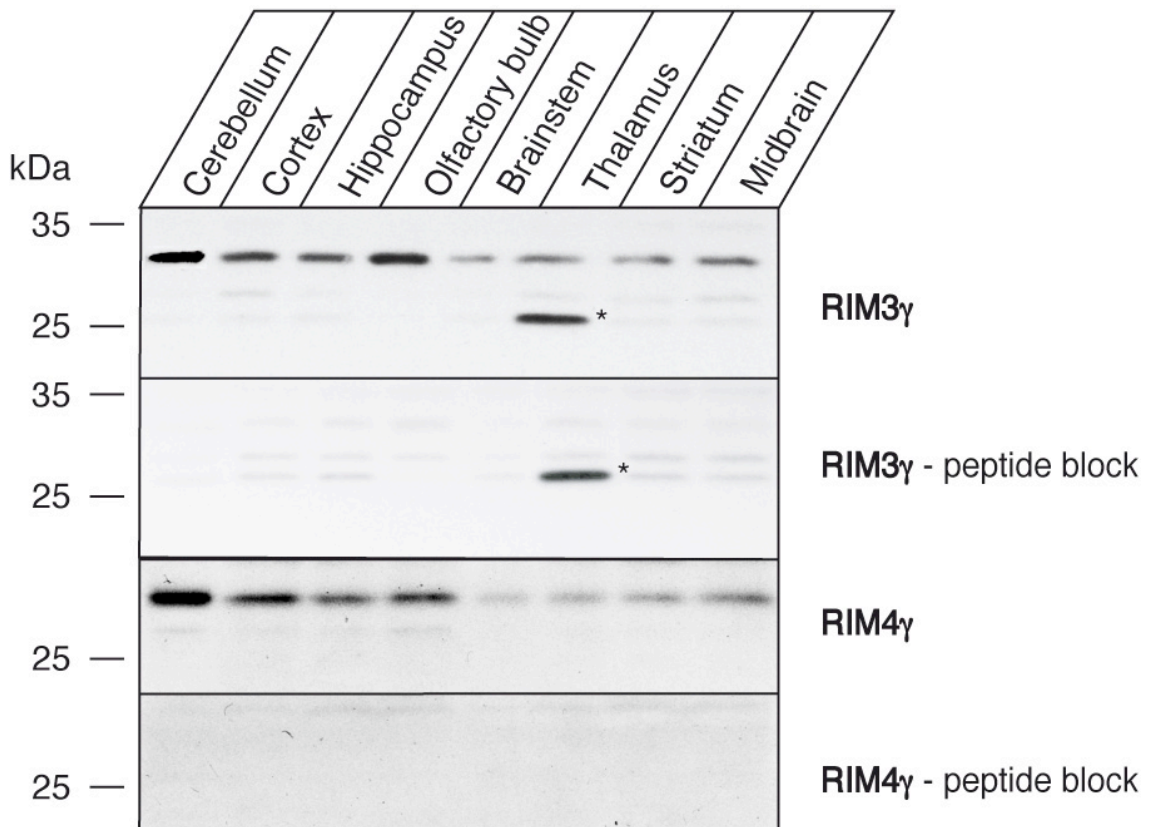


Fig. 5.5 RIM3 γ and RIM4 γ expression in different brain regions

Homogenates from the specified brain regions were analyzed by immunoblotting with isoform-specific antibodies. Incubation of the blot with RIM3 γ antibody revealed a 26 kDa band in the thalamus. The peptide block identified this band as an unspecific crossreactive band (*). RIM3 γ and RIM4 γ proteins were found to be ubiquitously expressed in the brain. However, the expression levels differed between the isoforms in various brain regions.

5.1.1.2.4 Developmental expression in rat brain

Expression of many synaptic proteins first appears around birth and increases during the time of synaptogenesis. Western blot analysis was performed to examine the expression profile of both γ -isoforms during brain development. In order to assess a putative developmental regulation of the expression of the RIM γ -isoforms, whole brain homogenates of rat were prepared at different time points, and equal amounts of protein were loaded on a SDS-Page gel for subsequent immunoblot analysis. Both proteins first appear around birth and the protein levels increased during postnatal week 2-3. Expression levels were stable after postnatal day 20 (Fig. 5.6).

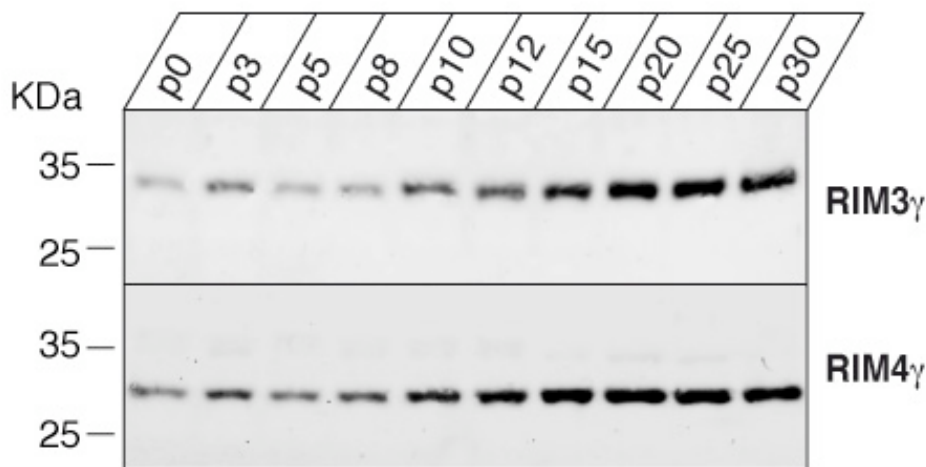


Fig. 5.6 RIM3 γ and RIM4 γ expression levels increase during synaptogenesis

Whole brain homogenates from rats of the indicated ages (p0-p30) were analyzed by immunoblotting with specific antibodies against RIM3 γ and RIM4 γ . Expression of both isoforms increased during postnatal brain development.

5.1.1.2.5 Association of γ -RIMS with the insoluble synaptic fraction

RIM1 α is an integral component of the cytomatrix at the presynaptic Active Zone. However, in contrast to α -RIMs that are composed of multiple protein

interaction domains, the RIM γ -isoforms only contain a single C2B domain that might not be sufficient to tightly link these proteins to the scaffold of proteins composing the cytomatrix at the active zone. To examine if γ -RIMs are associated with the pre- and postsynaptic densities, subcellular fractionation of synaptosomes from rat forebrain was carried out.

Synaptosomes are isolated synapses, which constitute sealed presynaptic nerve terminals that are attached to resealed postsynaptic compartments. They result from separating and isolating axon terminals from the rest of the neuron, after brain tissue has been homogenized under controlled conditions. The crude synaptosomal fraction was further purified by gradient centrifugation. After a first centrifugation step the nuclear fraction (P1) was discarded and the remaining crude synaptosomal fraction centrifuged again to obtain the synaptosomal cytosol fraction (S2) and the crude synaptosomal pellet fraction (P2) containing mitochondria and nerve endings. P2 was overlaid on a sucrose density gradient and ultracentrifuged obtaining a mitochondrial pellet, a myelin and a synaptosomal fraction. The synaptosomes were carefully collected and divided into two fractions. One was used for postsynaptic density (PSD) preparation and the other for synaptic vesicle (SV) and synaptic plasma membrane (SPM) enrichment. A two-time extraction of the PSD fraction with Triton X-100, resulted in the separation of the triton soluble fraction including synaptic vesicle proteins, and the TX-100 resistant fraction containing proteins associated to the synaptic density. The different subcellular fractions of the brain homogenate were analyzed by immunoblotting with antibodies against RIM3 γ and RIM4 γ . The quality of the subcellular fractionation was assessed by examining the distribution of pre- and postsynaptic markers: the presynaptic synaptic vesicle protein Rab3A, and postsynaptic density protein PSD-95. The typical distribution patterns for Rab3A and PSD-95 were observed; the first was highly enriched in the synaptic vesicle fraction (SV) and virtually absent from

the triton X-100 resistant fractions (TX1, TX2) in which PSD-95 was predominantly found (Fig. 5.7).

Even though RIM3 γ and RIM4 γ could be partially solubilized by Triton X-100 extraction, surprisingly, the majority of the protein remained associated with the Triton X-100 insoluble fractions. This result indicates that the short RIM isoforms are linked in part to the pre- and postsynaptic densities. In addition, both proteins could not be detected in the myelin and synaptic vesicle fraction (Fig. 5.7).

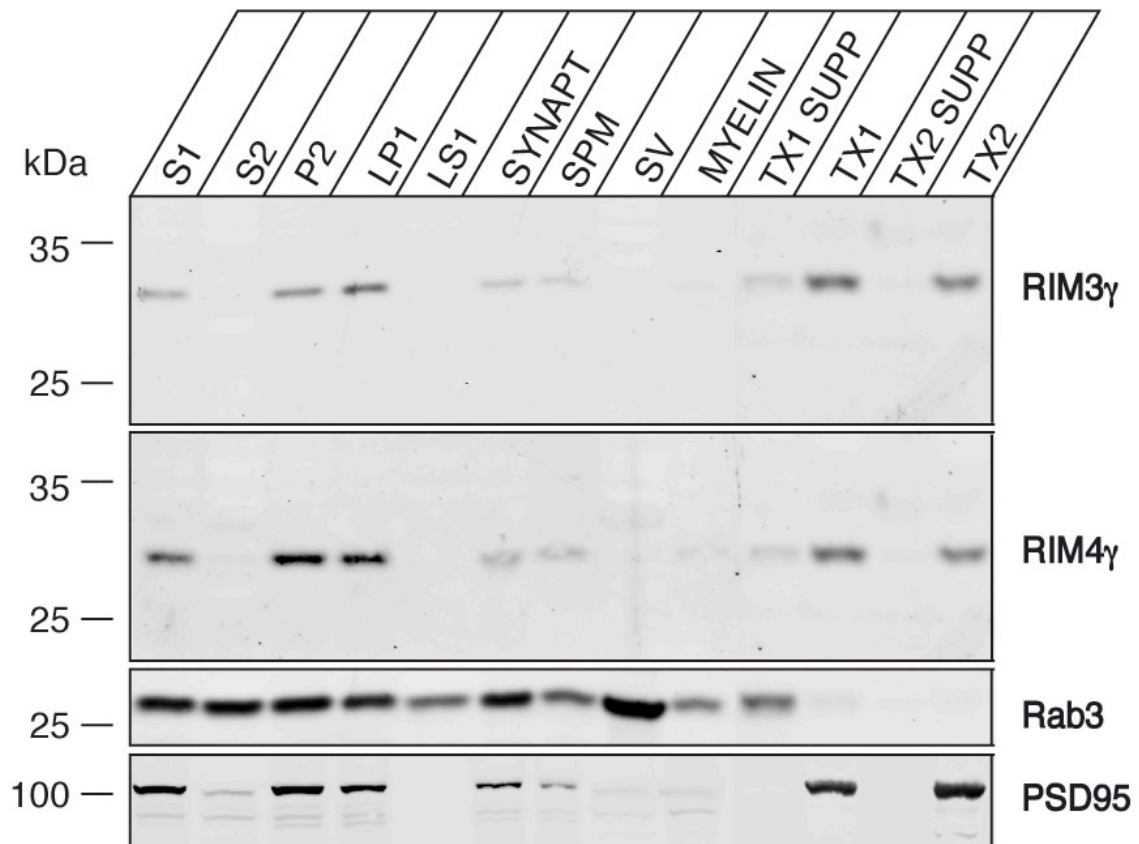


Fig. 5.7 Subcellular fractionation of rat synaptosomes

Homogenates were separated into nuclear fraction and crude synaptosomal fraction (S1), the synaptosomal cytosol fraction (S2); the crude synaptosomal pellet fraction (P2); the lysed synaptosomal membrane fraction (LP1); the crude synaptic vesicle fraction (SV) and the synaptic plasma membrane fraction (SPM). Supernatant of the 0,5% (w/v) or 1% (w/v) Triton X-100 soluble fraction (TX1 supp and TX2 supp respectively) and the Triton X-100 insoluble fraction of the SPM (TX1 and TX2). Fractions were analyzed using antibodies for RIM3 γ and RIM4 γ , as well as Rab3 and PSD95 that were used as control. After extraction with Triton X-100, the majority of RIM3 γ and RIM4 γ was found in the insoluble synaptic membrane fraction.

5.1.1.3 IMMUNOFLUORESCENCE ANALYSES IN RAT BRAIN

5.1.1.3.1 Light microscopy analysis of RIM3 γ and RIM4 γ localization in rat brain

The newly generated RIM3 γ and RIM4 γ antibodies detected proteins with the corresponding molecular weight proteins in rat brain homogenates. To further confirm the previously observed mRNA expression pattern and study the localization of RIM3 γ and RIM4 γ proteins in rat brain, immunohistochemistry analysis was performed. Therefore, 4 μ m saggital paraffin sections were labeled using antibodies against RIM3 γ and RIM4 γ and colabeled with an antibody against the synaptic vesicle protein Synapsin. RIM3 γ was strongly expressed in the granule cell layer and molecular layer of the cerebellum (Fig. 5.8, upper panel). In contrast, RIM4 γ was highly enriched in Purkinje cells, and also localized in the granular layer (Fig. 5.9, upper panel). In the olfactory bulb, both proteins were mainly found in the external plexiform layer and in the glomeruli where the axons of the olfactory neurons make synapses with the apical dendrites of mitral cells (Fig. 5.8 and Fig. 5.9 middle panels). In cortex, RIM4 γ was homogenously distributed (Fig. 5.8 lower panels) whereas RIM3 γ showed a higher expression level in layers II and III (Fig. 5.9 lower panels). In all brain regions, both proteins colocalized with synapsin.

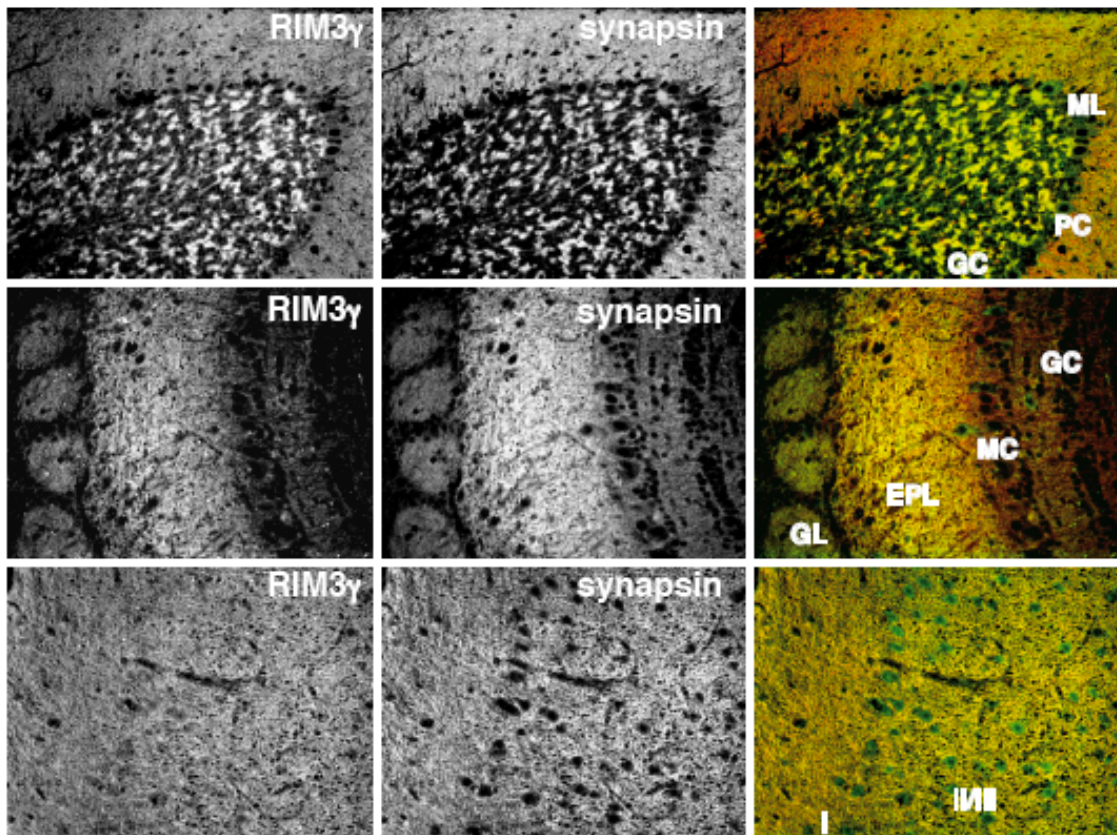


Fig. 5.8 Immunohistochemical analysis of RIM3 γ in rat brain

4 μ m paraffin sections were stained using RIM3 γ antibody (green) and colabeled with an antibody against the synaptic vesicle protein synapsin (red). High expression levels of RIM3 γ were observed in the cerebellar granular layer, and the II-III cortical layers. In the olfactory bulb, RIM3 γ was most strongly expressed in the external plexiform layer and the glomeruli. Abbreviations: EPL external plexiform; layer GC granular cells; PC Purkinje cells; GL glomerular layer; MC mitral cells ML molecular layer; I cortical layer I; II/III cortical layer II and III.

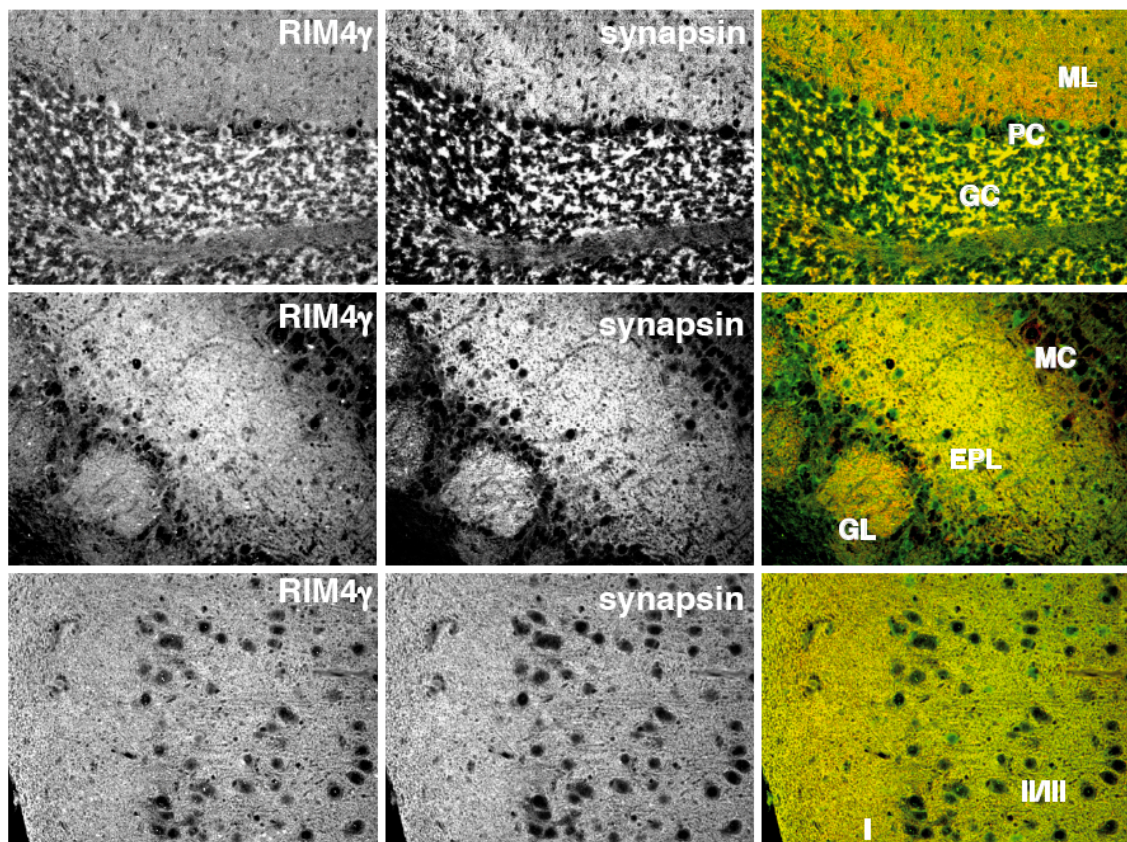


Fig. 5.9 Immunohistochemical analysis of RIM4 γ in rat brain

4 μ m paraffin sections were stained using RIM4 γ antibody (green) and colabeled with an antibody against the synaptic vesicle protein Synapsin (red). RIM4 γ was detected throughout the brain, showing a higher expression in cerebellar Purkinje cells, and the olfactory bulb external plexiform layer. RIM4 γ was highly and uniformly detected in different cortical layers. Abbreviations: EPL external plexiform layer; GC granular cells; GL glomerular layer; ML molecular layer; MC mitral cells; PC Purkinje cells; I cortical layer I; II/III cortical layer II and III.

5.1.1.3.1.1 Immunofluorescence analysis of RIM3 γ and RIM4 γ in primary cultured neurons

To further investigate the subcellular localization of RIM3 γ and RIM4 γ , immunocytochemistry analyses were performed using different markers. Synapsin and Bassoon antibodies were used as presynaptic markers, PSD-95 as postsynaptic marker, and MAP2 for dendritic labeling. Primary cortical neurons were double-immunolabeled at DIV14. RIM3 γ revealed a punctate expression pattern, colocalizing with Synapsin (Fig. 5.10, upper panels), bassoon (data not shown) and partially overlapping with PSD-95 (Fig. 5.10,

middle panels). In addition RIM3 γ did not colocalize with the dendritic marker MAP2 (Fig. 5.10, lower panels), pointing to a presynaptic localization of RIM3 γ . In contrast, RIM4 γ was rather uniformly distributed, and visible in axons and dendrites (Fig. 5.11).

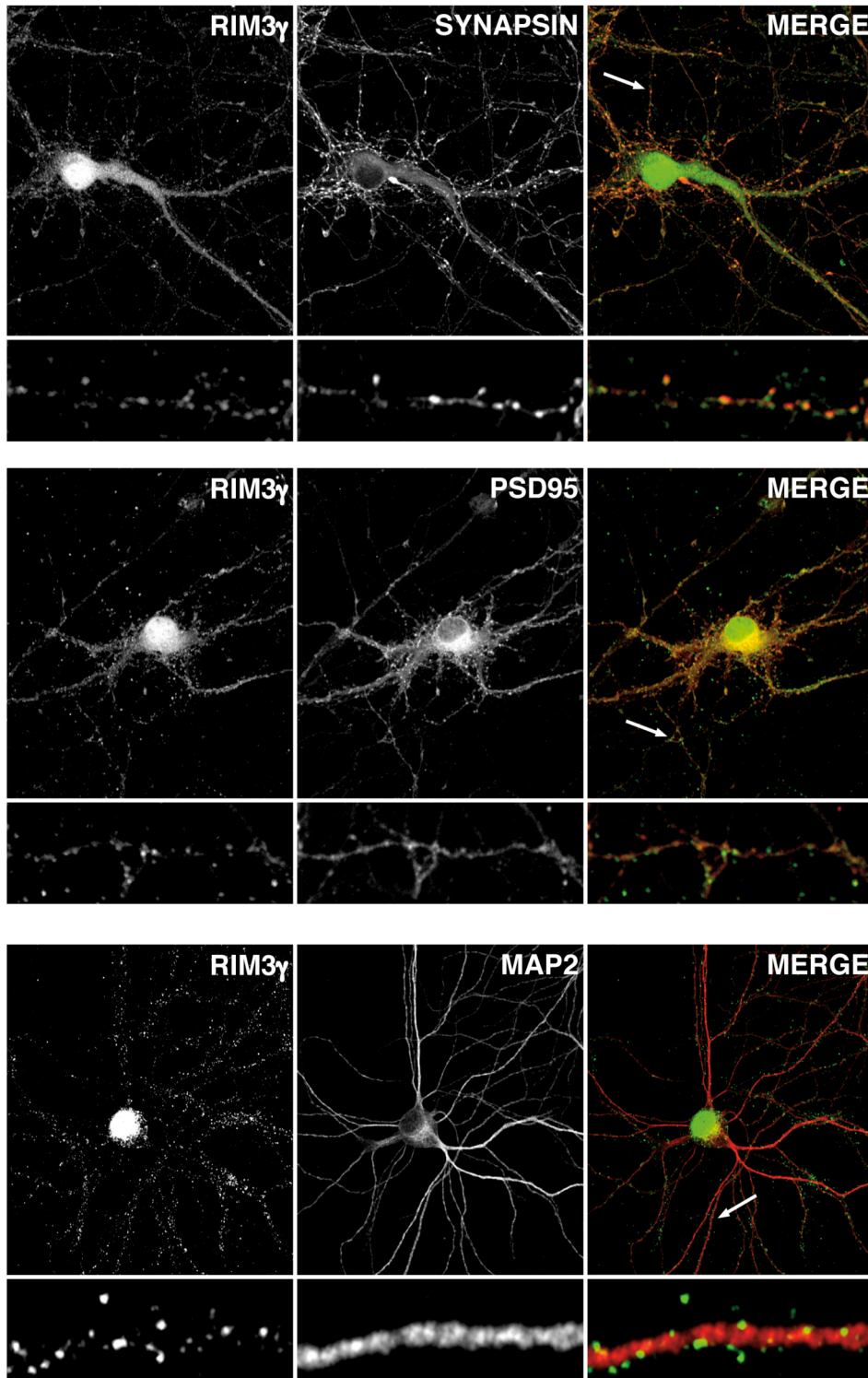


Fig. 5.10 Synaptic localization of RIM3 γ in cortical primary neurons

Cortical neurons were cultured for two weeks (DIV14), fixed and double-stained. Immunofluorescence analysis of endogenous RIM3 γ (green) was performed with various neuronal markers (red): synapsin (presynaptic), PSD95 (postsynaptic), MAP2 (dendritic). RIM3 γ showed a punctate expression pattern colocalizing with the presynaptic marker synapsin and partially overlapping with PSD-95 (postsynaptic). RIM3 γ was absent in MAP2 labeled dendrites.

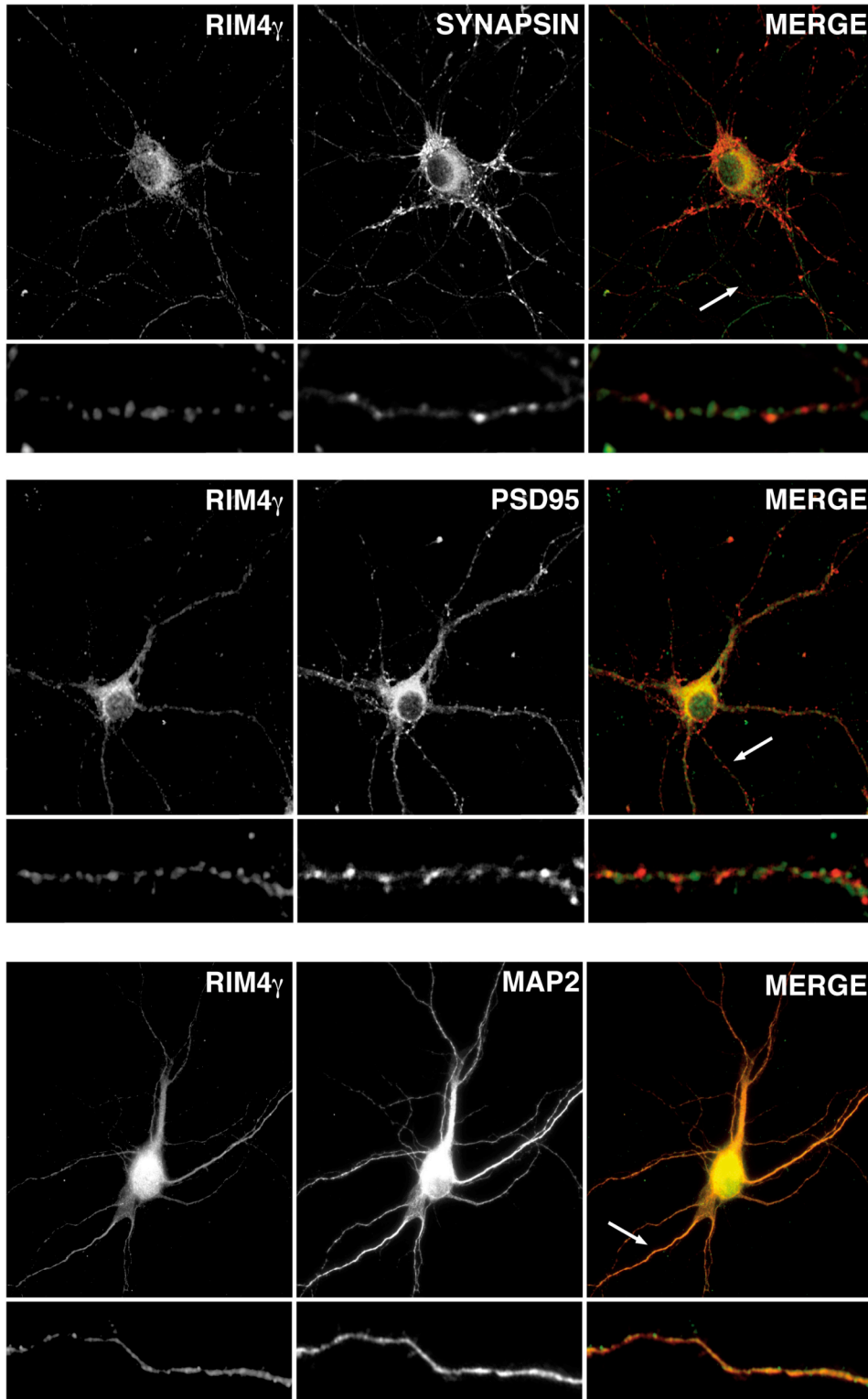


Fig. 5.11 Localization of RIM4 γ in cortical primary neurons

DIV14 cortical neurons were fixed and colabeled with anti-RIM4 γ antibody (green) and different markers (red): synapsin (presynaptic), PSD95 (postsynaptic), MAP2 (dendritic). RIM4 γ was found to be more uniformly distributed along the dendrites and partially colocalized with synaptic markers Synapsin and PSD-95.

5.1.1.3.2 Immunofluorescence analysis of RIM3 γ and RIM4 γ expression in the retina

Ribbon synapses are specialized synapses, present in sensory systems that undergo fast, continuous and graded neurotransmitter release (Parsons and Sterling, 2003; Sterling and Matthews, 2005; tom Dieck and Brandstätter, 2006). The structure and physiology of Ribbon synapses differ from conventional synapses. Ribbon synapses contain a specialized molecular machinery, lacking proteins such as Synapsin and comprising other specific proteins like RIBEYE/CtBP2 (tom Dieck and Brandstätter, 2006).

In order to study the presence or absence of RIM3 γ and RIM4 γ in the ribbon synapse, immunohistochemical labeling of bovine and rodent retina sections was performed. RIM3 γ staining revealed specific labeling in the synaptic layers, the inner and the outer plexiform layer. Both nuclear layers were virtually devoid of signal. In contrast, RIM4 γ was homogeneously distributed throughout all layers of the retina (Fig. 5.12).

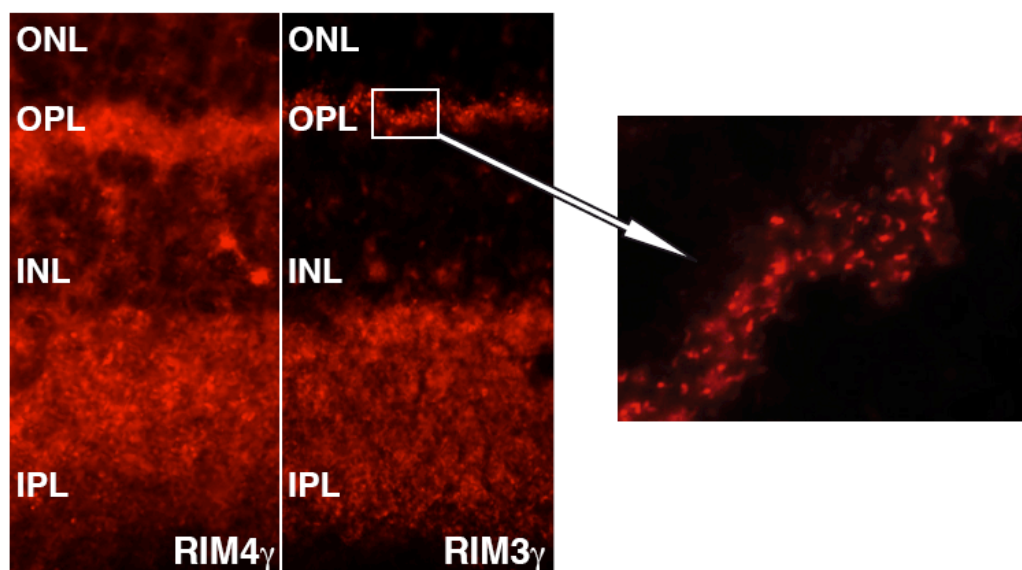


Fig. 5.12 RIM3 γ and RIM4 γ localization in the retina

Confocal micrographs of rat retina vertical cryosections showed synaptic localization of RIM3 γ in both synaptic layers, the outer and the inner plexiform layer (OPL, IPL). In contrast, RIM4 γ

was not only synaptically localized, but also present in the nuclear layers (ONL, INL). Magnification of the RIM3 γ marked OPL nicely showed RIM3 γ -labeled synaptic ribbons.

Synaptic coimmunostaining with the presynaptic marker CtBP2/RIBEYE was performed in order to confirm the subcellular localization of the RIM γ -isoforms in the retina. CtBP2/RIBEYE antibody labeled both synaptic layers: the outer plexiform layer (OPL) where rods and cones form synapses, and the inner plexiform layer, composed of ribbon synapses from bipolar cells (tom Dieck and Brandstätter, 2006). Both γ -isoforms colocalized with CtBP2/RIBEYE in the ribbon synapses, but in contrast to RIM3 γ , which displayed specific synaptic localization (Fig. 5.13, upper panels), RIM4 γ was also present in both nuclear layers (Fig. 5.13, lower panels). These data reconfirmed the synaptic localization of RIM3 γ in contrast to the uniform expression pattern of RIM4 γ .

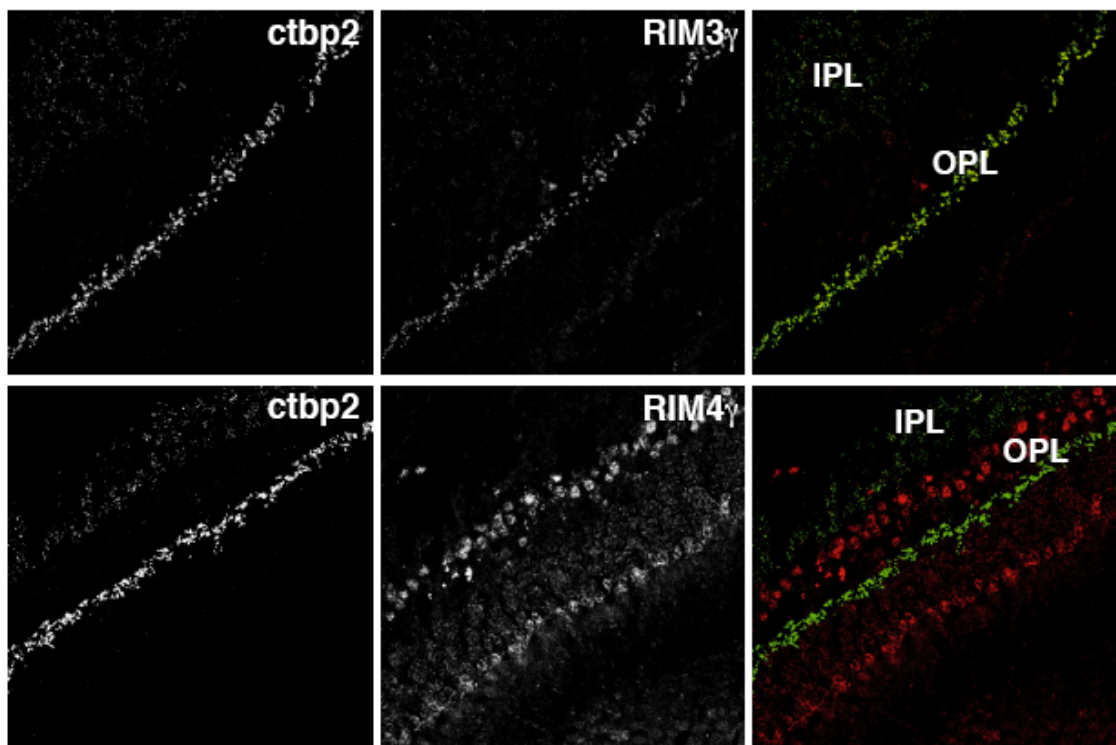


Fig. 5.13 Colocalization of γ -RIMs with the presynaptic ribbon protein CtBP2/RIBEYE

10 μ m cryosections of bovine retina were labeled with Ctbp2 (green) and RIM3 γ (red) or RIM4 γ (red) antibodies. Ctbp2 labeled photoreceptors and the bipolar cell ribbon synapse and colocalized with RIM3 γ , and partially with RIM4 γ .

5.1.1.3.3 RIM3 γ and RIM4 γ expression in inhibitory neurons

RIM1 α plays an essential role in neurotransmitter release in excitatory as well as inhibitory synapses (Castillo *et al.*, 2002; Chevaleyre *et al.*, 2007; Schoch *et al.*, 2002). Nevertheless, there are other synaptic proteins selectively enriched in excitatory or inhibitory synapses. Different isoforms of the presynaptic proteins Munc13 and Synapsin play a distinct role in GABAergic synapses (Rosenmund *et al.*, 2002; Terada *et al.*, 1999). In order to assess expression of γ -RIMs in inhibitory neurons, 4 μ m paraffin embedded brain slices were immunostained, using antibodies against RIM3 γ and RIM4 γ and colabeled with different markers for interneurons (Klausberger and Somogyi, 2008; Monyer and Markram, 2004). Inhibitory neurons release γ -aminobutyric acid (GABA) that is synthesized from glutamate by the enzyme glutamic acid decarboxylase (GAD), present in two different isoforms GAD-65 and GAD-67 (Monyer and Markram, 2004). GAD-67 antibody was used to identify most inhibitory neurons. In addition, colabeling with Parvalbumine was used to detect subpopulations of interneurons with fast firing behavior such as basket cells (Paxinos, 2004).

In the cerebellum, RIM4 γ showed a prominent expression in the Purkinje cell layer that constitutes the main gabaergic cell population. Purkinje cells were immuno-positive for both γ -isoforms that colocalized with different inhibitory markers such as GAD67 (Fig. 5.14, lower panel) and Parvalbumine (Fig. 5.14, upper panel). In the molecular layer, basket cells represent the GABAergic subpopulation. RIM4 γ was found to be expressed in some of the basket cells, whereas RIM3 γ was absent (Fig. 5.14, upper panels).

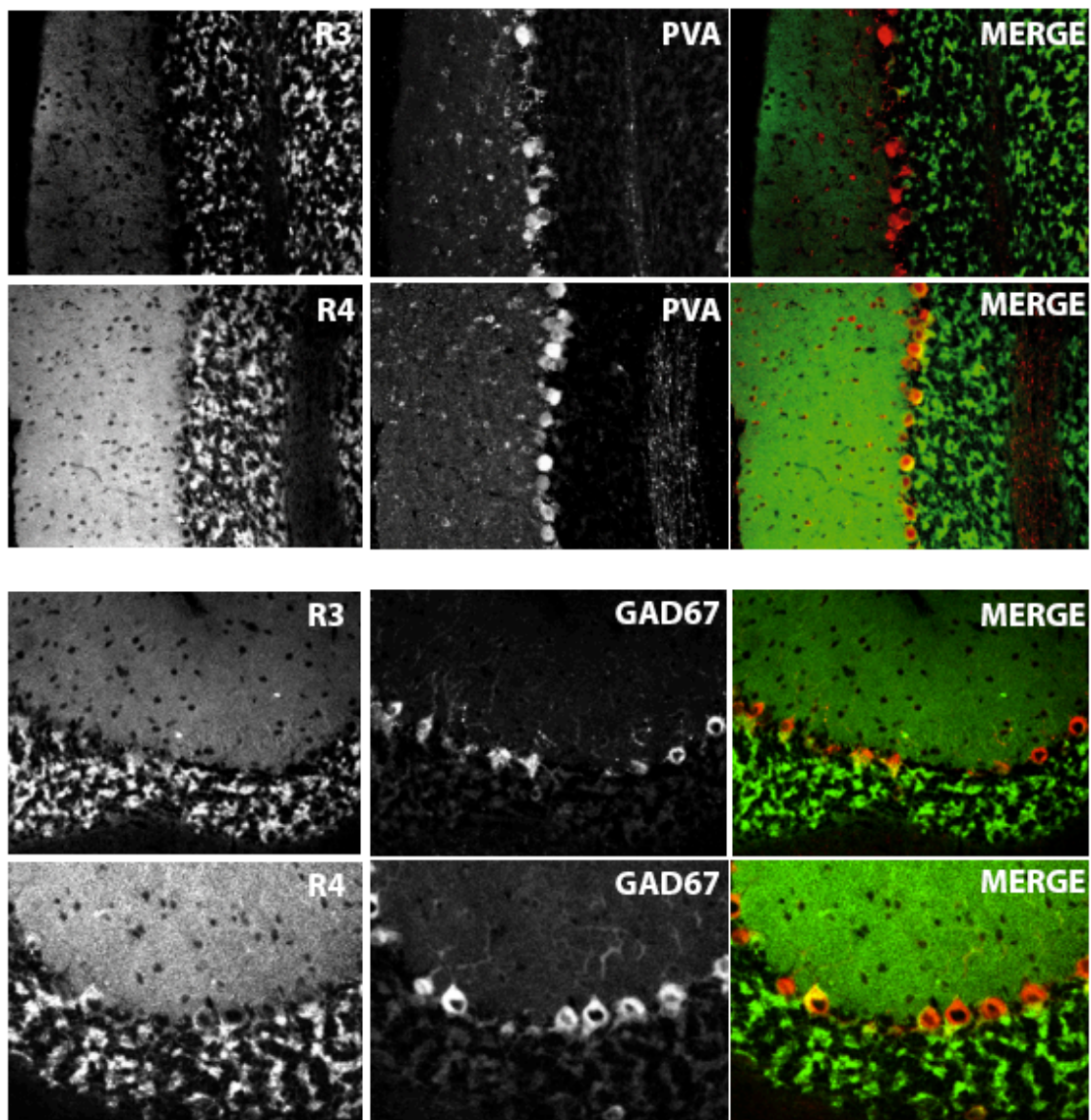


Fig. 5.14 RIM3 γ and RIM4 γ colocalized with different inhibitory markers in cerebellar cells

4 μ m paraffin sections were labeled using antibodies to differentiate inhibitory from excitatory neurons. Parvalbumine (red) und GAD67 (red) markers colocalized with γ -RIMs (green) in Purkinje cells, the main gabaergic cell population in cerebellum. In the molecular cell layer, basket cells (Parvalbumine positive) partially expressed RIM4 γ but not RIM3 γ . Abbreviations: R3 RIM3 γ ; R4 RIM4 γ ; PVA Parvalbumin.

Many different interneuron populations are present in the Hippocampus. Interneurons can be classified following different criteria: electrophysiology properties, morphology or neuropeptide content (Klausberger and Somogyi, 2008). Here, we used GAD67 as marker for most hippocampal interneurons

and Parvalbumin for basket cells. Interestingly, both isoforms could be found in hippocampal inhibitory neurons, colocalizing with Parvalbumin and GAD67, but not in all interneurons (Fig. 5.15).

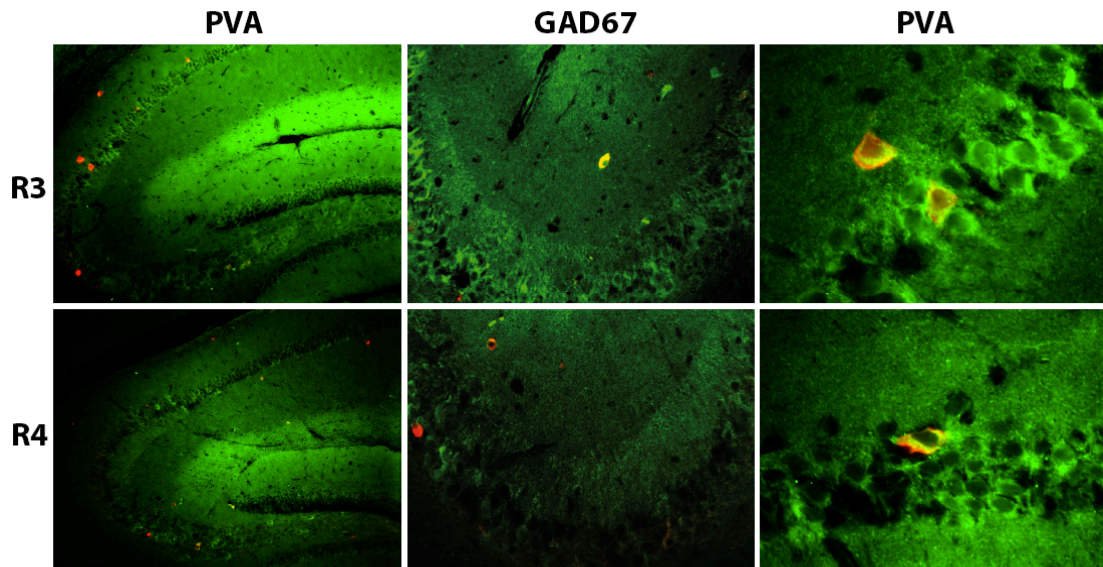


Fig. 5.15 γ -RIMs are present in hippocampal interneurons

4 μ m paraffin slices were colabeled using specific antibodies against RIM3 γ and RIM4 γ (green) and different antibodies to identify hippocampal interneurons (red). Both γ -isoforms were present in a fraction of GAD67 and Parvalbumin positive interneurons. R3 RIM3 γ ; R4 RIM4 γ ; PVA Parvalbumin.

A large population of Parvalbumin/ γ -RIMs positive inhibitory neurons was found in the superior colliculus, a brain region that has an important role in the integration of sensory information (Fig. 5.16).

In summary, RIM3 γ and RIM4 γ are expressed in GABAergic as well as in glutamatergic synapses. However, neither of them was found to be ubiquitously present in all inhibitory neuron subtypes.

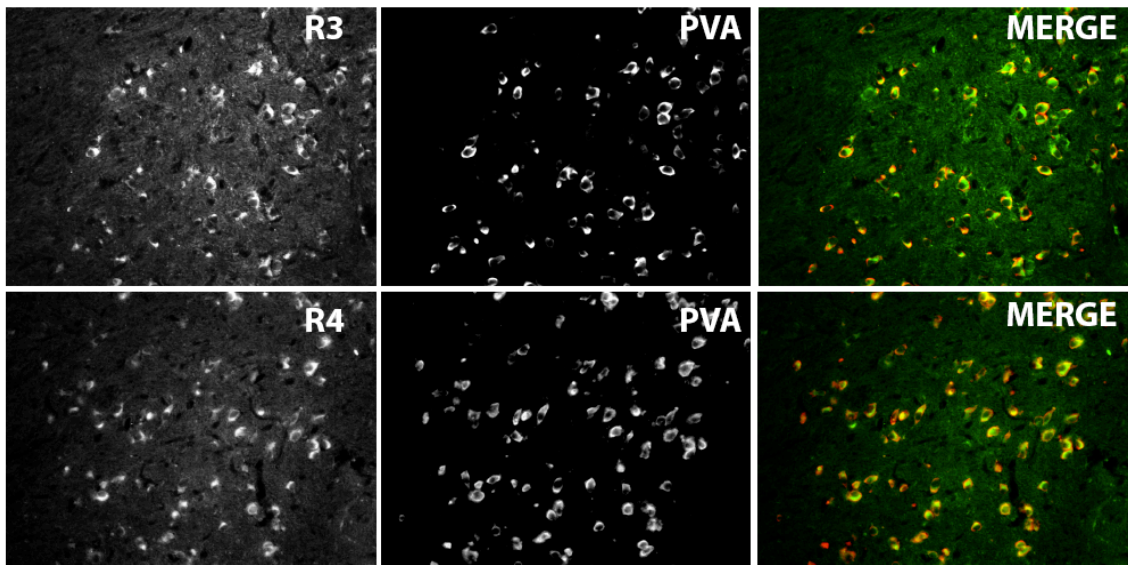


Fig. 5.16 Both γ -RIMs are present in the Parvalbumin positive cell population in the superior colliculus

γ -RIMs/ Parvalbumin colabeled paraffin slices showing colocalization of these proteins. RIM3 γ and RIM4 γ (green) were found in Parvalbumin positive (red) superior colliculus interneurons. R3 RIM3 γ ; R4 RIM4 γ ; PVA Parvalbumin.

5.1.2 Functional investigation of RIM3 γ and RIM4 γ proteins

5.1.2.1 CHARACTERIZATION OF γ -RIMS TARGETING SEQUENCES

γ -RIMs constitute a minimal variant of the RIM protein family as they contain only the C2B domain and a short isoform-specific N-terminal sequence. However, the RIM C2B domain mediates several interactions, important for its function. It has been shown to interact with Liprin- α 3 (Wang and Südhof, 2003), the presynaptic ubiquitin ligase SCRAPER (Yao *et al.*, 2007), and the calcium channel β -subunit (Kiyonaka *et al.*, 2007).

All RIM isoforms were shown to interact *in vitro*, in pull down assays, with Liprin- α 3 (Wang and Südhof, 2003). Furthermore, this interaction was hypothesized to

play an important role in RIM1 α trafficking. However, so far there is no *in vivo* data confirming this hypothesis, and crystallography studies have shown that the minimal Liprin binding domain is not enough to bind isolated RIM-C2B domains (Guan *et al.*, 2007). In order to study the possible role of Liprins- α in γ -RIM trafficking and identify the minimal RIM sequence necessary to interact with Liprins- α , a series of cotransfections and double immunofluorescence experiments were performed.

5.1.2.1.1 Analysis of the interaction between γ -RIMS and Liprins- α in chromaffin cells

To analyse the binding between γ -RIMs and Liprins- α in living cells, pCDNA expression vectors encoding full length and truncated γ -RIMs with a N-terminal green fluorescent protein (GFP) tag were generated (Fig. 5.21). Transfection efficacy in neurons is generally low. In contrast, HEK cells produce large amounts of proteins, which lead frequently to aberrant protein aggregation. Therefore, PC12 cells were used for this experiment. This cell line has neuronal properties, including calcium dependent secretion and synaptic like microvesicles.

As a first step, PC12 cells were transfected with expression plasmids for RIM1 α , RIM3 γ and RIM4 γ , with or without N-terminal GFP tag, to examine if the localization would be influenced by the fusion to the fluorescent marker. 36 hours after transfection, cells were analyzed by confocal microscopy. GFP-tagged and non-tagged proteins revealed the same localization (only GFP-tagged constructs shown, Fig. 5.17). PC12 cells expressing GFP-RIM1 α formed aggregates in the cytoplasm. Furthermore, GFP-RIM1 α was present in the nucleus, an unexpected distribution that had been previously described (Sun *et al.*, 2003). Overexpressed GFP-RIM3 γ was mainly located in nucleus (Fig. 5.17), similarly to RIM1 α with lower amounts present in the cytosol. In contrast,

GFP-RIM4 γ was absent from the nucleus and showed a diffuse distribution in the cytoplasm (Fig. 5.17).

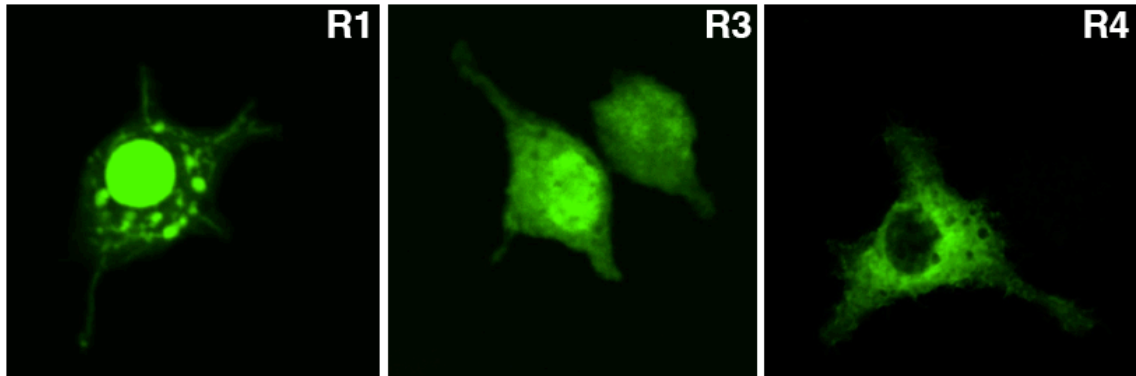


Fig. 5.17 Subcellular distribution of RIM3 γ and RIM4 γ GFP fusion proteins in PC12 cells

PC12 cells were transfected with expression plasmids encoding N-terminally tagged GFP- γ -RIMs. 36 hours after transfection, cells were fixed and examined using a confocal microscope. Unexpectedly, RIM1 α was mainly detected in the nucleus and in cytoplasmic clusters. RIM3 γ was localized in the nucleus and cytoplasm, whereas RIM4 γ was only expressed in the cytoplasm. Abbreviations: R1 RIM1 α ; R3 RIM3 γ ; R4 RIM4 γ .

Subsequently, subcellular localization of Liprin-1 α , -3 α and -4 α was examined. All overexpressed Liprin- α isoforms showed a diffuse cytoplasmic localization and were not present in the nucleus.

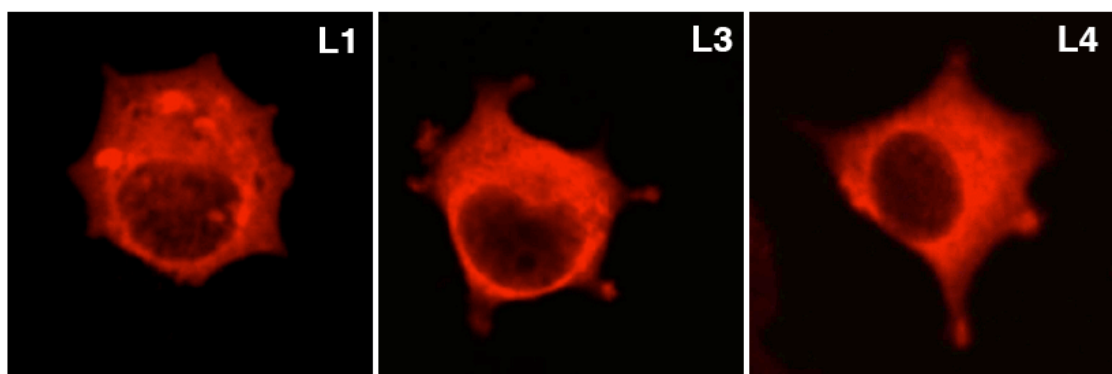


Fig. 5.18 Localization of different Liprin- α isoforms in PC12 cells

PC12 cells were transfected with different Liprin- α isoforms, PFA fixed after 36 hours and immunostained using specific antibodies for each isoforms. All transfected liprin- α family members showed a cytoplasmic localization. Abbreviations: L1 Liprin- α 1; L3 Liprin- α 3; L4 Liprin- α 4.

After examining RIM and Liprins- α localization in PC12 cells, cotransfections of γ -RIMs with different members of the Liprin- α family were carried out. PC12 cells, coexpressing pCDNA-GFP- γ -RIMs and pCMV-Liprin- α vectors, were fixed in 4% PFA 36 hours after transfection and immunolabeled using pan-antibodies recognizing all Liprin- α isoforms.

After cotransfection with all Liprin- α isoforms, GFP-RIM1 α and GFP-RIM3 γ were not concentrated in the nucleus anymore but mainly found the cytoplasm without apparent plasma membrane or chromaffin localization (Fig. 5.19). As expected, the cytoplasmic distribution of GFP-RIM4 γ did not change upon coexpression of Liprins- α (Fig. 5.19). Throughout the cytoplasm, the three GFP- γ -RIMs and the Liprins- α exhibited a highly overlapping distribution.

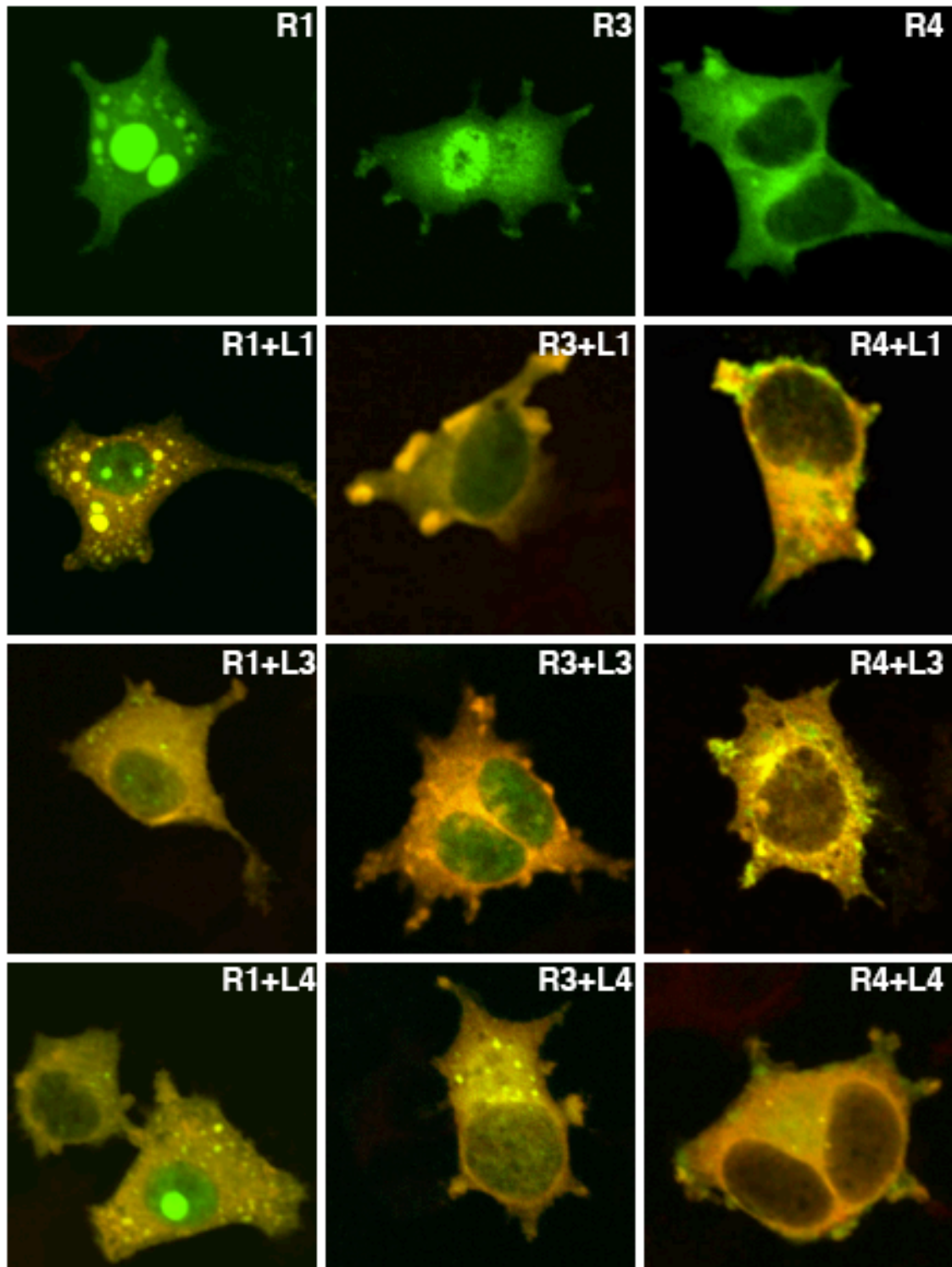


Fig. 5.19 Effect of liprin- α proteins on the subcellular localization of γ -RIMs and RIM1 α

Expression plasmids for GFP-tagged RIM fusion proteins were cotransfected, at an equimolar ratio, with plasmids expressing Liprins- α . GFP-tagged RIM1 α and RIM3 γ proteins, previously concentrated in the nucleus, were translocated to the cytoplasm upon cotransfection with any of the Liprins- α . No changes in RIM4 γ localization were evident in the presence of Liprins- α .

Cotransfection of all three GFP-tagged RIM isoforms with Liprins- α revealed an overlapping cytoplasmic distribution. Abbreviations: R1 RIM1 α ; R3 RIM3 γ ; R4 (RIM4 γ); L1 Liprin- α 1; L3 Liprin- α 3; L4 Liprin- α 4.

The sequence of the C2B domains is highly conserved within the RIM protein family. In addition to the C2B domain, γ -RIMs contain, a highly homologous sequence between the N-terminal and the C2B domain (Wang *et al.*, 2000), which consequently could be necessary to mediate the binding of proteins to the C2B domain. Therefore, we generated different deletion constructs coding for the C2B domain (C), the C2B domain and the homologous sequence (D), and for RIM3 γ lacking the N-terminal (E) (Table 5.1, Fig. 5.20)

| NAME | SEQUENCE | PROT. SIZE | PROT. SIZE + GFP |
|------------------------------------|--------------------|------------|------------------|
| GFP-RIM3 γ F (full length) | 1-924 bp; 308 aa | 32 kDa | 59 kDa |
| GFP-RIM3 γ E | 115-924 bp; 268 aa | 29 kDa | 56 kDa |
| GFP-RIM3 γ D | 217-924 bp; 236 aa | 25 kDa | 52 kDa |
| GFP- RIM3 γ C | 436-924 bp; 163 aa | 17 kDa | 44 kDa |
| GFP- RIM4 γ F (full length) | 1-810 bp; 270 aa | 29 kDa | 56 kDa |
| GFP-RIM4 γ D | 100-810 bp; 237 aa | 25 kDa | 64 kDa |
| GFP-RIM4 γ C | 340-810 bp; 157 aa | 17 kDa | 44 kDa |

Table 5.1 Properties of the various GFP γ -RIMs deletion constructs

The table lists the names, position and size of the subcloned fragments. No RIM4 γ E construct was designed due to the small size of the RIM4 γ N-terminus.

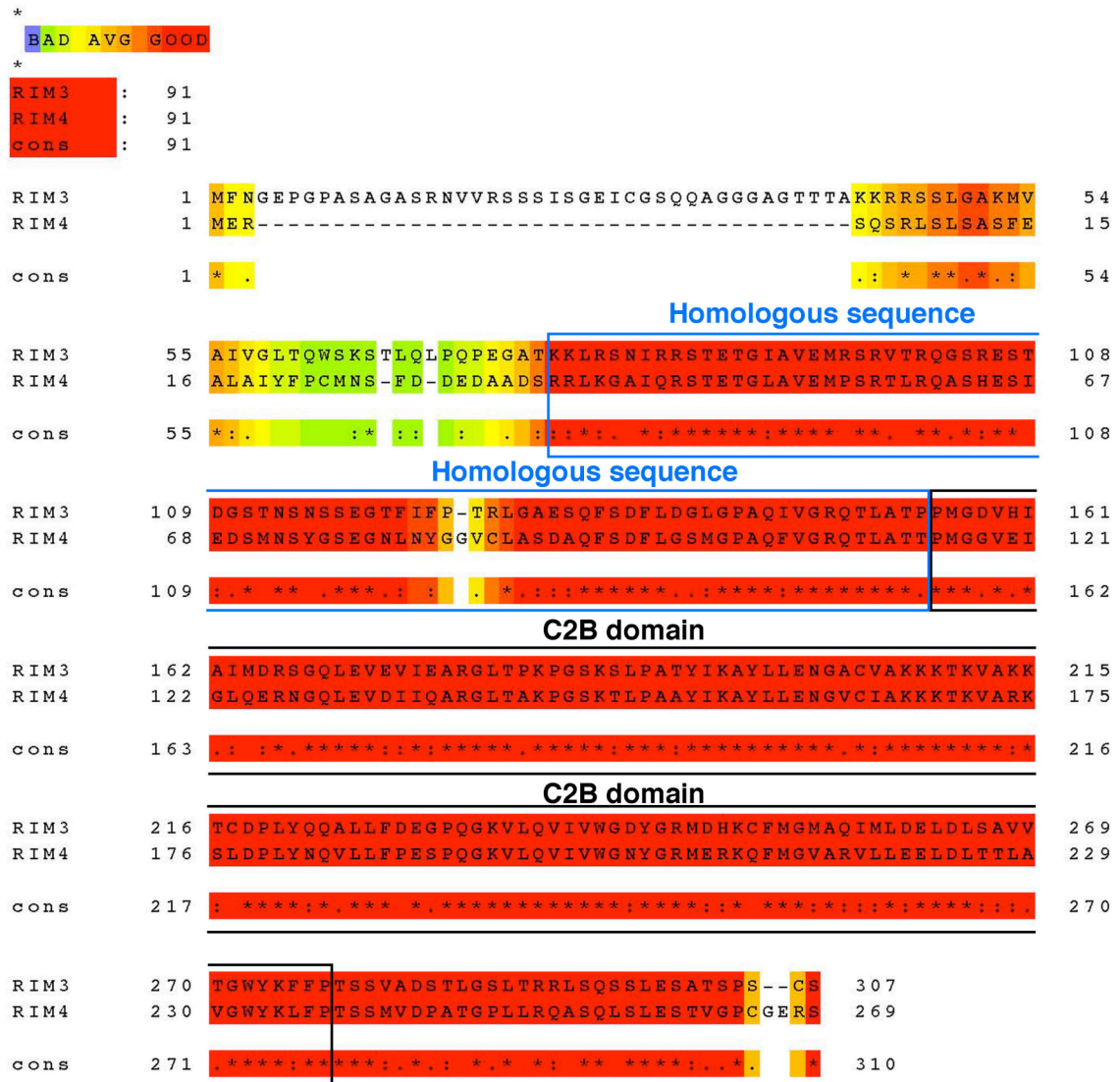


Fig. 5.20 RIM3 γ and RIM4 γ protein alignment
Protein alignment show the similarities in the sequence of both γ -isoforms. The highly homologous C2B domain is marked with a black box, whereas the homologous sequence is highlighted by a blue box.

To verify that expression of the various GFP- γ -RIM fusion proteins resulted in stable proteins of the expected size, an immunoblot analysis was performed (Fig. 5.21). HEK cells were transfected with the GFP- γ -RIM expression plasmids, lysed 48 hours after transfection, and analysed by SDS-Page and immunoblotting. An antibody against GFP was used for immunoblotting because γ -RIM specific antibodies were raised against a small N-terminal

peptide. The western blot showed bands corresponding to the calculated sizes of the GFP- γ -RIM fusion proteins (Table 5.1).

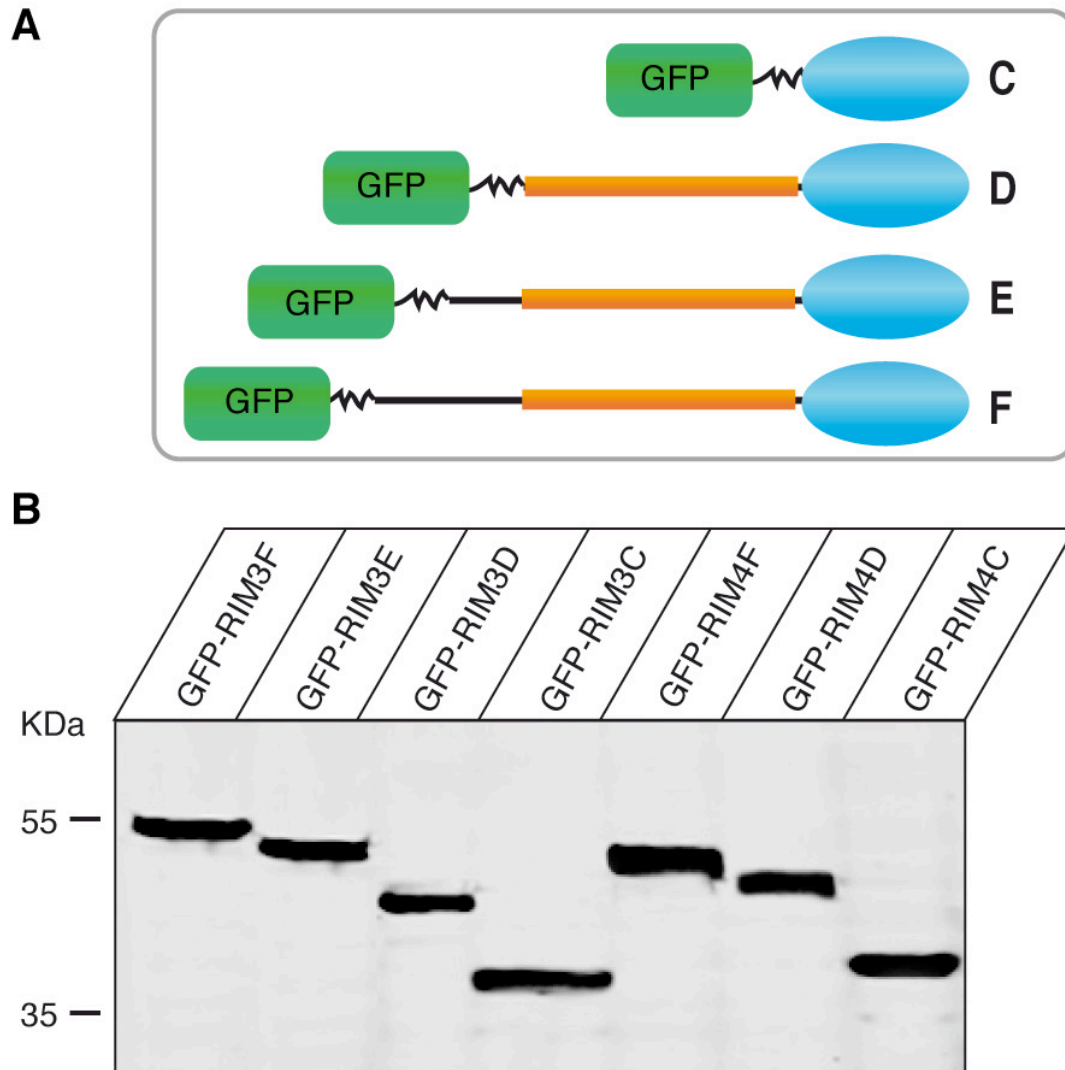


Fig. 5.21 Western blot analysis of RIM3 γ and RIM4 γ GFP fusion proteins
A. The cartoon shows a graphic overview of the composition of the full length and truncated GFP- γ -RIM fusion proteins used for the analysis. The isoform specific N-terminal sequence is depicted by a black bar, the homology sequence between the N-terminus and the C2B domain by an orange bar and the C2B domain is represented by a blue oval. **B.** All GFP tagged RIM3 γ and RIM4 γ deletion as well as full length expression plasmids were overexpressed in HEK 293T cells and analyzed by immunoblotting using an antibody against GFP. GFP-tagged proteins showed the predicted sizes.

To examine how deletion of the different N-terminal γ -RIMs sequences affects the subcellular localization, PC12 cells were transfected with the above described expression plasmids and analyzed by confocal microscopy. Truncated GFP-RIM3 γ -E protein was strongly expressed in the nucleus, and diffusely localized in the cytoplasm (Fig. 5.22). In contrast GFP-RIM3 γ -C and GFP-RIM3 γ -D were more uniformly expressed all through the cell. In the case of GFP-RIM4 γ truncated proteins, none of the deletions had a strong effect on the protein localization. GFP-RIM4 γ -C and GFP-RIM4 γ -D appeared diffusely distributed throughout the cytoplasm, as GFP-RIM4 γ did (Fig. 5.22). Protein localization was not modified and no aberrant aggregates were formed

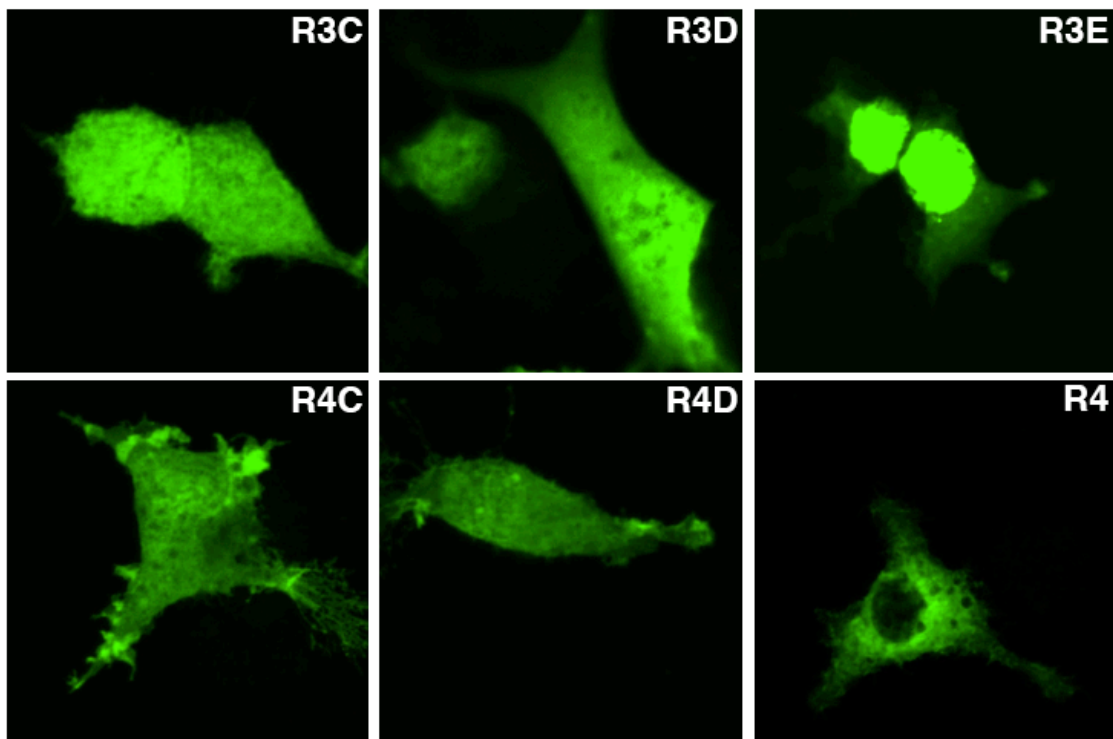


Fig. 5.22 Subcellular localization of the truncated GFP- γ -RIM fusion proteins in PC12 cells

All RIM4 deletion mutants showed the same expression pattern as the full length protein. In contrast truncated RIM3 proteins showed an increased cytoplasmic localization depending on the size. The smallest RIM3 γ fusion protein (R3C), only containing the C2B domain, and the one containing the homology fragment and the C2B domain (R3D) displayed a more diffuse cytoplasmic localization as compared to the full length and the RIM3 γ fusion protein only lacking the N-terminal isoform specific sequence (R3E), that are mainly concentrated in the nucleus.

After cotransfection of GFP-RIM3 γ -E fusion protein with Liprin- α 3, it was not detected in the nucleus anymore but rather distributed throughout the cytoplasm, colocalizing with Liprin- α 3 (Fig. 5.23). In the presence of Liprin- α 3, GFP-RIM3 γ -E, in which only the isoform-specific N-terminal sequence was missing, was only found in the cytoplasm and absent from the nucleus as previously shown for the GFP-RIM3 γ full length fusion protein, pointing to an interaction of both proteins (Fig. 5.23). In contrast, the truncated GFP-RIM3 γ -D protein, including the central homology sequence and the C2B domain, was found uniformly expressed throughout the cell when expressed alone or coexpressed with Liprin- α 3 (Fig. 5.23, middle panel). Coexpression of Liprin- α 3 and GFP-RIM3 γ -C fusion protein, containing only the C2B domain, did also not generate any change in the localization of the truncated GFP-RIM3 γ -C protein, which was diffusely expressed throughout the cell (Fig. 5.23, upper panel). GFP-RIM3 γ -D and GFP-RIM3 γ -C strongly colocalized with Liprin- α 3 in the cytoplasm. However, no major changes in the localization of both proteins could be detected when they were co-expressed with Liprin- α 3. In summary, the experiments show that the first 38 amino acids of the N-terminal isoform-specific sequence is not required for the interaction with Liprin- α 3, however, no unequivocal conclusion can be drawn about the shorter variants.

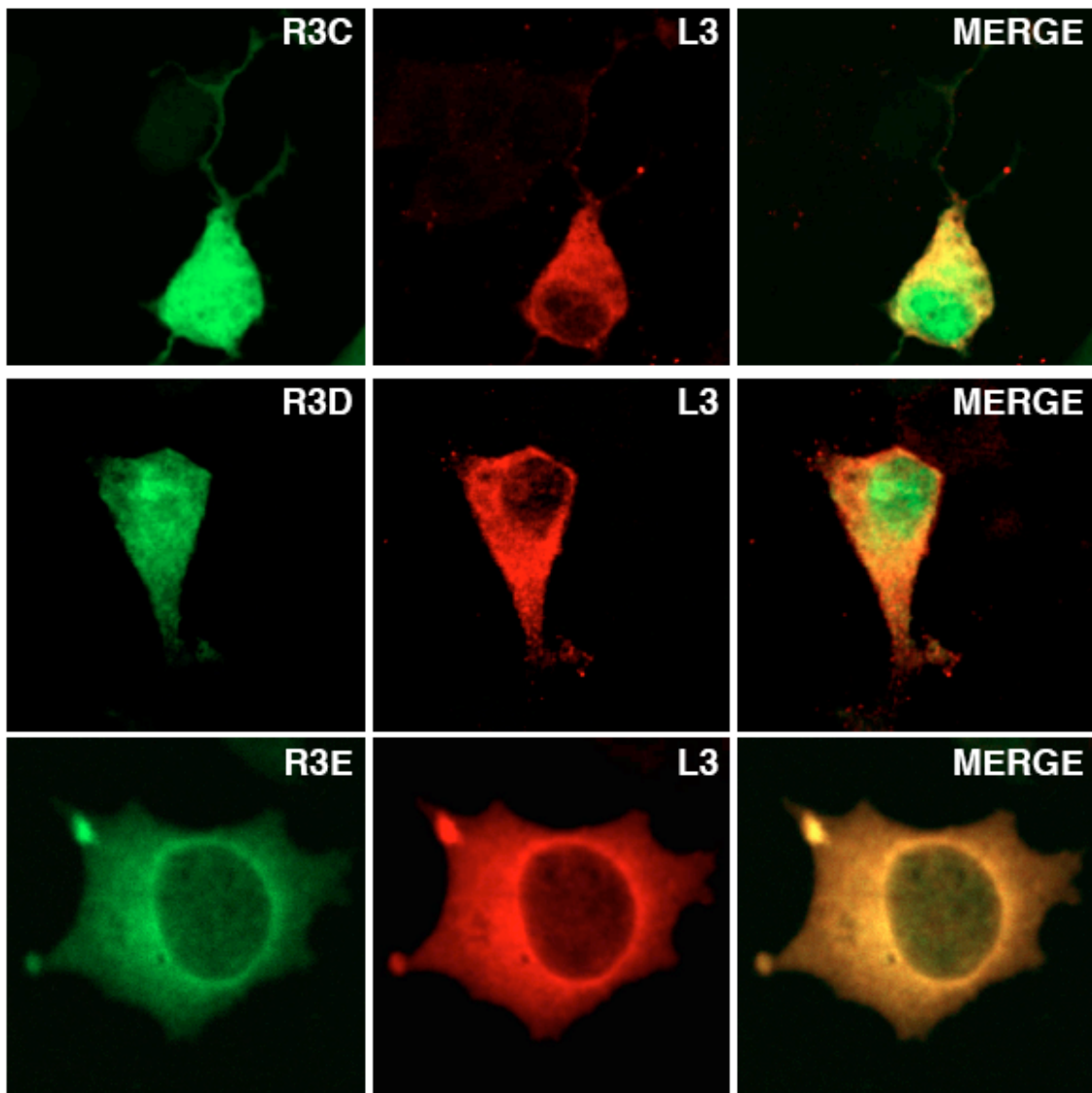


Fig. 5.23 Co-expression of GFP- RIM3 γ truncated proteins and Liprin- α 3 in PC12 cells

GFP-tagged RIM3 γ truncated proteins were cotransfected with pCMV-Liprin- α 3 full length. 36 hours after transfection, cells were fixed and immunolabeled using a specific antibody against Liprin- α followed by Cy3-coupled secondary antibody. GFP-RIM3 γ -E truncated proteins revealed cytoplasmic localization when cotransfected with Liprin- α 3, in contrast to the additional nuclear localization in cells not overexpressing Liprin- α 3. GFP-RIM3 γ -D and GFP-RIM3 γ -C proteins were more uniformly distributed throughout the cell and showed partial colocalization with overexpressed Liprin- α 3.

The presence of Liprin- α 3 did not change the localization of GFP-RIM4 γ fusion proteins examined, both proteins showed diffuse expression in the cytosol, overlapping with Liprin- α 3. Therefore it was not possible to conclude if an

interaction between these proteins took place or the expression just overlapped (Fig. 5.24).

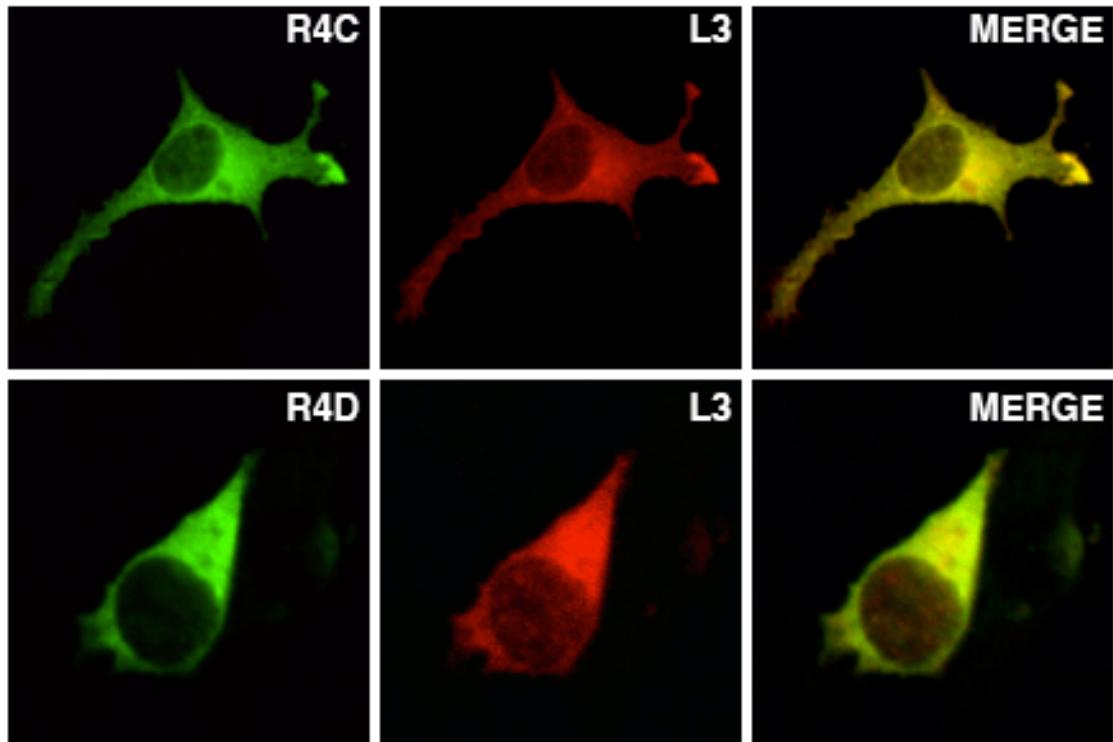


Fig. 5.24 Co-expression of GFP-RIM4 γ truncated proteins and Liprin- α 3 in PC12 cells

GFP-tagged RIM4 γ truncated proteins were cotransfected with pCMV-Liprin- α 3 (full length) fixed and immunolabeled using a specific antibody to Liprins- α followed by Cy3-coupled secondary antibody. All GFP-tagged RIM4 γ deletion constructs showed a cytosolic localization, without changes upon cotransfection with Liprin- α 3.

In summary, co-expression analyses in PC12 cells confirmed that RIM3 γ binds to Liprin- α 1, α 3, α 4. However, these experiments did not result in the identification of the minimal region required for binding Liprin- α .

5.1.2.2 ANALYSIS OF RIM3 γ AND RIM4 γ INTRACELLULAR TRAFFICKING IN PRIMARY HIPPOCAMPAL NEURONS

The use of fluorescently tagged-proteins offers many advantages when studying the function and localization of a protein. Fluorescent tags allow for the analysis of a protein in live cells, following its subcellular localization and

dynamics. However, the tag might influence the biological function or localization of the protein. In order to study the intracellular trafficking of RIM3 γ and RIM4 γ in cultured neurons, expression plasmids for RIM3 γ and RIM4 γ tagged with fluorescent marker proteins were developed.

Traditional methods using calcium phosphate or lipofectamine result in a very low transfection efficiencies, and may alter cell membrane properties. In contrast, incorporation of foreign DNA in neurons using lentiviral particles yield a high transfection efficiency without cell toxicity. Therefore, lentiviral expression plasmids for RIM3 γ and RIM4 γ with a C-terminally attached red fluorescent protein (mcherry), under control of the Synapsin promoter was generated. These plasmids were used to generate purified lentiviral particles in order to transduce hippocampal and cortical primary cultures. Neurons were infected on DIV 2-5 and analyzed on DIV 13-15. The transduction efficiency was always over 80%

Overexpression of RIM4 γ -mcherry resulted in a diffuse localization along the axon and dendrites. A similar expression pattern as observed in the immunocytochemistry analyses (Fig. 5.11). In contrast, transduction with the RIM3 γ -mcherry expressing viral particles resulted in low levels of the fusion protein, which was found in the nucleus and the main neuronal processes (Fig. 5.22). This expression pattern differs from the one observed by immunocytochemistry analyses of RIM3 γ , which showed a clear synaptic localization of the protein (Fig. 5.10). Differences in the expression pattern of the endogenous and overexpressed proteins might have different causes. The observed expression pattern of RIM3 γ -mcherry might be a consequence of low expression levels of the protein because of a weak promoter activity. In addition, the protein localization and/or stability might also be influenced by the tag. Therefore, a new N-terminal construct was generated coding for GFP-RIM3 γ and GFP-RIM4 γ under control of the stronger EF1 α promoter. GFP-

RIM3 γ had a much higher expression level and was synaptically localized, as the endogenous protein. In addition to being present at the synapse, GFP-RIM3 γ protein was also detectable in dendrites. In contrast, no significant differences in the localization of RIM4 γ were observed. C-terminal-RIM4 γ -mcherry and N-terminal-GFP-RIM4 γ exhibited the same diffuse localization along the neuronal processes.

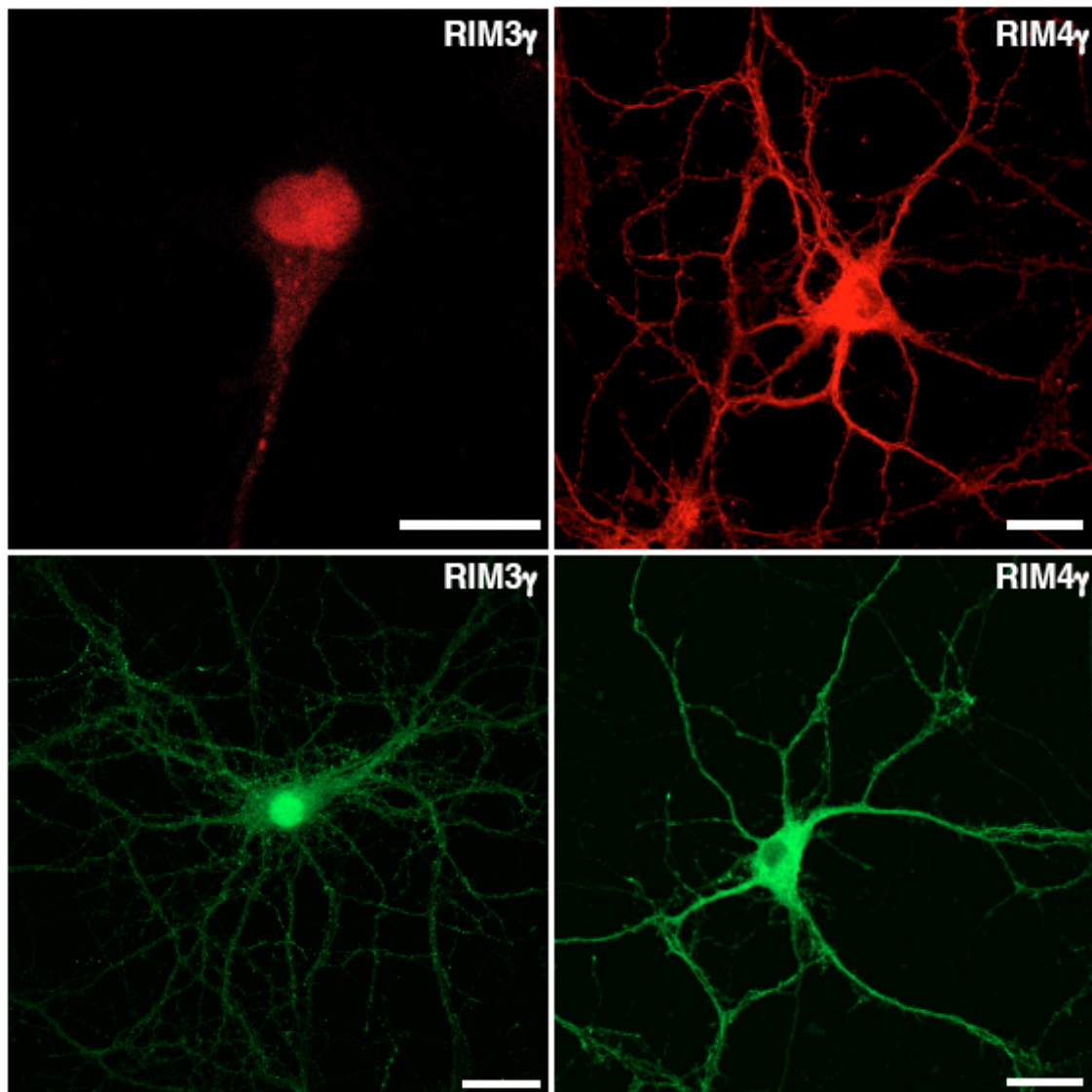


Fig. 5.25 Overexpression of fluorescently tagged RIM3 γ and RIM4 γ in primary hippocampal neurons

C-terminally mcherry-tagged γ -RIMs under the control of the Synapsin promoter and N-terminally GFP-tagged γ -RIMs under the control of the EF1 α promoter were used to produce lentiviral particles in order to overexpress RIM3 γ and RIM3 γ in primary neurons. Overexpression of C-terminal RIM3 γ -mcherry resulted in low levels of the protein, which was

found in the nucleus and the main neuronal process. C-terminal RIM4 γ -mcherry was diffusely localized in axon and dendrites. GFP-RIM3 γ expression, under the EF1 α promoter, resulted in a higher expression level. GFP-RIM3 γ was presynaptically localized at the synapses, but also detected in dendrites. GFP-RIM4 γ showed a similar expression pattern as RIM4 γ -mcherry. Scale bar 30 μ m.

5.1.2.3 ANALYSIS OF γ -RIMS TARGETING SEQUENCES IN NEURONS

In order to analyze the structural requirements for the localization of γ -RIMs, the previously designed deletion variants (Fig. 5.21) were subcloned in a lentiviral vector under the control of the EF1 α promoter. Primary hippocampal neurons were transduced with purified lentiviral particles at DIV3-5 and analyzed at DIV14-21, or transfected at DIV7-9 when low transfection efficiency was desired. The subcellular distribution of all designed GFP- γ -RIM truncated proteins was examined and compared with the full length protein.

All GFP-RIM3 γ truncated proteins showed a very similar subcellular localization. They were present in the axonal boutons, showing a punctate expression pattern, and also in the dendrites, where they were diffusely localized. Noteworthy, GFP-RIM3 γ -C, and GFP-RIM3 γ -D truncated proteins did not show the nuclear localization previously observed for the GFP-RIM3 γ full length protein, and also showed by GFP-RIM3 γ -E.

GFP-RIM4 γ truncated proteins were also localized in synaptic boutons and in dendrites. The distribution of GFP-RIM4 γ -D and GFP-RIM4 γ -C truncated proteins did not differ from the one observed for the full length protein.

These data suggest that the C2B domain alone is sufficient for the localization of RIM3 γ and RIM4 γ at the synapse.

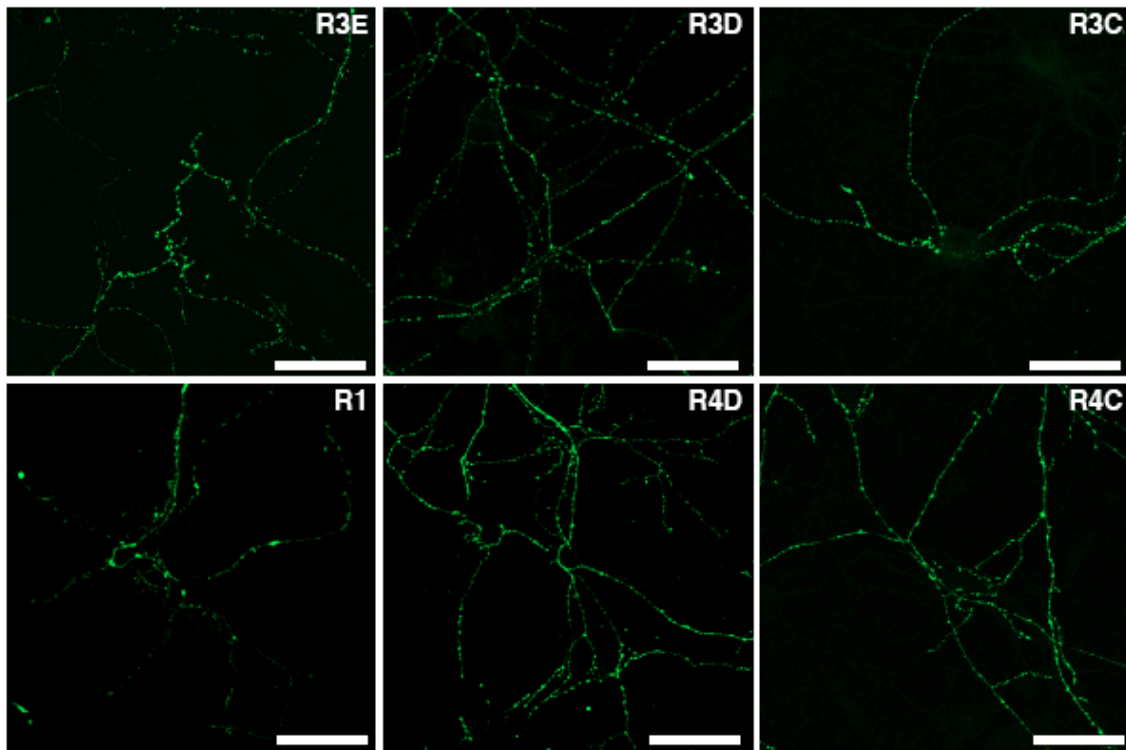


Fig. 5.26 Axonal localization of GFP- γ -RIMs truncated proteins

Hippocampal primary neurons were transfected with GFP-RIM3 γ full length or truncated proteins at DIV 7-9 and maintained in culture until synapses were mature (DIV14-DIV21). Subsequently, the neurons were fixated and analyzed by confocal microscopy. Low transfection efficiency was desired in order to be able to follow the neuronal processes of a single cell. RIM1 α was used as control for axonal localization. Scale bar 50 μ m.

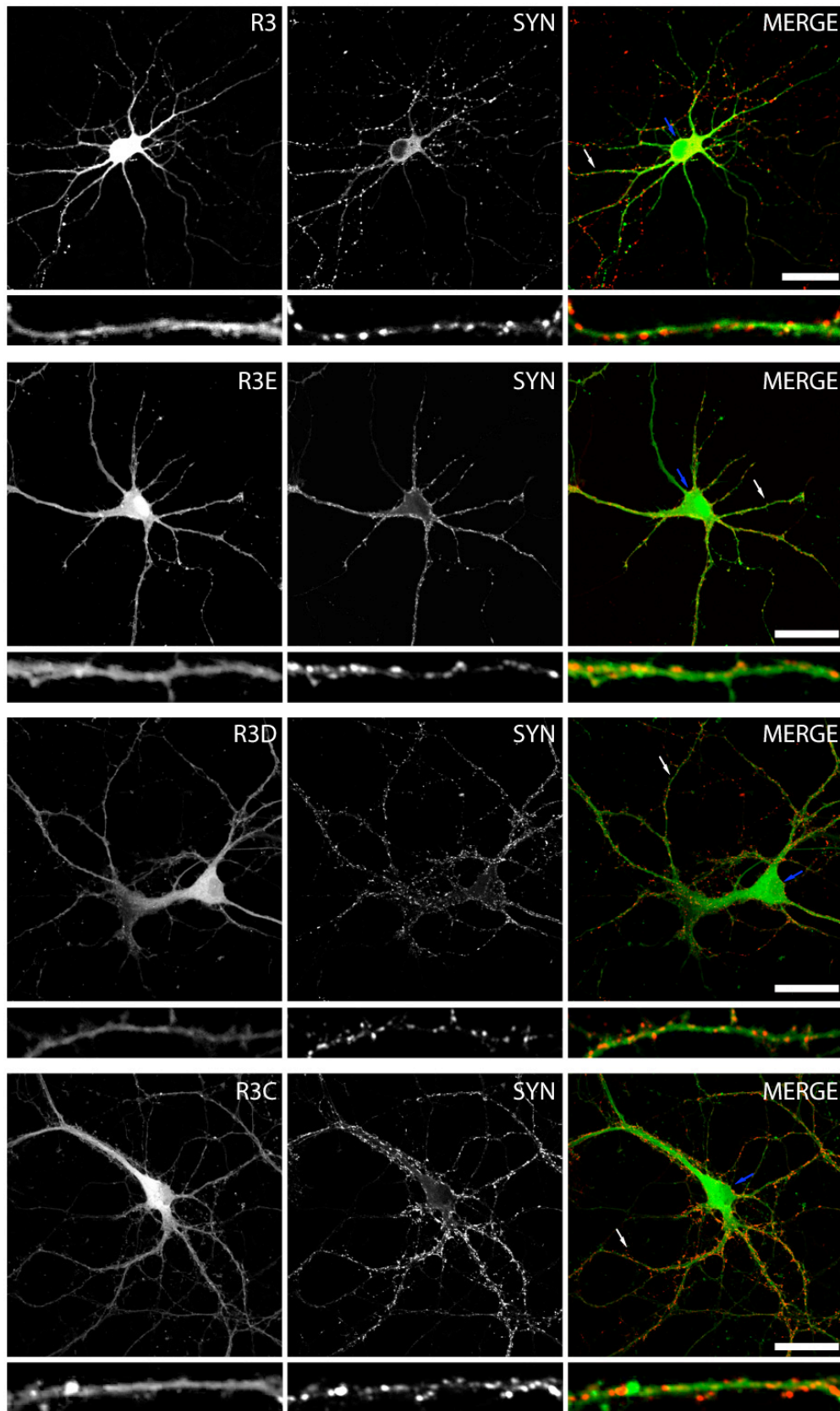


Fig. 5.27 GFP-RIM3 γ truncated proteins are present in dendrites

Hippocampal primary neurons were transduced with lentiviral particles expressing GFP-RIM3 γ full length or truncated proteins at DIV 3-5 and maintained in culture until analysis at DIV14. The

neurons were fixated and immunolabeled with an antibody against the synaptic vesicle protein synapsin to mark the synapses. Full length and truncated GFP-RIM3 γ proteins were diffusely present along the dendrites. No major differences could be found between the expression pattern of GFP-RIM3 γ full length and truncated proteins, except for the nuclear localization (blue arrows signalize nuclear localization). GFP-RIM3 γ full length and GFP-RIM3 γ -E were enriched in the nucleus, whereas GFP-RIM3 γ -D and GFP-RIM3 γ -C were not nuclear localized. White arrows indicate the dendrites chosen for magnification. Scale bar 30 μ m.

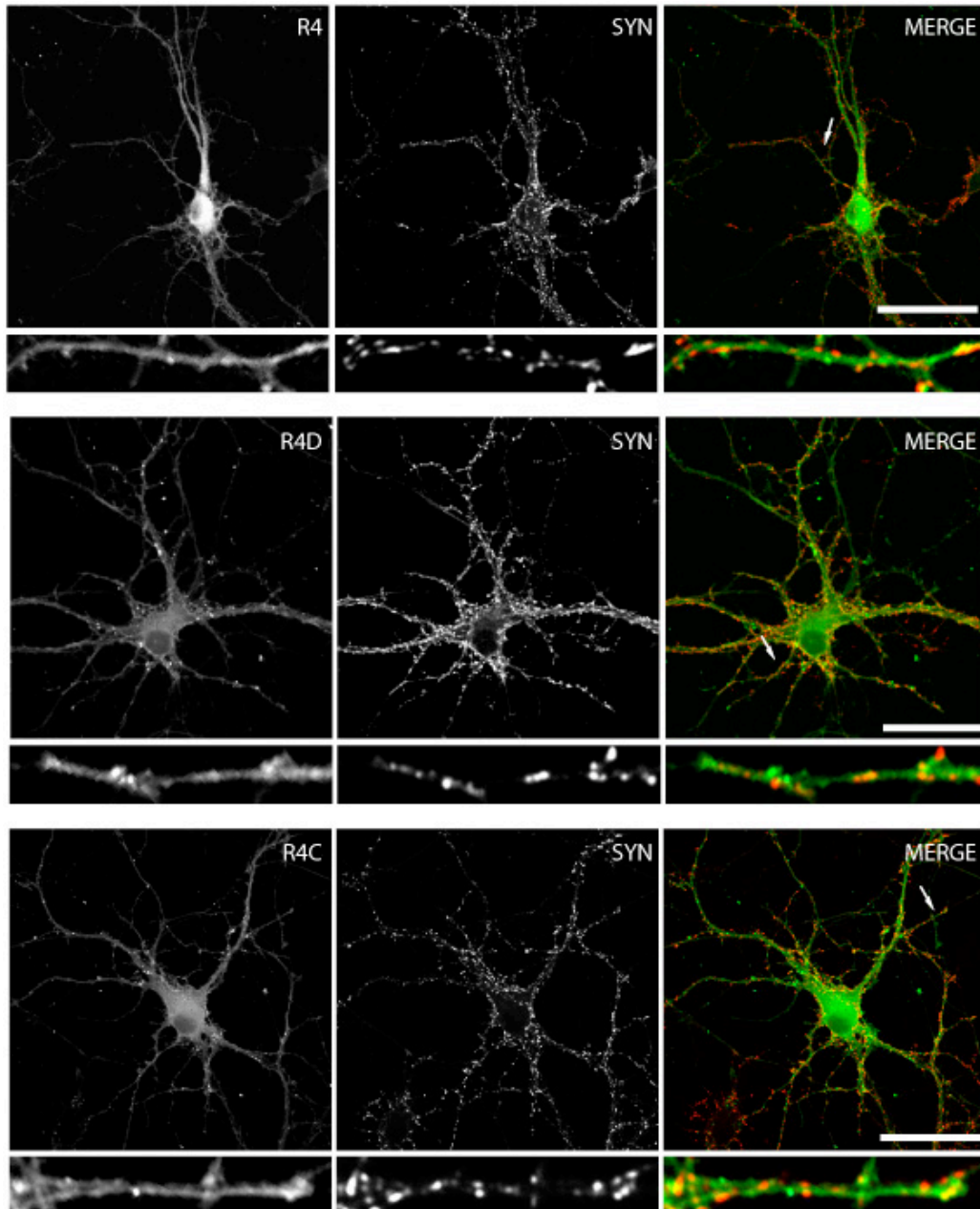


Fig. 5.28 GFP-RIM γ truncated proteins are present in dendrites

Hippocampal primary neurons were transduced with lentiviral particles expressing GFP-RIM4 γ full length or truncated proteins at DIV 3-5 and maintained in culture until analysis at DIV14. The

neurons were fixated and immunolabeled with an antibody against the synaptic vesicle protein Synapsin to mark the synapses. Full length and truncated GFP-RIM4 γ proteins were diffusely present along the dendrites. No major difference could be found between the expression patterns of GFP-RIM4 γ full length and truncated proteins. White arrows indicate the dendrites chosen for magnification. Scale bar 30 μ m.

5.1.2.4 POTENTIAL ROLE OF LIPRINS- α AND RIM1 α IN THE SYNAPTIC LOCALIZATION OF γ -RIMS

Previous studies have shown that Liprin- α is involved in the transport of several proteins, eg. AMPARs, GRIP1, GIT1 (Okada *et al.*, 1995; Shin *et al.*, 2003). In addition, Liprin- α has been shown to interact *in vitro* with the RIM1 α C2B domain (Schoch *et al.*, 2002). These data suggest that Liprin- α might be involved in RIM1 α trafficking, acting as linker between the motor proteins and RIMs.

In order to examine if Liprins- α plays a role in the localization and trafficking of γ -RIMs, lentiviral vectors coding for RIM3 γ -cherry, RIM4 γ -cherry under the control of the synapsin promoter, were used to overexpress γ -RIMs. Neurons were transfected with N-terminally GFP tagged Liprin- α on DIV3-5, and subsequently transduced with γ -RIMs-mcherry infected on DIV7-9. This approach allowed us to examine a putative role of Liprins- α in the localization of RIM3 γ and RIM4 γ within the same culture. Liprin- α 3 and Liprin- α 2 are the most abundant isoforms of the Liprin family in brain (Zürner and Schoch, 2008). Overexpression of γ -RIM-mcherry in neurons led to a diffuse expression of the proteins along the axon and the dendrites in the case of RIM4 γ . In contrast, both Liprin- α isoforms, showed a synaptic localization, as expected. No changes in the localization of γ -RIMs were detectable when coexpressed together with Liprins- α (Fig. 5.29). This data differed from previous observations in PC12 cells where Liprins- α were able to change RIM3 γ localization. These data indicate that Liprins- α do not promote the synaptic localization of γ -RIMs.

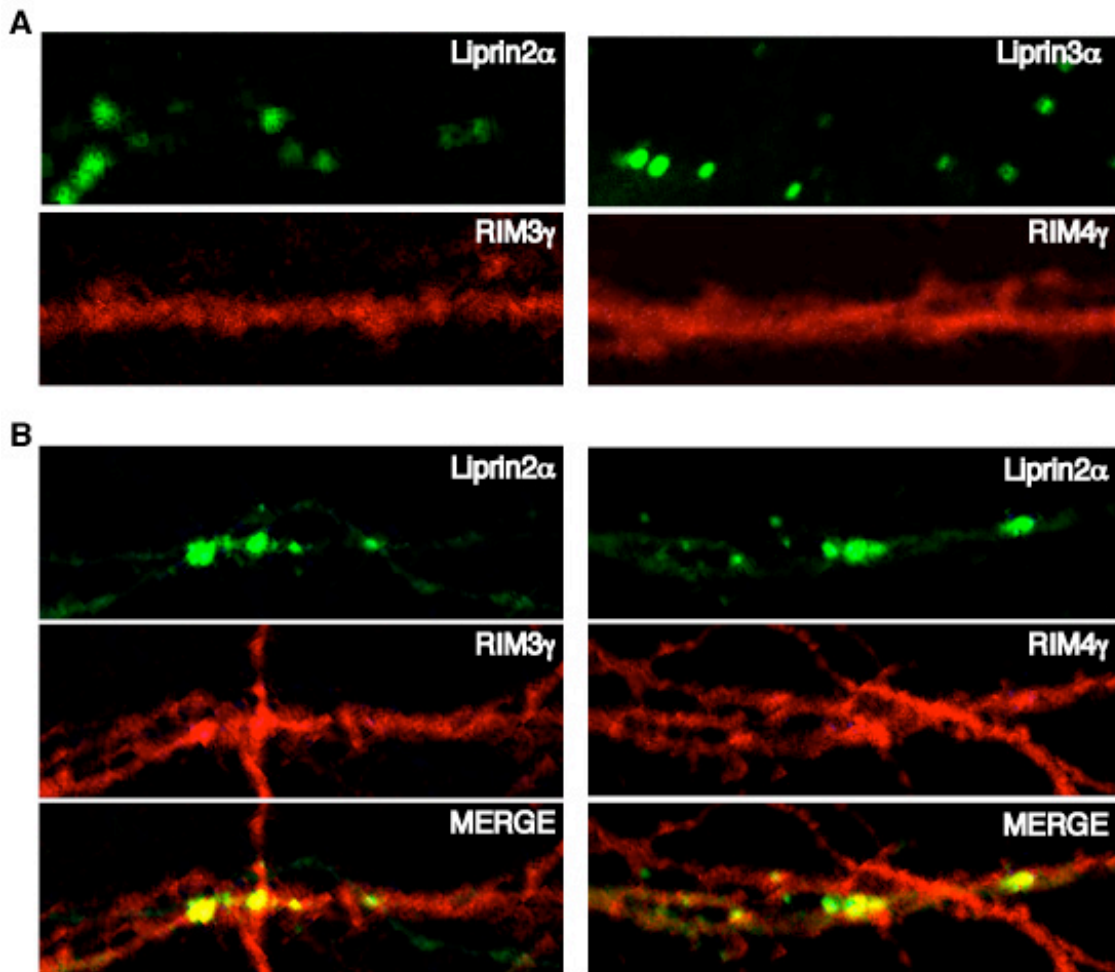


Fig. 5.29 Overexpression of Liprin- α 2, - α 3 does not affect localization of γ -RIMs in cultured neurons

Primary hippocampal neurons were transfected with Liprin- α 2/ α 3 (DIV3-5), subsequently transduced with viral particles expressing γ -RIMs-mcherry (DIV7-9) and analyzed by confocal microscopy. A, Exemplary neuron processes showing the localization of Liprin- α 2, Liprin- α 3, RIM3 γ and RIM4 γ when they were single transfected. B, Transfection of GFP-Liprin- α 2/ α 3 did not affect the localization of RIM3 γ -mcherry and RIM4 γ -mcherry.

The C2B domains of RIM2 α have been shown to dimerize (Guan *et al.*, 2007). In order to test the hypothesis that the C2B domains of α -RIMs and γ -RIMs could interact, leading to heterodimer formation, N-terminally GFP tagged RIM1 α was overexpressed in primary neurons at DIV3-5. Subsequently, neurons were transduced with the C-terminally mcherry tagged γ -isoforms, as described before. As previous shown, RIM3 γ -mcherry and RIM4 γ -mcherry were distributed diffusely, whereas RIM1 α showed the expected punctate

distribution. Interestingly, when RIM1 α and γ -RIMs were co-expressed, both γ -isoforms colocalized with RIM1 α and also exhibited a punctate distribution pattern. In addition, RIM3 γ -mcherry-expression levels were increased in the presence of RIM1 α , and specifically targeted to the synapse (Fig. 5.30A). The mainly diffuse localization of RIM4 γ -mcherry changed to a punctuated expression pattern, colocalizing with RIM1 α (Fig. 5.30B). These data indicate that RIM1 α promotes the presynaptic localization of RIM3 γ and RIM4 γ .

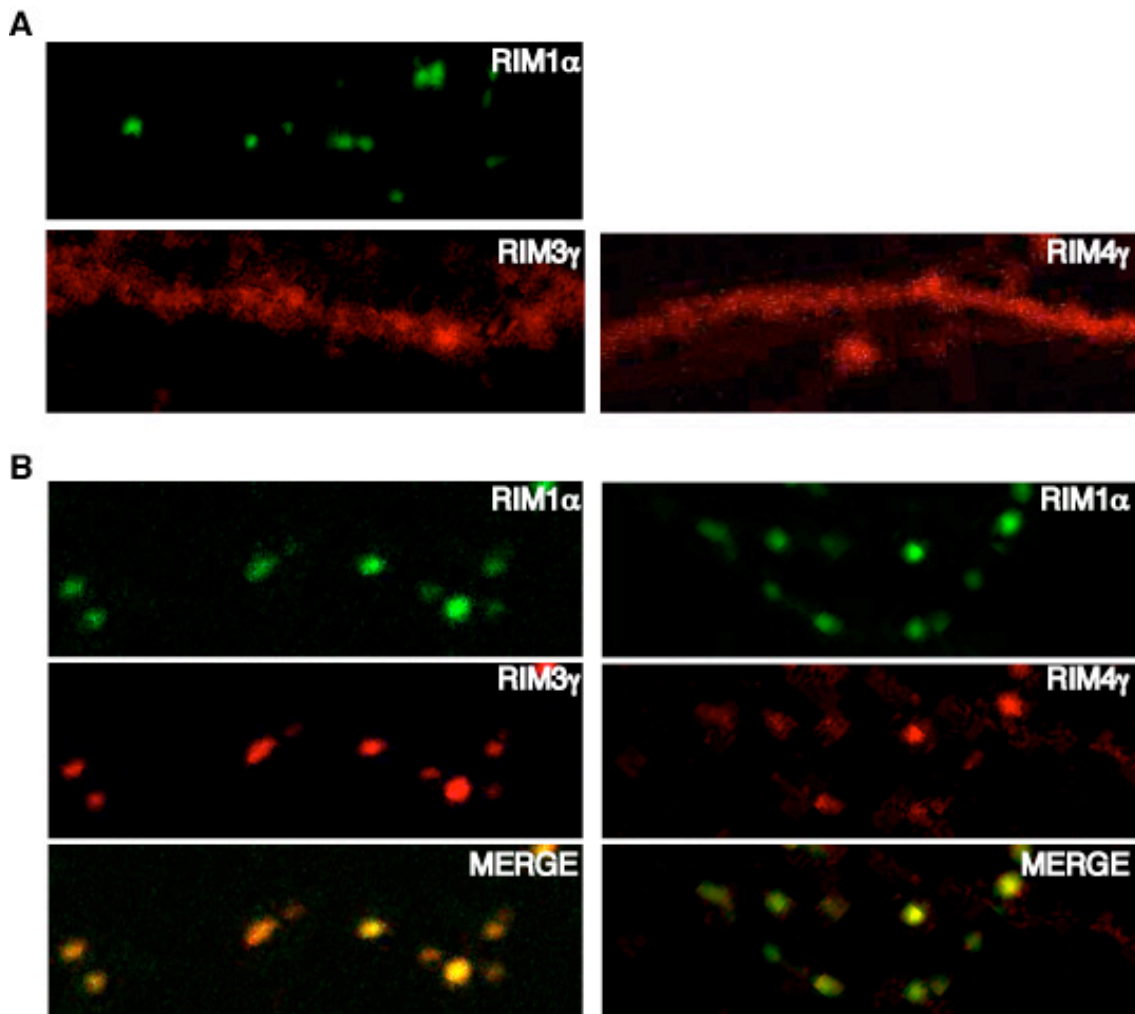


Fig. 5.30 Colocalization analysis of γ -RIMs and RIM1 α in primary neurons
Primary hippocampal neurons were transfected with RIM1 α (DIV3-5), subsequently infected with viral particles expressing mcherry-tagged γ -RIMs (DIV7-9) and analyzed by confocal microscopy. A, Exemplary neuronal processes showing the localization of RIM1 α , RIM3 γ and RIM4 γ if transfected individually. B, Cotransfection of RIM1 α resulted in a significant change in the localization of both γ -RIM isoforms. RIM3 γ -mcherry, previously diffusely distributed, was in

the presence of RIM1 α synaptically localized. RIM4 γ -cherry showed no more diffuse localization. Coexpression of RIM1 α resulted in the specific targeting of RIM4 γ to the synapse.

5.1.2.5 THE C2B DOMAIN OF γ -RIMS IS SUFFICIENT FOR THE INTERACTION WITH RIM1 α

In order to study if the C2B domains alone are sufficient to achieve the interaction between the γ -RIMs and RIM1 α , or if other sequences are required for this binding, primary hippocampal neurons were transfected with mcherry-RIM1 α on DIV5-7 and subsequently transduced with lentiviral particles expressing the GFP-tagged RIM3 γ or RIM4 γ truncated proteins. On DIV14, the hippocampal neurons were fixated and immunolabeled with antibodies against the synaptic vesicle protein Synapsin, in order to label the synapses. All γ -RIM truncated proteins colocalized with RIM1 α and Synapsin at the synapses, showing no major differences among the various truncated proteins.

In summary, these data suggest that the C2B domain alone might be sufficient for the interaction with RIM1 α and therefore for the presynaptic localization of RIM3 γ and RIM4 γ .

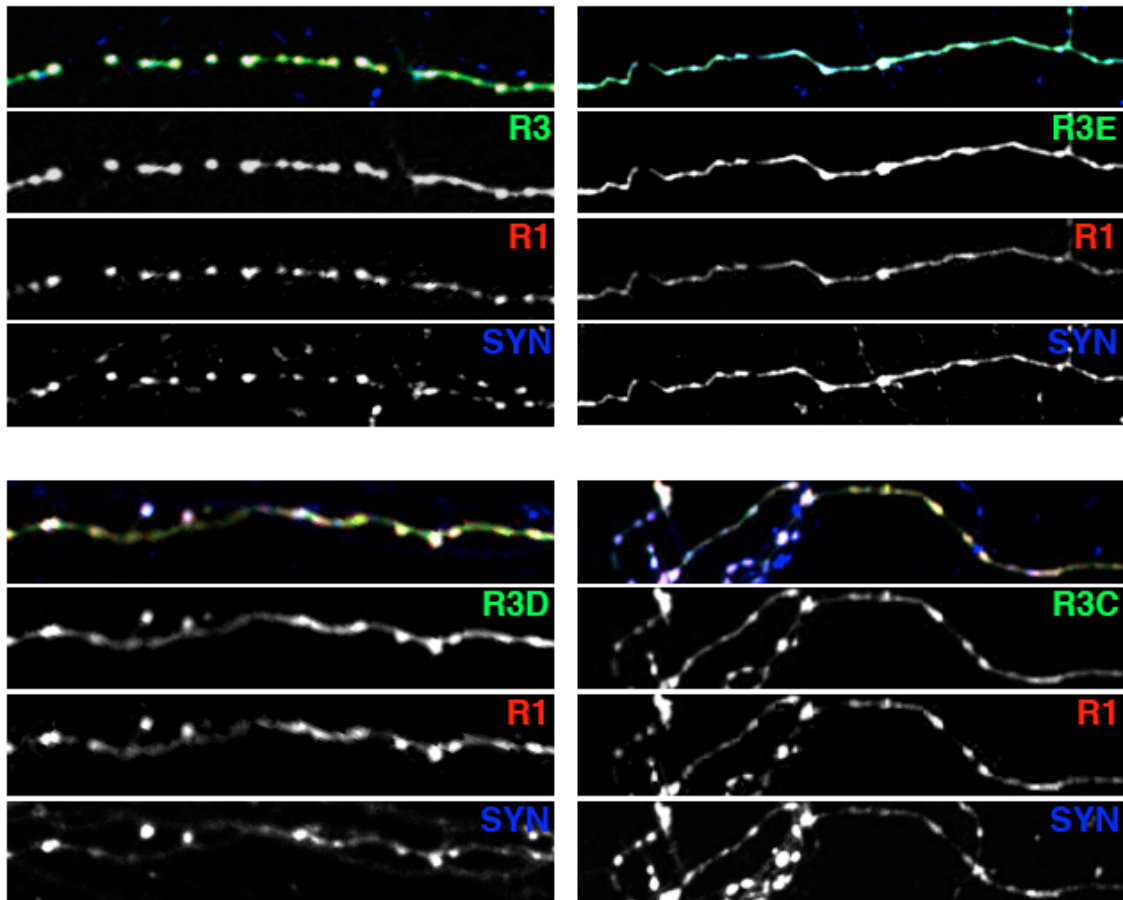


Fig. 5.31 GFP-RIM3 γ truncated proteins colocalize with RIM1 α at the synapses

Hippocampal cultured neurons were transfected with a plasmid expressing mCherry-RIM1 α (red) at DiV5-7 and subsequently transduced with lentiviral particles expressing GFP-RIM3 γ truncated proteins (green). At DIV14, the neurons were fixated and immunolabeled with an antibody against the synaptic vesicle protein Synapsin (blue). mCherry-RIM1 α and GFP-RIM3 γ full length and truncated proteins colocalized with Synapsin at the presynaptic boutons. Abbreviations: R1 RIM1 α ; R3 RIM3 γ ; SYN Synapsin.

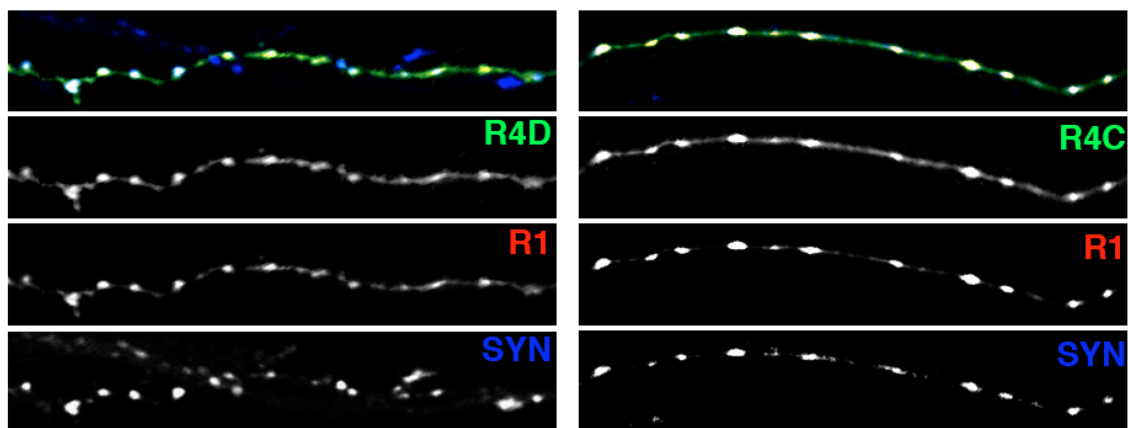


Fig. 5.32 GFP-RIM4 γ truncated proteins colocalize with RIM1 α at the synapses

Hippocampal cultured neurons were transfected with a plasmid expressing mCherry-RIM1 α (red) at DIV5-7 and subsequently transduced with lentiviral particles expressing GFP-RIM4 γ truncated proteins (green). At DIV14, the neurons were fixated and immunolabeled with an antibody against the synaptic vesicle protein Synapsin (blue). mCherry-RIM1 α and GFP-RIM4 γ truncated proteins colocalized with Synapsin at the presynaptic boutons. Abbreviations: R1 RIM1 α ; R3 RIM3 γ ; SYN Synapsin.

5.1.2.6 FUNCTIONAL CONSEQUENCES OF REDUCED γ -RIM LEVELS IN NEURONS

For evaluating the functional role of a protein, different approaches might be carry out in order to study a gain or a loss of function of the protein of interest. Studies involving loss of function include classical gene knockout approaches, mutations in the amino acid sequence of the protein and RNA interference techniques. In this work, to eliminate the expression of RIM3 γ and RIM4 γ , RNA interference technology was applied. Considering that the level of down-regulation achieved varies between different shRNAs, multiple shRNAs were designed following the shRNA design tech guide advice (Genome technology) and using several algorithms. To assess the efficiency of down-regulation each shRNA to downregulate γ -RIM expression, fluorescent immunocytochemistry and quantitative immunoblotting were applied. Eight (four for each) potential shRNA constructs were generated to decrease/suppress RIM3 γ and RIM4 γ expression (3.6.3).

5.1.2.6.1 *Analysis of knockdown efficiency in heterologous cells*

The efficiency of the different shRNAs was first tested in HEK 293T cells. Knockdown of overexpressed proteins of interest in HEK 293T allows for a quick and efficient screening of efficiency of the shRNAs because these cells

produce large amounts proteins that can be easily analyzed by Western-blotting.

HEK 293T cells were transfected with the pLVHTM vector containing the shRNA sequence under the H1 promoter and the green fluorescent marker GFP under the EF1 α promoter, to control for transfection/transduction efficiency together with a RIM3 γ and RIM4 γ expression plasmid. After the evaluation of different DNA amounts for transfection, a ratio of 5:1 shRNA-DNA/overexpressing plasmid was chosen for the experiments. Cells were lysed 48h after transfection and the protein expression levels were determined by western blot analysis. pLVHTM plasmid without shRNA was used as control. Since transfection efficiency in all experiments was over 98%, Tubulin was used as internal standard.

The immunoblot analysis showed that all RIM3 shRNAs resulted in a decrease of RIM3 γ protein levels to around 20% of the control (Fig. 5.33). In contrast, only shRNA 4.1 and 4.3 had a clear effect on RIM4 γ expression, reducing protein levels to 20-30% of the control (Fig. 5.34).

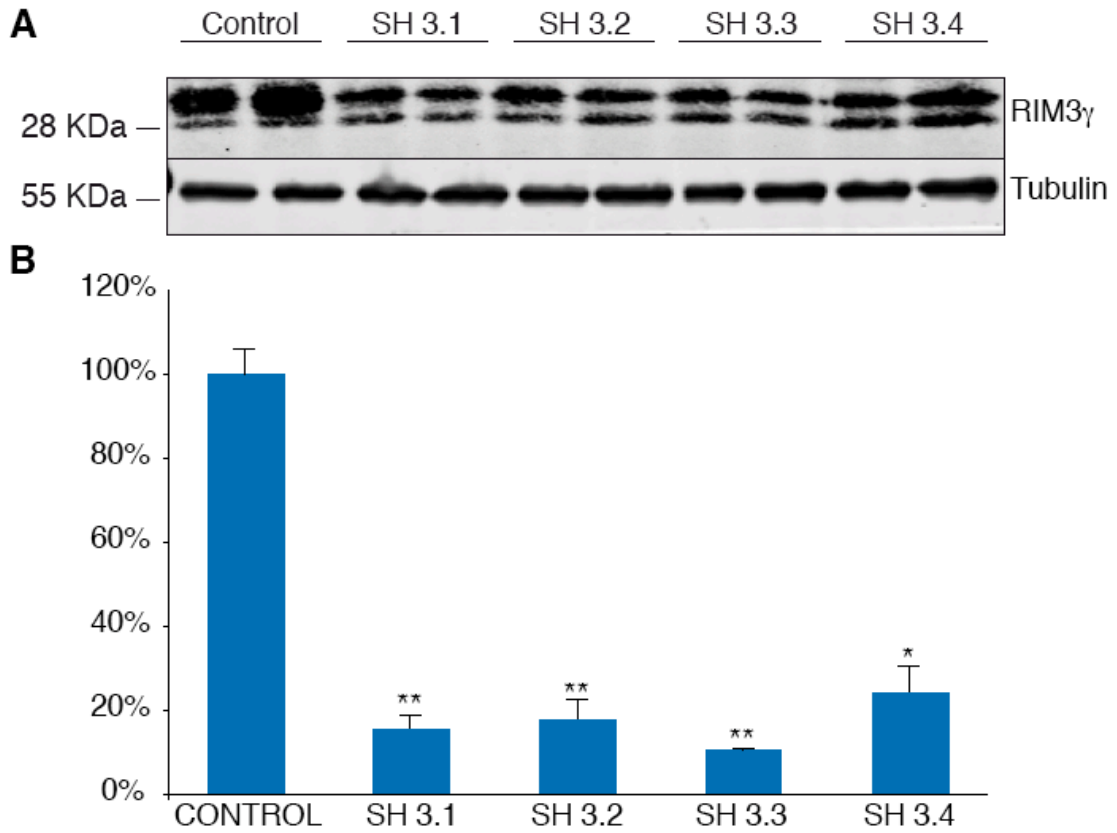


Fig. 5.33 RIM3 shRNAs efficiently reduce overexpressed RIM3 γ protein levels in HEK 293T cells

A, Immunoblot analysis was performed to test for the knockdown efficacy of various shRNA sequences against RIM3 γ . The pLVHTM plasmid containing the shRNA sequence and the pCMV-RIM3 γ expression plasmid were cotransfected, ratio DNA (6:1) in HEK 293T cells. 48h after transfection, cells were lysed and used for western blot analyses. B, All shRNAs designed for RIM3 γ showed a clear effect, decreasing the protein expression levels as compared to control. Tubulin was used as loading control, since transfection efficiency was over 98%. Quantification is presented as means \pm SEM, n=4.

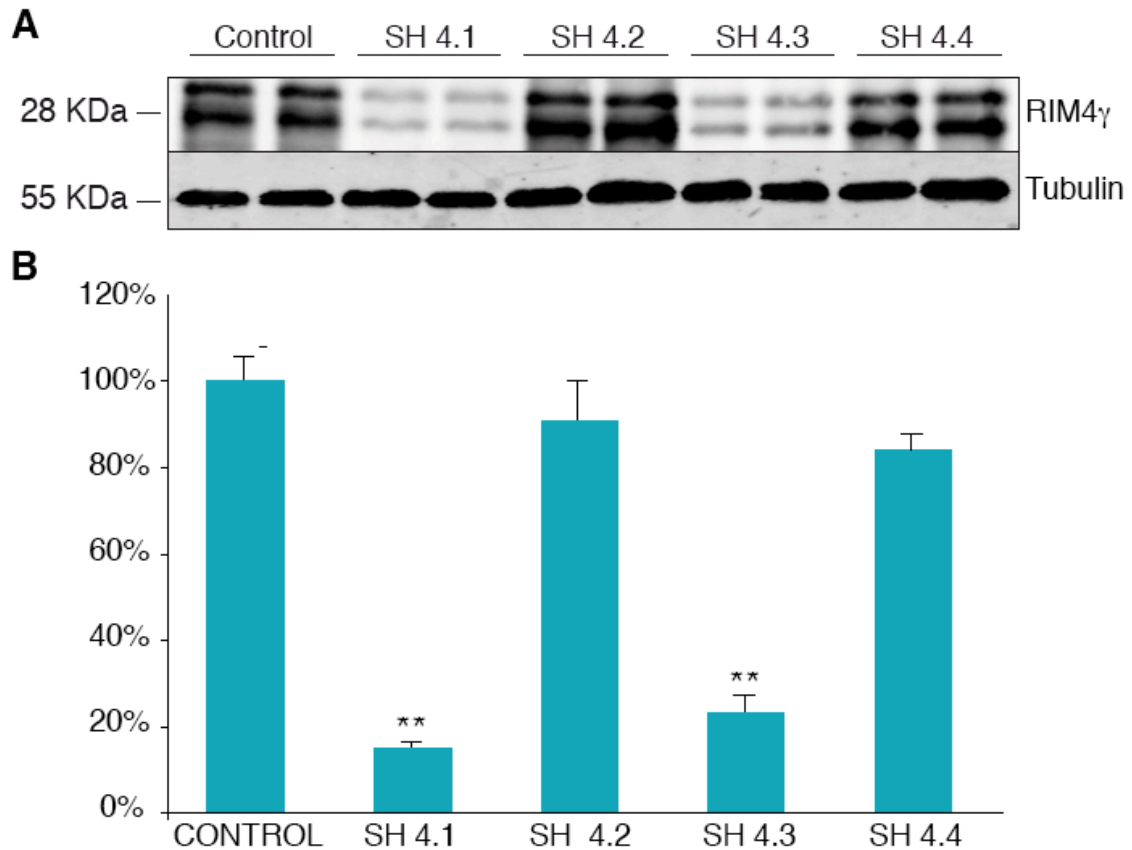


Fig. 5.34 RIM4 γ shRNAs efficiently reduce overexpressed RIM4 γ protein levels in HEK 293T cells

A, Immunoblot analysis was performed to test for the knockdown efficacy of various shRNA sequences against RIM4 γ . The pLVHTM plasmid containing the shRNA sequence and the pCMV-RIM4 γ expression plasmid were cotransfected, ratio DNA (6:1) in HEK 293T cells. 48h after transfection, cells were lysed and used for western blot analyses. B, Only two of the anti-RIM4 shRNA, shRNA 4.1 and 4.3, showed a significant downregulation of expression levels. Tubulin was used as loading control, since transfection efficiency was over 98%. Data analysis is shown as means \pm SEM, n= 4.

5.1.2.6.2 shRNAs are isoform specific

To verify that the shRNAs do not exhibit a cross reactivity due to sequence similarity, we tested the specificity of the shRNAs on their targets. Therefore, HEK cells were transfected with RIM3 γ and RIM4 γ expression plasmids and plasmids containing shRNAs targeted against the different γ -RIM isoforms. 48 hours after transfection, cells were lysed and equal amounts of protein were loaded for immunoblotting. Western blot analyses showed no effect of the RIM3

shRNAs on the expression level of RIM4 γ and vice versa. The results proof that the shRNAs are specific for the targeted isoform (Fig. 5.35).

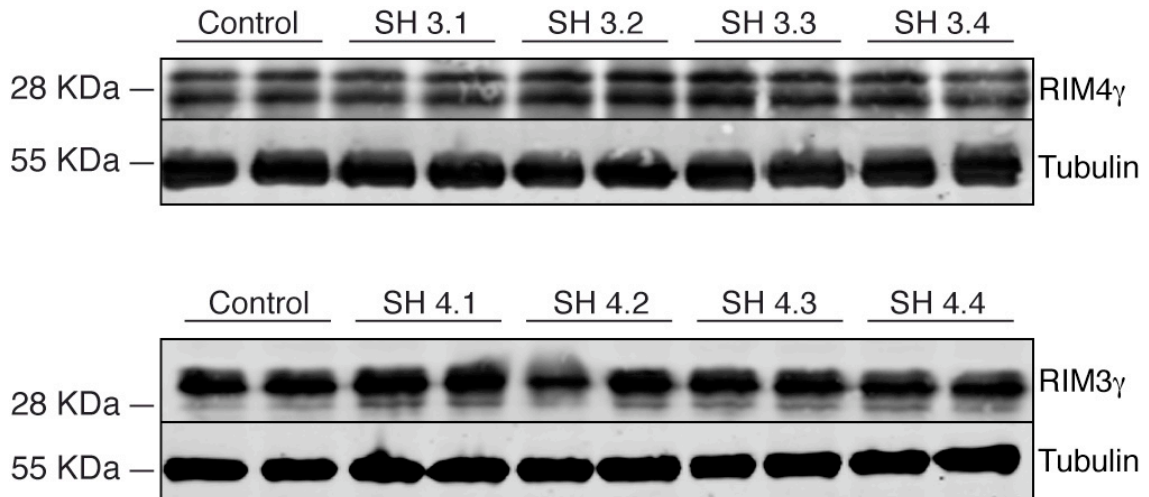


Fig. 5.35 RIM3 γ and RIM4 γ shRNAs are isoform-specific

Western Blot analyses were performed to test for possible crossreactivities of the shRNAs. ShRNA constructs and RIM3 γ or RIM4 γ expression plasmids were cotransfected (DNA ratio 6:1) in HEK 293T cells. 48h after transfection, cells were lysed and analyzed by immunoblotting. All shRNAs designed against RIM3 γ showed no effect on overexpressed protein levels of RIM4 γ , and vice versa.

5.1.2.6.3 Analysis of knockdown efficiency in neurons

Non-functional shRNAs can be quickly identified by testing their efficiency in HEK 293T cells, overexpressing the protein of interest. However, not all shRNAs having an effect in heterologous cells on the levels of overexpressed proteins, result in a downregulation of endogenous protein levels in the target cells. To examine the efficiency of shRNA downregulation on neuronal endogenous RIM3 γ and RIM4 γ primary cortical neurons were infected with lentiviral particles expressing the different shRNAs and GFP to control for transduction under the EF1 α promoter. Neurons were infected at DIV1 and analyzed at DIV14, when mature synapses are present. In contrast to the data obtained in HEK 293T cells, western blot analyses of homogenates from

primary cells, showed that sh3.4 (for RIM3 γ) and sh4.3 (for RIM4 γ) had a stronger effect than all other designed shRNAs (Fig. 5.36). The down-regulation efficacy also depended on the quality and titer of the purified viral particles, ranging from 1-42% (Fig. 5.37). In order to achieve a high infection rate, the number of viral particles has to exceed the number of targeted cells. In addition multiple viral particles can infect the same cell, thereby influencing the knockdown efficacy.

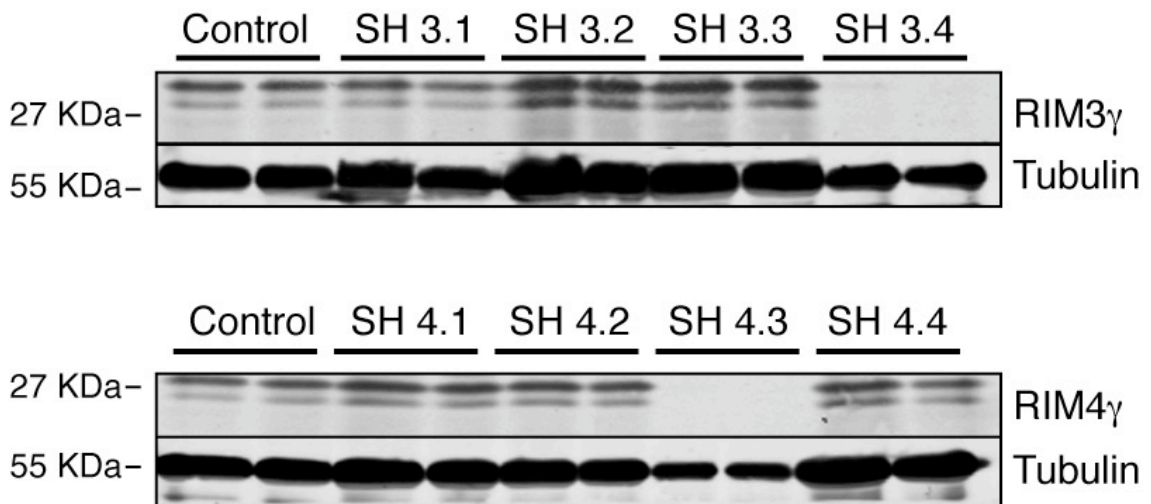


Fig. 5.36 shRNA effect on endogenous RIM3 γ and RIM4 γ protein expression

Western blot of cellular lysates from cortical primary neurons was performed at DIV14. Tubulin was used as loading control. In contrast to knockdown experiments in HEK cells, just one of the shRNAs showed a clear downregulation effect for each isoform.

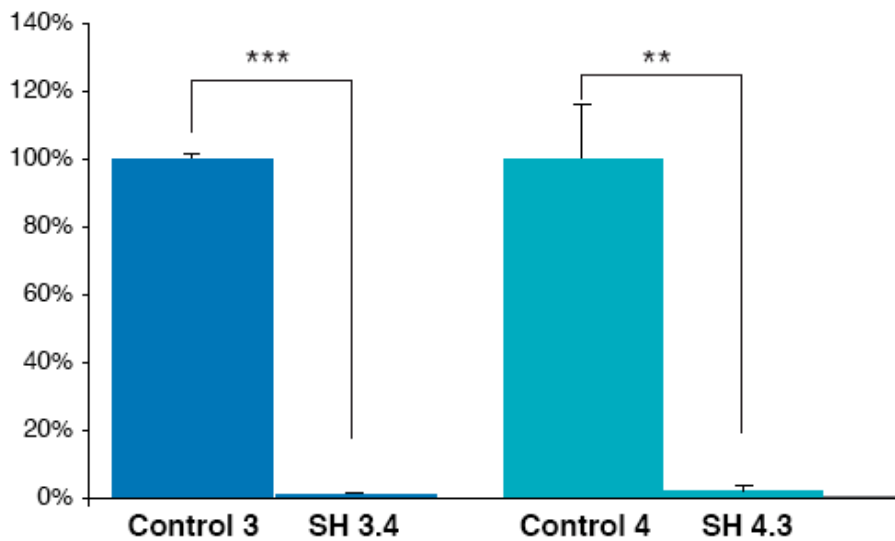


Fig. 5.37 Quantification of RIM3 γ and RIM4 γ shRNA mediated downregulation in primary cell neurons

Immunoblot quantification of homogenated primary neurons showed a significant reduction of endogenous protein expression levels after application of sh3.4 for RIM3 γ and sh4.3 for RIM4 γ , using Tubulin as loading control and neurons infected with empty pLVHTM vector as expression control. Data is presented as means \pm SEM.

5.1.2.6.4 RIM3 γ and RIM4 γ knockdown inhibits dendrite morphogenesis

After shRNA efficiency had been verified by immunoblot analysis, immunocytochemistry of primary hippocampal neurons deficient for RIM3 γ or RIM4 γ was carried out in order to evaluate the effects of RIM3 γ and RIM4 γ downregulation.

Therefore, dissociated hippocampal primary cultured neurons were transduced at DIV1 and examined at DIV14. Neuronal morphology was visualized by co-expression of the marker GFP, and expression levels of RIM3 γ or RIM4 γ by immunocytochemistry. Transduced cells were washed, fixed and immunolabeled with antibodies against RIM3 γ and RIM4 γ (Fig. 5.38). RIM3 γ -shRNA and RIM4 γ -shRNA transduced neurons showed stunted dendritic arbors compared with neurons transduced with viral particles containing the empty

shRNA plasmid. Neuron morphology was reduced to the main processes, showing a massive decrease in secondary and tertiary extensions (Fig. 5.38). To quantify the pattern of dendritic branching, Sholl analysis was performed (Fig. 5.37). This method measures the number of dendrites crossing circles at various radial distances from the cell soma. The estimate number of dendrites per unit area (number of intersections divide by the area of each circle) is plotted against distance. Sholl analysis followed by t-test revealed statistical differences among the control group and the shRNA groups. In neurons transduced with shRNA 3.4 for 13days (DIV1+13), the number of crossings stagnated between 20 and 120 μm from the soma. Neurons transduced with shRNA 4.3 showed a reduced number of crossings over the entire measured distance. These results reflect a simplified dendritic tree in which branching is severely impaired.

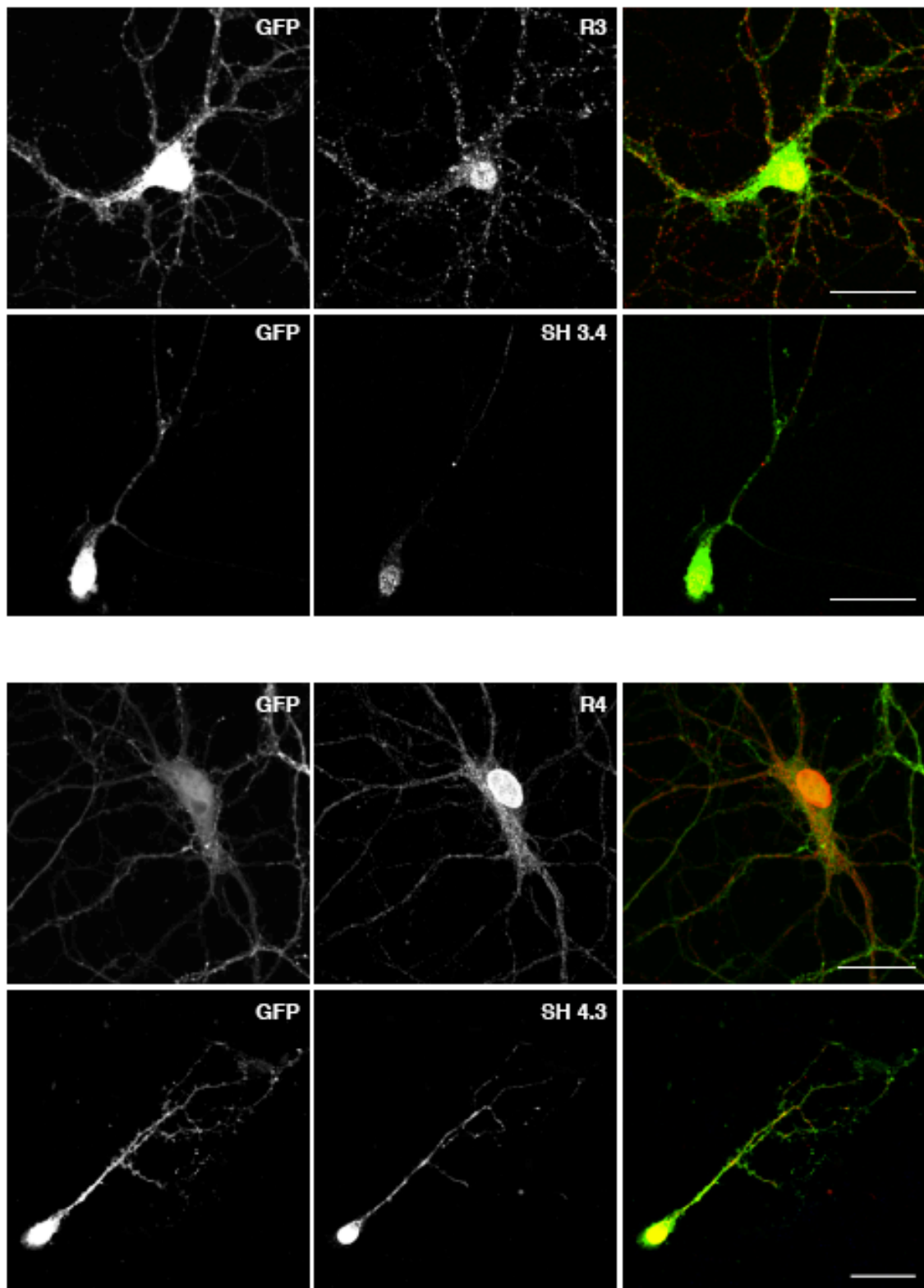


Fig. 5.38 Knockdown of RIM3 γ and RIM4 γ results in alteration of neuronal morphology

Hippocampal neurons infected with lentivirus carrying shRNA or control pLVHTM vector were fixed on DIV14 and immunolabeled with antibodies against RIM3 γ and RIM4 γ (red). Infected

neurons (GFP positive) expressing the shRNAs, showed a clear decrease of RIM3 γ or RIM4 γ immunoreactivity. Neurons with reduced levels of RIM3 γ and RIM4 γ exhibited significant alterations in dendritic arborization. Scale bar 30 μ m.

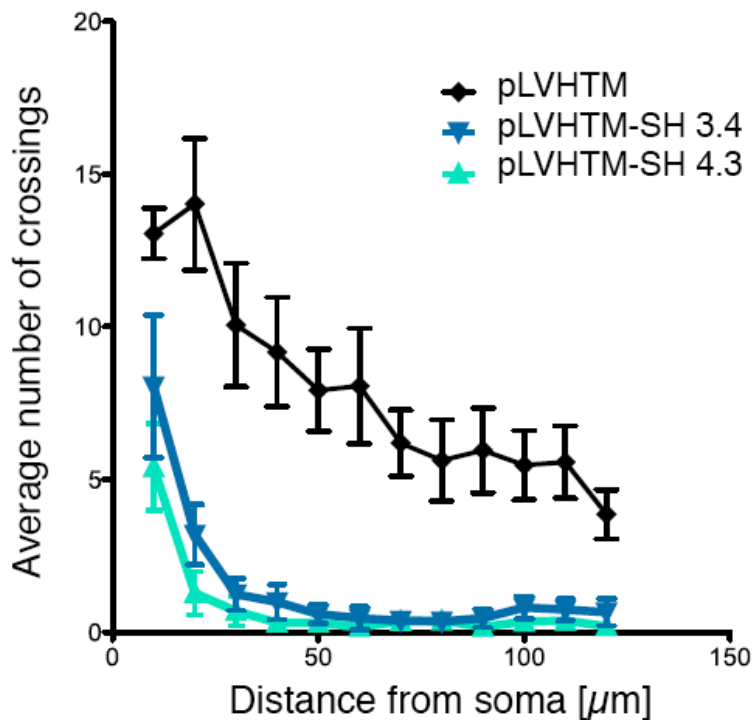
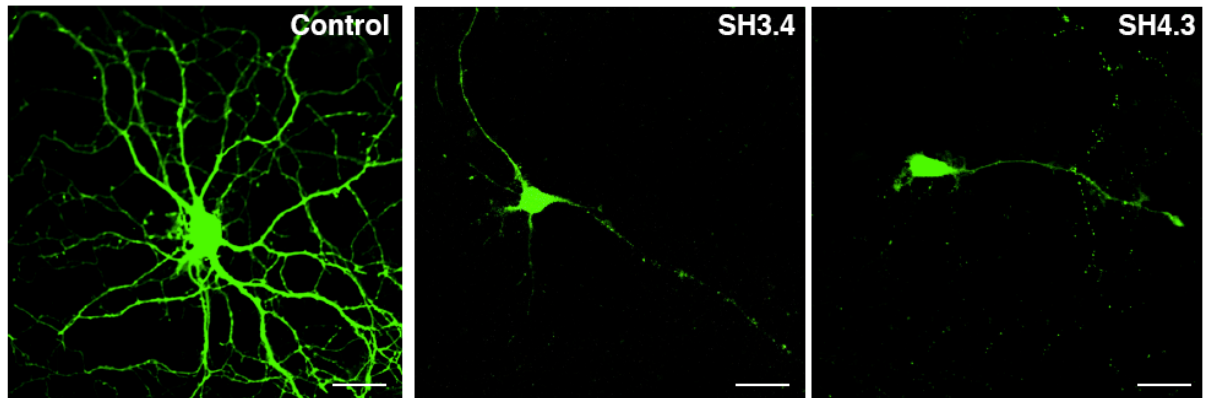


Fig. 5.39 Quantification of neuronal branching by Sholl analysis

Sholl analysis was performed to quantify the loss of neuronal processes. Sholl analysis quantifies the number of dendrite intersections for concentric circles centered at the soma. The estimate number of intersections are divided by the area of each circle and the result is plotted against the distance to the soma. Pictures above show exemplary pictures of neurons used for the analysis. Scale bar 30 μ m; n=8. Quantification revealed a significant reduction in the dendritic arbor ($P < 0.001$).

5.1.2.7 IN VIVO EXPERIMENTS

The dramatic loss in neuronal arborisation was an unexpected finding. To exclude that the effect was caused by problems related to cultured neurons, the effect of the shRNAs was also evaluated *in vivo* in order to validate the results obtained in the cell culture. Therefore, p0 rat brains were infected with viruses containing control vector or the different shRNAs. After intraventricular brain injection of the viral particles, the pups were kept with the mother until analysis. To examine the effect of the downregulation at different stages of synaptogenesis, brains were isolated and analyzed by immunohistochemistry at p7, p14 and p21. At all time points examined neurons expressing GFP could be identified.

At all time points, at least three animals per group were sacrificed. The brains were extracted after PFA fixation via transcardial perfusion, cut in 100 µm slices and analyzed by immunocytochemistry using FITC-couple antibody to GFP.

Analyses at p7 already showed a difference in neuronal morphology between control and shRNAs infected animals. Transduced control neurons around the infection point were green and displayed a normal morphology, with a high number of projections. In contrast shRNA-expressing neurons revealed a considerable decrease in the number of processes as compared to control (Fig. 5.40, left panels). Viral particles spread out after injection into different brain regions, such as thalamus, striatum, and cortex. In all brain regions, GFP positive cells expressing the shRNAs showed an evident loss in their neuronal processes (Fig. 5.40, right panels).

At p14, in both cases, animals infected with viral particles expressing the control plasmid or the shRNA sequences, showed that viruses migrated properly reaching the cortex, thalamus, hippocampus, striatum and midbrain. The projections of GFP positive control neurons expanded from the midbrain into

the striatum, in contrast to neurons expressing the shRNAs that were almost devoid of neuronal projections (Fig. 5.41, left panels). Cortical control neurons showed a proper dendritic growth. In contrast, branching was greatly compromised in neurons lacking RIM3 γ and RIM4 γ (Fig. 5.41, right panels).

At p21 days, a large number of GFP positive cells could be detected in the cortex, hippocampus, thalamus and striatum of rats injected with viral particles expressing control as well as shRNAs sequences, indicating a stable integration of the viral DNA into host DNA. Control neurons lacking RIM3 γ and RIM4 γ showed a significant decrease in the number of neuronal processes (Fig. 5.44), confirming the loss of dendrites shown at earlier time points, as well as in cell culture experiments (Fig. 5.38).

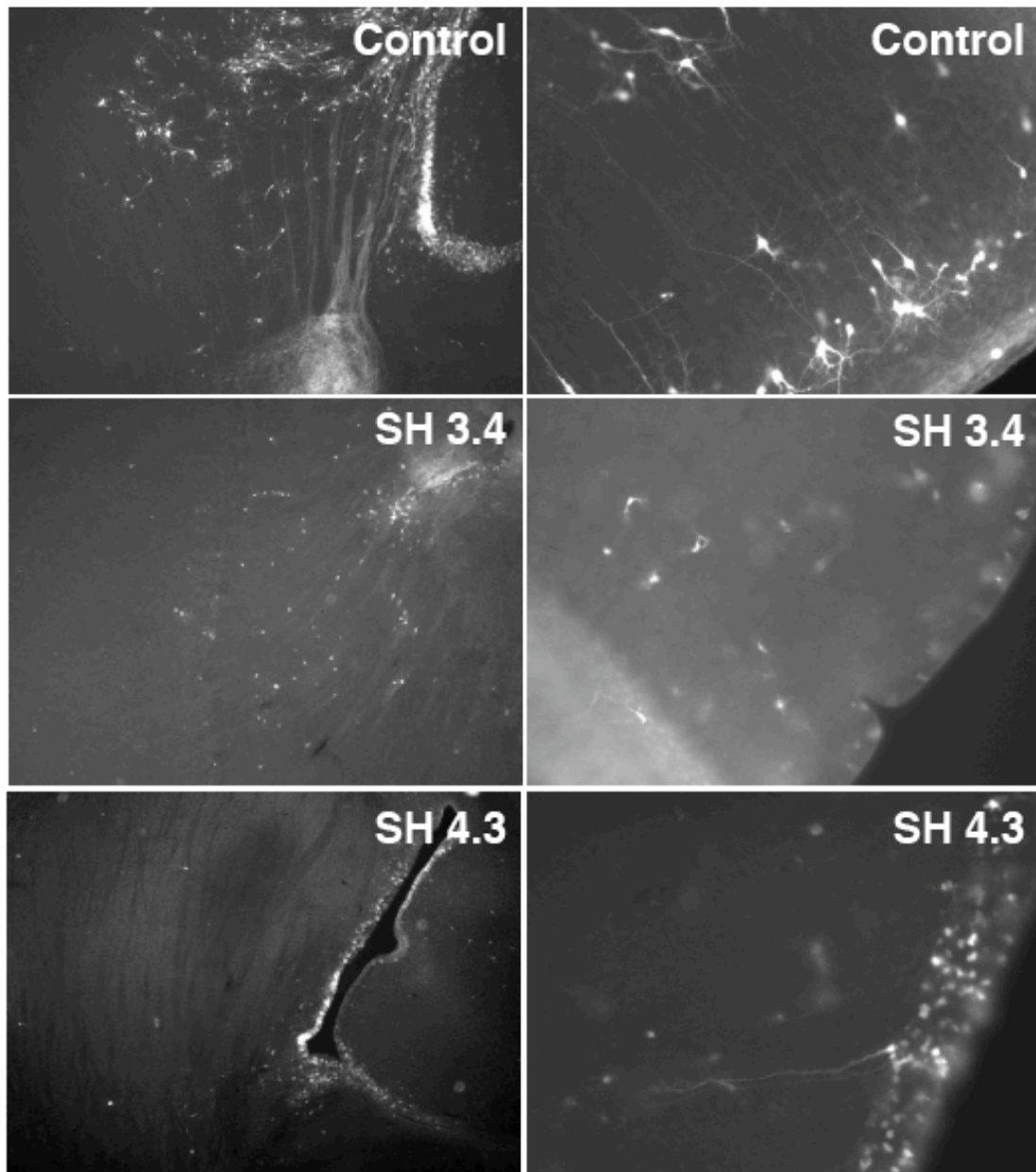


Fig. 5.40 *In vivo* knockdown of RIM3 γ and RIM4 γ at P7

Transduced neurons expressing the control or the shRNA sequences were identified by GFP labeling. Representative neurons in the cortex exhibit an obvious deficit in dendritic branching (right pictures). Striatal neurons surrounding the lateral ventricle where the virus was injected, show a noticeable difference in the number of processes between control and shRNA expressing neurons (left pictures). Neurons with decrease of RIM3 γ and RIM4 γ normal expression levels were smaller and deprived of the proper number of neurites.

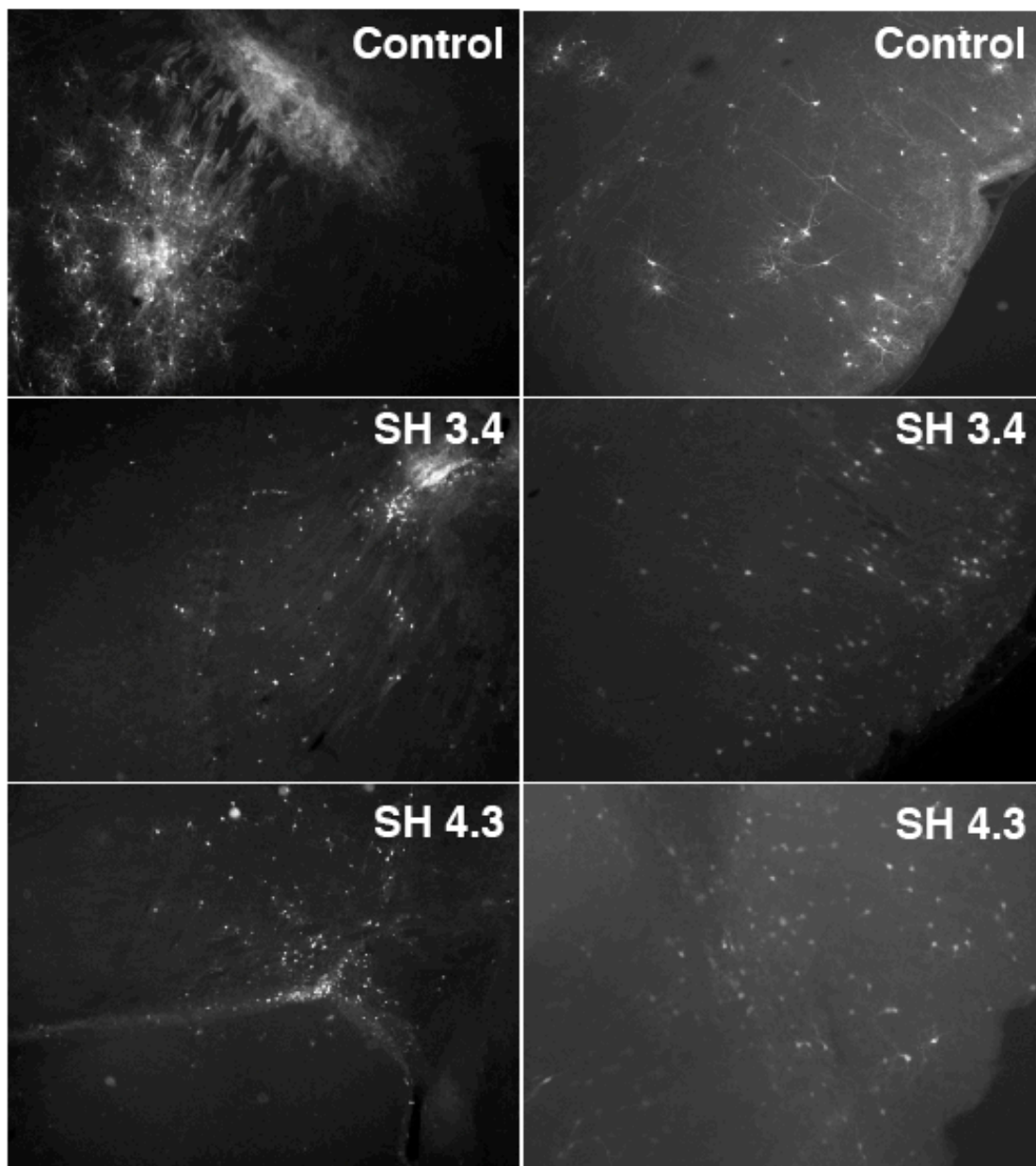


Fig. 5.41 *In vivo* knockdown of RIM3 γ and RIM4 γ at P14

At p14, neurons expressing the control or the shRNA sequences were identified by GFP labeling. Cortical control neurons displayed a normal morphology, in contrast to neurons transduced with the shRNA sequence, which exhibit a significant deficit in the number of dendrites (right pictures). Striatal neurons lacking RIM3 γ and RIM4 γ showed a clear loss of dendritic projection when compared to control (left pictures).

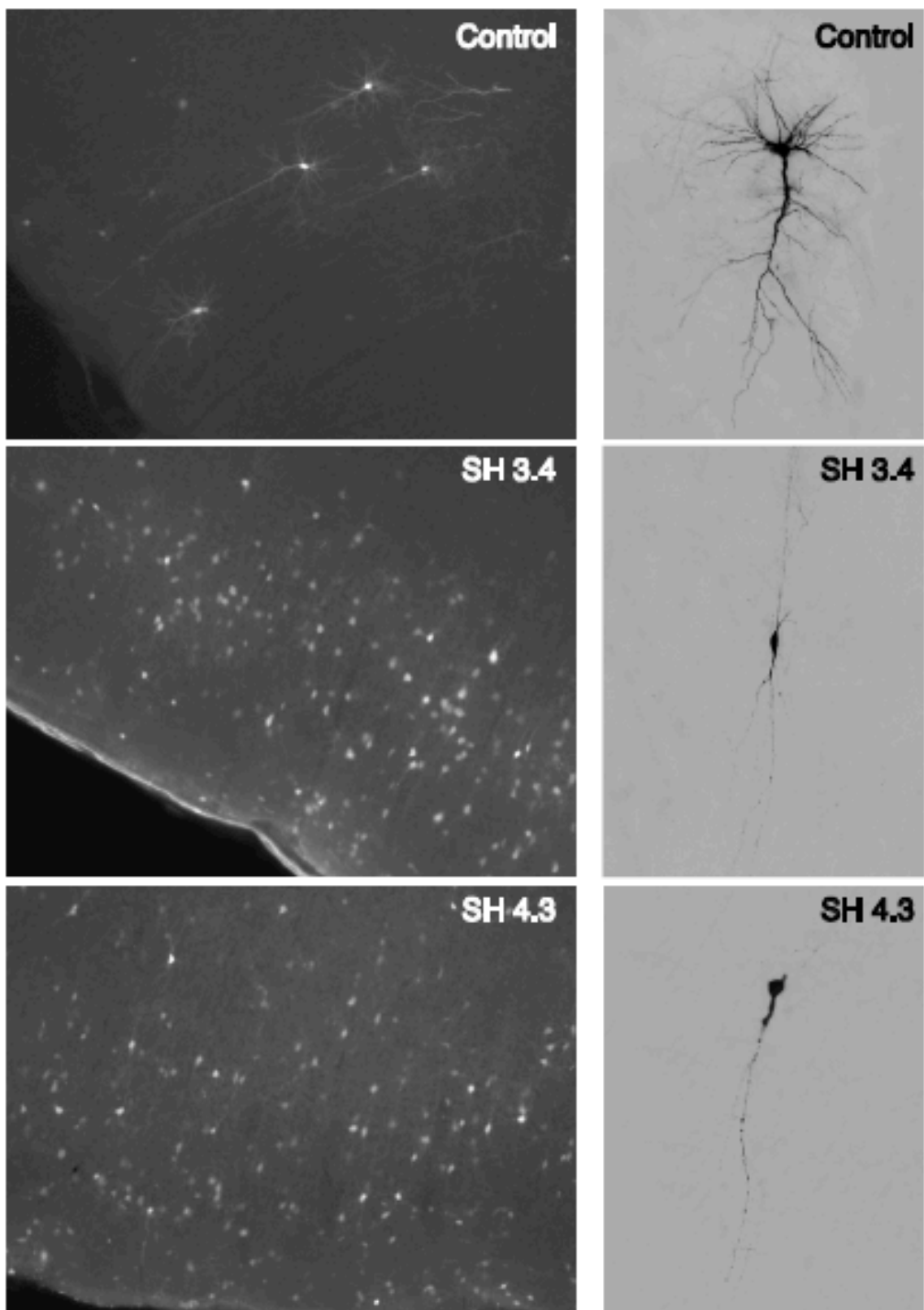


Fig. 5.42 *In vivo* knockdown of RIM3 γ and RIM4 γ at P21

At p21, neurons transduced with lentiviral particles containing the control or the shRNA sequences were identified by GFP labeling. Cortical control neurons displayed a normal

morphology, showing a regular dendritic growth. In contrast, neurons transduced with the shRNA sequence, exhibited a significant deficit in the number of neurites, indicating a greatly compromised neuronal branching (left pictures). (left pictures). Higher magnification of control and knockdown cortical neurons showed a significant loss in the dendritic arbor of neurons deficient in the expression of RIM3 γ and RIM4 γ as compared to control (right pictures).

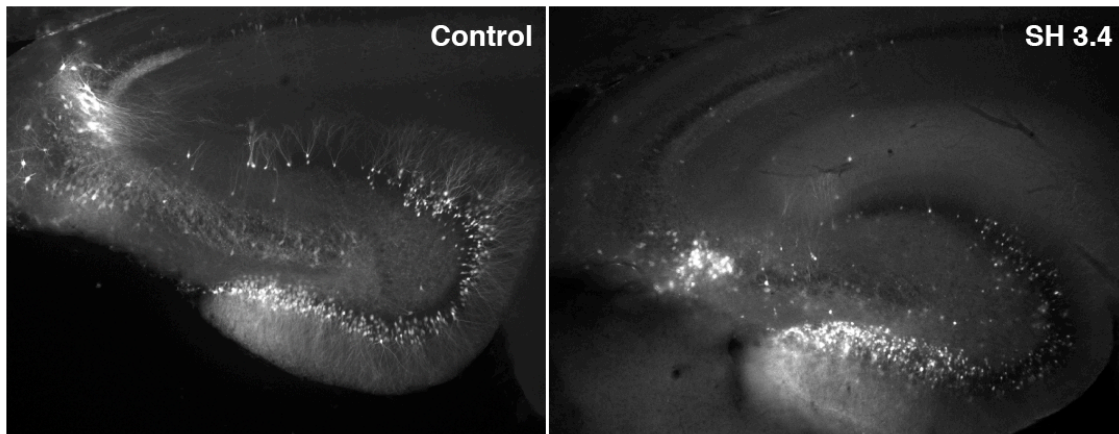


Fig. 5.43 *In vivo* knockdown of RIM3 γ and RIM4 γ at P21

At p21, hippocampal GFP positive control neurons displayed a normal morphology. Exemplary pictures of control neurons show a normal formation of the projections of the dentate gyrus granular cells and the CA3 pyramidal cells. In contrast, exemplary neurons lacking RIM3 γ showed a dramatic loss of neuronal processes. Granular cells and CA3 neurons displayed a compromised dendritic tree.

5.1.2.8 PHENOTYPE RESCUE

It has been shown that expression of RNAi sequences can result in off-target effects, e.g. structural changes of neurons (Alvarez *et al.*, 2006). Therefore, it is critical to show that the observed phenotype is induced by the reduction in the levels of the targeted gene. For this purpose, two different approaches were performed. First, point mutations were introduced in the shRNA sequences 3.4 and 4.3, the shRNAs that resulted in the strongest downregulation of RIM3 γ and RIM4 γ , respectively. These mutations are thought to interfere with the binding between the shRNAs and the target mRNA, thereby preventing the downregulation of the endogenous protein.

In the second approach, silent point mutations were introduced into the cDNA sequence of RIM3 γ and RIM4 γ at the region, which is targeted by the shRNA.

The introduction of silent mutations should result in shRNA resistant cDNAs, allowing for phenotype rescue experiments.

5.1.2.8.1 RIM3 γ and RIM4 γ shRNA sequence with point mutations are ineffective

To verify that RIM3 and RIM4 shRNAs with 3 to 5 nucleotide exchanges do not result in a down-regulation, cells were transfected with plasmids containing the shRNAs with or without mutations, or the empty control vector, together with RIM3 γ and RIM4 γ overexpression plasmids. 48h after transfection, the cells were lysed and analyzed by immunoblotting using specific antibodies against RIM3 γ and RIM4 γ . After overexpression of RIM3 γ and RIM4 γ shRNAs carrying point mutations, protein levels were unaffected, as compared to control. In contrast, cells transfected with the regular shRNAs showed a significant decrease in the amount of RIM3 γ and RIM4 γ (Fig. 5.44)

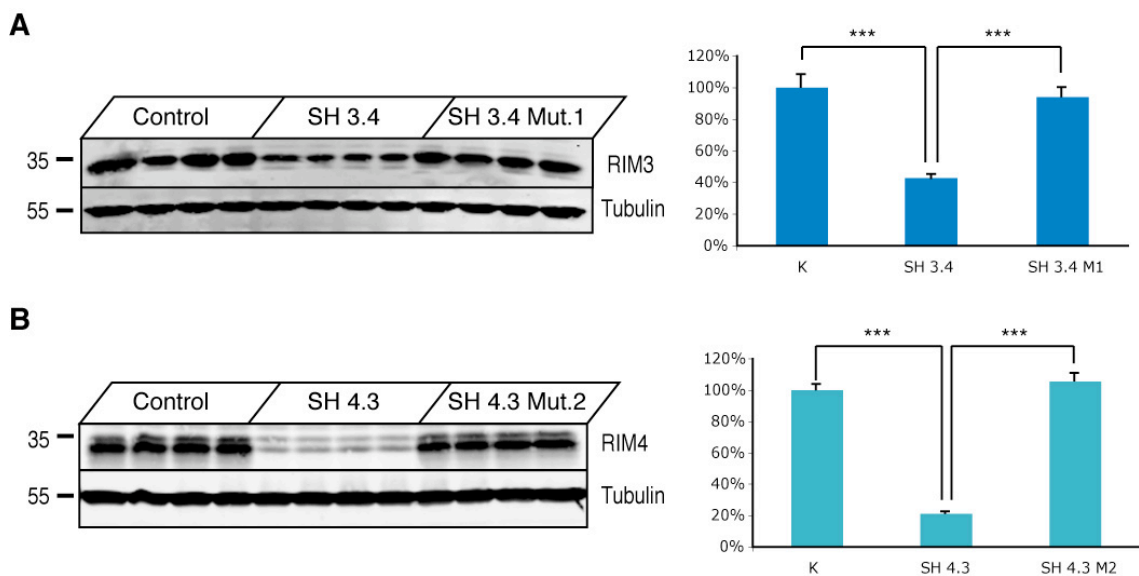


Fig. 5.44 shRNAs with nucleotide exchanges are unable to change RIM3 γ and RIM4 γ expression levels

Quantitative immunoblot analyses of HEK 293T cells co-expressing RIM3 γ (A) and RIM4 γ (B) and the regular or mutated shRNA sequences revealed that only the regular shRNAs resulted in

downregulation. Since transfection efficiency was over 98%. Tubulin was used as internal standard. Data is presented as means \pm SEM.

5.1.2.9 RESCUE EXPERIMENTS IN HIPPOCAMPAL NEURONS

After verifying that mutated shRNAs did not affect RIM3 γ and RIM4 γ overexpression levels in HEK 293T cells, lentiviral particles containing these shRNAs were produced and used to transduce primary hippocampal neurons. Cultured neurons were infected at DIV1 and analyzed at DIV14. Neurons expressing mutated shRNAs were directly compared to neurons expressing the functional shRNAs and control neurons infected with virus containing control vector without shRNA. Hippocampal cultured neurons expressing mutated shRNAs did not show any overt morphological alterations (Fig. 5.45, rescue I), in contrast to RIM3 γ and RIM4 γ deficient neurons, which exhibited a dramatic decrease in the number of dendrites (Fig. 5.38, Fig. 5.45 shRNA). Moreover, to ensure the target-specificity of the RIM3 and RIM4 shRNAs, an shRNA-resistant vector was generated by site-directed mutagenesis. Therefore, silent mutations (exchange of nucleotide without altering the amino acid sequence) were introduced in RIM3 γ and RIM4 γ cDNA sequence, so that the overexpressed protein could replace the endogenous that is affected by the shRNA. Hippocampal neurons coexpressing functional shRNAs together with plasmids containing mutated RIM3 γ and RIM4 γ exhibited a normal morphology, confirming that the loss of neuronal process was indeed due to a loss of RIM3 γ and RIM4 γ .

In summary, both rescue approaches confirmed the specificity of the shRNAs for their target.

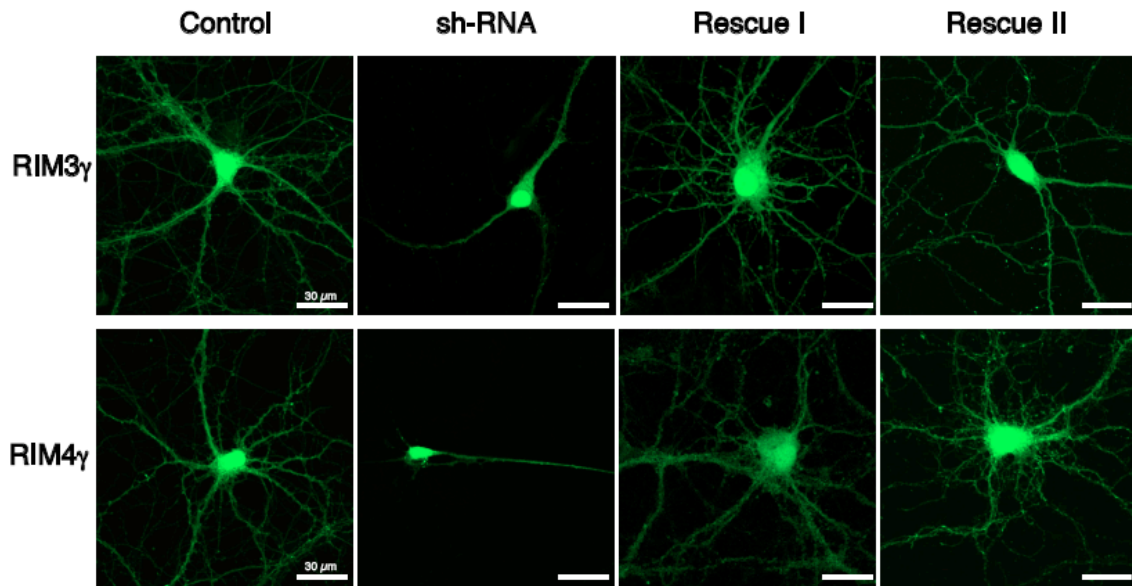


Fig. 5.45 RIM3 γ and RIM4 γ shRNA rescue experiments

Hippocampal neurons were transduced at DIV1 using viral particles expressing green fluorescent proteins for identification, together with different shRNA constructs. All neurons were analyzed at DIV14 using confocal microscopy. Neurons expressing shRNAs against RIM3 γ and RIM4 γ showed a clear loss of neuronal processes. In contrast, neurons infected with viral particles expressing point-mutated shRNAs (rescue I) revealed no difference in the number of neurites as compared to control. In the case of rescue II, in addition to virus expressing the functional shRNAs, neurons were also infected with lentiviral particles overexpressing shRNA-resistant RIM3 γ and RIM4 γ sequences. Overexpression of shRNA-resistant RIM3 γ and RIM4 γ rescued the downregulation phenotype. Scale bar 30 μ m.

5.1.2.10 RIM3 γ AND RIM4 γ ARE NECESSARY FOR NEURITE DEVELOPMENT

To examine if the knockdown of RIM3 γ and RIM4 γ prevents the formation of new processes, hippocampal cultured neurons were infected at different time points after preparation. Neurons were infected at DIV1, DIV3 and DIV7, with viral particles containing control or shRNA vector, and analyzed at DIV14 by immunocytochemistry. Viruses used for this experiment were from the same preparation to avoid variability due to the quality of different virus batches.

Infection at early time points (DIV1, DIV3) resulted in a dramatic decrease in the number of neurites, being reduced to the main processes. In contrast, neurons

infected at DIV7 displayed a higher number of neuronal processes, containing primary and secondary neurites. However, whereas control neurons developed an extensively branched dendritic tree, all infected neurons showed a decreased number of processes compared to control neurons.

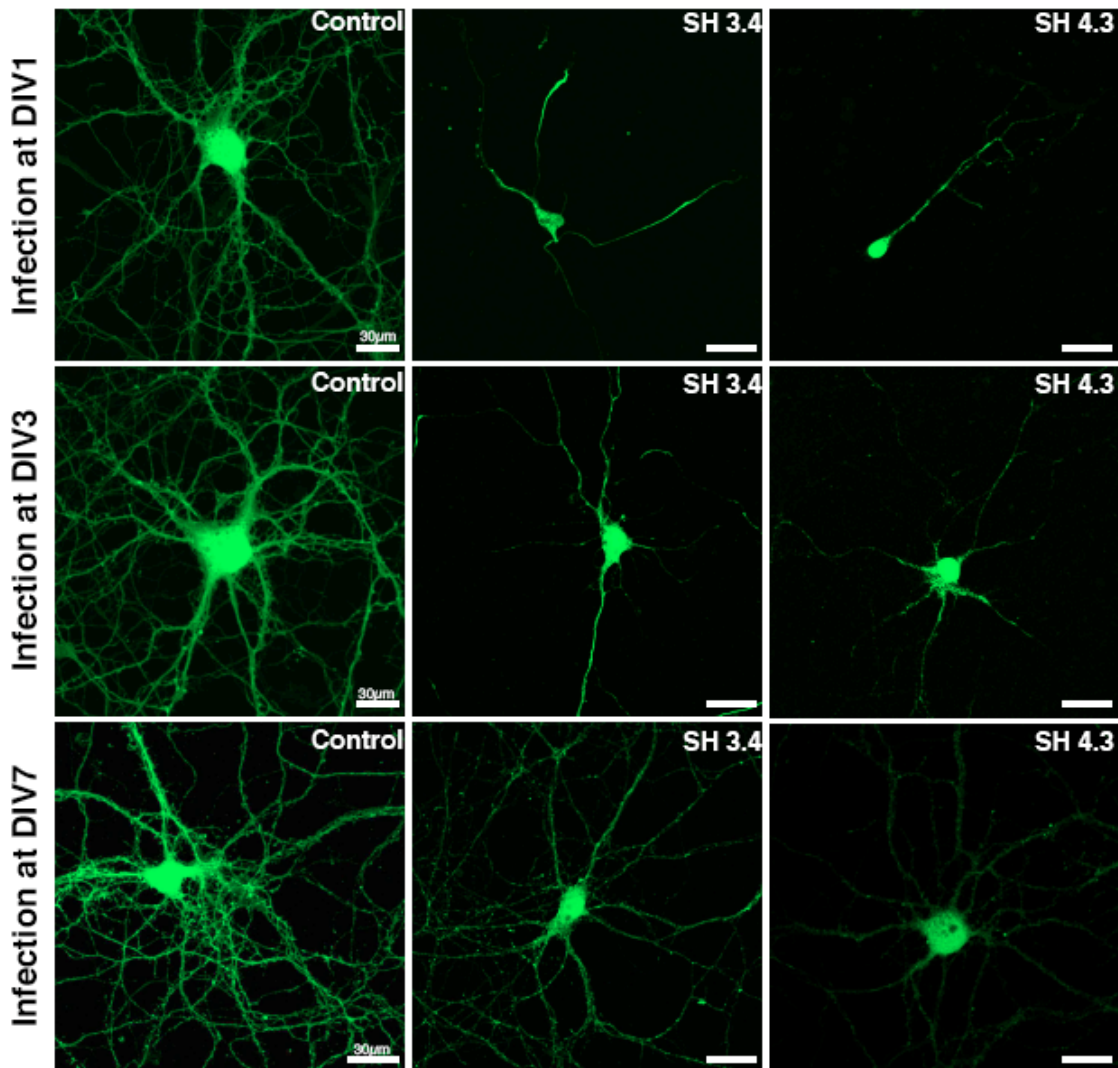


Fig. 5.46 Development of neuronal processes in neurons deficient for RIM3 γ or RIM4 γ

Hippocampal cultured neurons were transduced at different time points with shRNA-expressing lentiviral particles, and analyzed at DIV14. Shown are representative pictures of neurons at DIV14 after infection at different time points (DIV1, 3 and 7). Neurons infected later during development showed more dendrites than those in which knockdown had been performed earlier. However, at all time points shRNA treated neurons showed a lower number of processes as compared to control. Scale bar 30 μ m.

5.1.2.11 LOSS OF RIM3 γ AND RIM4 γ SPECIFICALLY AFFECTED RIM1 α EXPRESSION LEVELS

After establishing the efficacy of RIM3 γ and RIM4 γ downregulation and the specificity of the different shRNAs, as we had found RIM1 α to promote synaptic localization of both γ -RIMs, and to enhance RIM3 γ protein levels, we examined the consequences of γ -RIM knock down on RIM1 α expression. Primary cortical neurons were transduced with lentiviral particles containing control or shRNA sequences at DIV1 and analyzed at DIV14 by immunoblotting. The infection efficiency was around 80%. Cells were collected at DIV14, lysated and loaded on a SDS-Page gel for immunoblotting. Western Blot analyses showed that RIM1 α expression levels decreased proportionally to the reduction of RIM3 γ or RIM4 γ protein levels.

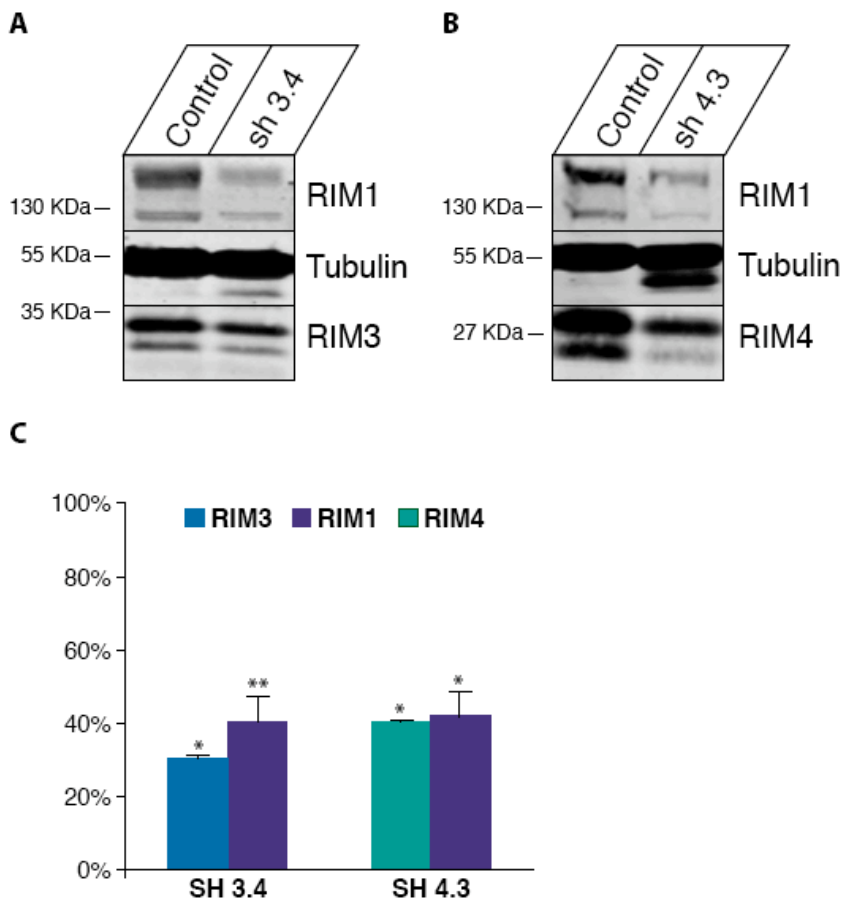


Fig.5.47 Downregulation of RIM3 γ or RIM4 γ results in a decrease in endogenous RIM1 α levels

A B, Representative western blot pictures illustrate the decrease in RIM1 α protein levels that is detected if RIM3 γ or RIM4 γ are downregulated via shRNA in primary neurons. C, Quantification of the immunoblot revealed that RIM1 α levels were decreased to a similar level as RIM3 γ and RIM4 γ , after shRNA treatment. Data is presented as means \pm SEM using Tubulin as loading control. Values were normalized to expression levels in control cells (neurons infected with empty pLVHTM vector).

To exclude a potential unspecific effect of the shRNAs on RIM1 α expression levels, due to sequence similarity, pLVHTM vector, empty or containing the shRNAs, was co-transfected with the expression plasmid pCMV-RIM1 α in HEK 293T cells. As in previous experiments the overexpression vector/shRNA vector ratio used was 1:6. None of the tested shRNAs altered RIM1 α protein expression levels, showing no unspecific effect on RIM1 α expression levels (Fig. 5.48). These results confirmed the specificity of the shRNA sequences and that the decrease in RIM1 α levels in neurons deficient in RIM3 γ and RIM4 γ , is due to the absence of γ -RIMs and not to an unspecific targeting of RIM1 α .

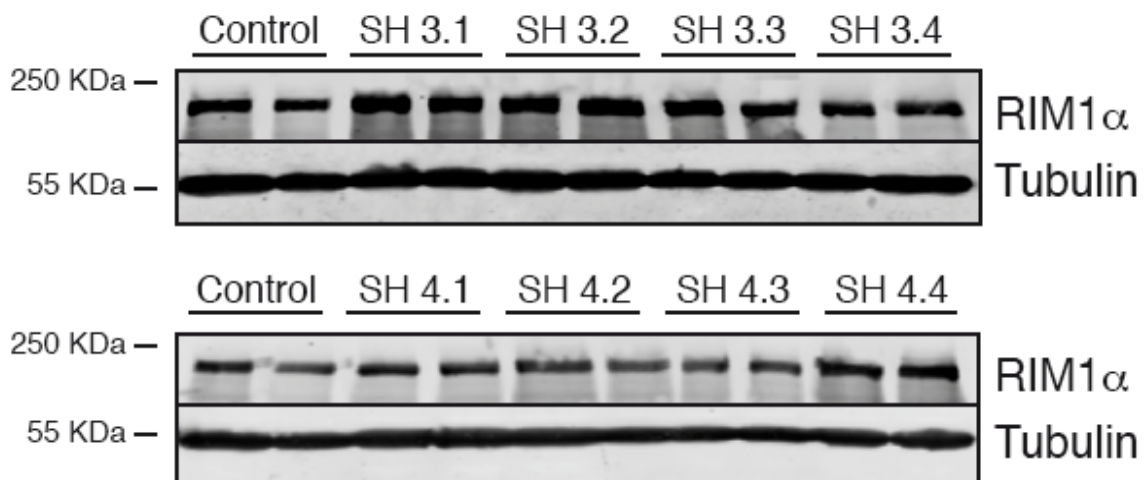


Fig. 5.48 RIM3 γ and RIM4 γ shRNAs did not alter RIM1 α overexpression levels

HEK 293T cells were transfected with shRNA vector and pCMV-RIM1 α (DNA ratio 1:6). 48 hours after transfection, cells were lysed and examined by immunoblot analysis. None of the shRNAs tested affected RIM1 α protein levels.

5.1.2.12 LOSS OF RIM3 γ INDUCES A REDUCTION OF LIPRINS- α AND GRIP1 EXPRESSION LEVELS

To further analyze the loss of dendrites and the possible mechanism underlying this effect, we hypothesized that downregulation of RIM3 γ may also affect protein levels of Liprins- α expression, and thereby alter the expression or localization of GRIP1. Liprins- α have been shown to be necessary for the trafficking of GRIP1, which is necessary for the proper localization of the EphB receptor. Mislocalization of this receptor induces a loss of neuronal processes, as shown in GRIP1 knockdown neurons, which is identical to the phenotype we observed for RIM3 γ and RIM4 γ knockdown neurons. Primary cortical neurons were transduced with lentiviral particles containing control or shRNA sequences at DIV1 and analyzed at DIV14 by immunoblotting. The Infection efficiency was around 90%. Cells were collected at DIV14, lysed and loaded on a SDS-Page gel for immunoblotting.

Western blot analysis (Fig. 5.49) showed no changes in the expression levels of Tubulin indicating that the amount of neurons analyzed was comparable, and no changes in the levels of Synaptophysin, suggesting no mayor axonal modification. As shown before, neurons lacking RIM3 γ and RIM4 γ displayed a dramatic loss of dendrites, but conserved their axons. Expression levels of the postsynaptic marker PSD-95, were reduced as a result of the decrease in the number of dendrites. Furthermore, Liprin- α , as well as its interaction partner GRIP1 showed also a reduction in the expression levels. In order to resolve whether the decrease of GRIP1 was a consequence of the reduction in the number of dendrites, or a direct effect of RIM3 γ downregulation, immunocytochemistry analyses were performed. Primary hippocampal neurons were transduced with lentiviral particles containing control or shRNA sequences at DIV1 and analyzed at DIV14 by confocal microscopy. Neurons infected with virus containing shRNA sequences showed a reduction in the number of

neuronal processes as shown before. Furthermore, the remaining dendrites displayed a significant loss of spines, which were almost non-existent (Fig. 5.50). In addition, GRIP1 expression levels were reduced, as shown before in the immunoblot analysis. However, these first observations have to be quantified in order to draw unequivocal conclusions.

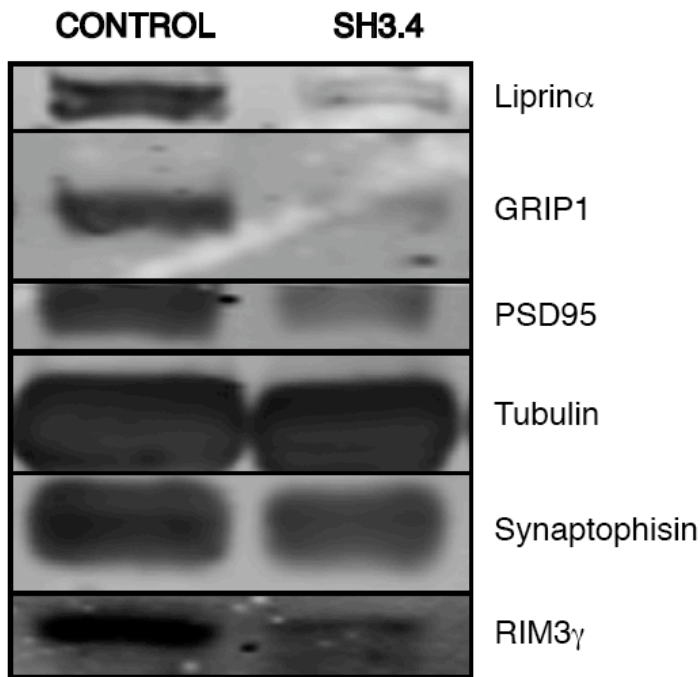


Fig. 5.49 Downregulation of RIM3 γ results in a reduction of the expression levels of several proteins

Representative western blot pictures illustrate the decrease in the protein levels of several proteins detected in RIM3 γ deficient primary neurons. Synaptophysin protein amount did not change between neurons transduced with control or shRNA sequences, suggesting no axonal changes. In contrast, the expression levels of the postsynaptic marker PSD-95 were reduced in neurons lacking RIM3 γ , as a result of the loss of dendrites. Expression levels of RIM3 γ interacting protein Liprins- α and its interaction partner GRIP1 were also reduced. As loading control Tubulin was used.

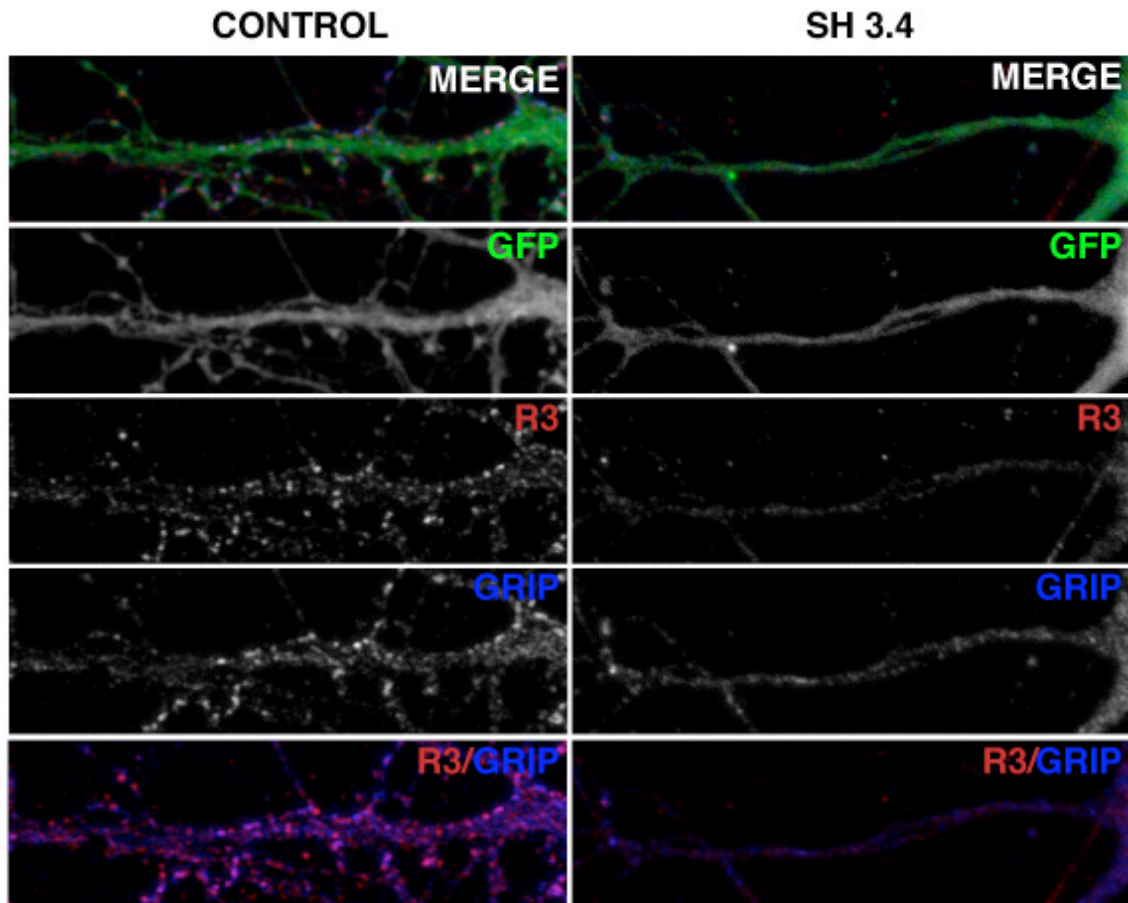


Fig. 5.50 Reduction of GRIP1 expression levels in neurons deficient in RIM3 γ

Exemplary confocal pictures show a reduction in the expression of RIM3 γ and GRIP1, in neurons transduced with viral particles expressing shRNA sequences against RIM3 γ , as compared to control neurons. Reduction of GRIP1 might be a direct effect of RIM3 γ downregulation.

5.1.2.13 SPONTANEOUS SYNAPTIC ACTIVITY IN RIM3 γ AND RIM4 γ KNOCKDOWN NEURONS

Ablation of most synaptic proteins as well as loss of neurites induces changes in neurotransmission. Therefore, in order to functionally investigate if neurons are still synaptically connected after the loss of neuronal processes due to the lack of RIM3 γ and RIM4 γ , preliminary electrophysiological measurements were performed in collaboration with Dr. Opitz (AG Beck).

Hippocampal cultured neurons were transduced with viral particles expressing control or shRNA sequences at DIV1, and spontaneous synaptic

transmission was analyzed using whole-cell patch clamp recordings at DIV14-17. Recordings of the miniature glutamatergic postsynaptic currents from hippocampal cultured neurons were performed in the presence of 0.5 μ M TTX, in order to block APs and 20 μ M Bicuculine to block spontaneous GABAergic activity.

Primary hippocampal neurons with downregulated RIM3 γ or RIM4 γ showed no difference in the frequency of miniature EPSCs, as compared to control neurons. However, neurons lacking RIM3 γ or RIM4 γ exhibited a significant reduction in the amplitude of mEPSCs (Fig. 5.51).

This data suggest either a reduced quantal content of spontaneous release or a reduced number of postsynaptic AMPARs.

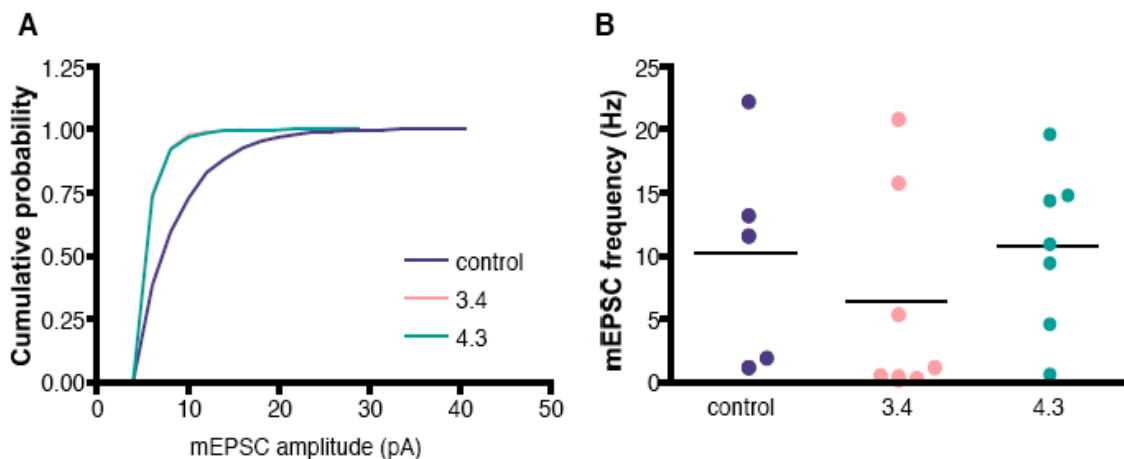


Fig. 5.51 RIM3 γ and RIM4 γ knockdown in neurons lead to a reduction of the mEPSC amplitude, without affecting the frequency

A, The cumulative probability of mEPSC amplitude displays a significant left-shift in cells with downregulated levels of RIM3 γ and RIM4 γ . B, Mean instantaneous frequency of mEPSCs of single neurons are represented by dots, the mean of every group is given by horizontal lines. No statistically significant difference between control and shRNA neurons could be detected (ANOVA $p > 0,05$). Control $n=5$; sh3.4 $n=7$; sh4.3 $n=7$.

5.2 *Presynaptic proteins in epilepsy*

Changes in presynaptic proteins have been associated with several neurological disorders in the last years, e.g. Alzheimer, Parkinson, autism, schizophrenia and epilepsy (Krüger *et al.*, 1998; Lynch *et al.*, 2004; Shankar and Walsh, 2009; Terada *et al.*, 1999; Weidenhofer *et al.*, 2006; Weidenhofer *et al.*, 2009). Furthermore, diverse subgroups of epilepsy patients have shown alterations in the expression of different presynaptic proteins. Several epilepsy cases were described in a family with a mutation in the synaptic vesicle protein Synapsin1 (Garcia *et al.*, 2004). Lately, reduced levels of another synaptic vesicle protein, Synaptotagmin1 have been associated with human refractory epilepsy (Xiao *et al.*, 2009). In addition, the synaptic vesicle protein protein SV2 is the target for the antiepileptic drug levetiracetam (Lynch *et al.*, 2004).

Rasmussen encephalitis (RE) is a rare form of epilepsy that mainly affects children. Characteristic features of RE are severe seizures and progressive neurological deficits, T cell infiltration and progressive degeneration of a single cerebral hemisphere. Originally thought to be a chronic form of viral encephalitis, Rasmussen encephalitis is now considered to be an autoimmune disease. In 2000, the presence of autoantibodies against in the serum of a single patient with RE previously shown to have anti-GluR3 antibodies was reported (Yang *et al.*, 2000). Subsequent studies demonstrated that anti-GluR3 antibodies are not specific for RE (Wiendl *et al.*, 2001), suggesting a possible role of Munc18-1 in the origin of this neurological alteration.

5.2.1 **Antibodies against Munc18-1 in serum of Rasmussen encephalities patients**

In order to further characterize the relevance of Munc18-1 autoantibodies for Rasmussen encephalitis, ten biopsy-proven RE sera, and eight healthy control

sera were screened by Western blot analysis. Extracts from HEK 293T cells transfected with full-length Munc18-1 were compared with untransfected HEK293 extracts as well as with protein homogenates of adult mouse brain. Munc18-1 was recognized in Munc18-1 transfected cell extracts and in mouse brain homogenate by anti-munc18-1 antibodies (Fig. 5.52A, left panel) and by two out of ten RE patient sera (Fig. 5.52A, middle panel; patient 1 and 2). By contrast, no immunoreactivity was detected in untransfected HEK cells. Furthermore, the autoantigen observed in the transfected HEK 293T cells and the mouse brain homogenate was specific for the RE serum as all healthy control human sera failed to recognize Munc18-1. All serum samples of patients 1 and 2 collected at different time points showed immunoreactivity against Munc18-1. The latest time point was 2.7 years after onset of the disease (in patient 1), indicating that the anti-T cell immunosuppressant tacrolimus had no effect on the antibody positivity.

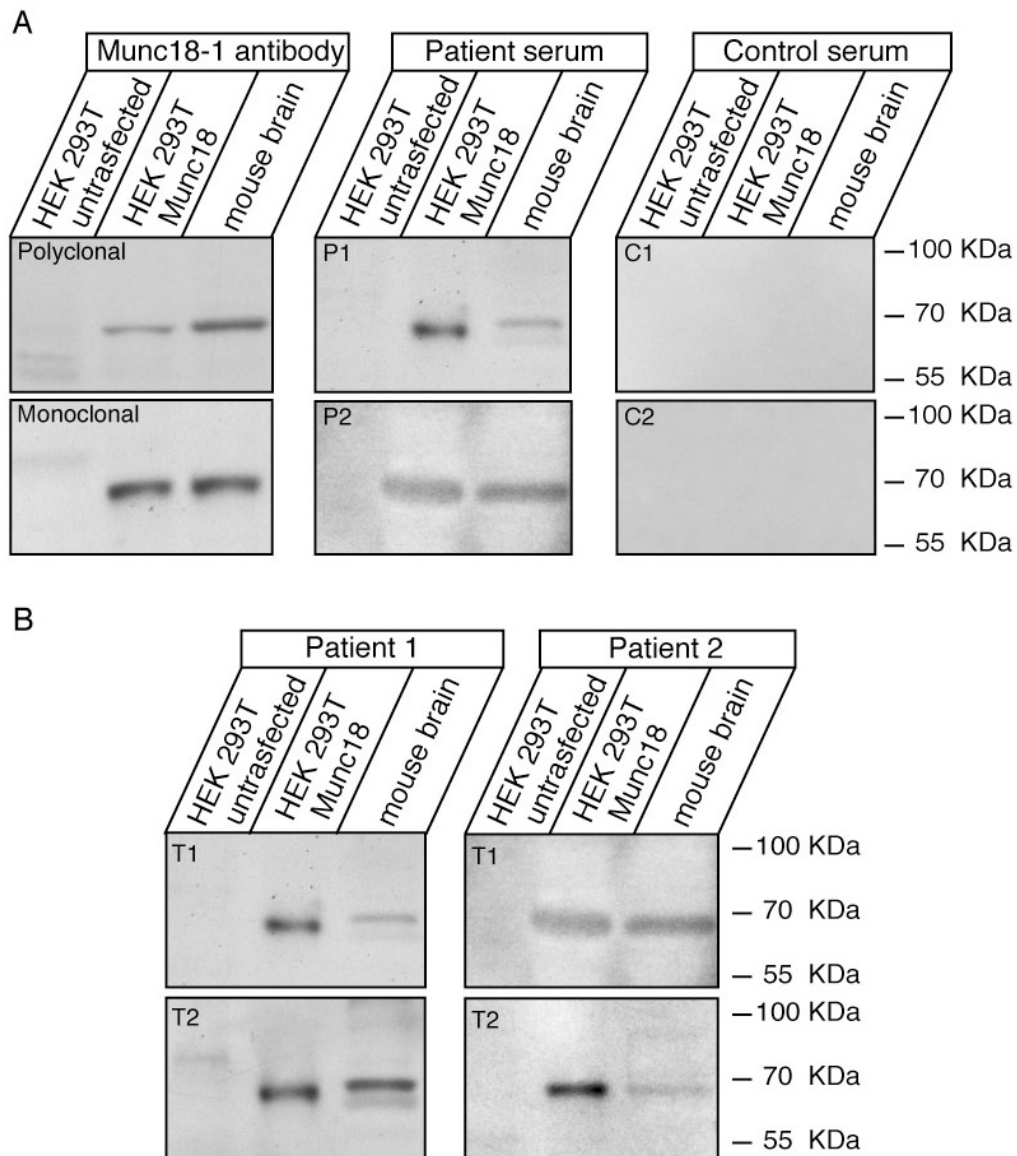


Fig. 5.52 Immunoreactivity of sera of biopsy-proven RE patients

A, Homogenates of untransfected HEK293 cells, of HEK293 cells transfected with an expression plasmid for rat Munc18-1, and of adult mouse brain were blotted and analyzed by immunoblotting. Polyclonal (P) and monoclonal (M) antibodies against Munc18-1 reacted with Munc18-1 expressed in HEK293 cells and endogenously present in adult mouse brain (left panel). Sera of two (P1 and P2) out of ten patients examined specifically recognized Munc18-1 only in transfected HEK293 cells and mouse brain homogenate (middle panel). Sera of healthy controls showed no response to Munc18-1 (right panel). B, Sera of patients 1 and 2 taken at different time points after the onset of the disease (t1, t2) all specifically reacted with Munc18-1.

5.2.2 Neuropathological evaluation of post-surgery biopsy specimens

In biopsy specimens of RE patients neuropathological changes such as neuronal cell loss, microglial activation and astrogliosis are observed (Bien *et al.*, 2002). Furthermore, major neuropathological hallmarks are T lymphocytic infiltration, and microglial nodules.

Neurosurgical biopsy samples were obtained in order to establish the diagnosis of RE. Paraffin embedded material of seven patients was available for this study and evaluated. The neuropathological specimens contained portions of grey and white matter. Characteristic microglia nodules as well as lymphocytic perineuronal arrangements were present in brain tissue samples of all patients. Immunophenotyping of perivascular and parenchymal mononuclear leukocyte infiltrates was performed with post-surgery biopsy sections of the available 7 RE patients. Most of the parenchymal leukocytes were CD8⁺ cytotoxic T-cells/lymphocytes or CD68⁺ macrophages/microglial cells (Fig 2A). Four patients exhibited (at a lower density than T cells and microglial cells) some perivascular and parenchymal CD20⁺ B-lymphocytes and plasma cells in the brain tissue. Plasma cells contained IgG (data not shown). Intriguingly, the two patients (P1 and P2, table) in which Munc18-1 autoantibodies were present, revealed prominent B-lymphocytic and plasma cell infiltrates with perivascular accumulation of B-lymphocytes (Fig 2A).

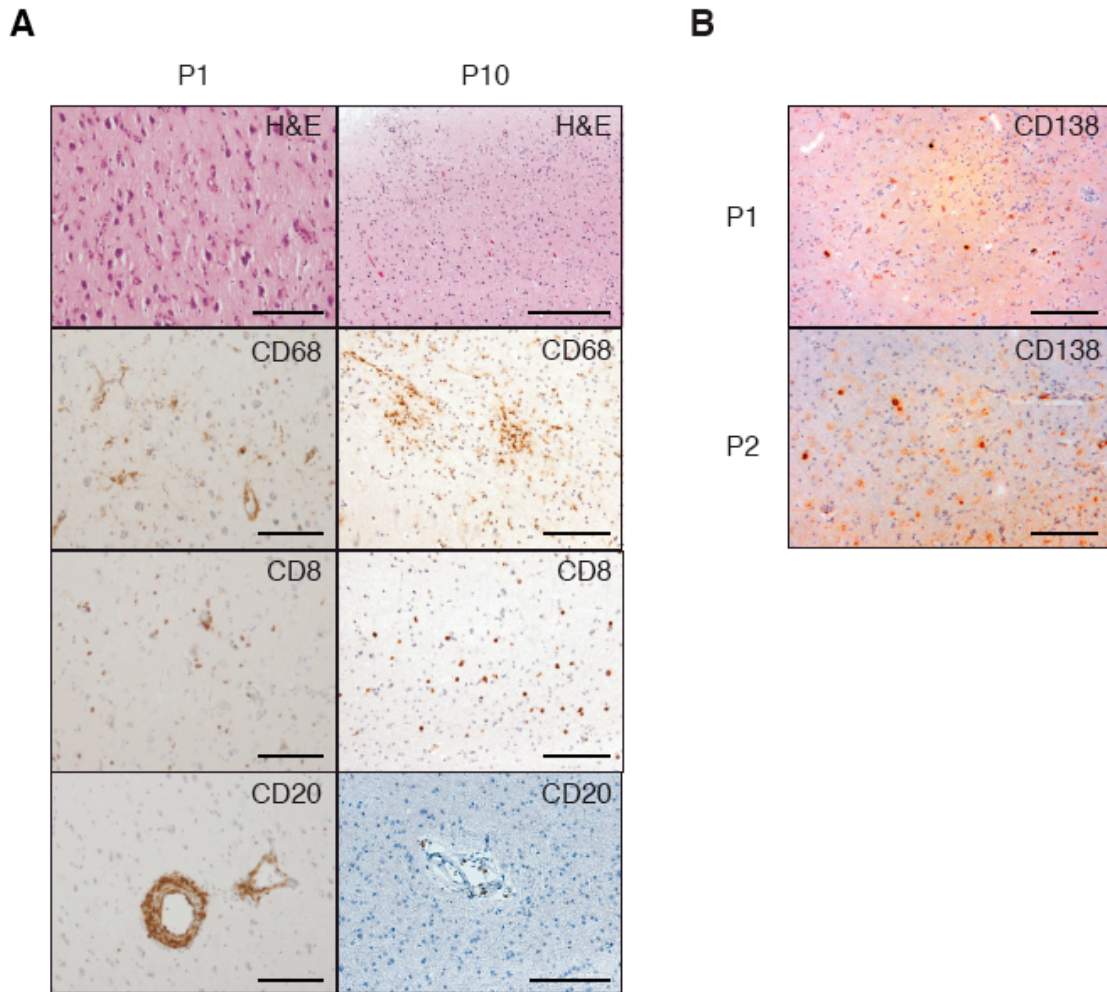


Fig.2 Immunohistochemistry of biopsy brain sections from RE patients

A, biopsy sections of all 10 RE patients were stained with H&E and processed immunohistochemically with antibodies against CD68, CD8, and CD20. In all patients immunoreactivity against CD68 and CD8 was observed. However, only the patients 1 (P1) and 2 that had autoantibodies against Munc18-1 showed a strong perivascular infiltration of B-lymphocytes (CD20). P10 patient with biopsy-proven RE lacking autoantibodies against Munc18-1 did not show a significant perivascular or intraparenchymal CD20-positive B-lymphocytic component. B, Both P1 and P2 also reacted strongly with antibodies against plasma cells (CD138). Scale bar = 200 μ m

| Patient | | Serum | | | Brain biopsy | |
|---------|----------------------------|--------------------------------|-------------------|-------------------------|----------------------------------|--------------------------------|
| No.. | Age at disease onset (yrs) | Disease duration at collection | Munc18-1 antibody | Treatment at collection | Treatment duration at collection | Disease duration at collection |
| 1, f | 11.4 | 2.2 mo | Positive | None | | |
| | | 2.7 mo | Positive | None | | |
| | | 2.7 yrs | Positive | Tacrolimus | 2.5 yrs | 2.5 mo |
| 2, m | 11.9 | 2.1 mo | Positive | None | | |
| | | 2,3 mo | Positive | Tacrolimus | 1.0 day | 2.0 mo |
| 3, f | 9.9 | 3.3 yrs | Negative | None | | 3.2 yrs |
| 4, m | 15.5 | 1.0 yrs | Negative | None | | |
| | | 2.3 yrs | Negative | IVIg | 1.3 yrs | 9.6 mo |
| 5, m | 4.4 | 8.5 mo | Negative | IVIg | 1.0 day | 8.3 mo |
| 6, m | 9.3 | 4.8 yrs | Negative | MMF. Prednisolon | 4.5 yrs | 1.6 yrs |
| 7, f | 37.6 | 1.1 yrs | Negative | None | | |
| | | 2.1 yrs | Negative | IVIg | 1.0 yrs | |
| | | 3.1 yrs | Negative | IVIg | 2.0 yrs | 1.1 yrs |
| 8, f | 5 | 11.0 mo | Negative | None | 1.0 wk | 10.8 mo |
| 9, f | 2.1 | 7.8 mo | Negative | Tacrolimus | 2.0 mo | |
| | | 3.0 yrs | Negative | Tacrolimus | 2.6 yrs | 5.6 mo |
| 10, m | 6.6 | 2.8 yrs | Negative | Tacrolimus | 2.5 yrs | |
| | | 2.9 yrs | Negative | Tacrolimus | 2.6 yrs | 2.7 mo |

Table.2 Summary clinical data

Abbreviations: Mo months; yrs years; MMF mycophenolate mofetil; IVIG intravenous immunoglobulin G

6 DISCUSSION

At the synapse, efficient synaptic transmission requires a tight spatial and temporal regulation. Synaptic vesicle fusion is a very fast process that only takes place at specialized areas of the presynaptic membrane, the so called Active Zones. To date, five families of Active Zone enriched proteins have been described: ELKS, Piccolo/ Bassoon, Munc13, Liprins- α and RIMs (reviewed in Schoch and Gundelfinger, 2006).

The RIM (Rab3 interacting molecule) family contains seven known members (1 α/β , 2 $\alpha/\beta/\gamma$, 3 γ and 4 γ), encoded by four different genes RIM (1-4). α -RIMs are multidomain proteins composed of several domains: a zinc finger domain, a PDZ domain and two C-terminal C2 domains (Wang *et al.*, 2000). Through these domains, they interact directly or indirectly with most other known Active Zone proteins (reviewed in Schoch and Gundelfinger, 2006). Interestingly, not all members of the family contain the whole set of domains (Wang *et al.*, 2000). RIM2 γ , RIM3 γ and RIM4 γ , the smallest members of the RIM protein family, are only composed of a C-terminal C2B domain and an isoform specific N-terminal sequence. Generation of the truncated variants of the RIM protein family stands out among components of the presynaptic release machinery and the CAZ. The other Active Zone enriched families Piccolo/Bassoon, Munc13, ELKS and Liprin- α families are composed of several highly conserved members (reviewed in Schoch and Gundelfinger, 2006). In contrast to the RIM protein family, in which the γ -isoforms only contain one of the whole set of domains, the Liprin- α protein family comprises four members which are highly homologous (Zürner and Schoch, 2008). All Liprins- α isoforms contain the entire set of domains, as well as ELKS1 and ELKS2 that only differ in their C-terminus, and Munc13 proteins that diverge in the composition of the N-terminus (Augustin *et al.*,

1999a; Koch *et al.*, 2000). Furthermore, Bassoon and Piccolo proteins are also very conserved, Bassoon only lacks the PDZ and the C2 domain of Piccolo (Fenster *et al.*, 2000). Only for Rabphilin, the other Rab3 effector protein, deletion variants similar to γ -RIMs have been described. The Rabphilin family contains two shorter isoforms, of which Noc2 consists of the N-terminal zinc finger domain of Rabphilin seems not to be a brain specific protein (Kotake *et al.*, 1997) and Doc2 comprises two C-terminal C2-like domains of Rabphilin (Orita *et al.*, 1995).

In recent years, RIM1 and RIM2 have been shown to be essential for synaptic vesicle maturation and different forms of presynaptic plasticity (Castillo *et al.*, 2002; Kaeser *et al.*, 2008a; Schoch *et al.*, 2002; Schoch *et al.*, 2006). However, to date little is known about RIM3 γ and RIM4 γ . The fact that RIMs are the only presynaptic Active Zone-enriched protein family, which generates brain-specific truncated isoforms, raised the question of their physiological relevance.

Therefore, we hypothesized that in dependence of their subcellular localization, several potential modes of action can be envisioned for γ -RIMs: if γ -RIMs were associated with the CAZ, they could occupy the “slots” for the full length RIMs. Thereby, γ -RIMs would act as dominant negative, interfering with the connection between calcium channels and synaptic vesicles mediated by α -RIMs via Rab3A (Fig. 6.1,A). γ -RIMs might also be present at the Active Zone but acting in concert with RIM1 α by stabilizing them via dimerization or by modulating their function (Fig. 6.1,B). Furthermore, in case γ -RIMs were absent from the Active Zone, but cytoplasmically localized, they might function as a quencher and sequester α -RIM-binding proteins (Fig. 6.1,C).

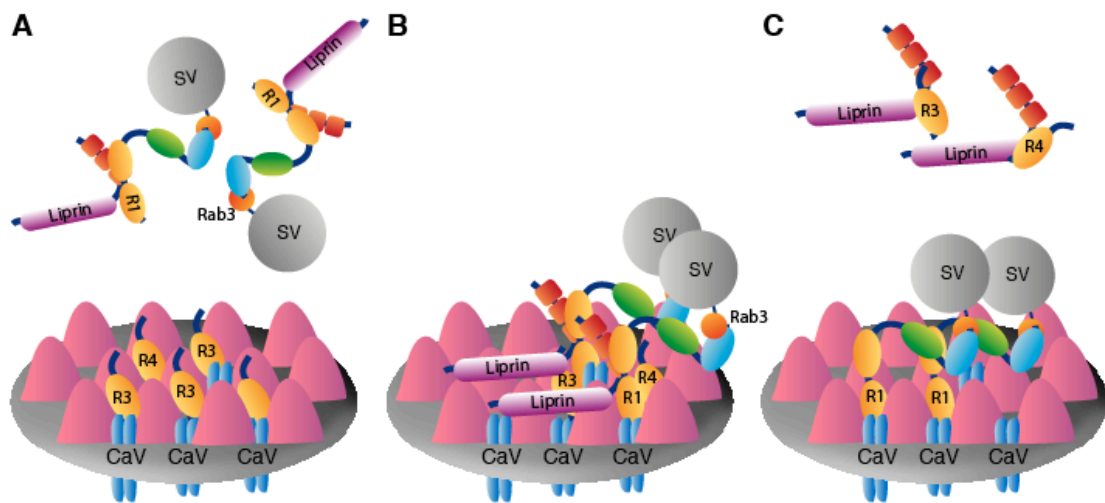


Fig. 6.1 Several possible modes of action for γ -RIMs

A, γ -RIMs are part of the cytomatrix at the Active Zone and interact with calcium channels, thereby blocking the slots for the full-length RIMs, acting as dominant negative. B, γ -RIMs are localized at the Active Zone cytomatrix and exert a positive action by stabilizing α -RIMs via dimerization, or modulate the function of the α -isoforms. C, γ -RIMs are not specifically localized at the Active Zone, but present in the cytoplasm arresting α -RIMs binding proteins.

6.1 Expression and subcellular localization of *RIM3 γ* and *RIM4 γ*

The first step to understand the physiological role of *RIM3 γ* and *RIM4 γ* was to study their localization. In the present study we investigated the expression pattern of *RIM3 γ* and *RIM4 γ* , and found that *RIM3 γ* and *RIM4 γ* , as *RIM1 α* and *RIM2 α* , are brain specific proteins (Wang *et al.*, 1997; Wang and Südhof, 2003) present throughout the brain in overlapping expression patterns. However, their mRNA and protein expression levels differ in various cell types. Our *in situ* hybridization and Western Blot data revealed that in the cerebellum, *RIM3 γ* is mainly expressed in the cerebellar granule cell layer, whereas *RIM4 γ* is highly enriched in Purkinje cells. In the cortex, *RIM4 γ* is uniformly localized throughout all cortical layers, and *RIM3 γ* is more concentrated in layers II-IV. In the hippocampal formation, both γ -RIM isoforms are strongly expressed in pyramidal and granule cells, as well as in interneurons. In addition, *RIM3 γ* is

detected in the thalamus at higher levels than RIM4 γ . Immunohistochemical analysis showed that both isoforms are present in excitatory and in inhibitory neurons, colocalizing with different interneuronal markers such as Parvalbumin and GAD67, indicating a potential role in the regulation of glutamatergic as well as of GABAergic neurotransmission. In addition, expression of RIM3 γ and RIM4 γ increased in parallel to synaptogenesis, a time course of expression that has been described for a large number of synaptic proteins (Song *et al.*, 1999; Stettler *et al.*, 1994).

The results of this study represent the first report about the localization of RIM4 γ . Our data of RIM3 γ distribution in various brain regions differs slightly from previous studies. Overall, our RIM3 γ *in situ* hybridization experiments agree with the data shown by Liang and collaborators (Liang *et al.*, 2007). However, small differences in the expression intensity, mainly in the CA3 region of the hippocampus and in cerebellar Purkinje cells were detected. These divergences could be due to their use of dioxigenin labelled probes. In contrast to the radioactively labeled probes we used, dioxigenin visualized signals depend on the reaction time. In addition, dioxigenin-labeled probes are longer than radioactively marked oligonucleotides, compromising the specificity of the results due to the sequence homology among all RIM family members. At the protein level, RIM3 γ is mostly found in cerebellum, cortex and hippocampus, confirming previous data (Wang *et al.*, 2000). But in contrast with the data of Wang *et al.*, and confirming the data of Liang *et al.*, RIM3 γ is not only present in the rostral brain regions but also in the caudal ones (Liang *et al.*, 2007).

The regional distribution of RIM1 α and RIM2 α has not been described at the protein level yet. However, *In situ* hybridization has shown RIM1 α to be abundantly expressed throughout the brain. RIM3 γ and RIM4 γ overlap with RIM1 α , with the highest levels in the cortex, cerebellum, hippocampus and thalamus, in contrast to RIM2 α , which is only highly concentrated in the

cerebellum, olfactory bulb and the gyrus dentatus of the hippocampus (Schoch *et al.*, 2006). Overall, α - and γ -RIMs are ubiquitously present throughout the brain, however the expression levels of these proteins vary among different cell types.

In summary, the regional distribution of RIM3 γ and RIM4 γ differs from the expression pattern of RIM1 α and RIM2 α in the subcellular localization and the protein levels. Interestingly, every brain region coexpresses one or both α -RIM isoforms and γ -RIMs. These data differ from the expression pattern of other presynaptic protein families, in which the different isoforms present distinct regional distribution, e.g. Synaptotagmins, Complexins. Synaptotagmins-1, -2, and -9, which are synaptic vesicle proteins that act as calcium sensors (reviewed in Südhof, 2002) are partially segregated. Synaptotagmin-1 is predominantly expressed in the forebrain, synaptotagmin-2 in the cerebellum and brain stem, and synaptotagmin-9 in the limbic system and striatum (Mittelsteadt *et al.*, 2009). Complexins, in addition to the differences in regional expression pattern, work in different synapses. Complexin I is preferentially localized in the axosomatic synapses, whereas Complexin II is mainly present in axodendritic terminals (Yamada *et al.*, 1999). Moreover, Active Zone enriched protein families Munc13 and ELKS comprise also several isoforms with different localizations. Munc13-1 is ubiquitously present throughout the brain, whereas Munc13-2 and Munc13-3 display complementary expression patterns. Munc13-2 is highly enriched in the rostral brain regions in contrast to Munc13-3 that is mainly localized in the caudal ones (Augustin *et al.*, 1999a). ELKS brain-specific isoforms are also differentially distributed. ELKS1B is mainly detected in the cerebellum and hippocampus, whereas ELKS2 is preferentially expressed in the hippocampus, cortex, olfactory bulb, and thalamus (Deguchi-Tawarada *et al.*, 2004; Wang *et al.*, 2002).

6.1.1 RIM3 γ is a presynaptic protein, also enriched in the nucleus

In order to affect the function of α -RIMs, γ -RIMs not only have to be coexpressed by a neuron but also have to be present in the same subcellular compartment. In our analysis we found RIM3 γ to be tightly linked to the synaptic plasma membrane, and absent from synaptic vesicles. Subcellular fractionation of crude synaptosomes showed that, even though RIM3 γ could be partially solubilized by Triton X-100 extraction, the majority of the protein remains associated with the Triton X-100 resistant fraction, as RIM1 α (Wang *et al.*, 1997) and the other components of the pre- and postsynaptic densities (Phillips *et al.*, 2001). However, this biochemical approach does not differentiate between pre- and postsynaptic localization.

Using immunocytochemistry we found RIM3 γ to be mainly located at the synapse, colocalizing with presynaptic markers such as Synapsin and Bassoon and partially overlapping with the postsynaptic protein PSD-95. However, the limited resolution of confocal microscopy does not allow for an unequivocal differentiation between a purely presynaptic or partially also postsynaptic distribution. Therefore, immunohistochemistry analysis on the retina was performed. Retinal neurons contain relatively large structures attached to the presynaptic plasma membrane, the so called synaptic ribbons, which have been shown to contain a specific set of proteins (tom Dieck and Brandstätter, 2006) and can be easily visualized by confocal microscopy. RIM3 γ is present in both synaptic layers of the retina, the outer plexiform and the inner plexiform layer. RIM3 γ is expressed at the Ribbon, colocalizing with the presynaptic marker Ctbp2/RIBEYE in the outer plexiform layer, and thereby confirming its presynaptic localization. Confocal images of the outer plexiform layer showed RIM3 γ to have a very similar distribution when compared to the α -RIM isoforms

(tom Dieck *et al.*, 2005; Wang *et al.*, 1997). However, RIM1 α and RIM2 α exhibit a different localization within the ribbon. Whereas RIM1 α is localized in the ribbon associated protein complex, RIM2 α is present in the plasma membrane-associated division (tom Dieck *et al.*, 2005). Further electron microscopy studies will be necessary to determine the exact localization of RIM3 γ at the Ribbon synapses.

The previously reported subcellular localization of RIM3 γ (Liang *et al.*, 2007) is in contradiction to the one observed in this study. Liang and colleagues described that RIM3 γ was mainly localized along the dendrites and did not show any specific presynaptic localization. However, they did not provide evidence that the antibody used was isoform specific. Liang *et al.* used the first 80 amino acids for immunization, probably leading to a cross-reactivity with RIM4 γ due to sequence homology. In contrast, our epitope analysis revealed only a short peptide sequence that was truly specific for RIM3 γ . We verified the specificity of our antibodies by overexpressing all RIM protein family members in HEK cells and immunoblotting analysis. In addition, immunoblotting and immunohistochemistry analysis, using antibodies against RIM3 γ previously blocked with the peptid they were raised against, led to a lack of signal, demonstrating the specificity of the expression pattern shown.

Unexpectedly, in addition to the presynaptic localization of RIM3 γ , immunocytochemistry analysis showed an enrichment of RIM3 γ in the nucleus. This observation was confirmed by overexpression of the protein tagged to a fluorescent marker protein in PC12 cells, as well as in neurons. Interestingly, bioinformatic prediction of the subcellular localization of RIM3 γ revealed a potential nuclear localization signal (NLS) composed of the polybasic residues KKRR, which are located in the N-terminus between residues 42 and 47 of the protein. This region is not present in RIM4 γ . Expression of a GFP-RIM3 γ deletion construct lacking the protein N-terminus, confirmed that the nuclear

localization of the protein is contained within the N-terminal sequence. The dual synaptic and nuclear localization of RIM3 γ suggests a possible role of this protein in the regulation of synapse-to-nucleus communication. Interestingly, RIM1 α has been also shown to be localized in the nucleus (Sun *et al.*, 2003). However, to date no information has been reported about the function of RIM1 α in this compartment.

6.1.2 RIM4 γ is uniformly localized along the axon and dendrites

RIM4 γ , as well as RIM3 γ , is associated with the synaptic plasma membrane, and absent from synaptic vesicles. RIM4 γ is partially solubilized by Triton X-100 extraction, however, the majority of the protein remains tightly associated with the Triton X-100 resistant fraction, indicating that RIM4 γ is part of the cytomatrix composing the synaptic densities. However, in neurons, RIM4 γ displays a diverging distribution from RIM3 γ . RIM4 γ is uniformly expressed along the dendrites and axons and is absent from the nucleus. This localization pattern was confirmed by immunocytochemistry in the retina where RIM4 γ expression was not restricted to the synaptic layers but also detected in both nuclear layers. These data point to a pre- and postsynaptic localization of the protein. In addition, bioinformatic prediction of protein subcellular localization verified the cytoplasmic localization of RIM4 γ . Furthermore, it also predicted a possible localization in the Golgi apparatus.

In summary, RIM3 γ and RIM4 γ are presynaptic proteins, as shown for RIM1 α and RIM2 α (Wang *et al.*, 1997; Wang *et al.*, 2000). But, in contrast to the α -RIM isoforms, which have been shown to be Active Zone specific proteins, γ -RIM proteins exhibit additional subcellular localizations. RIM3 γ is highly enriched in the nucleus, whereas RIM4 γ is uniformly expressed along axon and dendrites. Despite the high sequence homology, RIM3 γ and RIM4 γ possess a distinct

distribution but both colocalize with α -RIMs in the same synapses, allowing for a functional interplay of these proteins (Fig. 6.2).

The diverging subcellular localization of RIM3 γ and RIM4 γ , despite their high sequence homology, raises the question which regions of the protein mediate the common and which the distinct properties of the γ -RIMs.

6.2 γ -RIMs targeting sequences

In recent years, a large number of studies have been performed in order to elucidate the organization of CAZ proteins and the function of their domains. However, not much is known about the role of these domains in the anchoring of cytomatrix proteins to the Active Zone. Dresbach and colleagues could show that the central portion of Bassoon (amino acids 1692–3263), containing several coiled coil domains, is sufficient for its association with the Active Zone (Dresbach *et al.*, 2003). Nevertheless, this region is still very large and contains several domains. The targeting sequences of ELKS2 α (CAST) have also been studied. Ohtsuka *et al.* showed that the third and fourth coiled-coil domains of ELKS2 α are necessary for the synaptic localization of this protein (Ohtsuka *et al.*, 2002). In addition, the RIM1 α PDZ domain seems to be required for the association of RIM1 α to the Active Zone (Ohtsuka *et al.*, 2002), but deletion of the PDZ domain does not eliminate RIM1 α from the synapses (Deken *et al.*, 2005). To date, nothing has been reported about the minimal domains required for the proper localization of Piccolo and Liprins- α at the Active Zone. These data reflect that so far no “single” targeting sequence has been identified.

In this study we could demonstrate that the C2B domain of RIM3 γ and RIM4 γ is sufficient to specifically target both γ -RIM isoforms to the presynapse. For this purpose, we generated several truncated GFP- γ -RIM proteins containing the C2B domain, the C2B domain and the homologous sequence, and the full

length protein only lacking the isoform specific N-terminal sequence, and overexpressed them in PC12 cells, as well as in neurons.

Overexpression of GFP-RIM3 γ truncated proteins containing only the C2B domain or the C2B domain and the homologous sequence, but lacking the N-terminus of the protein, led to a loss of the nuclear localization of the proteins. However, these truncated proteins were still present at the axonal boutons, indicating that the C-terminal C2B domain directs the presynaptic localization of the protein, whereas the nuclear localization is controlled by the N-terminal sequence.

In contrast to the endogenous protein, overexpressed GFP-RIM3 γ full length and deletion proteins could also be detected in dendrites. However, similar observations have been made after overexpression of several tagged presynaptic proteins (Dresbach *et al.*, 2003). Reasons for this mislocalization could be the high expression levels of the overexpressed protein that might interfere with the sorting mechanism. In addition, the tagging of proteins with a fluorescent marker protein might induce a change in the conformation, which may obstruct the correct sorting of the protein.

Overexpression of GFP-RIM4 γ full length and truncated proteins containing only the C2B domain or the C2B domain together with the homologous sequence, but lacking the N-terminus of the protein, revealed an identical expression pattern as the full length protein. The truncated proteins were present in the axons, concentrated at the axonal boutons and along the dendrites, showing an identical localization as the endogenous protein and thereby demonstrating that the C2B domain is sufficient for the presynaptic localization of RIM4 γ .

Taken together, the RIM3 γ and RIM4 γ C2B domains are essential for the localization of the γ -RIM isoforms at the Active Zone. This result suggests that

the presynaptic localization might be promoted or mediated via the interaction between γ -RIMs and other Active Zone proteins.

6.3 Determinants of γ -RIM subcellular localization

After a first axo-dendritic contact, Active Zones are able to assemble within a few minutes. In this short time, all the cellular components must be delivered to the right position (Ahmari *et al.*, 2000; Friedman *et al.*, 2000). Considering the length of the axons, and the limitations in time, it has been postulated that there might be preassembled Active Zone precursor vesicles in the soma, which are axonally transported and fuse with the presynaptic membrane to form a new presynaptic bouton (Goldstein *et al.*, 2008). One of the mechanisms responsible for the delivery of proteins such as Munc13 and RIMs to the Active Zones are the PTVs (Piccolo/Bassoon transport vesicles) (Shapira *et al.*, 2003; Zhai *et al.*, 2001). However, subsequent studies have shown that Piccolo is not essential for the localization of these proteins (Leal-Ortiz *et al.*, 2008). ELKS proteins were also proposed to play a role in the localization of RIM1 at the Active Zone (Ohtsuka *et al.*, 2002). Nevertheless, RIM1 is localized to the Active Zone in the absence of ELKS, in *C.elegans*, and vice versa (Deken *et al.*, 2005). In addition, deletion of ELKS2 α in mice only slightly affects RIM1 α solubility (Kaesler *et al.*, 2009). To date, RIM1 α is the only Active Zone protein, which has been shown to be essential for the localization of another CAZ-protein. Deletion of RIM1 α in mice, significantly decreases the levels of Munc13 (Schoch *et al.*, 2002). Furthermore, a single mutation in Munc13-1 and ubMunc13-2 (I121N), perturbing the binding to RIM1 α , impedes the proper recruitment of Munc13 proteins to the synapse (Andrews-Zwilling *et al.*, 2006).

Besides, Liprins- α have been proposed as a possible candidate to play a role in the transport of presynaptic proteins, since deletion of Liprins- α in invertebrates leads to important changes in the Active Zone ultrastructure (Kaufmann *et al.*, 2002; Zhen and Jin, 1999). In addition, through their interaction with the Kinesin motor protein Kif1a, Liprins- α are involved in the trafficking of proteins such as AMPARs, GRIP1, and GIT1 (Okada *et al.*, 1995; Shin *et al.*, 2003; Wyszynski *et al.*, 2002).

6.3.1 Liprins- α do not influence the presynaptic localization of γ -RIMs

Based on *in vitro* assays, which showed that Liprins- α not only bind RIM1 α (Schoch *et al.*, 2002) but also RIM3 γ and RIM4 γ (Wang and Südhof, 2003), we hypothesized that Liprins- α might play a role in the trafficking to and synaptic localization of the γ -RIM isoforms at the presynaptic Active Zone. Therefore we asked whether the C2B domain alone mediates the interaction between RIMs and Liprins- α , or, as proposed by NMR and Crystallography studies, adjacent sequences are needed (Guan *et al.*, 2007).

To answer these questions, full length and truncated GFP- γ -RIM proteins were generated and coexpressed with Liprins- α in PC12 cells. RIM3 γ and RIM1 α were localized in the nucleus and the cytoplasm of PC12 cells if they were overexpressed individually. Interestingly, upon coexpression with Liprins- α they were not imported into the nucleus, showing a clear colocalization in the cytoplasm. Similar assays have been used to confirm the interaction partners of CAZ proteins. Ko and colleagues showed the interaction between Liprin1- α and ELKS (Ko *et al.*, 2003b), and co-clustering of Liprin1- α and GIT1 in COS cells (Ko *et al.*, 2003a). Furthermore, the affinity of RIM1 α and RIM2 α proteins for Rab3 has been tested by coexpression of GFP-tagged deletion and full length α -RIM proteins and Rab3 in PC12 cells (Fukuda, 2004).

The results of our experiments verified the interaction between different members of the Liprin- α family ($-\alpha 1$, $-\alpha 3$ and $-\alpha 4$) and RIM1 α , as well as RIM3 γ in living cells. These *in vivo* data confirm previous *in vitro* pull-down experiments that already showed an interaction between Liprin- $\alpha 3$ and RIM3 γ (Wang and Südhof, 2003) as well as RIM1 α (Schoch *et al.*, 2002). In contrast, we could not detect any change in the localization of RIM4 γ upon cotransfection with Liprins- α , although it had previously been shown to interact with Liprin- $\alpha 3$ *in vitro* (Wang and Südhof, 2003). However, both proteins were already localized in the cytoplasm and absent from the nucleus when they were overexpressed individually, therefore not allowing for unequivocal conclusions.

To address the question whether the C2B domain is sufficient to mediate the interaction between RIMs and Liprins- α , several GFP-tagged deletion proteins were generated and transfected in PC12 cells, alone or in combination with Liprin- $\alpha 3$. Analysis of the deletion mutants revealed that deletion of the isoform-specific N-terminus, resulted in a change in the localization of the protein which was no longer highly concentrated in the nucleus, but uniformly localized throughout the cell. Fusion proteins lacking the NLS showed cytoplasmic colocalization and did not change its localization when cotransfected with Liprin- $\alpha 3$ (Fig. 5.23). In contrast, GFP-RIM3 γ deletion construct only lacking the first 38 N-terminal amino acids, but conserving the NLS, displayed the same behavior as the full length protein, as it could not be detected in the nucleus in the presence of Liprin- $\alpha 3$. In the case of RIM4 γ , as expected from the localization of the full length protein, no changes in the protein localization could be detected for any of the GFP-RIM4 γ truncated variants.

Therefore, the PC12 coexpression assay only allows for an unequivocal determination of the interaction between RIM3 γ and Liprins- α if the NLS is present. To examine if the C2B domain by itself can mediate the interaction between Liprins- α and RIMs, Liprins- α could be fused to a membrane- or

mitochondrial-targeting sequence. Coexpression of membrane- or mitochondrial-tagged Liprin- α with interacting proteins previously localized in the cytoplasm would induce a translocation of the proteins to the plasma membrane/mitochondria, whereas non-interacting proteins would remain in the cytoplasm. However, weak interactions might not be detected by this *in vivo* assay, as shown by Patel and colleagues in the study of ELKS interaction with SYD2/ Liprin- α in the absence of SYD1 (Patel and Shen, 2009).

PC12 cells do not have special membrane compartments like Active Zones, therefore to examine the interaction in the endogenous environment and to further understand the interaction between RIMs and Liprins- α , additional experiments in neurons were performed. Our data suggests that Liprins- α are not involved in the targeting of γ -RIMs to the presynapse, since coexpression of RIM3 γ -mCherry and RIM4 γ -mCherry with GFP-Liprin- α ($-\alpha$ 2 and $-\alpha$ 3) in primary hippocampal neurons did not result in changes in the localization of RIMs. In contrast, coexpression of Liprin- α with ELKS and GIT1 increases the synaptic localization of these proteins (Dai *et al.*, 2006; Ko *et al.*, 2003a). Therefore, either Liprins- α are not involved in the targeting of γ -RIMs, or the C-terminal tagging of RIM3 γ and RIM4 γ with mCherry has somehow prevented the interaction between Liprins- α and γ -RIMs.

6.3.2 RIM1 α promotes the synaptic localization of RIM3 γ and RIM4 γ

To further investigate potential interactions that could influence the localization and function of RIM3 γ and RIM4 γ , we focused on the fact that both γ -RIM isoforms are mostly composed of the C2B domain. C2B domains are known to form multimers, as described for different members of the Synaptotagmin family (Damer and Creutz, 1996; Fukuda and Mikoshiba, 2000, 2001). In addition, crystallography analyses of the RIM2 α C2B domain revealed the competence of

this domain to dimerize (Guan *et al.*, 2007). Based on these observations and the fact that RIM1 α is necessary for the localization of the Active Zone protein Munc13 (Andrews-Zwilling *et al.*, 2006), we hypothesized that RIM1 α might play a role in the localization of RIM3 γ and RIM4 γ . To evaluate this hypothesis, GFP-RIM1 α was coexpressed with mCherry-tagged RIM3 γ or RIM4 γ in hippocampal neurons. Our data revealed that RIM1 α promotes the presynaptic localization of RIM3 γ as well as RIM4 γ . Coexpression of RIM4 γ and RIM1 α changed the distribution of RIM4 γ , which was previously uniformly localized along neuronal processes, to a mainly punctate expression pattern. Furthermore, coexpression of RIM1 α and RIM3 γ led to an increase in synaptic localization of RIM3 γ . In both cases, increased levels of RIM1 α led to an enrichment of RIM3 γ and RIM4 γ at the synapse.

To define the region of γ -RIMs required for this interaction, GFP- γ -RIMs full length and deletion proteins were overexpressed in hippocampal neurons in the presence and absence of mCherry-RIM1 α in order to examine whether the interaction between α -RIMs and γ -RIMs depends only on the C2B domain, or needs additional sequences. However, N-terminal GFP- γ -RIM full length and deletion proteins were localized at the axonal boutons in the presence and absence of RIM1 α . These results differ from the data obtained in previous experiments, in which γ -RIMs were C-terminally tagged with the fluorescent marker mCherry. γ -RIMs-mCherry were not enriched in axonal boutons, but diffusely localized along the axon.

Taking together, these data suggest firstly, that C-terminal tagging interferes with proper targeting of γ -RIMs, however this impediment can be overcome by increased levels of RIM1 α . Secondly, that endogenous RIM1 α or additional proteins are sufficient to promote the presynaptic localization of the overexpressed N-terminally tagged RIM3 γ and RIM4 γ .

Furthermore, these results point to a physical interaction of α - and γ -RIMS most likely by homo- and heterodimerization. Moreover, overexpression of RIM1 α promotes an enhancement of the synaptic localization of RIM3 γ and RIM4 γ , and downregulation of γ -RIMS induces a decrease of RIM1 α protein levels. These data suggest that formation of α -/ γ -heterodimers might play a role in the stabilization of α -RIMS at the Active Zone.

Based on these results, a hypothesis regarding the potential function of γ -RIMS can be formulated: at the Active Zone slots can be occupied by α -homo, α -/ γ -hetero and γ -homodimers (Fig. 6.2). In that way, the function of RIMS at the Active Zone, eg. synaptic vesicle coupling to calcium channels could be modulated by the ratio of the different complexes. Under the assumption that α -homodimers are the functional dimers, formation of α -/ γ -heterodimers would decrease the number of these functional complexes, thereby preventing an excess of primed vesicles, and γ -homodimers would completely inhibit the connection between calcium channels and synaptic vesicles, since they cannot bind to Rab3. A balance among the different dimers would be required for a proper synaptic transmission. Therefore, an increase of RIM1 α protein levels would induce an enhancement of γ -RIMS synaptic localization in order to keep the number of α -/ α -complexes at the Active Zone constant, and thereby the number of primed synaptic vesicles.

Formation of heterodimers has already been suggested as a mechanism to regulate the function and the stability of several synaptic proteins. Amphiphysin I has been shown to be important for the stability of amphiphysin II, and the formation of their heterodimers plays a role in clathrin-mediated endocytosis (Wigge et al., 1997). In addition, synapsin heterodimer formation has been proposed to modulate synapsin function (Hosaka and Südhof, 1999). Moreover, homodimerization of the C2A domain of Munc13-1 has been shown to compete with the heterodimerization of RIM1 α and Munc13-1 C2A domains. Formation

of these heterodimers has been reported to regulate neurotransmitter release (Lu et al., 2006). Therefore, a balance among α -homo, α - γ -hetero and γ -homodimers might play an important role in regulating the function of α -RIMs.

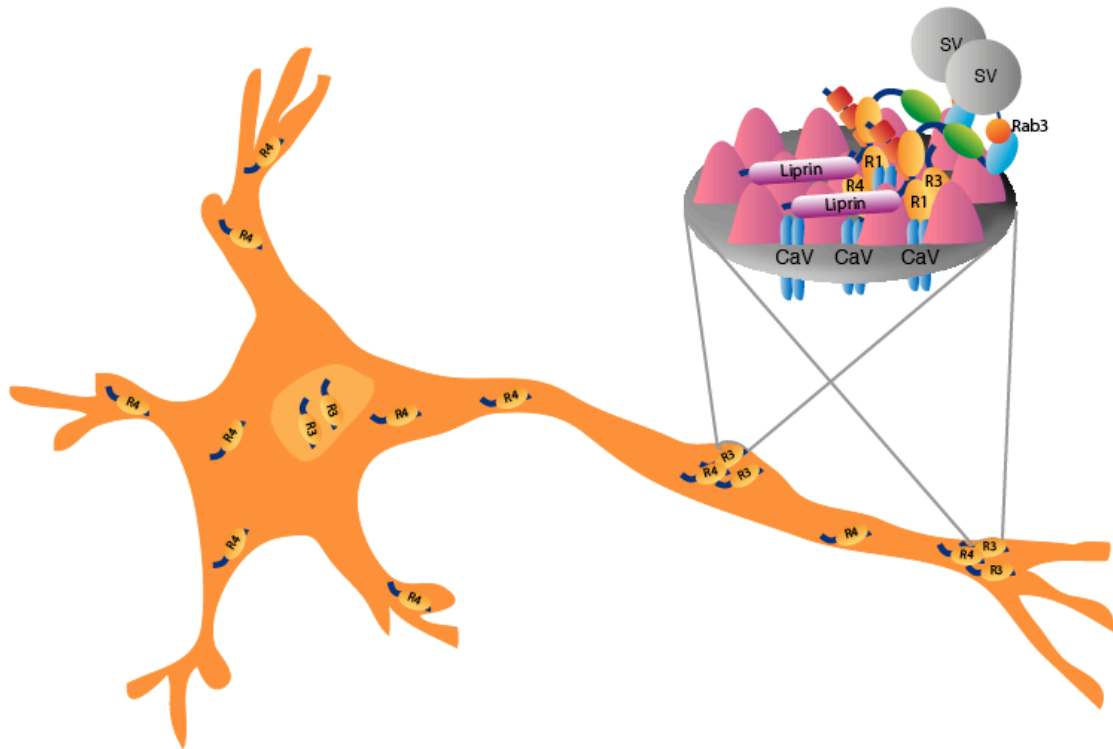


Fig. 6.2 RIM3 γ and RIM4 γ localization in the neuron

Both, RIM3 γ and RIM4 γ are localized at the Active Zone. This localization is promoted by the C2B domain, and enhanced by their interaction to RIM1 α . In addition to the presynaptic localization of both γ -RIMs, the N-terminal isoform specific sequence confers additional differential expression patterns. RIM3 γ is enriched in the nucleus, whereas RIM4 γ is localized in the cytoplasm along dendrites and axons.

6.4 RIM3 γ and RIM4 γ are necessary for the correct formation of neuronal processes

The five families composing the CAZ (Munc13, Piccolo/Basoon, ELKS, Liprin- α and RIMs) have been widely analyzed. Deletion of CAZ proteins, by knockout or RNA interference technology, has revealed the essential role of these proteins in neurotransmitter release, however, so far no mutant has been found to alter the physical structure of the Active Zone to any significant degree. Only

disruption of Liprins- α in invertebrates leads to alterations in the size and structure of the Active Zone (Kaufmann *et al.*, 2002; Zhen and Jin, 1999). Furthermore, overexpression of degradation resistant Liprin- α 1, leads to a reduction in the number of primary, secondary and tertiary dendrites (Yao *et al.*, 2007).

To gain insight into the function of RIM3 γ and RIM4 γ , short hairpin RNAs were designed to reduce protein expression in neurons, utilizing lentiviral transduction. Neurons deficient for RIM3 γ and RIM4 γ showed a surprising phenotype. All neurons with a decrease in the levels of either RIM3 γ or RIM4 γ maintained the axon, but suffered an extraordinary loss of neuronal arborization. Sholl analyses showed that the number of crossings stagnated at a low level (0-1 crossings) over the entire measured distance (120 μ m) in neurons transduced with the shRNAs, thus reflecting the severe impairment of the dendritic tree.

The loss of dendrites was an unexpected result considering that RIM1 α/β or RIM2 α knockout neurons do not show any morphological alterations, not even at the ultrastructural level (Kaesler *et al.*, 2008a; Schoch *et al.*, 2002; Schoch *et al.*, 2006). Furthermore, RIM1 α down-regulation in primary neurons, did not induce any alteration in the structure of the neurons (Yao *et al.*, 2007).

The striking phenotype resulting from the downregulation of RIM3 γ and RIM4 γ raised several questions. (1) Is the phenotype a consequence of a cell culture artefact? (2) Are the shRNAs specific for their targets? (3) Are the neurons functional after the massive loss of dendrites? (4) Is the loss of neurons a developmental or a maintenance problem?

(1) The possibility of a cell culture artefact, was excluded after *in vivo* experiments. Newborn rats were injected in the ventricle with a control- or shRNA-expressing viral suspension and analyzed at different time points (p7,

p14 and p21). Neurons lacking RIM3 γ or RIM4 γ showed a decrease in the number of neurites, as compared to infected control neurons. Therefore, the *In vivo* experiments confirmed the morphological changes observed in cultured neurons. Furthermore, these experiments showed that the loss of dendrites is unlikely to induce neuronal death, since 21 days after infection a very high number of neurons lacking RIM3 γ or RIM4 γ were still present.

(2). Off-target effects are the most significant problem when using RNA interference. These effects are usually due to two different factors: the binding of shRNAs to sequences other than the target, or the enhancement of immune response by effects independent of shRNA sequences (Alvarez et al., 2006; Hajeri and Singh, 2009). In addition, downregulation of synaptic proteins involves additional difficulties. Downregulation of synaptic proteins may compete with intracellular processes such as microRNAs (Alvarez et al., 2006; Schrott et al., 2006). Furthermore, Alvarez and colleagues observed changes in neuronal morphology when applying an shRNA a luciferase gene, which is not expressed by neurons (Alvarez et al., 2006). Therefore, the results obtained from downregulation of synaptic proteins should be carefully analyzed.

To test the target specificity, two different approaches were carried out. Firstly, four point mutations were introduced in the shRNA sequence to prevent the annealing to the mRNA. Neurons infected with mutated shRNAs did not show any morphological change, indicating no effect of the mutated shRNAs on RIM3 γ and RIM4 γ protein expression. A second rescue experiment was carried out to confirm shRNA target specificity. Silent point mutations were introduced in RIM3 γ and RIM4 γ cDNA sequences in order to avoid shRNA annealing without altering the amino acid sequence. Neurons coexpressing functional shRNA together with resistant RIM3 γ or RIM4 γ sequences showed a rescue of the phenotype, demonstrating thereby that the loss of dendrites is a direct effect

of RIM3 γ and RIM4 γ downregulation, and therefore proving the target specificity.

Nonspecific off-target effects are due to the activation of the innate immune response as it induces toxicity related effects that are based on the RNAi construct itself or its delivery vehicle (Rao *et al.*, 2009). Small RNA sequences have been shown to induce changes in cell viability, by immunity activation (Fedorov *et al.*, 2006). The use of Plasmid-based shRNA-vectors reduces the possibility of an immune response (Hajeri and Singh, 2009). Furthermore, if the loss of dendrites were an effect of the vehicle, all designed shRNAs and also the control plasmid would have induced the same outcome. Therefore, we can conclude that the impairment of the dendritic tree is a result of the loss of RIM3 γ and RIM4 γ .

(3) The development of a highly branched dendritic tree is essential for the establishment of functional neuronal connections, therefore we considered the possibility that neurons lacking RIM3 γ or RIM4 γ could be synaptically inactive as a consequence of the loss of neurites. For that reason electrophysiological analyses were performed. Spontaneous glutamatergic activity of RIM3 γ or RIM4 γ deficient neurons was measured and compared to control cells. Preliminary data from neurons expressing low levels of RIM3 γ and RIM4 γ confirmed that the neurons were electrophysiologically active, and so far showed no difference in the frequency of mEPSCs, indicating that the release probability is not changed. These data suggested that the number of synapses was unchanged. However, this finding would be unexpected since the number of dendrites is extremely decreased. This finding could be explained by a reduction in the number of synapses, but with an increase in the size of the synaptic vesicle pools within the remaining synapses. Nevertheless, the frequency data was very variable between individual neurons even within

control cells. Therefore, further experiments will be necessary to confirm that indeed there is no change in mEPSC frequency.

In contrast to the frequency data, statistic analyses showed a clear reduction of mEPSC amplitude in neurons lacking RIM3 γ or RIM4 γ . A reduction in the amplitude of spontaneous synaptic events might be a consequence of a decrease in the quantum size and therefore a presynaptic failing. Otherwise, the reduction in amplitude might be due to a decrease in the number of postsynaptic neurotransmitter receptors. Further experiments will be required to understand the mechanism underlying the decrease in mEPSC amplitude. Furthermore, these results differ from the data obtained in RIM1 KO primary neurons. Recordings of miniature excitatory postsynaptic currents (mEPSC) in RIM1 deficient hippocampal neurons showed no differences either in the frequency or in the amplitude of mEPSCs, as compared to wild type neurons (Calakos et al., 2004). These data suggest that the decrease in the amplitude of mEPSCs observed in RIM3 γ and RIM4 γ knock down neurons is not a direct consequence of the decrease on RIM1 α levels.

(4) To examine the dynamics of dendrite loss, primary hippocampal neurons were transduced with control and shRNAs expressing plasmids at different time points (DIV1, DIV3, and DIV7). Neurons infected at earlier time points displayed a more dramatic impairment of the dendritic tree than neurons transduced at DIV7, pointing to a possible developmental problem. However these experiments are not conclusive. To study this phenomom in more detail, time-lapse imaging will be necessary in order to conclusively show if neurons lacking RIM3 γ or RIM4 γ simplify their dendritic tree by retracting dendritic processes, or in contrast, do not establish appropriate neuronal morphology.

6.4.1 Possible mechanisms underlying the loss of neuronal processes

Dendrite morphogenesis consists of a sequence of interrelated steps, including outgrowth, branching, guidance, targeting, cessation of growth and arbor remodeling. All these processes depend on the rearrangement of cytoskeletal structures and can be regulated by intrinsic and extrinsic mechanisms in a spatio-temporally regulated manner (reviewed in Corty *et al.*, 2009; Ehlers, 2005; Jan and Jan, 2003; Miller and Kaplan, 2003; Poulain and Sobel, 2009). Neurotransmission triggers changes in intracellular calcium levels that act on calcium dependent intracellular signalling pathways. These calcium-induced signalling pathways seem to affect neuronal morphology and the development of the dendritic arborization by targeting nuclear transcription factors thereby controlling expression of genes required for dendritic development (Chen and Ghosh, 2005).

The loss of dendrites induced by downregulation of RIM3 γ and RIM4 γ , might be due to a direct or indirect effect on the actin cytoskeleton, triggered by protein-protein interactions, activity-regulated intracellular signals, nuclear transcription or ER-Golgi trafficking. An important step to understand the molecular mechanism underlying this arborization impairment will be to investigate if the C2B domain alone is sufficient to rescue the knock down phenotype. These results would reveal whether the shown effect is driven by the C2B domain and its interaction partners, or in contrast by the N-terminal sequence.

We hypothesize that this effect might be driven by Liprins- α and not by RIM1 α . Downregulation of RIM1 α cannot be responsible for the reduction in the number of dendrites since neurons lacking RIM1 α do not show any changes even in the ultrastructure of the presynapse (Schoch *et al.*, 2002; Yao *et al.*, 2007). In

contrast, several lines of evidence point towards a role of Liprins- α in mediating changes in the morphology of the neuron.

Liprin- α acts as adaptor protein for the motor protein Kif1a being responsible for the transport of GRIP1 (Wyszynski *et al.*, 2002). Downregulation of GRIP1 showed a similar phenotype to that observed in RIM3 γ and RIM4 γ knock down neurons. Loss of GRIP1 led to a loss of dendrites induced by the impairment of EphB2 receptor trafficking (Hoogenraad *et al.*, 2005). The interaction between GRIP1 and Liprins- α is responsible for the targeting of AMPARs, and might control the exit of AMPAR complexes from the ER/Golgi in association with stargazin (Wyszynski *et al.*, 2002). A loss of Liprins- α might induce a reduction in the transport of GRIP1 leading to a misslocalization of AMPARs and EphB2 receptor that result in a loss of dendrites (Fig. 6.3).

Furthermore, Liprins- α interact with and transport GIT1, a multidomain protein known to regulate protein trafficking and the actin cytoskeleton (Ko *et al.*, 2003a). GIT1 negatively modulates ARF (ADP-ribosylation factors), known to regulate intracellular neuronal transport (Chavrier and Goud, 1999). The interaction between GIT1 and Liprin- α 1 is also responsible for the transport of AMPARs (Shin *et al.*, 2003). In addition, cross-talking between the presynaptic EphrinB and its postsynaptic EphB receptor influences spine and dendrite morphology (Essmann *et al.*, 2008; Segura *et al.*, 2007). Loss of Liprin- α might affect the levels or the localization of GIT1 leading to an alteration on the cytoskeleton, directly or through its effector EphrinB.

Furthermore, GRIP1 interacts with PICK1, which has been shown to inhibit the effect of Arp2/3 on actin polymerization therefore altering neuronal morphology and the endocytosis of AMPARs (Rocca *et al.*, 2008).

Moreover, Liprins- α were first identified as interaction partners of the Leukocyte common antigen-related (LAR) family receptor protein tyrosine phosphatases

(LAR-RPTP) (Serra-Pagès *et al.*, 1998). Recent studies have shown that proper degradation of Liprin- α 1 by CAMKII is necessary for the distribution of LAR in dendrites. Inhibition of Liprin- α 1 degradation leads to a mislocalization of LAR, and thereby impairs dendrite morphogenesis (Hoogenraad *et al.*, 2007). However, in this case downregulation of Liprin- α 1 increases the number of spines, and up-regulation reduces the number of dendrites. This effect is in contradiction of our hypothesis. However Liprin- α 1 is, under normal conditions, poorly expressed in the brain (Zürner and Schoch, 2008). Up-regulation of Liprin- α 1 might induce down-regulation of Liprin- α 2 and Liprin- α 3, the isoforms that are highly enriched in the brain, thereby triggering the shown effects.

Taken together, downregulation of γ -RIMS might induce a specific reduction of the levels of Liprins- α , which could then induce alterations of the actin cytoskeleton and affect the localization of AMPARs, through several pathways. Furthermore, it might affect the EphrinB and its postsynaptic EphB receptor cascade and therefore promote a loss of neuronal arborization (Fig. 6.3,1).

However, it is also possible that the N-terminus of RIM3 γ and RIM4 γ regulates the loss of dendrites, pointing to a more general mechanism underlying the impairment of the neuronal tree. As mentioned above, RIM3 γ is not only localized presynaptically but also highly enriched in the nucleus. In recent years, several synaptic proteins have been shown to accumulate in the nucleus (reviewed in Jordan and Kreutz, 2009), executing diverging functions at the synapse and in the nucleus. An example of this dual behaviour is the CtBP family of proteins, first discovered as transcriptional corepressors. CtBP proteins have been shown to play an important role in intracellular trafficking and the organization of the ribbon synapses (Chinnadurai, 2003; Corda *et al.*, 2006). In addition to CtBPs, GRIP1, CASK and Jacob are synaptic proteins with a role as transcriptional regulators or involved in the trafficking of proteins out or in the nucleus (reviewed in Jordan and Kreutz, 2009). RIM3 γ , which is located

in the nucleus might also possess a role in transcription or trafficking of other proteins, and therefore affect neuronal morphogenesis (Fig. 6.3,2).

In contrast to RIM3 γ , RIM4 γ has been predicted to be associated to the Golgi apparatus. Several studies have suggested that dendritic growth, but apparently not axonal growth, can also be affected by defects in the secretory pathways (Tang, 2008). In addition, the Golgi apparatus operates as a scaffold for numerous signaling molecules, including kinases and phosphatases that are regulated by synaptic activity and may influence dendrite morphogenesis (Hanus and Ehlers, 2008). RIM4 γ might be involved in the sorting of proteins out of the Golgi apparatus. Therefore downregulation of RIM4 γ could induce an impairment of the trafficking of proteins that are implicated in the regulation of the actin cytoskeleton (Fig. 6.3,3).

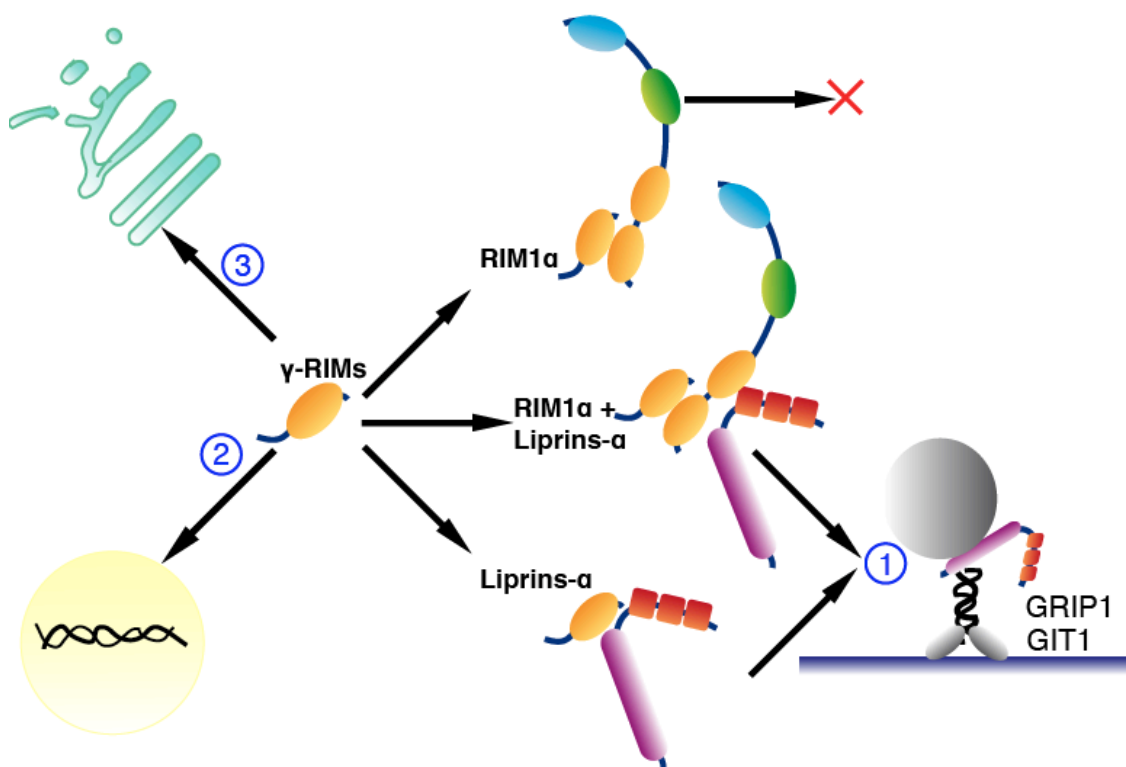


Fig. 6.3 Possible mechanisms underlying the loss of dendrites

1, γ -RIM downregulation might alter, directly or via RIM1 α , the expression levels of Liprin- α and Liprin- α binding proteins, thereby disrupting different cascades that are implicated in the

formation and maintenance of neuronal processes. 2, Nuclear RIM3 γ might function in regulating the expression of a group of genes involved in dendrite formation. 3, RIM4 γ might associate with the endoplasmic reticulum and the Golgi apparatus and thereby contribute to the trafficking of different proteins to their correct subcellular localization.

In summary, neurons deficient in RIM3 γ and RIM4 γ undergo an extreme loss of neuronal processes. This effect might be triggered by the alteration of the localization and/or expression levels of proteins downstream of γ -RIMs such as Liprin- α s and Liprin- α s binding proteins, or in contrast, by a more general process implicating Golgi-trafficking or the regulation of gene expression.

The phenotype observed in neurons lacking γ -RIMs is surprising as it differs from the data obtained for all other CAZ enriched proteins. Neurons lacking RIM1, Munc13, Bassoon or ELKS displayed an important impairment in neurotransmitter release but no significant changes in the structure of the Active Zone (Augustin et al., 1999b; Kaeser et al., 2009; Schoch et al., 2002). Only, deletion of Liprin- α s in invertebrates induces a change in the size and organization of the synapses (Kaufmann *et al.*, 2002; Zhen and Jin, 1999).

6.5 Autoantibodies to Munc18, cerebral plasma cells and B-lymphocytes in Rasmussen encephalitis

Our analyses reveal a subgroup of RE patients with a remarkable humoral immunoreaction based on autoantibodies targeted to Munc18-1 and cerebral B-lymphocyte and antibody producing plasma cell infiltrates.

Etiology and pathogenesis of RE are only incompletely understood. An autoimmune etiology for RE has been postulated based on the observation of inflammatory infiltrates in RE brains and of transient responses to immunomodulatory therapy. Whereas a major pathogenic contribution of

cytotoxic T-lymphocytes is well established (Bauer *et al.*, 2002), the role of humoral autoimmunity in RE has been challenged by recent data. Initially, auto-antibodies against the postsynaptic protein GluR3 were suggested to play a role in RE (Rogers *et al.*, 1994). However, in subsequent studies GluR3 antibodies were found to be not specific to RE and could only be identified infrequently in RE patients (Watson *et al.*, 2004; Wiendl *et al.*, 2001). Furthermore, the concentration of the GluR3 auto-antibodies in the RE patient sera was not sufficient to detect GluR3 protein in rat brain homogenates (Rogers *et al.*, 1994). In contrast, Yang *et al.* observed a strong, single immunoreactive band in immunoblots of rat synaptosomes probed with the serum of a RE patient who previously had been shown to have anti-GluR3 antibodies and identified the presynaptic SM protein Munc18-1 as autoantigen (Yang *et al.*, 2000). Here we found that a subgroup of two out of ten biopsy-proven RE patients tested has antibodies that detect Munc18-1, either expressed in HEK293 cells or endogenously present in mouse brain homogenate. Furthermore, we found an infiltration of B-lymphocytes and antibody producing plasma cells in the brain parenchyma in the two patients in which Munc18-1 antibodies were present. This suggests a propensity for local antibody production in brain parenchyma of RE patients. However, a potential clonality of these lymphocytes/plasma cells needs to be examined by future studies. Findings in favor of such clonal expansion of B cells have been provided in an earlier study (Baranzini *et al.*, 2002). In addition, a recently performed study describes the completely abrogation of seizure activity during six month in a patient treated with rituximab. Previously, this patient was treated with several antiepileptic and immunosuppressor drugs, however the seizure-free period with was not longer than 7 weeks (Thilo *et al.*, 2009). Rituximab is a chimeric anti-CD20 antibody that induces apoptosis of CD20+ cells (Maloney *et al.*, 1994). The successful treatment with Rituximab corroborates an implication of B-cells in Rasmussen

encephalitis.

Munc18-1 is a cytoplasmatic protein and an essential component of the presynaptic release machinery. In animals deficient for the protein neurotransmitter release is completely blocked and neurons undergo apoptosis after normal brain assembly (Verhage et al., 2000). If the Munc18-1 IgG were to be taken up into the presynaptic nerve terminal via endocytosis it could bind to Munc18-1 and reversibly interfere with synaptic transmission or trigger a signaling cascade resulting in neuronal cell death.

The presence of inflammatory T-cell infiltrates and microglial nodes is an integral aspect of RE pathology (Bien *et al.*, 2005). Recent findings suggest that the local immune response in RE includes restricted T-cell populations that have expanded from a few precursors T-cells responding to discrete antigenic epitopes (Bauer *et al.*, 2002). Our data demonstrates a subgroup of RE patients to exist that are defined by the presence of Munc18-1 auto-antibodies and cerebral B-lymphocyte and plasma cell infiltrates as characteristic neuropathological changes. Interestingly, Munc18-1 autoantibodies showed a long-lasting presence in patient 1 who was followed until 2.7 yrs after disease onset. On the other hand, none of the initially antibody negative patients became positive during the course of their disease. These pathological changes may reflect a distinct and stable humoral immune component within the pathogenesis of a subgroup of patients with RE in which Munc18-1 serves as target of the inflammatory reaction.

RE is a complex disease, which might be caused by several independent pathophysiological mechanisms. Antibodies against Munc18-1 may help to define a subgroup of patients and thereby be useful in gaining a more detailed understanding of the disorder.

7 CONCLUSIONS

The results of this study show for the first time that RIM3 γ and RIM4 γ , as the full length α -RIMs, are brain specific proteins present throughout the brain in overlapping but distinct expression patterns. Both isoforms are present in excitatory and inhibitory synapses and their expression is developmentally regulated, increasing during synaptogenesis. Subcellularly, RIM3 γ and RIM4 γ are tightly associated with the cytomatrix composing the synaptic densities. RIM3 γ is specifically localized at the presynapse and highly enriched in the nucleus. In contrast, RIM4 γ is uniformly expressed along axons and dendrites. These findings indicate that the subcellular localization of the individual γ -RIMs differs despite their high sequence homology. However, both are present within the same subcompartment as α -RIMs.

Furthermore, we analyzed the domain organization of RIM3 γ and RIM4 γ in order to identify the targeting sequences of both isoforms. We found that the C2B domain is sufficient to target RIM3 γ and RIM4 γ to the presynapse, suggesting the isoform specific N-terminal sequence to be responsible for their differential localization. In the case of RIM3 γ this region contains a nuclear localization signal.

We could verify the colocalization of γ -RIMs and Liprins- α in neurons as well as in PC12 cells after overexpression of the proteins, however, an unequivocal interaction could only be shown for RIM3 γ . Furthermore, we could show that the N-terminus of RIM3 γ is not required for its interaction with Liprins- α .

Interestingly, we found RIM1 α , in contrast to Liprin- α , to promote the synaptic localization of RIM3 γ and RIM4 γ , however this interaction was not required for the targeting of γ -RIMs.

To gain insight into the functional role of RIM3 γ and RIM4 γ , both proteins were downregulated using RNA interference technology. Surprisingly, downregulation of both γ -RIM isoforms induced a severe impairment of neuronal morphogenesis. Neurons lacking RIM3 γ and RIM4 γ conserved the axon but displayed a significant loss of dendrites. In addition, a reduction in the protein levels of RIM3 γ and RIM4 γ induced an equivalent decrease of RIM1 α protein levels and a decrease in the amount of Liprin- α and the Liprin- α binding protein GRIP1.

As RIM1 KO mice displayed no changes in neuronal morphology, not even at the ultrastructural level, the decrease in RIM1 α levels is unlikely to be the cause of the observed phenotype. Rather, the similar phenotype described in GRIP1 deficient neurons, points to a cascade/complex that links γ -RIMs to different Liprin- α binding proteins, e.g. GRIP1, GIT1. These data suggest that the reduction of the expression level of Liprin- α in neurons lacking γ -RIMs might induce the loss of dendrites via different mechanisms that alter protein trafficking and/or the actin cytoskeleton.

Overall, in spite of their small size, γ -RIMs exhibit common properties with α -RIMs, but also characteristics that are specific for the isoforms. Further experiments have to be performed to clarify the open questions.

8 OUTLOOK

The results obtained in this study raise several questions that need to be address in further experiments.

The next stage of the project would involve further experiments to fully resolve the mechanism underlying the loss of neuronal processes. In this regard, it will be necessary to examine whether the downregulation of RIM3 γ affects the expression levels of RIM4 γ and vice versa.

Additional experiments will be also a mandatory to determine which domain is sufficient to rescue the knock-down phenotype and identify the events involved in the observed loss of dendrites. Therefore, the identification of proteins downstream of γ -RIMs, overexpresion of which would rescue the phenotype, should be pursued.

In addition, it will be important to understand which is the physiological relevance of the differential subcellular distribution of both γ -RIMs, and determine if deletion of RIM1 α (RIM1 KO) might influence the localization of these proteins.

Furthermore, a more detailed electrophysiological study will be necessary to understand the role of RIM3 γ and RIM4 γ in neurotransmitter release and to determine if the reduction of RIM3 γ and RIM4 γ affect synaptic activity via a decrease of RIM1 α expression levels and/or other additional pathways.

9 REFERENCES

- Ahmari, S.E., Buchanan, J., and Smith, S.J. (2000). Assembly of presynaptic active zones from cytoplasmic transport packets. In *Nat Neurosci*, pp. 445-451.
- Ahmed, S., Maruyama, I.N., Kozma, R., Lee, J., Brenner, S., and Lim, L. (1992). The *Caenorhabditis elegans* unc-13 gene product is a phospholipid-dependent high-affinity phorbol ester receptor. In *Biochem J*, pp. 995-999.
- Altrock, W.D., tom Dieck, S., Sokolov, M., Meyer, A.C., Sigler, A., Brakebusch, C., Fässler, R., Richter, K., Boeckers, T.M., Potschka, H., *et al.* (2003). Functional inactivation of a fraction of excitatory synapses in mice deficient for the active zone protein bassoon. *Neuron* 37, 787-800.
- Alvarez, V.A., Ridenour, D.A., and Sabatini, B.L. (2006). Retraction of synapses and dendritic spines induced by off-target effects of RNA interference. In *J Neurosci*, pp. 7820-7825.
- Andrews-Zwilling, Y.S., Kawabe, H., Reim, K., Varoqueaux, F., and Brose, N. (2006). Binding to Rab3A-interacting molecule RIM regulates the presynaptic recruitment of Munc13-1 and ubMunc13-2. *J Biol Chem* 281, 19720-19731.
- Augustin, I., Betz, A., Herrmann, C., Jo, T., and Brose, N. (1999a). Differential expression of two novel Munc13 proteins in rat brain. *Biochem J* 337 (Pt 3), 363-371.
- Augustin, I., Rosenmund, C., Südhof, T.C., and Brose, N. (1999b). Munc13-1 is essential for fusion competence of glutamatergic synaptic vesicles. *Nature* 400, 457-461.
- Baranzini, S.E., Laxer, K., Saketkoo, R., Elkins, M.K., Parent, J.M., Mantegazza, R., and Oksenberg, J.R. (2002). Analysis of antibody gene rearrangement, usage, and specificity in chronic focal encephalitis. *Neurology* 58, 709-716.
- Barragan, I., Marcos, I., Borrego, S., and Antiñolo, G. (2005). Molecular analysis of RIM1 in autosomal recessive Retinitis pigmentosa. *Ophthalmic Res* 37, 89-93.
- Basu, J., Shen, N., Dulubova, I., Lu, J., Guan, R., Guryev, O., Grishin, N.V., Rosenmund, C., and Rizo, J. (2005). A minimal domain responsible for Munc13 activity. In *Nat Struct Mol Biol*, pp. 1017-1018.

- Bauer, J., Bien, C.G., and Lassmann, H. (2002). Rasmussen's encephalitis: a role for autoimmune cytotoxic T lymphocytes. *Curr Opin Neurol* 15, 197-200.
- Betz, A., Ashery, U., Rickmann, M., Augustin, I., Neher, E., Südhof, T.C., Rettig, J., and Brose, N. (1998). Munc13-1 is a presynaptic phorbol ester receptor that enhances neurotransmitter release. *Neuron* 21, 123-136.
- Betz, A., Okamoto, M., Benseler, F., and Brose, N. (1997). Direct interaction of the rat unc-13 homologue Munc13-1 with the N terminus of syntaxin. *J Biol Chem* 272, 2520-2526.
- Betz, A., Thakur, P., Junge, H.J., Ashery, U., Rhee, J.S., Scheuss, V., Rosenmund, C., Rettig, J., and Brose, N. (2001). Functional interaction of the active zone proteins Munc13-1 and RIM1 in synaptic vesicle priming. *Neuron* 30, 183-196.
- Bien, C.G., Bauer, J., Deckwerth, T.L., Wiendl, H., Deckert, M., Wiestler, O.D., Schramm, J., Elger, C.E., and Lassmann, H. (2002). Destruction of neurons by cytotoxic T cells: a new pathogenic mechanism in Rasmussen's encephalitis. *Ann Neurol* 51, 311-318.
- Bien, C.G., Granata, T., Antozzi, C., Cross, J.H., Dulac, O., Kurthen, M., Lassmann, H., Mantegazza, R., Villemure, J.G., Spreafico, R., and Elger, C.E. (2005). Pathogenesis, diagnosis and treatment of Rasmussen encephalitis: a European consensus statement. *Brain* 128, 454-471.
- Bronk, P., Deák, F., Wilson, M.C., Liu, X., Südhof, T.C., and Kavalali, E.T. (2007). Differential effects of SNAP-25 deletion on Ca²⁺-dependent and Ca²⁺-independent neurotransmission. In *J Neurophysiol*, pp. 794-806.
- Brose, N., Hofmann, K., Hata, Y., and Südhof, T.C. (1995). Mammalian homologues of *Caenorhabditis elegans* unc-13 gene define novel family of C2-domain proteins. *J Biol Chem* 270, 25273-25280.
- Burgoyne, R.D., Barclay, J.W., Ciufo, L.F., Graham, M.E., Handley, M.T.W., and Morgan, A. (2009). The functions of Munc18-1 in regulated exocytosis. In *Ann N Y Acad Sci*, pp. 76-86.
- C. Südhof, T., and Starke, K. (2008). Pharmacology of neurotransmitter release. p. 582.
- Calakos, N., Schoch, S., Südhof, T.C., and Malenka, R.C. (2004). Multiple roles for the active zone protein RIM1alpha in late stages of neurotransmitter release. In *Neuron*, pp. 889-896.
- Carr, C.M., and Munson, M. (2007). Tag team action at the synapse. In *EMBO Rep*, pp. 834-838.

- Castillo, P.E., Janz, R., Südhof, T.C., Tzounopoulos, T., Malenka, R.C., and Nicoll, R.A. (1997). Rab3A is essential for mossy fibre long-term potentiation in the hippocampus. In *Nature*, pp. 590-593.
- Castillo, P.E., Schoch, S., Schmitz, F., Südhof, T.C., and Malenka, R.C. (2002). RIM1alpha is required for presynaptic long-term potentiation. In *Nature*, pp. 327-330.
- Chandra, S., Gallardo, G., Fernández-Chacón, R., Schlüter, O.M., and Südhof, T.C. (2005). Alpha-synuclein cooperates with CSPalpha in preventing neurodegeneration. In *Cell*, pp. 383-396.
- Chavrier, P., and Goud, B. (1999). The role of ARF and Rab GTPases in membrane transport. In *Curr Opin Cell Biol*, pp. 466-475.
- Chen, Y., and Ghosh, A. (2005). Regulation of dendritic development by neuronal activity. In *J Neurobiol*, pp. 4-10.
- Chevaleyre, V., Heifets, B.D., Kaeser, P.S., Südhof, T.C., Purpura, D.P., and Castillo, P.E. (2007). Endocannabinoid-mediated long-term plasticity requires cAMP/PKA signaling and RIM1alpha. *Neuron* 54, 801-812.
- Chinnadurai, G. (2003). CtBP family proteins: more than transcriptional corepressors. In *Bioessays*, pp. 9-12.
- Cockrell, A., and Kafri, T. (2007). Gene delivery by lentivirus vectors. In *Mol Biotechnol*, pp. 184-204.
- Coppola, T., Magnin-Luthi, S., Perret-Menoud, V., Gattesco, S., Schiavo, G., and Regazzi, R. (2001). Direct interaction of the Rab3 effector RIM with Ca²⁺ channels, SNAP-25, and synaptotagmin. *J Biol Chem* 276, 32756-32762.
- Corda, D., Colanzi, A., and Luini, A. (2006). The multiple activities of CtBP/BARS proteins: the Golgi view. In *TRENDS in Cell Biology*, pp. 167-173.
- Corty, M.M., Matthews, B.J., and Grueber, W.B. (2009). Molecules and mechanisms of dendrite development in *Drosophila*. In *Development*, pp. 1049-1061.
- Crowder, K.M., Gunther, J.M., Jones, T.A., Hale, B.D., Zhang, H.Z., Peterson, M.R., Scheller, R.H., Chavkin, C., and Bajjalieh, S.M. (1999). Abnormal neurotransmission in mice lacking synaptic vesicle protein 2A (SV2A). In *P Natl Acad Sci Usa*, pp. 15268-15273.
- Crump, J.G., Zhen, M., Jin, Y., and Bargmann, C.I. (2001). The SAD-1 kinase regulates presynaptic vesicle clustering and axon termination. In *Neuron*, pp. 115-129.

- Dai, H., Tomchick, D.R., García, J., Südhof, T.C., Machius, M., and Rizo, J. (2005). Crystal structure of the RIM2 C2A-domain at 1.4 Å resolution. *Biochemistry* *44*, 13533-13542.
- Dai, Y., Taru, H., Deken, S.L., Grill, B., Ackley, B., Nonet, M.L., and Jin, Y. (2006). SYD-2 Liprin- α organizes presynaptic active zone formation through ELKS. *Nat Neurosci* *9*, 1479-1487.
- Damer, C.K., and Creutz, C.E. (1996). Calcium-dependent self-association of synaptotagmin I. In *J Neurochem*, pp. 1661-1668.
- Deák, F., Liu, X., Khvotchev, M., Li, G., Kavalali, E.T., Sugita, S., and Südhof, T.C. (2009a). Alpha-latrotoxin stimulates a novel pathway of Ca²⁺-dependent synaptic exocytosis independent of the classical synaptic fusion machinery. In *J Neurosci*, pp. 8639-8648.
- Deák, F., Schoch, S., Liu, X., Südhof, T.C., and Kavalali, E.T. (2004). Synaptobrevin is essential for fast synaptic-vesicle endocytosis. *Nat Cell Biol* *6*, 1102-1108.
- Deák, F., Xu, Y., Chang, W.-P., Dulubova, I., Khvotchev, M., Liu, X., Südhof, T.C., and Rizo, J. (2009b). Munc18-1 binding to the neuronal SNARE complex controls synaptic vesicle priming. In *J Cell Biol*, pp. 751-764.
- Deguchi-Tawarada, M., Inoue, E., Takao-Rikitsu, E., Inoue, M., Ohtsuka, T., and Takai, Y. (2004). CAST2: identification and characterization of a protein structurally related to the presynaptic cytomatrix protein CAST. In *Genes Cells*, pp. 15-23.
- Deken, S.L., Vincent, R., Hadwiger, G., Liu, Q., Wang, Z.W., and Nonet, M.L. (2005). Redundant localization mechanisms of RIM and ELKS in *Caenorhabditis elegans*. In *J Neurosci*, pp. 5975-5983.
- Dresbach, T., Hempelmann, A., Spilker, C., tom Dieck, S., Altroch, W.D., Zuschratter, W., Garner, C.C., and Gundelfinger, E.D. (2003). Functional regions of the presynaptic cytomatrix protein bassoon: significance for synaptic targeting and cytomatrix anchoring. In *Mol Cell Neurosci*, pp. 279-291.
- Dresbach, T., Qualmann, B., Kessels, M.M., Garner, C.C., and Gundelfinger, E.D. (2001). The presynaptic cytomatrix of brain synapses. *Cell Mol Life Sci* *58*, 94-116.
- Dulubova, I., Khvotchev, M., Liu, S., Huryeva, I., Südhof, T.C., and Rizo, J. (2007). Munc18-1 binds directly to the neuronal SNARE complex. *P Natl Acad Sci Usa* *104*, 2697-2702.
- Dulubova, I., Lou, X., Lu, J., Huryeva, I., Alam, A., Schneggenburger, R., Südhof, T.C., and Rizo, J. (2005). A Munc13/RIM/Rab3 tripartite complex: from priming to plasticity? *EMBO J* *24*, 2839-2850.

- Ehlers, M.D. (2005). Dendrite development: a surprising origin. In *J Cell Biol*, pp. 517-519.
- Essmann, C., Martinez, E., Geiger, J., Zimmer, M., Traut, M., Stein, V., Klein, R., and Acker-Palmer, A. (2008). Serine phosphorylation of ephrinB2 regulates trafficking of synaptic AMPA receptors. In *Nat Neurosci*.
- Fedorov, Y., Anderson, E.M., Birmingham, A., Reynolds, A., Karpilow, J., Robinson, K., Leake, D., Marshall, W.S., and Khvorova, A. (2006). Off-target effects by siRNA can induce toxic phenotype. In *RNA*, pp. 1188-1196.
- Fenster, S.D., Chung, W.J., Zhai, R., Cases-Langhoff, C., Voss, B., Garner, A.M., Kaempfer, U., Kindler, S., Gundelfinger, E.D., and Garner, C.C. (2000). Piccolo, a presynaptic zinc finger protein structurally related to bassoon. In *Neuron*, pp. 203-214.
- Fenster, S.D., Kessels, M.M., Qualmann, B., Chung, W.J., Nash, J., Gundelfinger, E.D., and Garner, C.C. (2003). Interactions between Piccolo and the actin/dynamin-binding protein Abp1 link vesicle endocytosis to presynaptic active zones. In *J Biol Chem*, pp. 20268-20277.
- Fernández-Chacón, R. (2004). The Synaptic Vesicle Protein CSP Prevents Presynaptic Degeneration
. In *Neuron*.
- Fischer von Mollard, G., Mignery, G.A., Baumert, M., Perin, M.S., Hanson, T.J., Burger, P.M., Jahn, R., and Südhof, T.C. (1990). rab3 is a small GTP-binding protein exclusively localized to synaptic vesicles. In *P Natl Acad Sci Usa*, pp. 1988-1992.
- Friedman, H.V., Bresler, T., Garner, C.C., and Ziv, N.E. (2000). Assembly of new individual excitatory synapses: time course and temporal order of synaptic molecule recruitment. In *Neuron*, pp. 57-69.
- Fukuda, M. (2004). Alternative splicing in the first alpha-helical region of the Rab-binding domain of Rim regulates Rab3A binding activity: is Rim a Rab3 effector protein during evolution? *Genes Cells* 9, 831-842.
- Fukuda, M., and Mikoshiba, K. (2000). Distinct self-oligomerization activities of synaptotagmin family. Unique calcium-dependent oligomerization properties of synaptotagmin VII. In *J Biol Chem*, pp. 28180-28185.
- Fukuda, M., and Mikoshiba, K. (2001). Mechanism of the calcium-dependent multimerization of synaptotagmin VII mediated by its first and second C2 domains. In *J Biol Chem*, pp. 27670-27676.
- Garcia, C.C., Blair, H.J., Seager, M., Coulthard, A., Tennant, S., Buddles, M., Curtis, A., and Goodship, J.A. (2004). Identification of a mutation in synapsin I,

a synaptic vesicle protein, in a family with epilepsy. In *J Med Genet*, pp. 183-186.

García-Junco-Clemente, P., Linares-Clemente, P., and Fernández-Chacón, R. (2005). Active zones for presynaptic plasticity in the brain. *Mol Psychiatry* 10, 185-200; image 131.

Gengyo-Ando, K., Kamiya, Y., Yamakawa, A., Kodaira, K., Nishiwaki, K., Miwa, J., Hori, I., and Hosono, R. (1993). The *C. elegans* unc-18 gene encodes a protein expressed in motor neurons. In *Neuron*, pp. 703-711.

Goldstein, A.Y.N., Wang, X., and Schwarz, T.L. (2008). Axonal transport and the delivery of pre-synaptic components. In *Curr Opin Neurobiol*, pp. 495-503.

Gracheva, E.O., Hadwiger, G., Nonet, M.L., and Richmond, J.E. (2008). Direct interactions between *C. elegans* RAB-3 and Rim provide a mechanism to target vesicles to the presynaptic density. *Neurosci Lett* 444, 137-142.

Grosshans, B.L., Ortiz, D., and Novick, P. (2006). Rabs and their effectors: achieving specificity in membrane traffic. In *P Natl Acad Sci Usa*, pp. 11821-11827.

Guan, R., Dai, H., Tomchick, D.R., Dulubova, I., Machius, M., Südhof, T.C., and Rizo, J. (2007). Crystal structure of the RIM1alpha C2B domain at 1.7 Å resolution. *Biochemistry* 46, 8988-8998.

Gundelfinger, E.D., and tom Dieck, S. (2000). Molecular organization of excitatory chemical synapses in the mammalian brain. *Naturwissenschaften* 87, 513-523.

Hajeri, P.B., and Singh, S.K. (2009). siRNAs: their potential as therapeutic agents--Part I. Designing of siRNAs. In *Drug Discov Today*, pp. 851-858.

Hanus, C., and Ehlers, M.D. (2008). Secretory outposts for the local processing of membrane cargo in neuronal dendrites. In *Traffic*, pp. 1437-1445.

Hata, Y., Slaughter, C.A., and Südhof, T.C. (1993). Synaptic vesicle fusion complex contains unc-18 homologue bound to syntaxin. In *Nature*, pp. 347-351.

Hibino, H., Pironkova, R., Onwumere, O., Vologodskaya, M., Hudspeth, A.J., and Lesage, F. (2002). RIM binding proteins (RBPs) couple Rab3-interacting molecules (RIMs) to voltage-gated Ca(2+) channels. In *Neuron*, pp. 411-423.

Higashio, H., Nishimura, N., Ishizaki, H., Miyoshi, J., Orita, S., Sakane, A., and Sasaki, T. (2008). Doc2 alpha and Munc13-4 regulate Ca(2+) -dependent secretory lysosome exocytosis in mast cells. In *J Immunol*, pp. 4774-4784.

Hoogenraad, C.C., Feliu-Mojer, M.I., Spangler, S.A., Milstein, A.D., Dunah, A.W., Hung, A.Y., and Sheng, M. (2007). Liprinalpha1 degradation by

calcium/calmodulin-dependent protein kinase II regulates LAR receptor tyrosine phosphatase distribution and dendrite development. In *Dev Cell*, pp. 587-602.

Hoogenraad, C.C., Milstein, A.D., Ethell, I.M., Henkemeyer, M., and Sheng, M. (2005). GRIP1 controls dendrite morphogenesis by regulating EphB receptor trafficking. In *Nat Neurosci*, pp. 906-915.

Hosaka, M., and Südhof, T.C. (1999). Homo- and heterodimerization of synapsins. In *J Biol Chem*, pp. 16747-16753.

Huang, Y.-Y., Zakharenko, S.S., Schoch, S., Kaeser, P.S., Janz, R., Südhof, T.C., Siegelbaum, S.A., and Kandel, E.R. (2005). Genetic evidence for a protein-kinase-A-mediated presynaptic component in NMDA-receptor-dependent forms of long-term synaptic potentiation. In *P Natl Acad Sci Usa*, pp. 9365-9370.

Inoue, E., Mochida, S., Takagi, H., Higa, S., Deguchi-Tawarada, M., Takao-Rikitsu, E., Inoue, M., Yao, I., Takeuchi, K., Kitajima, I., *et al.* (2006). SAD: a presynaptic kinase associated with synaptic vesicles and the active zone cytomatrix that regulates neurotransmitter release. *Neuron* 50, 261-275.

Inoue, H., Nojima, H., and Okayama, H. (1990). High efficiency transformation of *Escherichia coli* with plasmids. In *Gene*, pp. 23-28.

Jan, Y.-N., and Jan, L.Y. (2003). The control of dendrite development. In *Neuron*, pp. 229-242.

Janin, J. (1979). Surface and inside volumes in globular proteins. In *Nature*, pp. 491-492.

Johnson, S., Halford, S., Morris, A.G., Patel, R.J., Wilkie, S.E., Hardcastle, A.J., Moore, A.T., Zhang, a.K., and Hunt, D.M. (2003). Genomic organisation and alternative splicing of human RIM1, a gene implicated in autosomal dominant cone-rod dystrophy (CORD7). *Genomics* 81, 304-314.

Jordan, B.A., and Kreutz, M.R. (2009). Nucleocytoplasmic protein shuttling: the direct route in synapse-to-nucleus signaling. In *Trends Neurosci*, pp. 392-401.

Junge, H.J., Rhee, J.-S., Jahn, O., Varoqueaux, F., Spiess, J., Waxham, M.N., Rosenmund, C., and Brose, N. (2004). Calmodulin and Munc13 form a Ca²⁺ sensor/effector complex that controls short-term synaptic plasticity. In *Cell*, pp. 389-401.

Kaeser, P.S., Deng, L., Chávez, A.E., Liu, X., Castillo, P.E., and Südhof, T.C. (2009). ELKS2alpha/CAST deletion selectively increases neurotransmitter release at inhibitory synapses. In *Neuron*, pp. 227-239.

Kaeser, P.S., Kwon, H., Chiu, C.Q., Deng, L., Castillo, P.E., and Südhof, T.C. (2008a). RIM1alpha and RIM1beta are synthesized from distinct promoters of

the RIM1 gene to mediate differential but overlapping synaptic functions. *J Neurosci* *28*, 13435-13447.

Kaesler, P.S., Kwon, H.B., Blundell, J., Chevaleyre, V., Morishita, W., Malenka, R.C., Powell, C.M., Castillo, P.E., and Südhof, T.C. (2008b). RIM1alpha phosphorylation at serine-413 by protein kinase A is not required for presynaptic long-term plasticity or learning. *P Natl Acad Sci Usa* *105*, 14680-14685.

Kashima, Y., Miki, T., Shibasaki, T., Ozaki, N., Miyazaki, M., Yano, H., and Seino, S. (2001). Critical role of cAMP-GEFII--Rim2 complex in incretin-potentiated insulin secretion. In *J Biol Chem*, pp. 46046-46053.

Kaufmann, N., DeProto, J., Ranjan, R., Wan, H., and Van Vactor, D. (2002). *Drosophila* liprin-alpha and the receptor phosphatase Dlar control synapse morphogenesis. In *Neuron*, pp. 27-38.

Kavalali, E.T., Klingauf, J., and Tsien, R.W. (1999). Activity-dependent regulation of synaptic clustering in a hippocampal culture system. In *P Natl Acad Sci Usa*, pp. 12893-12900.

Khanna, R., Li, Q., Sun, L., Collins, T.J., and Stanley, E.F. (2006). N type Ca²⁺ channels and rim scaffold protein covary at the presynaptic transmitter release face but are components of independent protein complexes. In *Neuroscience*, pp. 1201-1208.

Kim, S., Ko, J., Shin, H., Lee, J.-R., Lim, C., Han, J.-H., Altroock, W.D., Garner, C.C., Gundelfinger, E.D., Premont, R.T., *et al.* (2003). The GIT family of proteins forms multimers and associates with the presynaptic cytomatrix protein Piccolo. In *J Biol Chem*, pp. 6291-6300.

Kishi, M., Pan, Y.A., Crump, J.G., and Sanes, J.R. (2005). Mammalian SAD kinases are required for neuronal polarization. In *Science*, pp. 929-932.

Kiyonaka, S., Wakamori, M., Miki, T., Uriu, Y., Nonaka, M., Bito, H., Beedle, A.M., Mori, E., Hara, Y., De Waard, M., *et al.* (2007). RIM1 confers sustained activity and neurotransmitter vesicle anchoring to presynaptic Ca²⁺ channels. *Nat Neurosci* *10*, 691-701.

Klausberger, T., and Somogyi, P. (2008). Neuronal diversity and temporal dynamics: the unity of hippocampal circuit operations. In *Science*, pp. 53-57.

Ko, J., Kim, S., Valtschanoff, J.G., Shin, H., Lee, J.-R., Sheng, M., Premont, R.T., Weinberg, R.J., and Kim, E. (2003a). Interaction between liprin-alpha and GIT1 is required for AMPA receptor targeting. In *J Neurosci*, pp. 1667-1677.

Ko, J., Na, M., Kim, S., Lee, J.-R., and Kim, E. (2003b). Interaction of the ERC family of RIM-binding proteins with the liprin-alpha family of multidomain proteins. In *J Biol Chem*, pp. 42377-42385.

- Koch, H., Hofmann, K., and Brose, N. (2000). Definition of Munc13-homology-domains and characterization of a novel ubiquitously expressed Munc13 isoform. *Biochem J* 349, 247-253.
- Kohn, R.E., Duerr, J.S., McManus, J.R., Duke, A., Rakow, T.L., Maruyama, H., Moulder, G., Maruyama, I.N., Barstead, R.J., and Rand, J.B. (2000). Expression of multiple UNC-13 proteins in the *Caenorhabditis elegans* nervous system. In *Mol Biol Cell*, pp. 3441-3452.
- Kotake, K., Ozaki, N., Mizuta, M., Sekiya, S., Inagaki, N., and Seino, S. (1997). Noc2, a putative zinc finger protein involved in exocytosis in endocrine cells. In *J Biol Chem*, pp. 29407-29410.
- Koushika, S.P., Richmond, J.E., Hadwiger, G., Weimer, R.M., Jorgensen, E.M., and Nonet, M.L. (2001). A post-docking role for active zone protein Rim. *Nat Neurosci* 4, 997-1005.
- Krüger, R., Kuhn, W., Müller, T., Voitalla, D., Graeber, M., Kösel, S., Przuntek, H., Epplen, J.T., Schöls, L., and Riess, O. (1998). Ala30Pro mutation in the gene encoding alpha-synuclein in Parkinson's disease. In *Nat Genet*, pp. 106-108.
- Lang, T., and Jahn, R. (2008). Core proteins of the secretory machinery. In *Handb Exp Pharmacol*, pp. 107-127.
- Leal-Ortiz, S., Waites, C.L., Terry-Lorenzo, R., Zamorano, P., Gundelfinger, E.D., and Garner, C.C. (2008). Piccolo modulation of Synapsin1a dynamics regulates synaptic vesicle exocytosis. In *J Cell Biol*, pp. 831-846.
- Li, L., and Chin, L.S. (2003). The molecular machinery of synaptic vesicle exocytosis. *Cell Mol Life Sci* 60, 942-960.
- Liang, F., Zhang, B., Tang, J., Guo, J., Li, W., Ling, E.A., Chu, H., Wu, Y., Chan, Y.G., and Cao, Q. (2007). RIM3 gamma is a postsynaptic protein in the rat central nervous system. In *J Comp Neurol*, pp. 501-510.
- Lonart, G., Schoch, S., Kaeser, P.S., Larkin, C.J., Südhof, T.C., and Linden, D.J. (2003). Phosphorylation of RIM1alpha by PKA triggers presynaptic long-term potentiation at cerebellar parallel fiber synapses. In *Cell*, pp. 49-60.
- Lu, J., Li, H., Wang, Y., Südhof, T.C., and Rizo, J. (2005). Solution structure of the RIM1alpha PDZ domain in complex with an ELKS1b C-terminal peptide. *J Mol Biol* 352, 455-466.
- Lu, J., Machius, M., Dulubova, I., Dai, H., Südhof, T.C., Tomchick, D.R., and Rizo, J. (2006). Structural basis for a Munc13-1 homodimer to Munc13-1/RIM heterodimer switch. In *PLoS Biol*, p. e192.
- Lynch, B.A., Lambeng, N., Nocka, K., Kensel-Hammes, P., Bajjalieh, S.M., Matagne, A., and Fuks, B. (2004). The synaptic vesicle protein SV2A is the

binding site for the antiepileptic drug levetiracetam. In *P Natl Acad Sci Usa*, pp. 9861-9866.

Maloney, D.G., Liles, T.M., Czerwinski, D.K., Waldichuk, C., Rosenberg, J., Grillo-Lopez, A., and Levy, R. (1994). Phase I clinical trial using escalating single-dose infusion of chimeric anti-CD20 monoclonal antibody (IDEC-C2B8) in patients with recurrent B-cell lymphoma. In *Blood*, pp. 2457-2466.

Malsam, J., Kreye, S., and Söllner, T.H. (2008). Membrane fusion: SNAREs and regulation. In *Cell Mol Life Sci*, pp. 2814-2832.

Maruyama, I.N., and Brenner, S. (1991). A phorbol ester/diacylglycerol-binding protein encoded by the *unc-13* gene of *Caenorhabditis elegans*. In *P Natl Acad Sci Usa*, pp. 5729-5733.

Maximov, A., Tang, J., Yang, X., Pang, Z.P., and Südhof, T.C. (2009). Complexin controls the force transfer from SNARE complexes to membranes in fusion. In *Science*, pp. 516-521.

McBain, C.J., and Kauer, J.A. (2009). Presynaptic plasticity: targeted control of inhibitory networks. In *Curr Opin Neurobiol*, pp. 254-262.

Michaelides, M., Holder, G.E., Hunt, D.M., Fitzke, F.W., Bird, A.C., and Moore, A.T. (2005). A detailed study of the phenotype of an autosomal dominant cone-rod dystrophy (CORD7) associated with mutation in the gene for RIM1. *The British journal of ophthalmology* *89*, 198-206.

Miller, F.D., and Kaplan, D.R. (2003). Signaling mechanisms underlying dendrite formation. In *Curr Opin Neurobiol*, pp. 391-398.

Miller, K.E., DeProto, J., Kaufmann, N., Patel, B.N., Duckworth, A., and Van Vactor, D. (2005). Direct observation demonstrates that Liprin-alpha is required for trafficking of synaptic vesicles. In *Curr Biol*, pp. 684-689.

Misura, K.M., Scheller, R.H., and Weis, W.I. (2000). Three-dimensional structure of the neuronal-Sec1-syntaxin 1a complex. In *Nature*, pp. 355-362.

Mittelsteadt, T., Seifert, G., Alvarez-Baron, E., Steinhaeuser, C., Becker, A.J., and Schoch, S. (2009). Differential mRNA Expression Patterns of the Synaptotagmin Gene Family in the Rodent Brain. *J Comp Neurol* *512*, 514-528.

Monyer, H., and Markram, H. (2004). Interneuron Diversity series: Molecular and genetic tools to study GABAergic interneuron diversity and function. In *Trends Neurosci*, pp. 90-97.

Nonet, M.L., Staunton, J.E., Kilgard, M.P., Fergestad, T., Hartwig, E., Horvitz, H.R., Jorgensen, E.M., and Meyer, B.J. (1997). *Caenorhabditis elegans* rab-3 mutant synapses exhibit impaired function and are partially depleted of vesicles. *J Neurosci* *17*, 8061-8073.

- Ohtsuka, T., Takao-Rikitsu, E., Inoue, E., Inoue, M., Takeuchi, M., Matsubara, K., Deguchi-Tawarada, M., Satoh, K., Morimoto, K., Nakanishi, H., and Takai, Y. (2002). Cast: a novel protein of the cytomatrix at the active zone of synapses that forms a ternary complex with RIM1 and munc13-1. *J Cell Biol* 158, 577-590.
- Okada, Y., Yamazaki, H., Sekine-Aizawa, Y., and Hirokawa, N. (1995). The neuron-specific kinesin superfamily protein KIF1A is a unique monomeric motor for anterograde axonal transport of synaptic vesicle precursors. In *Cell*, pp. 769-780.
- Olsen, O., Moore, K.A., Fukata, M., Kazuta, T., Trinidad, J.C., Kauer, F.W., Streuli, M., Misawa, H., Burlingame, A.L., Nicoll, R.A., and Brecht, D.S. (2005). Neurotransmitter release regulated by a MALS-liprin-alpha presynaptic complex. In *J Cell Biol*, pp. 1127-1134.
- Orita, S., Naito, A., Sakaguchi, G., Maeda, M., Igarashi, H., Sasaki, T., and Takai, Y. (1997). Physical and functional interactions of Doc2 and Munc13 in Ca²⁺-dependent exocytotic machinery. *J Biol Chem* 272, 16081-16084.
- Orita, S., Sasaki, T., Naito, A., Komuro, R., Ohtsuka, T., Maeda, M., Suzuki, H., Igarashi, H., and Takai, Y. (1995). Doc2: a novel brain protein having two repeated C2-like domains. In *Biochem Biophys Res Commun*, pp. 439-448.
- Ozaki, N., Shibasaki, T., Kashima, Y., Miki, T., Takahashi, K., Ueno, H., Sunaga, Y., Yano, H., Matsuura, Y., Iwanaga, T., *et al.* (2000). cAMP-GEFII is a direct target of cAMP in regulated exocytosis. In *Nat Cell Biol*, pp. 805-811.
- Parker, J.M., Guo, D., and Hodges, R.S. (1986). New hydrophilicity scale derived from high-performance liquid chromatography peptide retention data: correlation of predicted surface residues with antigenicity and X-ray-derived accessible sites. In *Biochemistry*, pp. 5425-5432.
- Parsons, T.D., and Sterling, P. (2003). Synaptic ribbon. Conveyor belt or safety belt? In *Neuron*, pp. 379-382.
- Patel, M.R., and Shen, K. (2009). RSY-1 is a local inhibitor of presynaptic assembly in *C. elegans*. In *Science*, pp. 1500-1503.
- Paxinos, G. (2004). The rat nervous system - Page 643. p. 1309.
- Phillips, G.R., Huang, J.K., Wang, Y., Tanaka, H., Shapiro, L., Zhang, W., Shan, W.S., Arndt, K., Frank, M., Gordon, R.E., *et al.* (2001). The presynaptic particle web: ultrastructure, composition, dissolution, and reconstitution. In *Neuron*, pp. 63-77.
- Pilpel, N., Landeck, N., Klugmann, M., Seeburg, P.H., and Schwarz, M.K. (2009). Rapid, reproducible transduction of select forebrain regions by targeted

- recombinant virus injection into the neonatal mouse brain. In *J Neurosci Methods*, pp. 55-63.
- Poulain, F., and Sobel, A. (2009). The microtubule network and neuronal morphogenesis: Dynamic and coordinated orchestration through multiple players. In *Mol Cell Neurosci*.
- Powell, C.M., Schoch, S., Monteggia, L., Barrot, M., Matos, M.F., Feldmann, N., Südhof, T.C., and Nestler, E.J. (2004). The presynaptic active zone protein RIM1alpha is critical for normal learning and memory. *Neuron* 42, 143-153.
- Rao, D.D., Vorhies, J.S., Senzer, N., and Nemunaitis, J. (2009). siRNA vs. shRNA: similarities and differences. In *Advanced Drug Delivery Reviews*, pp. 746-759.
- Richmond, J.E., Weimer, R.M., and Jorgensen, E.M. (2001). An open form of syntaxin bypasses the requirement for UNC-13 in vesicle priming. In *Nature*, pp. 338-341.
- Rickman, C., and Duncan, R. (2009). MUNC18/syntaxin interaction kinetics control secretory vesicle dynamics. In *J Biol Chem*.
- Rizo, J., and Rosenmund, C. (2008). Synaptic vesicle fusion. *Nat Struct Mol Biol* 15, 665-674.
- Rizo, J., and Südhof, T.C. (2002). Snares and Munc18 in synaptic vesicle fusion. *Nat Rev Neurosci* 3, 641-653.
- Rocca, D.L., Martin, S., Jenkins, E.L., and Hanley, J.G. (2008). Inhibition of Arp2/3-mediated actin polymerization by PICK1 regulates neuronal morphology and AMPA receptor endocytosis. In *Nat Cell Biol*, pp. 259-271.
- Rodkey, T.L., Liu, S., Barry, M., and McNew, J.A. (2008). Munc18a scaffolds SNARE assembly to promote membrane fusion. *Mol Biol Cell* 19, 5422-5434.
- Rogers, S.W., Andrews, P.I., Gahring, L.C., Whisenand, T., Cauley, K., Crain, B., Hughes, T.E., Heinemann, S.F., and McNamara, J.O. (1994). Autoantibodies to glutamate receptor GluR3 in Rasmussen's encephalitis. *Science* 265, 648-651.
- Rosenmund, C., Rettig, J., and Brose, N. (2003). Molecular mechanisms of active zone function. *Curr Opin Neurobiol* 13, 509-519.
- Rosenmund, C., Sigler, A., Augustin, I., Reim, K., Brose, N., and Rhee, J.S. (2002). Differential control of vesicle priming and short-term plasticity by Munc13 isoforms. *Neuron* 33, 411-424.
- Schaub, J.R., Lu, X., Doneske, B., Shin, Y.-K., and McNew, J.A. (2006). Hemifusion arrest by complexin is relieved by Ca²⁺-synaptotagmin I. In *Nat Struct Mol Biol*, pp. 748-750.

- Schlüter, O.M., Schmitz, F., Jahn, R., Rosenmund, C., and Südhof, T.C. (2004). A complete genetic analysis of neuronal Rab3 function. *J Neurosci* *24*, 6629-6637.
- Schoch, S., Castillo, P.E., Jo, T., Mukherjee, K., Geppert, M., Wang, Y., Schmitz, F., Malenka, R.C., and Südhof, T.C. (2002). RIM1alpha forms a protein scaffold for regulating neurotransmitter release at the active zone. In *Nature*, pp. 321-326.
- Schoch, S., Deák, F., Königstorfer, A., Mozhayeva, M., Sara, Y., Südhof, T.C., and Kavalali, E.T. (2001). SNARE function analyzed in synaptobrevin/VAMP knockout mice. *Science* *294*, 1117-1122.
- Schoch, S., and Gundelfinger, E.D. (2006). Molecular organization of the presynaptic active zone. *Cell Tissue Res* *326*, 379-391.
- Schoch, S., Mittelstaedt, T., Kaeser, P.S., Padgett, D., Feldmann, N., Chevaleyre, V., Castillo, P.E., Hammer, R.E., Han, W., Schmitz, F., *et al.* (2006). Redundant functions of RIM1alpha and RIM2alpha in Ca(2+)-triggered neurotransmitter release. *EMBO J* *25*, 5852-5863.
- Schratt, G.M., Tuebing, F., Nigh, E.A., Kane, C.G., Sabatini, M.E., Kiebler, M., and Greenberg, M.E. (2006). A brain-specific microRNA regulates dendritic spine development. In *Nature*, pp. 283-289.
- Segura, I., Essmann, C.L., Weinges, S., and Acker-Palmer, A. (2007). Grb4 and GIT1 transduce ephrinB reverse signals modulating spine morphogenesis and synapse formation. In *Nat Neurosci*, pp. 301-310.
- Serra-Pagès, C., Medley, Q.G., Tang, M., Hart, A., and Streuli, M. (1998). Liprins, a family of LAR transmembrane protein-tyrosine phosphatase-interacting proteins. *J Biol Chem* *273*, 15611-15620.
- Shankar, G.M., and Walsh, D.M. (2009). Alzheimer's disease: synaptic dysfunction and Abeta. In *Mol Neurodegener*, p. 48.
- Shapira, M., Zhai, R.G., Dresbach, T., Bresler, T., Torres, V.I., Gundelfinger, E.D., Ziv, N.E., and Garner, C.C. (2003). Unitary assembly of presynaptic active zones from Piccolo-Bassoon transport vesicles. *Neuron* *38*, 237-252.
- Shibasaki, T., Sunaga, Y., Fujimoto, K., Kashima, Y., and Seino, S. (2004). Interaction of ATP sensor, cAMP sensor, Ca²⁺ sensor, and voltage-dependent Ca²⁺ channel in insulin granule exocytosis. In *J Biol Chem*, pp. 7956-7961.
- Shin, H., Wyszynski, M., Huh, K.-H., Valtschanoff, J.G., Lee, J.-R., Ko, J., Streuli, M., Weinberg, R.J., Sheng, M., and Kim, E. (2003). Association of the kinesin motor KIF1A with the multimodular protein liprin-alpha. In *J Biol Chem*, pp. 11393-11401.

- Siksou, L., Rostaing, P., Lechaire, J.P., Boudier, T., Ohtsuka, T., Fejtová, A., Kao, H.T., Greengard, P., Gundelfinger, E.D., Triller, A., and Marty, S. (2007). Three-dimensional architecture of presynaptic terminal cytomatrix. *J Neurosci* 27, 6868-6877.
- Simsek-Duran, F., Linden, D.J., and Lonart, G. (2004). Adapter protein 14-3-3 is required for a presynaptic form of LTP in the cerebellum. In *Nat Neurosci*, pp. 1296-1298.
- Song, J.Y., Ichtchenko, K., Südhof, T.C., and Brose, N. (1999). Neuroligin 1 is a postsynaptic cell-adhesion molecule of excitatory synapses. In *P Natl Acad Sci Usa*, pp. 1100-1105.
- Sørensen, J.B., Matti, U., Wei, S.-H., Nehring, R.B., Voets, T., Ashery, U., Binz, T., Neher, E., and Rettig, J. (2002). The SNARE protein SNAP-25 is linked to fast calcium triggering of exocytosis. In *P Natl Acad Sci Usa*, pp. 1627-1632.
- Spangler, S.A., and Hoogenraad, C.C. (2007). Liprin-alpha proteins: scaffold molecules for synapse maturation. *Biochem Soc Trans* 35, 1278-1282.
- Sterling, P., and Matthews, G. (2005). Structure and function of ribbon synapses. In *Trends Neurosci*, pp. 20-29.
- Stettler, O., Moya, K.L., Zahraoui, A., and Tavitian, B. (1994). Developmental changes in the localization of the synaptic vesicle protein rab3A in rat brain. In *Neuroscience*, pp. 587-600.
- Stevens, C.F. (2003). Neurotransmitter release at central synapses. In *Neuron*, pp. 381-388.
- Stryker, E., and Johnson, K.G. (2007). LAR, liprin alpha and the regulation of active zone morphogenesis. In *J Cell Sci*, pp. 3723-3728.
- Südhof, T.a.S., Klaus (2008a). Pharmacology of neurotransmitter release. p. 582.
- Südhof, T.C. (2002). Synaptotagmins: why so many? In *J Biol Chem*, pp. 7629-7632.
- Südhof, T.C. (2004). The synaptic vesicle cycle. *Annu Rev Neurosci*.
- Südhof, T.C. (2008b). Neuroligins and neurexins link synaptic function to cognitive disease. In *Nature*, pp. 903-911.
- Südhof, T.C., and Rothman, J.E. (2009). Membrane fusion: grappling with SNARE and SM proteins. In *Science*, pp. 474-477.
- Sun, L., Bittner, M.A., and Holz, R.W. (2003). Rim, a component of the presynaptic active zone and modulator of exocytosis, binds 14-3-3 through its N terminus. *J Biol Chem* 278, 38301-38309.

- Tai, H.-C., and Schuman, E.M. (2008). Ubiquitin, the proteasome and protein degradation in neuronal function and dysfunction. In *Nat Rev Neurosci*, pp. 826-838.
- Takao-Rikitsu, E., Mochida, S., Inoue, E., Deguchi-Tawarada, M., Inoue, M., Ohtsuka, T., and Takai, Y. (2004). Physical and functional interaction of the active zone proteins, CAST, RIM1, and Bassoon, in neurotransmitter release. *J Cell Biol* 164, 301-311.
- Tang, B.L. (2008). Emerging aspects of membrane traffic in neuronal dendrite growth. In *Biochim Biophys Acta*, pp. 169-176.
- Tang, J., Maximov, A., Shin, O.-H., Dai, H., Rizo, J., and Südhof, T.C. (2006). A complexin/synaptotagmin 1 switch controls fast synaptic vesicle exocytosis. In *Cell*, pp. 1175-1187.
- Terada, S., Tsujimoto, T., Takei, Y., Takahashi, T., and Hirokawa, N. (1999). Impairment of inhibitory synaptic transmission in mice lacking synapsin I. In *J Cell Biol*, pp. 1039-1048.
- Thilo, B., Stingele, R., Knudsen, K., Boor, R., Bien, C.G., Deuschl, G., and Lang, N. (2009). A case of Rasmussen encephalitis treated with rituximab. In *Nat Rev Neurol*, pp. 458-462.
- tom Dieck, S., Altroch, W.D., Kessels, M.M., Qualmann, B., Regus, H., Brauner, D., Fejtová, A., Bracko, O., Gundelfinger, E.D., and Brandstätter, J.H. (2005). Molecular dissection of the photoreceptor ribbon synapse: physical interaction of Bassoon and RIBEYE is essential for the assembly of the ribbon complex. *J Cell Biol* 168, 825-836.
- tom Dieck, S., and Brandstätter, J.H. (2006). Ribbon synapses of the retina. *Cell Tissue Res* 326, 339-346.
- tom Dieck, S., Sanmartí-Vila, L., Langnaese, K., Richter, K., Kindler, S., Soyke, A., Wex, H., Smalla, K.H., Kämpf, U., Fränzer, J.T., *et al.* (1998). Bassoon, a novel zinc-finger CAG/glutamine-repeat protein selectively localized at the active zone of presynaptic nerve terminals. In *J Cell Biol*, pp. 499-509.
- Varoqueaux, F., Sigler, A., Rhee, J.S., Brose, N., Enk, C., Reim, K., and Rosenmund, C. (2002). Total arrest of spontaneous and evoked synaptic transmission but normal synaptogenesis in the absence of Munc13-mediated vesicle priming. *P Natl Acad Sci Usa* 99, 9037-9042.
- Verhage, M., Maia, A.S., Plomp, J.J., Brussaard, A.B., Heeroma, J.H., Vermeer, H., Toonen, R.F., Hammer, R.E., van den Berg, T.K., Missler, M., *et al.* (2000). Synaptic assembly of the brain in the absence of neurotransmitter secretion. *Science* 287, 864-869.

- Wagh, D.A., Rasse, T.M., Asan, E., Hofbauer, A., Schwenkert, I., Dürrbeck, H., Buchner, S., Dabauvalle, M.C., Schmidt, M., Qin, G., *et al.* (2006). Bruchpilot, a protein with homology to ELKS/CAST, is required for structural integrity and function of synaptic active zones in *Drosophila*. *Neuron* *49*, 833-844.
- Wang, X., Hu, B., Zimmermann, B., and Kilimann, M.W. (2001). Rim1 and rabphilin-3 bind Rab3-GTP by composite determinants partially related through N-terminal alpha-helix motifs. *J Biol Chem* *276*, 32480-32488.
- Wang, Y., Liu, X., Biederer, T., and Südhof, T.C. (2002). A family of RIM-binding proteins regulated by alternative splicing: Implications for the genesis of synaptic active zones. *P Natl Acad Sci Usa* *99*, 14464-14469.
- Wang, Y., Okamoto, M., Schmitz, F., Hofmann, K., and Südhof, T.C. (1997). Rim is a putative Rab3 effector in regulating synaptic-vesicle fusion. *Nature* *388*, 593-598.
- Wang, Y., and Südhof, T.C. (2003). Genomic definition of RIM proteins: evolutionary amplification of a family of synaptic regulatory proteins(small star, filled). *Genomics* *81*, 126-137.
- Wang, Y., Sugita, S., and Südhof, T.C. (2000). The RIM/NIM Family of Neuronal C2 Domain Proteins. In *P Natl Acad Sci Usa*, pp. 20033-20044.
- Washbourne, P., Thompson, P.M., Carta, M., Costa, E.T., Mathews, J.R., Lopez-Bendito, G., Molnár, Z., Becher, M.W., Valenzuela, C.F., Partridge, L.D., and Wilson, M.C. (2002). Genetic ablation of the t-SNARE SNAP-25 distinguishes mechanisms of neuroexocytosis. In *Nat Neurosci*, pp. 19-26.
- Watson, R., Jiang, Y., Bermudez, I., Houlihan, L., Clover, L., McKnight, K., Cross, J.H., Hart, I.K., Roubertie, A., Valmier, J., *et al.* (2004). Absence of antibodies to glutamate receptor type 3 (GluR3) in Rasmussen encephalitis. In *Neurology*, pp. 43-50.
- Weidenhofer, J., Bowden, N.A., Scott, R.J., and Tooney, P.A. (2006). Altered gene expression in the amygdala in schizophrenia: up-regulation of genes located in the cytomatrix active zone. In *Mol Cell Neurosci*, pp. 243-250.
- Weidenhofer, J., Scott, R.J., and Tooney, P.A. (2009). Investigation of the expression of genes affecting cytomatrix active zone function in the amygdala in schizophrenia: effects of antipsychotic drugs. In *Journal of psychiatric research*, pp. 282-290.
- Weimer, R.M., Gracheva, E.O., Meyrignac, O., Miller, K.G., Richmond, J.E., and Bessereau, J.-L. (2006). UNC-13 and UNC-10/rim localize synaptic vesicles to specific membrane domains. In *J Neurosci*, pp. 8040-8047.
- Wiendl, H., Bien, C.G., Bernasconi, P., Fleckenstein, B., Elger, C.E., Dichgans, J., Mantegazza, R., and Melms, A. (2001). GluR3 antibodies: prevalence in

focal epilepsy but no specificity for Rasmussen's encephalitis. In *Neurology*, pp. 1511-1514.

Wigge, P., Köhler, K., Vallis, Y., Doyle, C.A., Owen, D., Hunt, S.P., and McMahon, H.T. (1997). Amphiphysin heterodimers: potential role in clathrin-mediated endocytosis. In *Mol Biol Cell*, pp. 2003-2015.

Wyszynski, M., Kim, E., Dunah, A.W., Passafaro, M., Valtschanoff, J.G., Serra-Pagès, C., Streuli, M., Weinberg, R.J., and Sheng, M. (2002). Interaction between GRIP and liprin-alpha/SYD2 is required for AMPA receptor targeting. In *Neuron*, pp. 39-52.

Xiao, Z., Gong, Y., Wang, X.-F., Xiao, F., Xi, Z.-Q., Lu, Y., and Sun, H.-B. (2009). Altered expression of synaptotagmin I in temporal lobe tissue of patients with refractory epilepsy. In *J Mol Neurosci*, pp. 193-200.

Xue, M., Reim, K., Chen, X., Chao, H.-T., Deng, H., Rizo, J., Brose, N., and Rosenmund, C. (2007). Distinct domains of complexin I differentially regulate neurotransmitter release. In *Nat Struct Mol Biol*, pp. 949-958.

Yamada, M., Saisu, H., Ishizuka, T., Takahashi, H., and Abe, T. (1999). Immunohistochemical distribution of the two isoforms of synaphin/complexin involved in neurotransmitter release: localization at the distinct central nervous system regions and synaptic types. In *Neuroscience*, pp. 7-18.

Yang, R., Puranam, R.S., Butler, L.S., Qian, W.H., He, X.P., Moyer, M.B., Blackburn, K., Andrews, P.I., and McNamara, J.O. (2000). Autoimmunity to munc-18 in Rasmussen's encephalitis. In *Neuron*, pp. 375-383.

Yao, I., Takagi, H., Ageta, H., Kahyo, T., Sato, S., Hatanaka, K., Fukuda, Y., Chiba, T., Morone, N., Yuasa, S., *et al.* (2007). SCRAPPER-dependent ubiquitination of active zone protein RIM1 regulates synaptic vesicle release. *Cell* *130*, 943-957.

Yoon, T.-Y., Lu, X., Diao, J., Lee, S.-M., Ha, T., and Shin, Y.-K. (2008). Complexin and Ca²⁺ stimulate SNARE-mediated membrane fusion. In *Nat Struct Mol Biol*, pp. 707-713.

Zampighi, G.A., Fain, N., Zampighi, L.M., Cantele, F., Lanzavecchia, S., and Wright, E.M. (2008). Conical Electron Tomography of a Chemical Synapse: Polyhedral Cages Dock Vesicles to the Active Zone. *Journal of Neuroscience* *28*, 4151.

Zhai, R.G., and Bellen, H.J. (2004). The architecture of the active zone in the presynaptic nerve terminal. *Physiology (Bethesda, Md)* *19*, 262-270.

Zhai, R.G., Vardinon-Friedman, H., Cases-Langhoff, C., Becker, B., Gundelfinger, E.D., Ziv, N.E., and Garner, C.C. (2001). Assembling the

presynaptic active zone: a characterization of an active one precursor vesicle. *Neuron* 29, 131-143.

Zhen, M., and Jin, Y. (1999). The liprin protein SYD-2 regulates the differentiation of presynaptic termini in *C. elegans*. In *Nature*, pp. 371-375.

Zilly, F.E., Sørensen, J.B., Jahn, R., and Lang, T. (2006). Munc18-bound syntaxin readily forms SNARE complexes with synaptobrevin in native plasma membranes. In *PLoS Biol*, p. e330.

Ziv, N.E., and Garner, C.C. (2004). Cellular and molecular mechanisms of presynaptic assembly. *Nat Rev Neurosci* 5, 385-399.

Zürner, M., and Schoch, S. (2008). The mouse and human Liprin-alpha family of scaffolding proteins: Genomic organization, expression profiling and regulation by alternative splicing. *Genomics*.

10 LIST OF FIGURES

| | |
|---|----|
| <i>Fig. 1.1 Electron micrograph of a synapse</i> | 2 |
| <i>Fig. 1.2 The synaptic vesicle cycle</i> | 3 |
| <i>Fig. 1.3 Models of Active Zone ultrastructure</i> | 6 |
| <i>Fig. 1.4 Components of the “core machinery” for synaptic vesicle fusion and of the “cytomatrix at the Active Zone”</i> | 11 |
| <i>Fig. 1.5 Alternatively spliced exons in RIM1α and RIM2α.</i> | 21 |
| <i>Fig. 1.6 Domain structure of the RIM protein family</i> | 22 |
| <i>Fig. 1.7 Interacting molecules of α-RIMs</i> | 25 |
| <i>Fig. 1.8. Direct and indirect proteins interaction of RIM1α at the Active Zone</i> | 30 |
| <i>Fig. 3.1 TOPO TA cloning vector (Invitrogen)</i> | 49 |
| <i>Fig. 3.2 pCDNA 3.1 CT-GFP TOPO vector (Invitrogen)</i> | 50 |
| <i>Fig. 3.3 pCDNA 3.1 NT-GFP TOPO vector (Invitrogen)</i> | 51 |
| <i>Fig. 3.4 pCMV5 vector (T.S Lab)</i> | 52 |
| <i>Fig. 3.5 pCDNA 3.1 vector (Invitrogen)</i> | 53 |
| <i>Fig. 3.6 pL26 vector (M.Schwarz Lab)</i> | 54 |
| <i>Fig. 3.7 pLVTHM vector (Trono Lab)</i> | 55 |
| <i>Fig. 3.8 pLentiLN-EGFP-EF1α plasmid (Trono Lab)</i> | 56 |
| <i>Fig. 3.9 psPAX2 packaging plasmid second generation (Trono Lab)</i> | 57 |
| <i>Fig. 3.10 pMD2.G envelope plasmid second generation (Trono Lab)</i> | 58 |
| <i>Fig. 4.1 Cloning strategy for pcDNA3.1 and pL26 vectors</i> | 71 |
| <i>Fig. 4.2 Schematic depiction of the overexpression plasmids</i> | 71 |
| <i>Fig. 4.3 Structural organization of lentiviral shRNA constructs</i> | 72 |
| <i>Fig. 4.4 Schematic depiction of the injection of lentiviral particles in the ventricle and Hippocampus</i> | 83 |
| <i>Fig. 5.1 Localization of RIM3γ mRNA in adult rat brain</i> | 86 |
| <i>Fig. 5.2 Localization of RIM4γ mRNA in adult rat brain</i> | 87 |
| <i>Fig. 5.3 Specificity of newly generated RIM3γ and RIM4γ antibodies</i> | 88 |
| <i>Fig. 5.4 γ-RIMs are brain specific proteins</i> | 89 |
| <i>Fig. 5.5 RIM3γ and RIM4γ expression in different brain regions</i> | 90 |

| | |
|--|-----|
| <i>Fig. 5.6 RIM3γ and RIM4γ expression levels increase during synaptogenesis</i> | 91 |
| <i>Fig. 5.7 Subcellular fractionation of rat synaptosomes</i> | 93 |
| <i>Fig. 5.8 Immunohistochemical analysis of RIM3γ in rat brain</i> | 95 |
| <i>Fig. 5.9 Immunohistochemical analysis of RIM4γ in rat brain</i> | 96 |
| <i>Fig. 5.10 Synaptic localization of RIM3γ in cortical primary neurons</i> | 98 |
| <i>Fig. 5.11 Localization of RIM4γ in cortical primary neurons</i> | 99 |
| <i>Fig. 5.12 RIM3γ and RIM4γ localization in the retina</i> | 100 |
| <i>Fig. 5.13 Colocalization of γ-RIMs with the presynaptic ribbon protein CtBP2/RIBEYE</i> | 101 |
| <i>Fig. 5.14 RIM3γ and RIM4γ colocalized with different inhibitory markers in cerebellar cells</i> | 103 |
| <i>Fig. 5.15 γ-RIMs are present in hippocampal interneurons</i> | 104 |
| <i>Fig. 5.16 Both γ-RIMs are present in the Parvalbumin positive cell population in the superior colliculus</i> | 105 |
| <i>Fig. 5.17 Subcellular distribution of RIM3γ and RIM4γ GFP fusion proteins in PC12 cells</i> | 107 |
| <i>Fig. 5.18 Localization of different Liprin-α isoforms in PC12 cells</i> | 107 |
| <i>Fig. 5.19 Effect of liprin-α proteins on the subcellular localization of γ-RIMs and RIM1α</i> | 109 |
| <i>Fig. 5.20 RIM3γ and RIM4γ protein alignment</i> | 111 |
| <i>Fig. 5.21 Western blot analysis of RIM3γ and RIM4γ GFP fusion proteins</i> | 112 |
| <i>Fig. 5.22 Subcellular localization of the truncated GFP-γ-RIM fusion proteins in PC12 cells</i> | 113 |
| <i>Fig. 5.23 Co-expression of GFP- RIM3γ truncated proteins and Liprin-α3 in PC12 cells</i> | 115 |
| <i>Fig. 5.24 Co-expression of GFP-RIM4γ truncated proteins and Liprin-α3 in PC12 cells</i> | 116 |
| <i>Fig. 5.25 Overexpression of fluorescently tagged RIM3γ and RIM4γ in primary hippocampal neurons</i> | 118 |
| <i>Fig. 5.26 Axonal localization of GFP-γ-RIMs truncated proteins</i> | 120 |
| <i>Fig. 5.27 GFP-RIM3γ truncated proteins are present in dendrites</i> | 121 |
| <i>Fig. 5.28 GFP-RIMγ truncated proteins are present in dendrites</i> | 122 |
| <i>Fig. 5.29 Overexpression of Liprin-α2, -α3 does not affect localization of γ-RIMs in cultured neurons</i> | 124 |
| <i>Fig. 5.30 Colocalization analysis of γ-RIMs and RIM1α in primary neurons</i> | 125 |
| <i>Fig. 5.31 GFP-RIM3γ truncated proteins colocalize with RIM1α at the synapses</i> | 127 |
| <i>Fig. 5.32 GFP-RIM4γ truncated proteins colocalize with RIM1α at the synapses</i> | 128 |
| <i>Fig. 5.33 RIM3 shRNAs efficiently reduce overexpressed RIM3γ protein levels in HEK 293T cells</i> | 130 |
| <i>Fig. 5.34 RIM4γ shRNAs efficiently reduce overexpressed RIM4γ protein levels in HEK 293T cells</i> | 131 |

| | |
|---|-----|
| <i>Fig. 5.35 RIM3γ and RIM4γ shRNAs are isoform-specific</i> | 132 |
| <i>Fig. 5.36 shRNA effect on endogenous RIM3γ and RIM4γ protein expression</i> | 133 |
| <i>Fig. 5.37 Quantification of RIM3γ and RIM4γ shRNA mediated downregulation in primary cell neurons</i> | 134 |
| <i>Fig. 5.38 Knockdown of RIM3γ and RIM4γ results in alteration of neuronal morphology</i> | 136 |
| <i>Fig. 5.39 Quantification of neuronal branching by Sholl analysis</i> | 137 |
| <i>Fig. 5.40 In vivo knockdown of RIM3γ and RIM4γ at P7</i> | 140 |
| <i>Fig. 5.41 In vivo knockdown of RIM3γ and RIM4γ at P14</i> | 141 |
| <i>Fig. 5.42 In vivo knockdown of RIM3γ and RIM4γ at P21</i> | 142 |
| <i>Fig. 5.43 In vivo knockdown of RIM3γ and RIM4γ at P21</i> | 143 |
| <i>Fig. 5.44 shRNAs with nucleotide exchanges are unable to change RIM3γ and RIM4γ expression levels</i> | 144 |
| <i>Fig. 5.45 RIM3γ and RIM4γ shRNA rescue experiments</i> | 146 |
| <i>Fig. 5.46 Development of neuronal processes in neurons deficient for RIM3γ or RIM4γ</i> | 147 |
| <i>Fig. 5.47 Downregulation of RIM3γ or RIM4γ results in a decrease in endogenous RIM1α levels</i> | 148 |
| <i>Fig. 5.48 RIM3γ and RIM4γ shRNAs did not alter RIM1α overexpression levels</i> | 149 |
| <i>Fig. 5.49 Downregulation of RIM3γ results in a reduction of the expression levels of several proteins</i> | 151 |
| <i>Fig. 5.50 Reduction of GRIP1 expression levels in neurons deficient in RIM3γ</i> | 152 |
| <i>Fig. 5.51 RIM3γ and RIM4γ knockdown in neurons lead to a reduction of the mEPSC amplitude, without affecting the frequency</i> | 153 |
| <i>Fig. 5.52 Immunoreactivity of sera of biopsy-proven RE patients</i> | 156 |
| <i>Fig. 6.1 Several possible modes of action for γ-RIMs</i> | 162 |
| <i>Fig. 6.2 RIM3γ and RIM4γ localization in the neuron</i> | 176 |
| <i>Fig. 6.3 Possible mechanisms underlying the loss of dendrites</i> | 184 |

11 LIST OF TABLES

| | |
|---|-----|
| <i>Table 3.1 Lab equipment</i> | 41 |
| <i>Table 3.2 Chemicals</i> | 42 |
| <i>Table 3.3 Commercial kits</i> | 43 |
| <i>Table 3.4 Cell culture media and solutions</i> | 43 |
| <i>Table 3.5 Primary antibodies</i> | 44 |
| <i>Table 3.6 Secondary antibodies</i> | 45 |
| <i>Table 3.7 Primer for sequencing</i> | 45 |
| <i>Table 3.8 In situ hybridization probe sequences</i> | 45 |
| <i>Table 3.9 Primers used for DNA amplification</i> | 48 |
| <i>Table 5.1 Properties of the various GFP γ-RIMs deletion constructs</i> | 110 |
| <i>Table 5.2 Summary clinical data</i> | 159 |

12 ABBREVIATIONS

| Abbreviation | Full name |
|--------------|--|
| AB | Antibody |
| AMPA | α -amino-3-hydroxy-5-methyl-4-isoxazolepropionic acid |
| AMPAR | AMPA receptor |
| ATP | Adenosine tri-phosphate |
| AZ | Active Zone |
| BRP | Bruchpilot |
| cAMP | Cyclic adenosine-3,5-monophosphate |
| CAZ | Cytomatrix at the active zone |
| CB | Cerebellum |
| CC | Coiled-coil domain |
| cDNA | Complementary DNA |
| CSP α | Cysteine string protein α |
| CtBP | C-terminal Binding Protein |
| C-terminus | Carboxyl terminus |
| CTX | Cortex |
| DAB | 3,3'-Diaminobenzidine |
| DAG | diacylglycerol |
| dATP | Deoxyadenosine triphosphate |
| DEPC | Diethyl pyrocarbonate |
| DG | Dentate gyrus |
| DIV | Day in vitro |
| DKO | Double knockout |
| DMSO | Dimethyl sulfoxide |
| DNA | Deoxyribonucleic acid |
| dNTP | Deoxyribonucleotide triphosphate |
| E18,5 | Embryo at day 18.5 after fertilization |
| EDTA | Ethylenediaminetetraacetic acid |
| EGFP | Enhanced green fluorescent protein |
| EM | Electron microscopy |
| EPL | External plexiform layer |
| FW | Forward |
| GABA | γ -aminobutyric acid |
| GAD | Glutamic acid decarboxylase |

| | |
|------------|---|
| GC | Cerebellar granule cell layer |
| GEFII | Guanine nucleotide-exchange factor II |
| GFP | Green fluorescent protein |
| GIT1 | G protein-coupled receptor kinase-interacting protein 1 |
| GL | Glomerular layer |
| GRIP1 | Glutamate receptor-interacting protein 1 |
| GRL | Granule cell layer |
| GTPase | Guanosine triphosphatase |
| h | Hour |
| HBSS | Hank's Balanced Salt Solution |
| HC | Hippocampus |
| IR | infrared |
| ISH | <i>In situ</i> hybridization |
| Kb | Kilo base |
| kDa | Kilo Dalton |
| KIF1A | Kinesin family member 1A |
| KO | Knockout |
| l | Liter |
| LAR | Leukocyte common antigen-related |
| LB-medium | Luria broth medium |
| LH | Liprin homology domain |
| LTP | Long-term potentiation |
| MB | Midbrain |
| MCL | Mitral cell layer |
| mg | milligram |
| mGluR | Metabotropic glutamate receptors |
| ML | Molecular layer |
| ml | Mililiter |
| mM | Milimolar |
| mRNA | Messenger RNA |
| MUN | Munc homology-domain |
| NMDA | N-methyl-D-aspartic acid |
| NMDAR | NMDA receptor |
| NMJ | Neuromuscular junction |
| NMJ | Neuro-muscular junction |
| NSF | N-Ethylmaleimide-Sensitive Factor |
| N-terminus | Amino-terminus |
| OB | Olfactory bulb |
| OD | Optical density |
| Oligo | Oligonucleotide |

| | |
|------------------|--|
| P0, p7, p14, p21 | Postnatal day 0,7,14,21... |
| P28 | Animal at day 28 after (post) birth |
| PAGE | Polyacrylamide gel electrophoresis |
| PBS | Phosphate buffered saline |
| PC | Purkinje cells |
| PCR | Polymerase chain reaction |
| PDZ | PDZ-protein binding domain |
| PFA | Paraformaldehyde |
| PKA | Protein kinase A |
| PPF | Pair pulse facilitation |
| PSD | Postsynaptic density |
| PTV | Piccolo/Bassoon transport vesicle |
| RE | Rasmussen encephalitis |
| RIM | Rab interacting molecule |
| RIM-BPs | RIM-binding proteins |
| RNA | Ribonucleic acid |
| RPM | Revolutions per minute |
| RRP | Readily-releasable pool |
| RT | Room temperature |
| RT-PCR | Reverse transcription PCR |
| RV | Reverse |
| SAM | Sterile- α -motif interaction domain |
| SAP | shrimp alkaline phosphatase |
| SDS | Sodium dodecyl sulfate |
| SEM | Standard error of the mean |
| Ser | Serine |
| SH3 | Src homology 3 domain |
| SNAP | Synaptosome associated protein |
| SNARE | Soluble N-ethylmaleimide-sensitive factor (NSF) attachment protein receptors |
| SPM | Synaptic plasma membranes |
| SRP | Slowly releasable pool |
| SS | Splice site |
| SSC | Saline sodium citrate buffer |
| STP | Short-term potentiation |
| STR | Striatum |
| SV | Synaptic vesicle |
| SV2 | Synaptic vesicle protein 2 |
| TH | Thalamus |
| TMD | Transmembrane domain. |

| | |
|--------|--------------|
| TX-100 | Triton X-100 |
| UV | Ultraviolet |
| WT | Wild type |
| μl | Microliter |

13 ACKNOWLEDGMENTS

First I would like to thank my thesis director, **Prof. Dr. Susanne Schoch**, for giving me the opportunity to do this PhD and for her great mentoring. She has been an example of enthusiasm, support and patience. She has been always there, having the right words and giving me good advices for live and work. Thanks for everything.

I would like to express my gratitude to **Prof. Dr. Albert Haas** for accepting being my supervisor. I extend my gratitude to Prof. Dr. **Albert Becker** and Prof. **Walter Witke** for their time as part of my thesis committee.

I wish to thank **Prof. Dr. med. T. Pietsch** and **Prof. Dr. med CE Elger** for the opportunity to carry out this work in their Institutes.

I would like to express my gratitude to **Prof. Dr. Albert Becker** for his good advises and help. Thanks also to **Prof. Dr. Heinz Beck** and **Prof. Dr. Dirk Dietrich** for their very helpful questions, critics, suggestions and comments.

I thank **Dr. Thoralf Opitz** for the great collaboration and for introducing me in the electrophysiology world.

I would like to thank all members of the Schoch and Becker group, it has been a real pleasure to work and share this time with you. Special thanks to my **Annes** and **Mario**, for the funny hours in the lab and in the office. Because, without you my last year would have been much more boring. To **Anne Alfter** (meine blondie), I thank for her patience, her support and trust, for making me cry from laughing. I thank **Gudrun** for the cell culture work, Sabine for the ordering, **Karen** for the corrections, and all others for your help.

I thank all the people I have met in the last five years. They have shared with

me good and bad moments. I specially thank **Barbara** for her support in L&B, even when she was always the one asking for my key. **Julius**, I am grateful for introducing me to the confocal microscopy and the Tango nights. I thank all the people I have met in Bonn, thanks **Kai, Bella, Pitt, Sandra, Trixy...** because without you my life would have been completely different. Particularly I would like to thank **Michel** for “giving me” his job and sharing with me the first lab hours and experiments.

I thank **Tobi** for so many things... he has been always at my side, from the very beginning.

Finally, and with a lot of love, I am thankful to my girls, **Leta, Lodo and Jana**, for being always there supporting me, for the many hours eating sushi and laughing, for the coffee breaks, dinners and shopping.

And of course, I thank my family and parents. A mis **padres**, a quien dedico este trabajo, por su paciencia y apoyo, por sus sabios consejos. Porque sin ellos todo esto no habría sido posible.

14 CURRICULUM VITAE

EDUCATION

RHEINISCHE FRIEDRICH-WILHEMS-UNIVERSITÄT BONN

PhD (Graduate studies in neurobiology/cell biology) 2010

Thesis: Localization and functional role of RIM3γ and RIM4γ, the small members of the RIM protein family

UNIVERSIDAD ESPAÑOLA A DISTANCIA (UNED)

Master of Business Administration (MBA) July 2008

1st course: accounting, finances, operation management, marketing strategies, and business plan. Executive game.

2nd course: marketing speciality. INTOP

UNIVERSIDAD COMPLUTENSE DE MADRID

Advanced Studies Degree (DEA) in Pharmaceutical Chemistry July 2006

Green Chemistry interuniversity postgraduate program (quality mentioned)

MSc in Pharmaceutical Sciences 1998-2003

Specialization in Biotechnology

Erasmus Grant: Pharmacy practical training. Rhein-Sieg Krankenhaus, Siegburg (Germany).

CONGRESS CONTRIBUTIONS

Alvarez-Barón E, Becker A, Bien C, Elger CE, Schoch S. Characterization of the presence of autoantibodies to Munc18 in Rasmussen's encephalitis, **Pharmaceutical Sciences World Congress (PSWC2007), Amsterdam, Netherlands, 22-25 April 2007.**

Alvarez-Barón E, Mittelstaedt T, Schoch S. Comprehensive analysis of the expression and cellular distribution of RIM3 γ and RIM4 γ in the developing and adult rat brain. **Annual Meeting of the Society of Neuroscience, San Diego, 3-7 November 2007.**

Alvarez-Barón E, Mittelstaedt T, Schoch S. Characterization of the synaptic role and localization of RIM3 and 4 γ , **Federation of European Neuroscience Societies (6th FENS Forum, 2008), Geneve, 12-16 July 2008.**

Mittelstaedt T, Seifert G, Alvarez-Barón E, Steinhäuser C, Schoch S. Differential mRNA expression patterns of synaptotagmin gene family members in the rodent brain. **Federation of European Neuroscience Societies (6th FENS Forum, 2008), Geneve, 12-16 July 2008.**

Alvarez-Barón E, Schmitz F, Schoch S Functional characterization of the small members of the RIM protein family, RIM3g and RIM4g. **Synaptopathies: dysfunction of synaptic function (Biochemical Society). Newquay, UK, 2-4 September 2009. SELECTED ORAL COMMUNICATION.**

Alvarez-Barón E, Schmitz F, Schoch S. g-RIMS : localization and functional role. **Active Zones as organizers of neuronal communication. Baeza, Spain, 22-24 October 2009. SELECTED ORAL COMMUNICATION.**

PUBLICATION RECORD

Alvarez-Báron E, Bien C, Schramm J, Elger CE, Becker AJ, Schoch S. Autoantibodies to Munc18, cerebral plasma cells and B-lymphocytes in Rasmussen encephalitis. **Epilepsy Res**, 80(1): 93-9, 2008.

Mittelstaedt T, Elena Alvárez-Barón E, und Schoch S. Die Cytomatrix der präsynaptischen Aktiven Zone: molekulare Organisation und Funktion. **Neuroforum** 03/2008.

Mittelstaedt T, Seifert G, Alvárez-Barón E, Steinhäuser C, Becker AJ, Schoch S. Differential mRNA expression patterns of the Synaptotagmingene family in the rodent brain. **Journal of comparative neurology**, 512(4): 514-28, 2009.

Mittelsteadt T, Álvarez-Barón E, und Schoch S. RIM proteins and their role in synapse function **Biological Chemistry**, submitted.

Álvarez-Barón E, Mittelstaedt T, Schmitz F, Schoch S. Gamma-RIMs: distribution and function in the mammalian brain (manuscript in preparation).